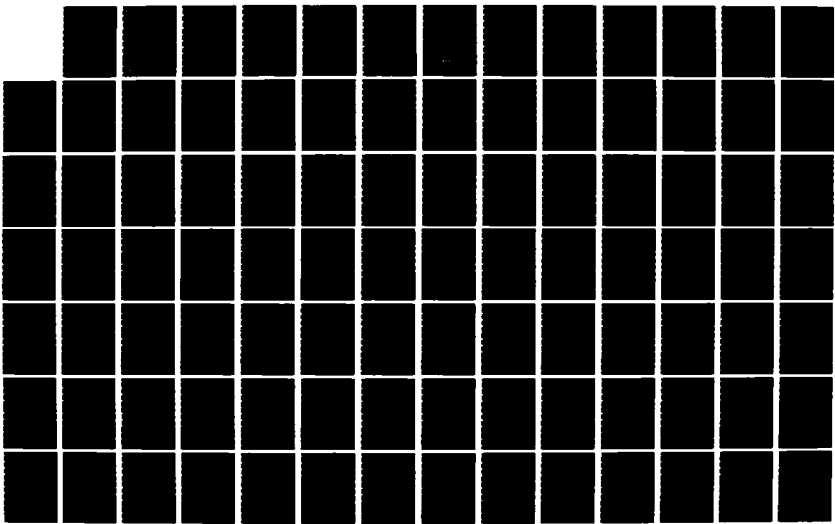
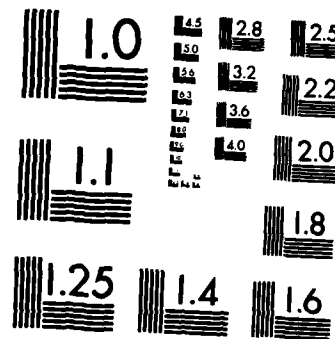


AD-A162 736 AN INVESTIGATION INTO PRINCIPLES FOR DESIGN OF A 1/2
MULTIPLE DIPOLE HF (HIGH (U) HOCHSCHULE DER BUNDESWEHR
MUNICH (GERMANY F R) INST FOR HIGH- G FLACHENECKER
UNCLASSIFIED 15 JUN 84 R/D-4419-EE-09 DAJA45-83-M-0274 F/G 9/5 NL





MICROCOPY RESOLUTION TEST CHART
NATIONAL BUREAU OF STANDARDS-1963-A

An Investigation
into Principles for Design of a
Multiple Dipole
HF-Antenna Configuration

AD-A162 736

Final Technical Report

June 15, 1984

DAJA 45-83-M-0274

DTIC
ELECTED
DEC 23 1984
S D

Gerhard Flachenecker

Institute for High-Frequency Techniques
University of the Bundeswehr Munich

1 COPY

This document has been approved
for public release and sale; its
distribution is unlimited.

85
58 - 12 - 23 005

**An Investigation
into Principles for Design of a
Multiple Dipole
HF-Antenna Configuration**

Final Technical Report

June 15, 1984

DAJA 45-83-M-0274

Gerhard Flachenecker

**Institute for High-Frequency Techniques
University of the Bundeswehr Munich**

An Investigation into Principles for Design of a
Multiple Dipole HF-Antenna Configuration

Gerhard Flachenecker
Institute for High-Frequency Techniques
University of the Bundeswehr Munich

Table of Contents:

1. Introduction	2
2. Sample Structure to be Analyzed	5
3. Feeder Systems	5
4. Calculation Method	14
5. Representation of the Results	17
6. Analysis at 3 MHz. Feeder Type: Cobra Head	19
7. Analysis at 5.1 MHz. Feeder Type: Cobra Head	48
8. Analysis at 8.66 MHz. Feeder Type: Cobra Head	66
9. Analysis at 14.71 MHz. Feeder Type: Cobra Head	79
10. Analysis at 25 MHz. Feeder Type: Cobra Head	92
11. Analysis for the Feeder Type: Baluns at the Dipole Centres	105
12. Conclusions - Recommendations	148
13. Acknowledgement	150

Accession For	
NTIS	CRA&I
DTIC	TAB
Unannounced	
Justification	
By _____	
Distribution / _____	
Availability Codes	
Dist	Avail and/or Special
A-1	



UNCLASSIFIED

SECURITY CLASSIFICATION OF THIS PAGE (When Data Entered)

REF 4419-EE-09

REPORT DOCUMENTATION PAGE		READ INSTRUCTIONS BEFORE COMPLETING FORM
1. REPORT NUMBER	2. GGOVT ACCESSION NO.	3. RECIPIENT'S CATALOG NUMBER
	AD-PK AD-4162 736	AD-4162 736
4. TITLE (and Subtitle) An Investigation into Principles for Design of a Multiple Dipole HF-Antenna Configuration	5. TYPE OF REPORT & PERIOD COVERED Technical Report Aug 83 - Feb 84	
7. AUTHOR(s) G./Flachenecker	6. PERFORMING ORG. REPORT NUMBER DAJA45-83-M-0274	
9. PERFORMING ORGANIZATION NAME AND ADDRESS Hochschule der Bundeswehr München Werner-Heisenberg-Weg 39 8014 Neubiberg, Germany	10. PROGRAM ELEMENT, PROJECT, TASK AREA & WORK UNIT NUMBERS 6.11.02A 1T161102BH57-03	
11. CONTROLLING OFFICE NAME AND ADDRESS USARDSG-UK Box 65, FPO NY 09510	12. REPORT DATE June 15, 1984	
14. MONITORING AGENCY NAME & ADDRESS (if different from Controlling Office)	13. NUMBER OF PAGES 150	
	15. SECURITY CLASS. (of this report) Unclassified	
	15a. DECLASSIFICATION/DOWNGRADING SCHEDULE	
16. DISTRIBUTION STATEMENT (of this Report) Approved for Public Release; distribution unlimited		
17. DISTRIBUTION STATEMENT (of the abstract entered in Block 20, if different from Report)		
18. SUPPLEMENTARY NOTES		
19. KEY WORDS (Continue on reverse side if necessary and identify by block number) Dipole, HF-range, multiple dipole HF-antenna site, mutual coupling, radiation pattern, current distribution, feeder systems, cobra head feeder, feeder line, parasitic currents, antenna, antenna resonance		
20. ABSTRACT (Continue on reverse side if necessary and identify by block number) Analysis of a dipole HF-antenna site configuration involving multiple dipole antennas, feeder lines, and supporting structures. Calculation of the current distribution along the antenna wires, and the distribution of the parasitic currents along the feeder lines and supporting structures depending on frequency and feeder system. Calculation of the radiation patterns concerning the parasitic currents. 3D-presentation of the results.		

An Investigation into Principles for Design of a
Multiple Dipole HF-Antenna Configuration

Gerhard Flachenecker
Institute for High-Frequency Techniques
University of the Bundeswehr Munich

1. Introduction.

The following report deals with multiple-frequency/multiple-user antenna configurations for the HF-range, as shown in Fig. 1 for a typical arrangement. Horizontally mounted dipoles are used to transmit or receive, respectively, via the space wave. To cover the whole HF-range several antennas of different length are used. Each antenna can be accessed by a separate transmitter/receiver. In order to obtain the proper transmitting and receiving pattern the antennas are mounted at certain heights and supported by a system of poles and messenger wires. In many cases a microwave tower is integrated into the structure.

It is a well-known fact that closely spaced antennas in such antenna arrays show disturbed effects which are not seen in the isolated antenna. Mutual coupling between the different antennas and between the antennas and the supporting structures can produce unexpected currents and affect the operation. In general, the mentioned coupling causes two effects:

(a) If two antennas (at different frequencies) are in transmit mode simultaneously, there could be a power feedback from one transmitter to the other and vice versa, due to the antenna coupling. If, in another case, one antenna is in transmit mode and another antenna is in receive mode, the power coupled from the transmitting field to the receive antenna can cause nonlinear effects in the front-end stage of the receiver. These effects are well-known and can be avoided by filtering. (As a result of filtering the feeding point of each antenna in a

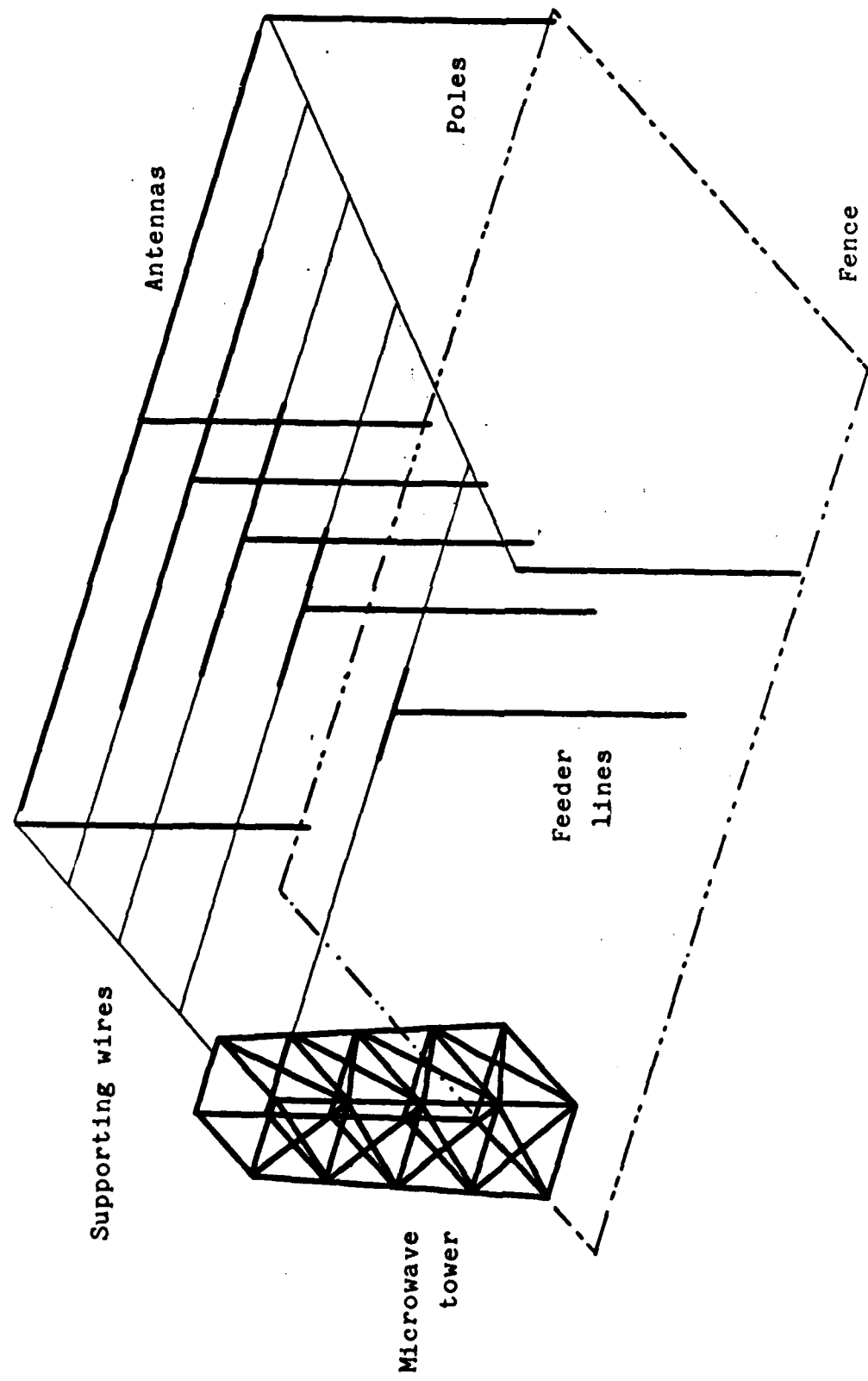


Fig. 1: Principle arrangement of a multiple-frequency/multiple-user HF-dipole antenna site.

multiple-frequency/multiple-user array is loaded with highly reactive impedances at all frequencies except its own operating frequency).

(b) The near field radiated from one of the antennas in transmit mode induces currents along the other antennas, the supporting wires, the poles, and the feeder lines of all antennas. These currents severely influence the radiation pattern of the transmitting antenna. This effect cannot be avoided by additional filtering within the feeder lines. The resulting radiation patterns (and also the receive patterns, due to the law of reciprocity) is only determined by the outer structure of the configuration and the load impedances of all the other antennas, which can appear at random.

The following report is restricted to item (b), since these influences cannot be altered after the construction of the sample antenna configuration. A typical antenna configuration is assumed for calculation purposes rather than an actual antenna site, but one which is very close to reality. It should be understood that the exact behavior of an antenna arrangement is very sensitive to the exact dimensions of the arrangement. The analysis of a sample configuration, however, shows a number of basic effects and leads to general rules which are very helpful for the design of new antenna sites. Furthermore, the computation programs which have been developed during the preparation of this report can be used for recursive calculation of a new antenna design which has been outlined after the general rules of the sample analysis.

One limitation on the analysis of a structure such as that shown in Fig. 1 is the available memory of the computer in use. The maximum available memory limits the total (combined) length of the analyzed structure components with respect to the free-space wavelength at the particular frequency. In the case of the computer used in the following analysis it was not possible to

model the microwave tower exactly nor to consider the supporting wires as conductive wires, only insulated from the dipole tips. Extensive investigations, which are not included in this report, showed, however, that the microwave tower can be replaced by a simple pole without generating major errors. The supporting wires have been considered to be non-conductive, which is true in the case of nylon rope in use, or in the case of conductive wires which are very frequently intersected by insulators. The results of the following analysis strongly suggest one of these two mentioned cases for the supporting wires. Therefore, the assumption of nonconductive supporting wires is not a real limitation of the analysis technique when considering a new trial antenna configuration.

2. Sample Structure to be Analyzed.

As previously discussed, the microwave tower has been replaced by a simple pole. Additionally, the influence of the supporting wires has been assumed to be negligible and these wires have been totally removed. The remaining structure is shown in Fig. 2. The array is assumed to cover the frequency range 3 through 25 MHz with a total of 5 antennas. These antennas are chosen in length to follow a geometrical series in order to cover equal relative bandwidths. The longest antenna has a length of 50 m which is half a wavelength at 3 MHz. The shortest antenna has a length of 6 m which is half a wavelength at 25 MHz. All poles and feeder lines have a height of 18.3 m (60 ft) which is close to the actual antenna array. Thus, all of the antennas are situated at a height of 18.3 m. All poles, including the pole which replaces the microwave tower, have diameters of 25 cm. Metal poles are used.

Fig. 3 shows the coordinates of the supporting poles and the feeder lines in (x/y) notation. Fig. 2 and 3 together completely describe the dimensions of the structure. For further reference, Fig. 4 indicates the half-wavelength frequencies of the various antennas. These frequencies are assumed to be the center operating frequencies of the respective antennas. All the following analyses will be performed at these center frequencies.

3. Feeder Systems.

A very important parameter for the behavior of the antenna array is the kind of feeders which are used. Figs. 5 through 7 show different feeder types which could be used.

The simplest feeder is shown in Fig. 5. In this case, which is called "cobra head feeder", the feeder line is a coaxial cable.

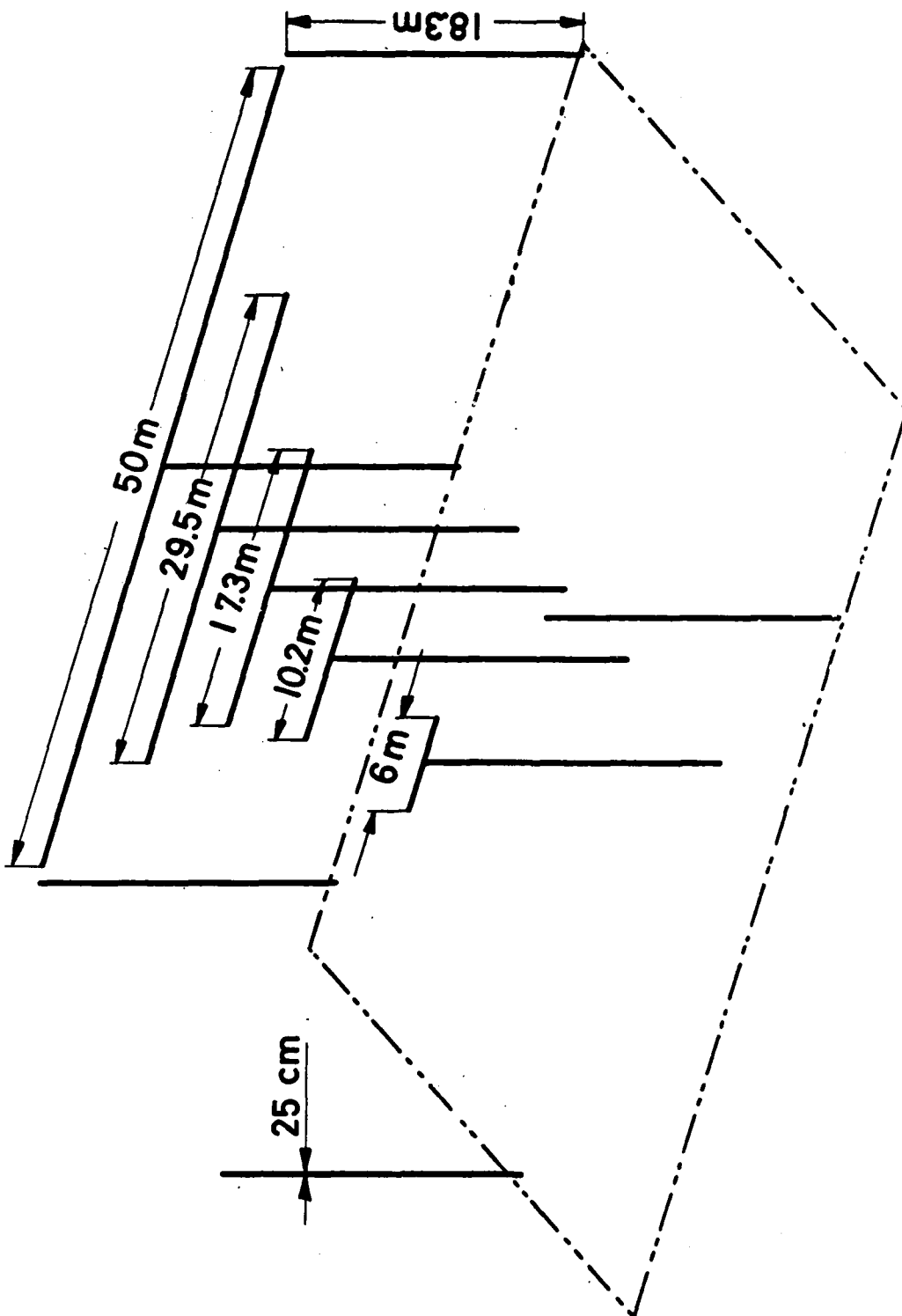


Fig. 2: Dimensions of the antennas and the supporting poles.
All poles: Height = 18.3 m; Diameter = 25 cm
All feeder lines: Height = 18.3 m.

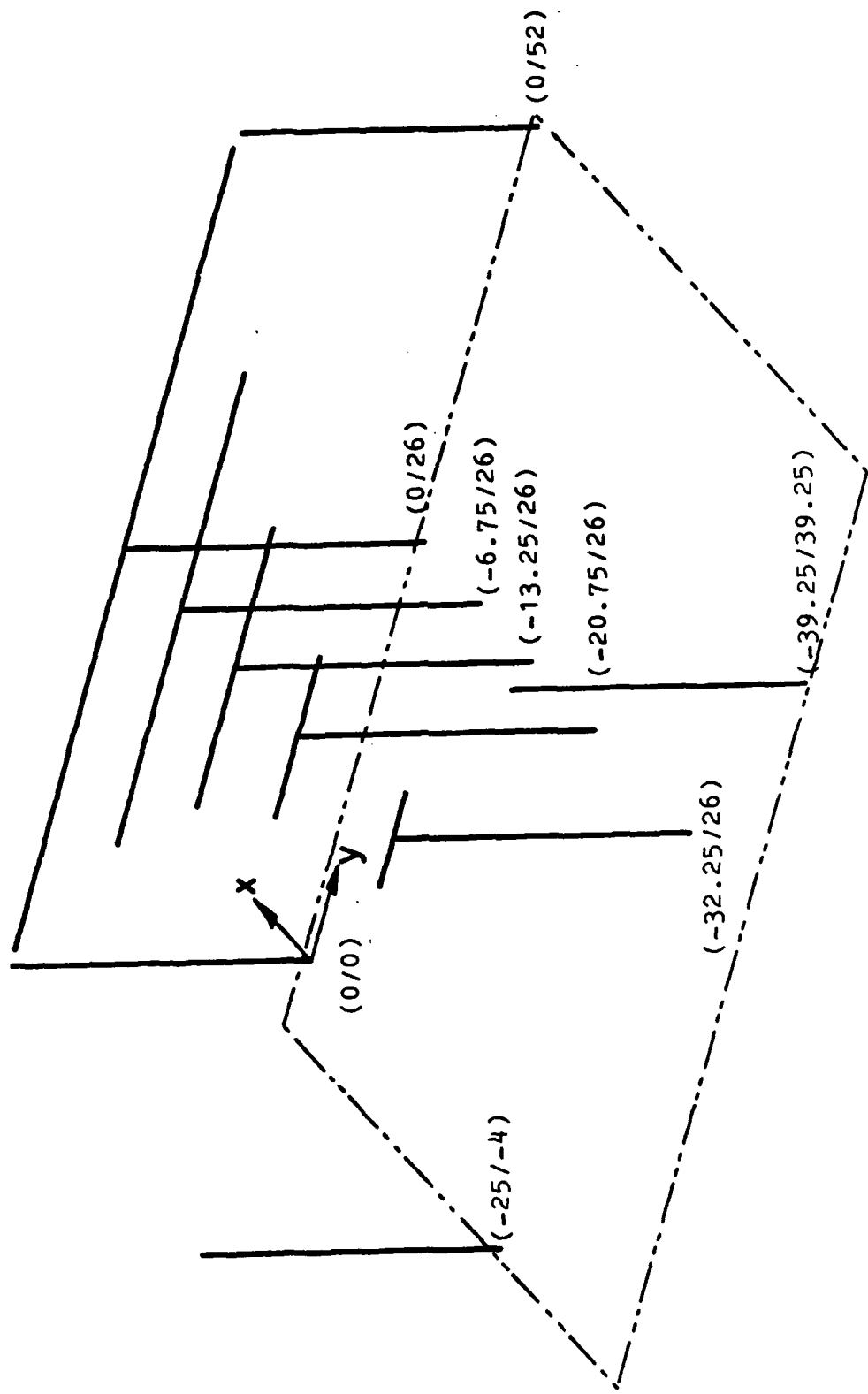


Fig. 3: Coordinates of the supporting poles and the feeders in (x/y) notation.

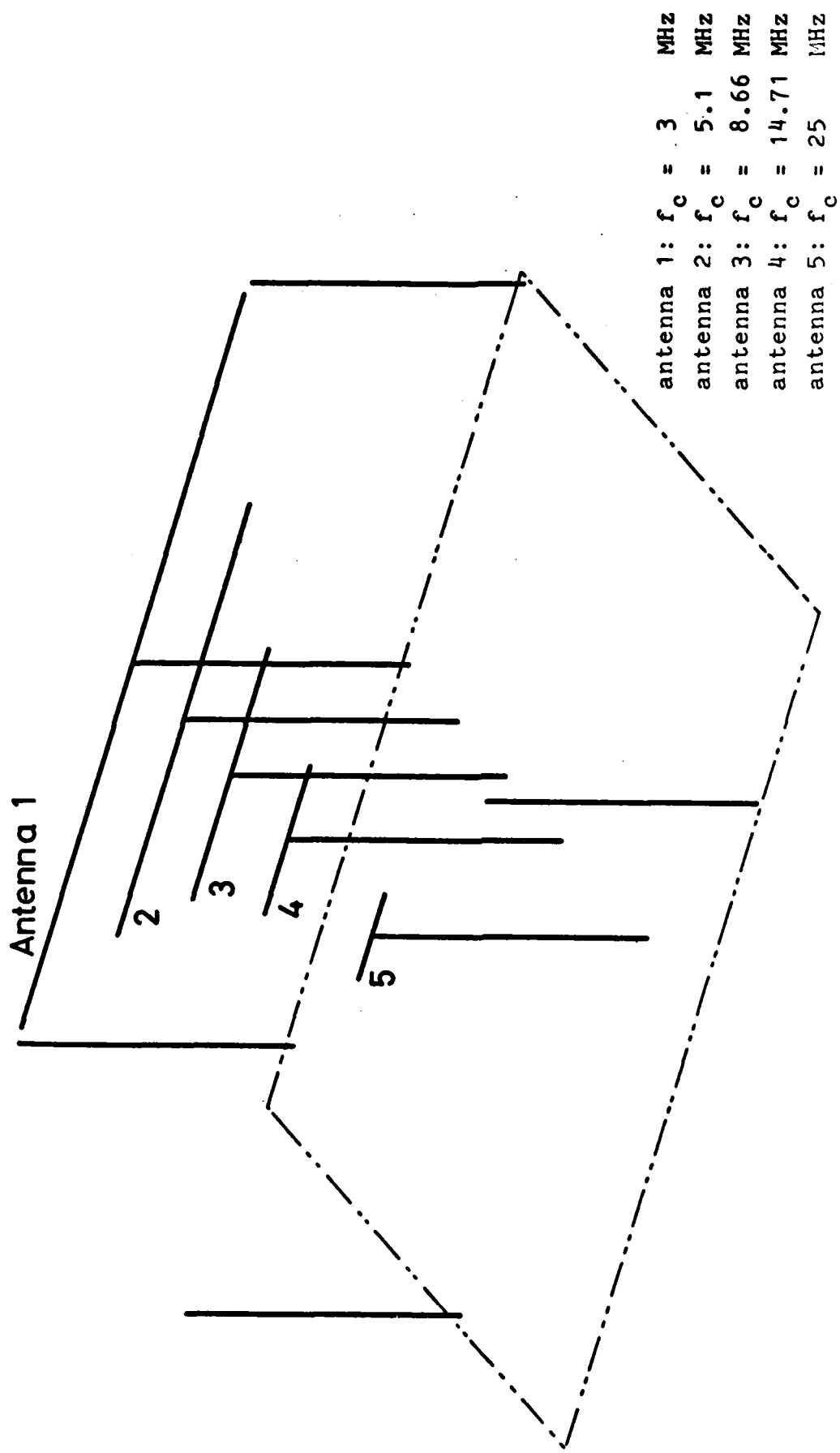


Fig. 4: Half-wavelength frequencies of the individual dipoles.

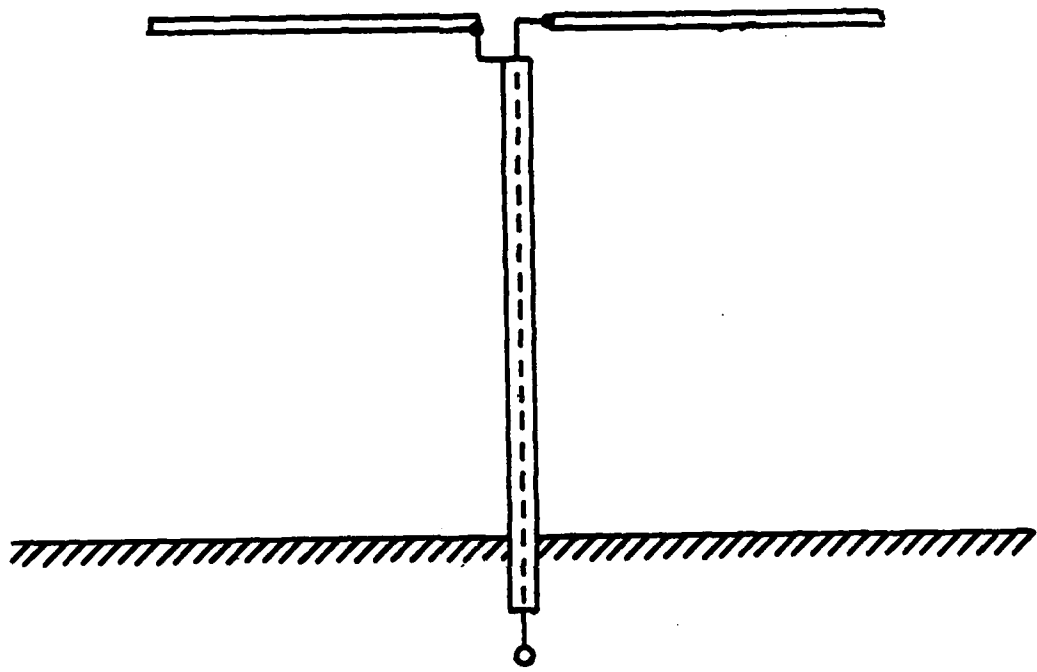


Fig. 5: Feeder type "Cobra head".

The outer conductor of the coaxial cable is simply connected to one half of the dipole antenna while the inner conductor is connected to the other half of the dipole. As will be pointed out during the analysis this feeder system has several serious drawbacks. As the outer conductor of the coaxial cable is directly connected to the antenna the feeder line can conduct high sheath currents compared to the dipole currents. In this case the radiation pattern of the dipole can be seriously disturbed.

Extended sheath currents along the feeder line can be avoided if baluns are used. Figs. 6 and 7 show four slightly different kinds of feeder systems using baluns. In Figs. 6a and b the baluns are located at the dipole centers. In both cases coaxial cables are used as feeder lines to the dipole centers and balancing is achieved close to the antenna connection points. The difference between the both arrangements is the presence or absence of a center ground to the balun or the dipole, respectively. The lowest sheath currents along the feeder line will be observed in the case of Fig. 6a with no grounding of the antenna. Lightning protection, however, could require a center grounding of the dipole, as shown in Fig. 6b. In this case even-mode sheath currents can be generated along the feeder line but these currents will be of much less magnitude than in the case of a cobra-head feeder.

Figs 7a and b show dipole antennas with symmetrical feeder lines. The baluns are located at ground level. The difference between both arrangements is the absence or the presence of a center ground. In general, the even-mode currents along the feeder line will be higher than in the cases of Figs. 6a and b due to the direct connecting of the feeder line to the dipole antenna.

The following report analyzes the two most opposite cases of feeder principles:

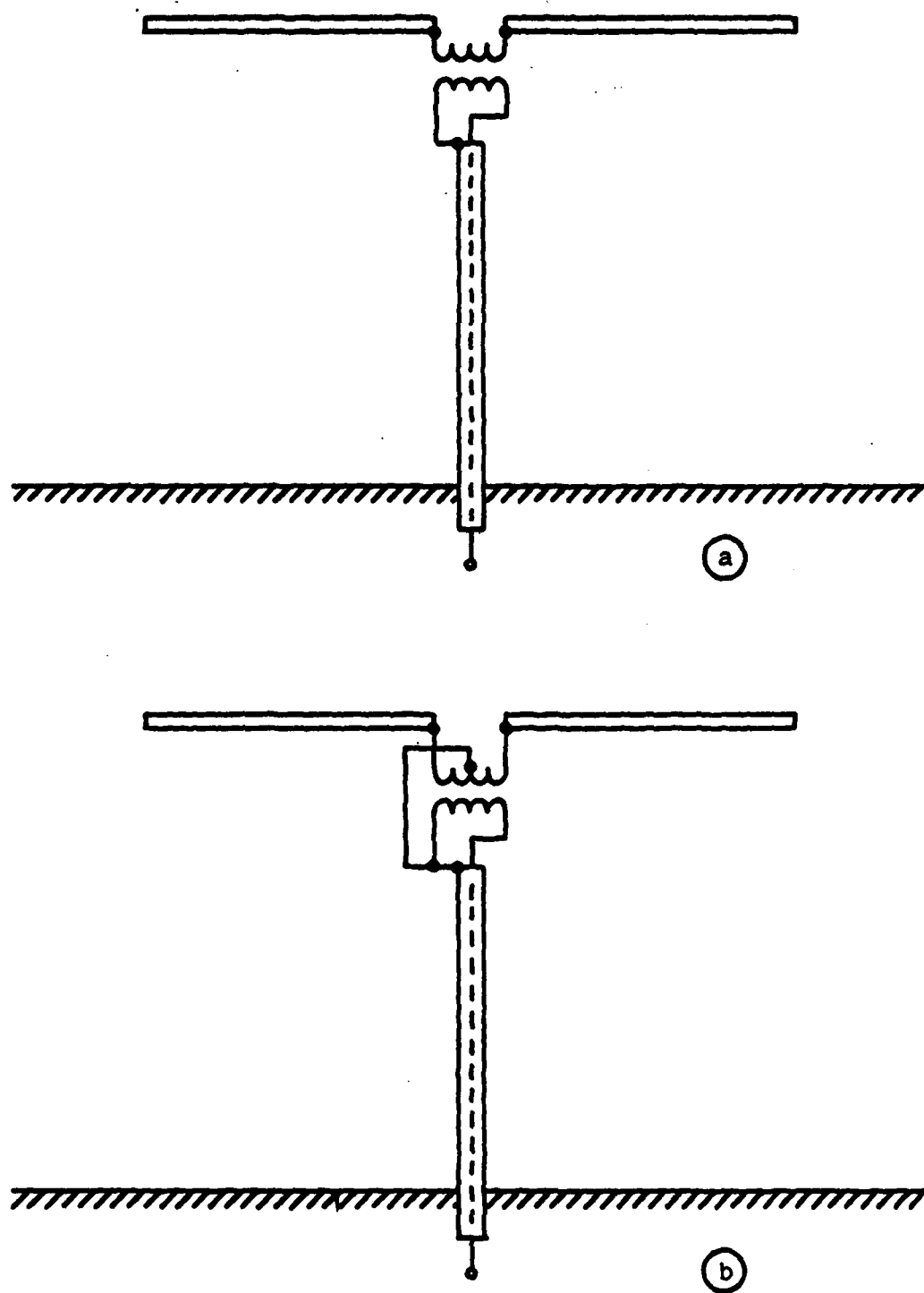


Fig. 6: Feeder type "Balun at the dipole center"

- a) not grounded
- b) grounded

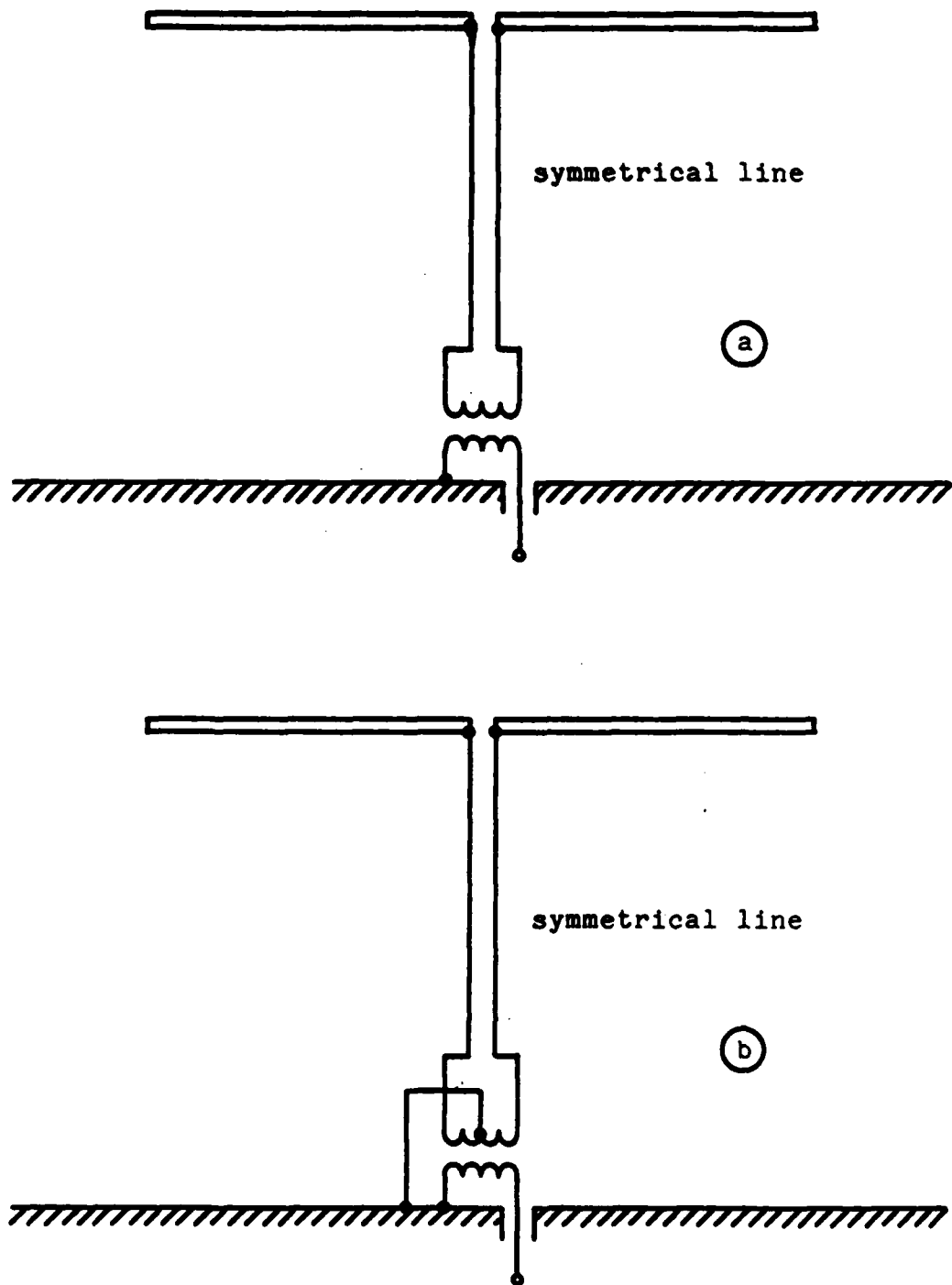


Fig. 7: Feeder type "Symmetrical feeder line"

- a) not grounded
- b) grounded

(a) First, the case of cobra-head feeders, which in general is the case showing the greatest influence of feeder lines on antenna behavior.

(b) Second, the balun feeder of Fig. 6a without center grounding, which in general will show the lowest influence of feeder lines on antenna behavior.

It can be assumed generally that any other feeder system will be between the two analyzed systems regarding the distortions of the radiating patterns. It should be mentioned once again that the exact behavior of an antenna array can only be calculated assuming the exact array measures and the exact antenna load impedances. The following analyses of two arrangements only show basic rules for the design. Once a new configuration has been proposed following these rules, a recalculation with the exact data is highly recommended.

4. Calculation Method.

A description of the complete calculation method which has been used for the following analyses is beyond the scope of this report. Therefore, only the principles will be sketched.

The current distribution along the whole structure and the radiation patterns (or receiving patterns, respectively) depend on the frequency with which a particular antenna is fed (or acts as receiving element), and on the load impedances of the remaining antennas. A computer program was used which is able to calculate the current distribution and the patterns for each combination of frequency, feeder point, and load impedances. This computer program splits the whole structure of the array into a great number of small elements, each of which is described as a spatial vector. Each element has to be small compared to the free-space wavelength at the frequency in use. A total of about 250 elements was used. This number is limited by the memory of the computer in use. For each element, two unknown currents, input and output, are assumed. The current difference is treated as a surface charge on the element. In a matrix the reaction of all elements is combined to fulfill the boundary conditions along the surface of the structure. Out of this matrix the unknown currents, the voltages at feeder gaps considering the load impedances, and finally the patterns can be determined.

Solving the matrix operations is very time consuming. Thus, it is not economical to solve the whole system for each case of interest. Instead, a superposition principle using basic solutions has been used. It can be shown that (for each frequency) only a limited number of basic solutions has to be known in order to determine the behavior of the structure for each possible load termination. This number of basic solutions is the number of the feeder gaps in the structure, which in this

case is the number of antennas. In the following analyses the five case

- antenna 1 is fed, all other antennas are open loop,
- antenna 2 is fed, all other antennas are open loop,
- antenna 3 is fed, all other antennas are open loop,
- antenna 4 is fed, all other antennas are open loop, and
- antenna 5 is fed, all other antennas are open loop,

have been used as basic solutions (generic cases). Each case produces a current distribution, a pattern, and open-loop voltages at the remaining antennas. If these five cases are solved, the antenna array can be treated as a five port with a known five-port Z-matrix (impedance matrix). The Z-matrix can be extracted from the open-loop voltages of the basic solutions. With the help of the Z-matrix the superposition of the basic solutions can be performed to describe each possible case of load terminations. With this method for any case of practical interest the current distribution and pattern of the configuration can be calculated very economically.

The Z-Matrix itself gives additional information. Along the main diagonal it shows the antenna impedances of the respective antenna. Z_{11} , for instance, is the internal impedance of antenna 1 if all other antennas are open loop terminated. The other elements represent the cross coupling of the respective antennas; Z_{12} , for instance, is given by

$$Z_{12} = U_2/I_1 \quad (1)$$

where U_2 is the open loop voltage of antenna 2 generated by the current I_1 (which is fed to antenna 1), while all other antennas are open loop terminated. Also, with the help of the Z-matrix, the antenna impedances can be calculated in the general case where the other antennas are not open loop terminated but terminated with certain impedances.

Due to the importance of the Z-matrix concerning the mutual coupling of the antennas in the array it is included in this report for every frequency which has been treated.

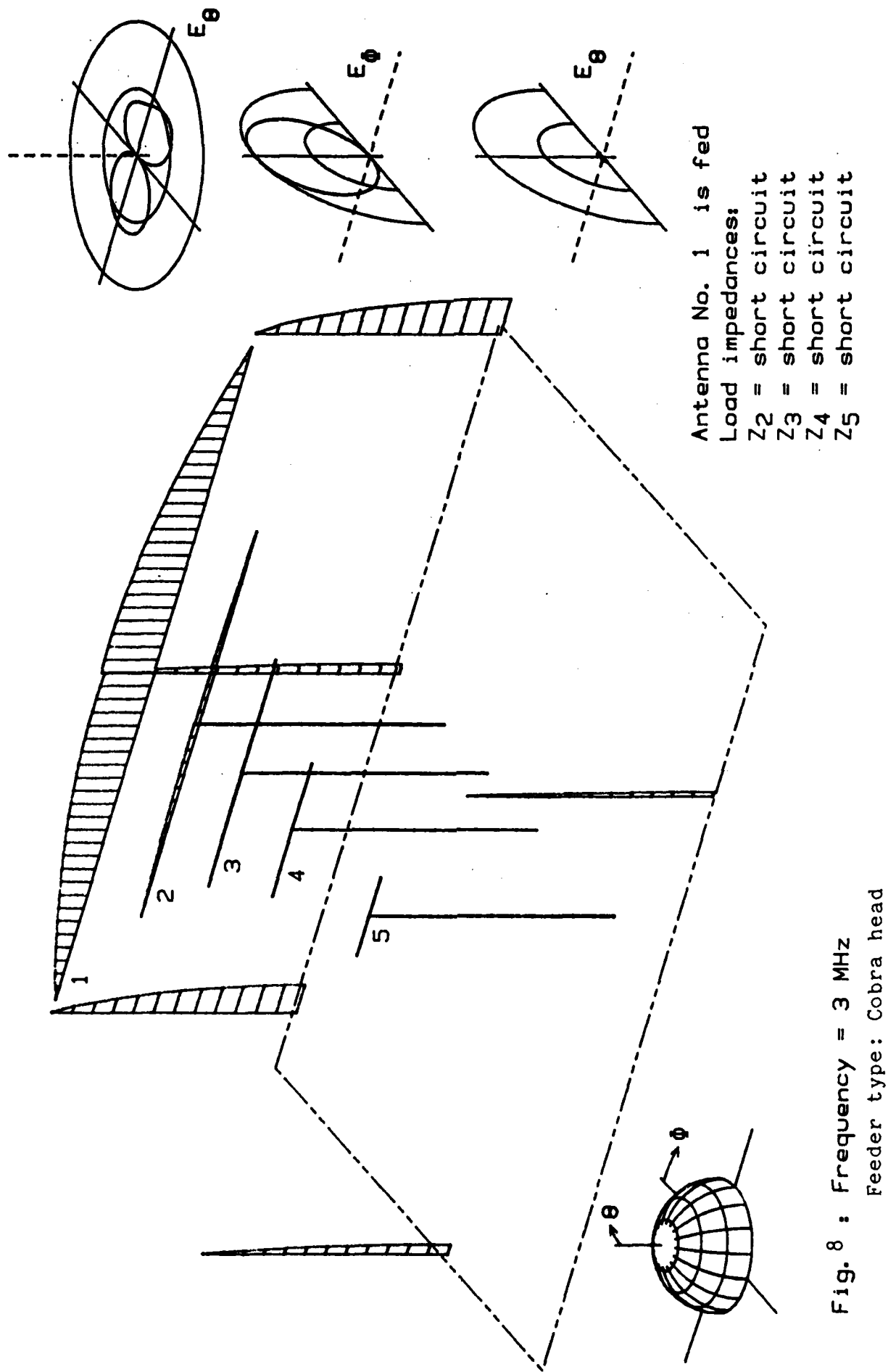
5. Representation of the Results.

An example of the results is in Fig. 8, which shows the antenna structure in a three-dimensional view. The current distribution along the structure is outlined with the help of the "hatched" areas, as usual in antenna theory. Each cross hatch represents one calculated value of a current magnitude. Keep in mind that this representation only shows magnitudes. Phase information, of course, is lost. The separation between cross hatch lines also shows the element length for the numeric calculation.

The labeled area at the bottom right gives information about load conditions. In the example, antenna 1 is fed and all other antennas are short circuited.

At the right-hand side are the main cross sections of the radiation pattern. The coordinate system which has been used is at the bottom left side. The top and bottom patterns shown are for vertical polarization; the middle pattern is the horizontal polarization pattern.

In the following, each treated frequency starts with the presentation of the five generic cases. It is, of course, never intended that any antenna be used except the one for that particular frequency. If, for instance, a frequency of about 3 MHz is in use, antenna 1 (see Fig. 4) will always be the transmitting or receiving antenna. Never will antennas 2 through 5 be used for 3 MHz. These "un-natural" cases are only used as the basic solutions out of which the behaviour of the entire structure under all load conditions can be calculated. On the other hand, the generic cases very clearly show the kind of "reaction" of the parasitic coupled antennas to the current distribution.



6. Analysis at 3MHz. Feeder type: Cobra head.

In Table 1 the Z-matrix for 3MHz and cobra-head feeding is presented. Figs. 9 through 13 show the generic cases as discussed above. As the center frequency of antenna 1 is 3 MHz only this antenna is intended for actual use at this frequency. Therefore, Fig. 9 (which deals with antenna 1 being fed) is of special interest.

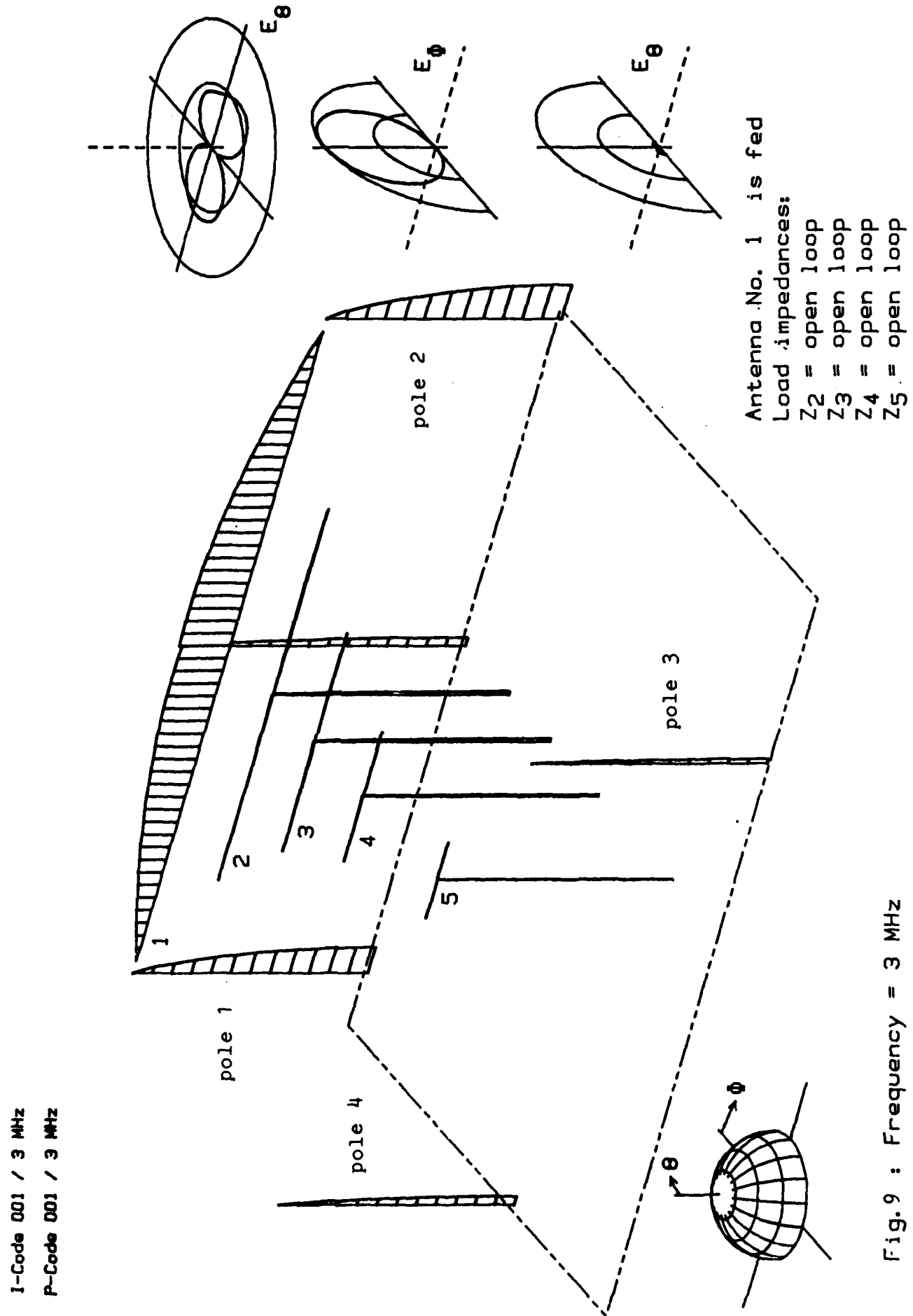
In Fig. 9 the remaining antennas are open loop terminated. This, of course, is only one special case in practice but it is well suited for the basic explanations. As can be seen from the current distribution the length of antenna 1 must be close to one half of the free-space wavelength. An unexpected effect is the high magnitude of the currents in the poles 1 and 2 close the tips of antenna 1. The currents in the other poles and in the feeder lines are less because poles 1 and 2 are very closely spaced to the antenna tips where a high radial electric field strength is generated. Figs. 2 and 3 show that the distances of these poles from the respective antenna tips are 1m each.

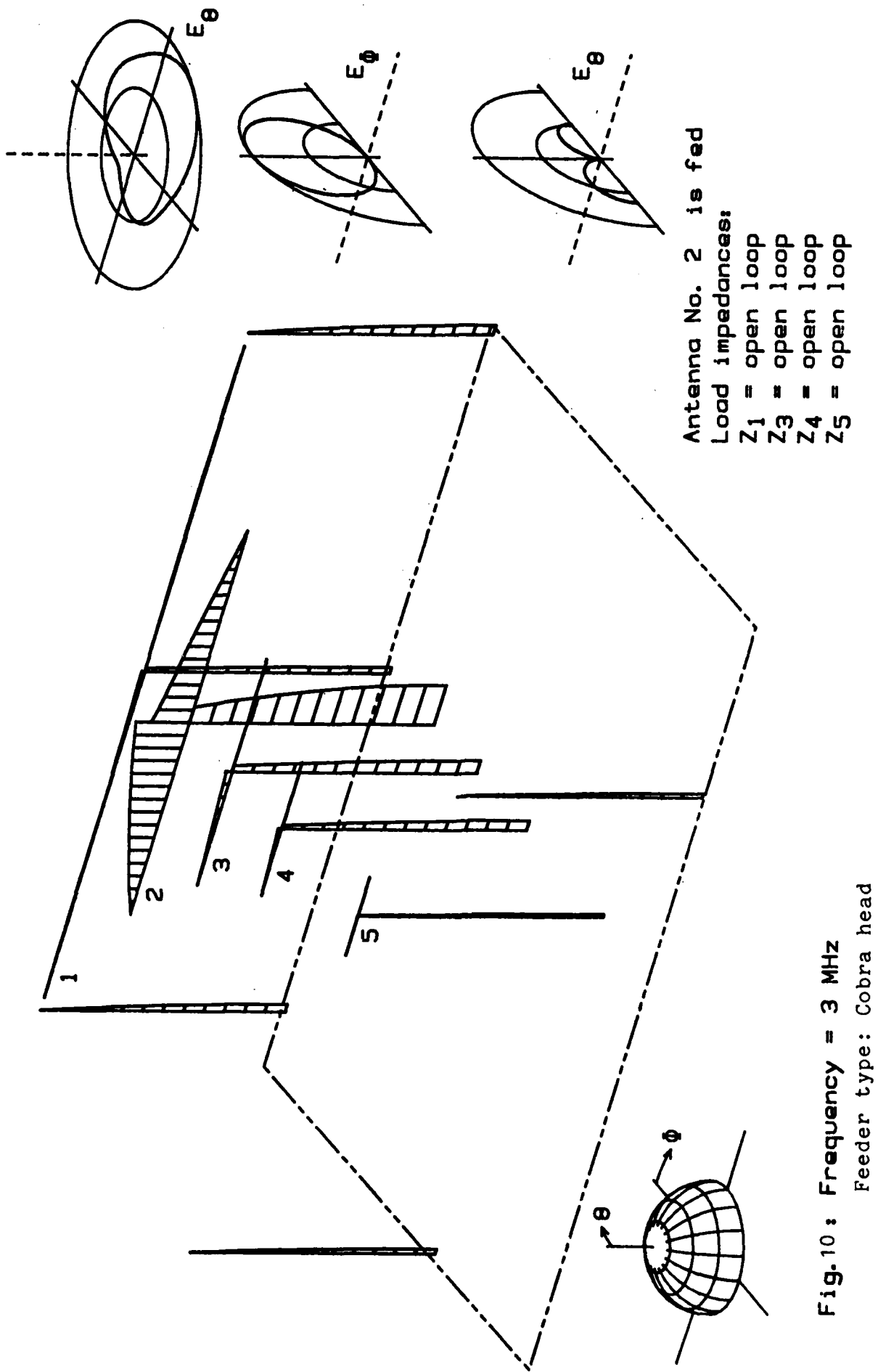
The current along antenna 1 has a discontinuity at the feeder gap due to the fact that at the left hand side of the feeder gap the current divides into two parts which flow into the left antenna rod and as a sheath current along the feeder line. These current representations lose phase informations. Thus, the linear sum of the left-side antenna current and the sheath current on the feeder at the feeding gap is not necessarily equal to the right-side antenna current. Only the complex sum (regarding phases) has to be equal.

The currents in poles 1 and 2 are slightly different as a consequence of the feeder type. The feeding of the right dipole half against the left dipole half and the feeder line involves the feeder line as part of the antenna. In this dipole-feed configuration the voltage at the left-side dipole half is less

$l_{11} = (-106.49+j133) \text{ ohms}$	$l_{12} = (51.20+j41) \text{ ohms}$	$l_{13} = (29.07+j29) \text{ ohms}$	$l_{14} = (3.28-j17) \text{ ohms}$	$l_{15} = (-4.74-j6) \text{ ohms}$
$l_{21} = (51.56+j41) \text{ ohms}$	$l_{22} = (41.38-j796) \text{ ohms}$	$l_{23} = (98.36+j58) \text{ ohms}$	$l_{24} = (-106.44-j26) \text{ ohms}$	$l_{25} = (-32.52+j27) \text{ ohms}$
$l_{31} = (29.85+j27) \text{ ohms}$	$l_{32} = (98.25+j57) \text{ ohms}$	$l_{33} = (550.06-j2877) \text{ ohms}$	$l_{34} = (-850.32-j245) \text{ ohms}$	$l_{35} = (-325.78+j172) \text{ ohms}$
$l_{41} = (3.81-j14) \text{ ohms}$	$l_{42} = (-105.96-j25) \text{ ohms}$	$l_{43} = (-849.38-j245) \text{ ohms}$	$l_{44} = (1538.17+j2223) \text{ ohms}$	$l_{45} = (692.89-j210) \text{ ohms}$
$l_{51} = (-3.49-j5) \text{ ohms}$	$l_{52} = (-32.15+j27) \text{ ohms}$	$l_{53} = (-324.79+j171) \text{ ohms}$	$l_{54} = (691.58-j210) \text{ ohms}$	$l_{55} = (370.10-j832) \text{ ohms}$

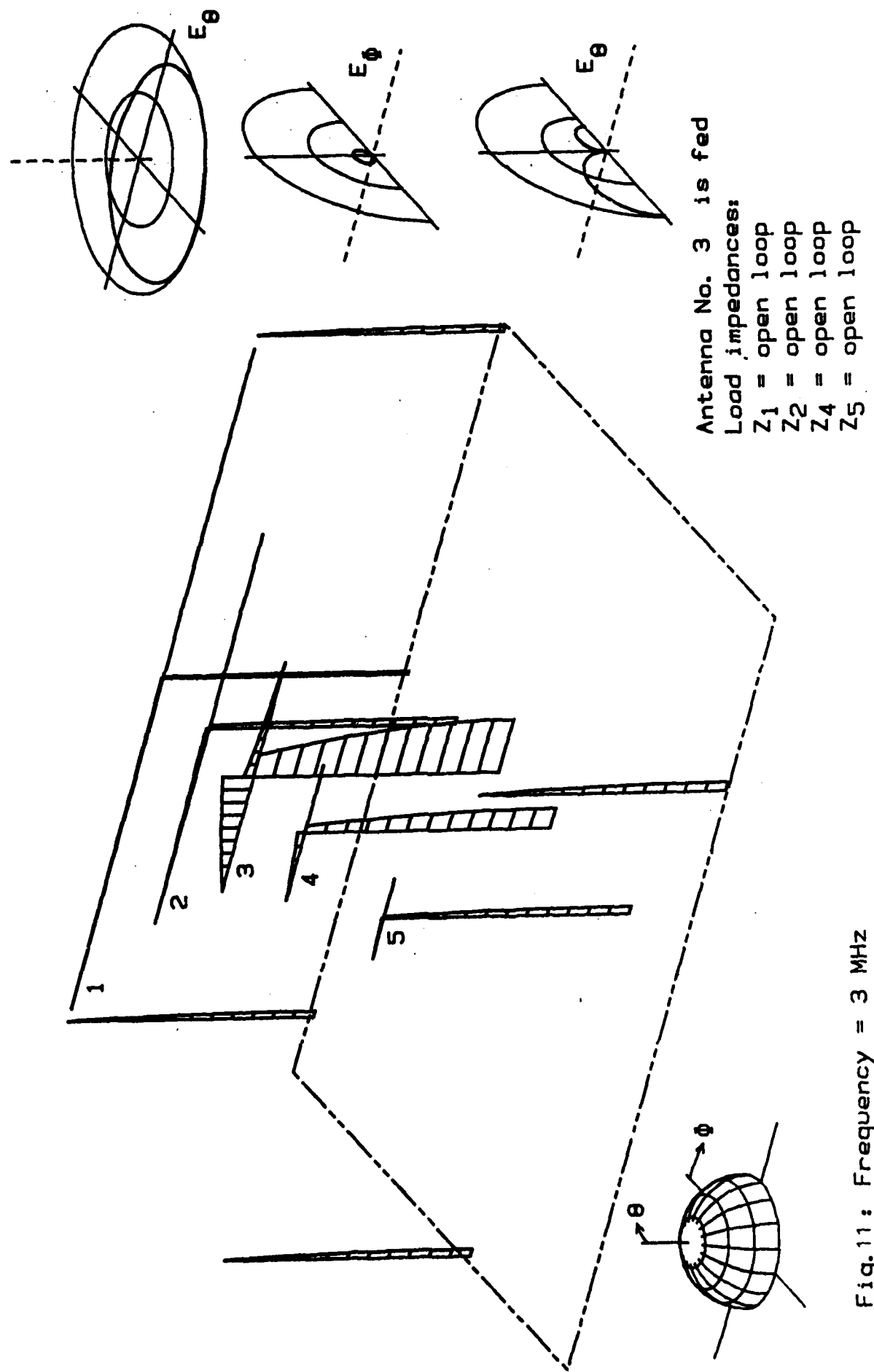
Table 1: L-Matrix for f = 3 MHz. Feeder type: Cobra head.

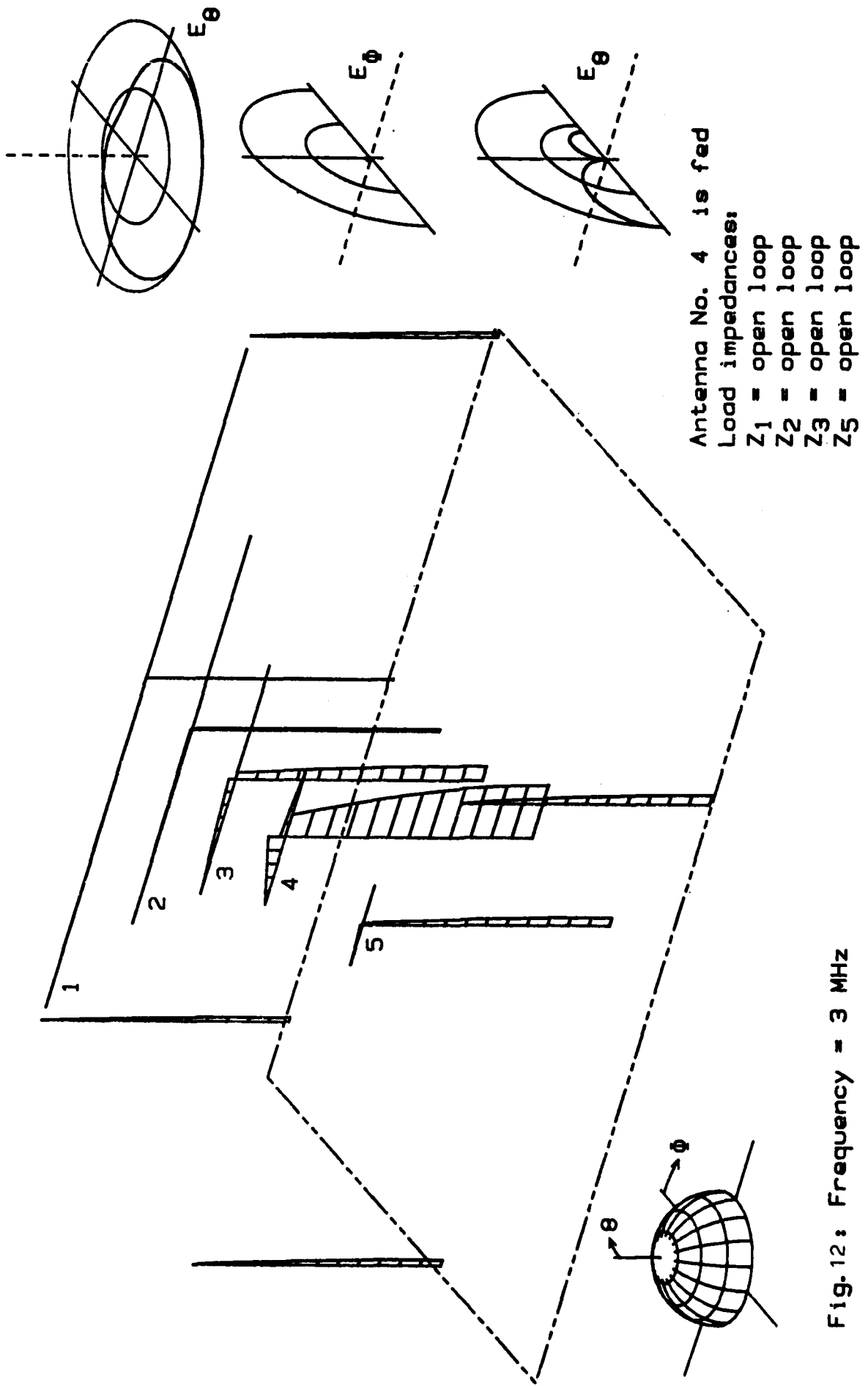


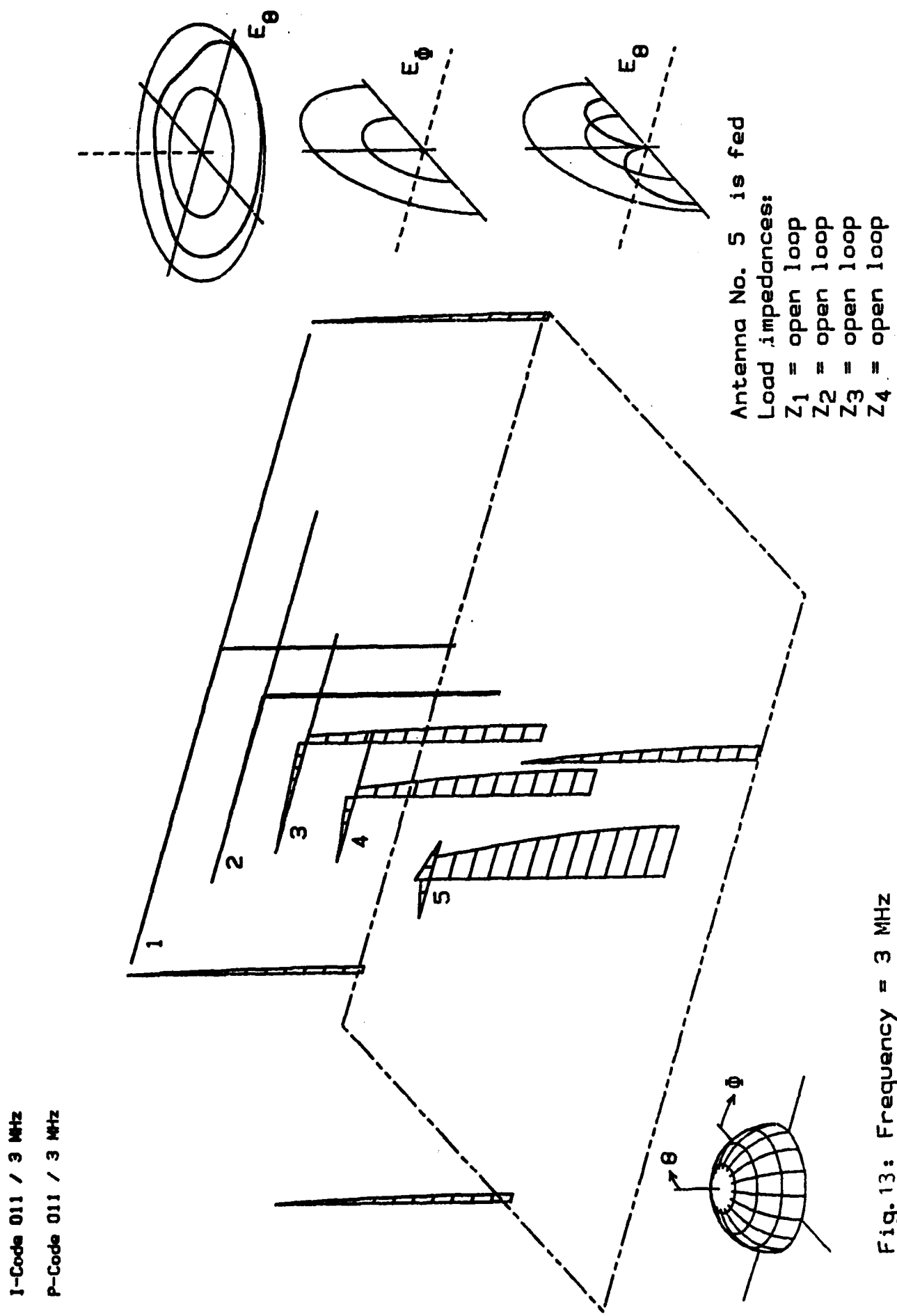


I-Code 009 / 3 MHz
P-Code 009 / 3 MHz

- 23 -







than the right-side dipole half. Therefore, the field exciting pole 1 is less than the field exciting pole 2.

It is interesting that even pole 4 has a current induced which has about the same magnitude as the current along the feeder line of antenna 1.

The currents along the poles and the feeder lines increase with decreasing distance from the ground plane. This is due to the conductivity of the ground plane which acts as a short circuit for the currents along the poles and the feeder lines. Also, the ground plane produces "mirror images" of the dipole currents and the currents along the poles and the feeder lines.

At the right-hand side the most important radiation patterns are shown. E-theta is the electrical field strength of the vertical polarization while E-phi is the electrical fieldstrength of the horizontal polarization. Due to the mirror image of antenna 1 the radiation of the horizontal polarization is cancelled along the ground plane as can be seen from the patterns. The maximum radiation is achieved for the horizontal polarization straight overhead due to the fact that antenna 1 is less than a quarter wavelength above ground and, therefore, the mirror image of antenna 1 is spaced apart less than half a wavelength.

A horizontally-oriented ideal dipole would not radiate vertically polarized components of the electrical fieldstrength. In our case, however, radiation of the vertical fieldstrength component E-theta is sizeable, as can be seen from the upper pattern. This radiation is generated from the currents along the poles and the feeder lines, mainly from poles 1 and 2 in this special case. As poles 1 and 2 are excited from the dipole 1 in counterphase the radiation of the vertically polarized electrical fieldstrength is almost zero for $\Phi=0^\circ$ and $\Phi=180^\circ$ and has maximum values for about $\Phi=90^\circ$ and $\Phi=270^\circ$.

The coupling of poles 1 and 2 to antenna 1 has an effect which can be seen from the current distribution and the Z-matrix. The poles act as capacitively coupled top capacities of antenna 1 and electrically lengthen antenna 1. In spite of the effect that the length of antenna 1 is exactly one half of the free space wavelength at 3 MHz the current distribution already "shrinks" around the feeder gap. This demonstrates an electrical length of greater than half a wavelength. In the Z-matrix the impedance Z_{11} represents the impedance of antenna 1. While an ideal half-wavelength dipole from theory shows an impedance of about $(70+j0)$ ohms in this case the real part (106 ohms) is slightly more and the imaginary part ($j133$ ohms) is considerably higher. The main reason for this is the coupling of the antenna to poles 1 and 2.

Figs. 10 through 13 show the remaining generic cases. They are not as obviously of interest practically. The behaviour shown in these figures, however, is always implicitly included in the behaviour of antenna 1 as soon as any load terminations other than open loop is given at antennas 2 through 5. Considering this point of view, Figs. 10 through 13 show some very interesting aspects. In Figs. 10 through 12, for instance, the left-side dipole half of the fed antenna has more current induced than the right-side dipole half. Additionally, the feeder line of the fed antenna has very high sheath currents. On the other hand, the sum of the left-side dipole current and the sheath current of the feeder line has to equal the current at the right-side dipole half because the total length of the feeder line plus the left-side dipole half is close to a quarter wavelength and generates a resonance. The feeding of the respective antenna excites a high current component which "by-passes" the feeder gap. The combined lengths of feeder line plus one dipole half are:

antenna 2: 33.05m or .3305 * wavelength
antenna 3: 26.95m or .2695 * wavelength

antenna 4: 23.40m or .2340 * wavelength

Due to these values the effect is most obvious in Figs. 11 and 12 where antennas 3 and 4 are assumed to be fed.

In the following figures some additional special cases of load impedances are analyzed. In all these cases antenna 1 is assumed to be fed as it will be in practice at this frequency. Fig. 14 shows the case where antennas 2 through 5 are short circuited. One might assume that the result should be quite different from the case of open-loop terminated antennas because the load conditions are most opposite. However, in both cases current distribution as well as radiation patterns are almost the same. This will be explained in more detail.

The currents at the feeder gaps of the different antennas can be calculated using the following matrix equation:

$$\begin{vmatrix} I_1 \\ I_2 \\ I_3 \\ I_4 \\ I_5 \end{vmatrix} = \begin{vmatrix} Z_{11} & Z_{12} & Z_{13} & Z_{14} & Z_{15} \\ Z_{21} & Z_{22} + Z_2 & Z_{23} & Z_{24} & Z_{25} \\ Z_{31} & Z_{32} & Z_{33} + Z_3 & Z_{34} & Z_{35} \\ Z_{41} & Z_{42} & Z_{43} & Z_{44} + Z_4 & Z_{45} \\ Z_{51} & Z_{52} & Z_{53} & Z_{54} & Z_{55} + Z_5 \end{vmatrix}^{-1} \begin{vmatrix} U_1 \\ 0 \\ 0 \\ 0 \\ 0 \end{vmatrix}$$

Equ. (2)

In this equation the elements Z_{mn} represent the Z-matrix of the antenna array and Z_2 through Z_5 represent the load impedances of antennas 2 through 5. The "-1" exponent indicates a matrix

I-Code 002 / 3 MHz
P-Code 002 / 3 MHz

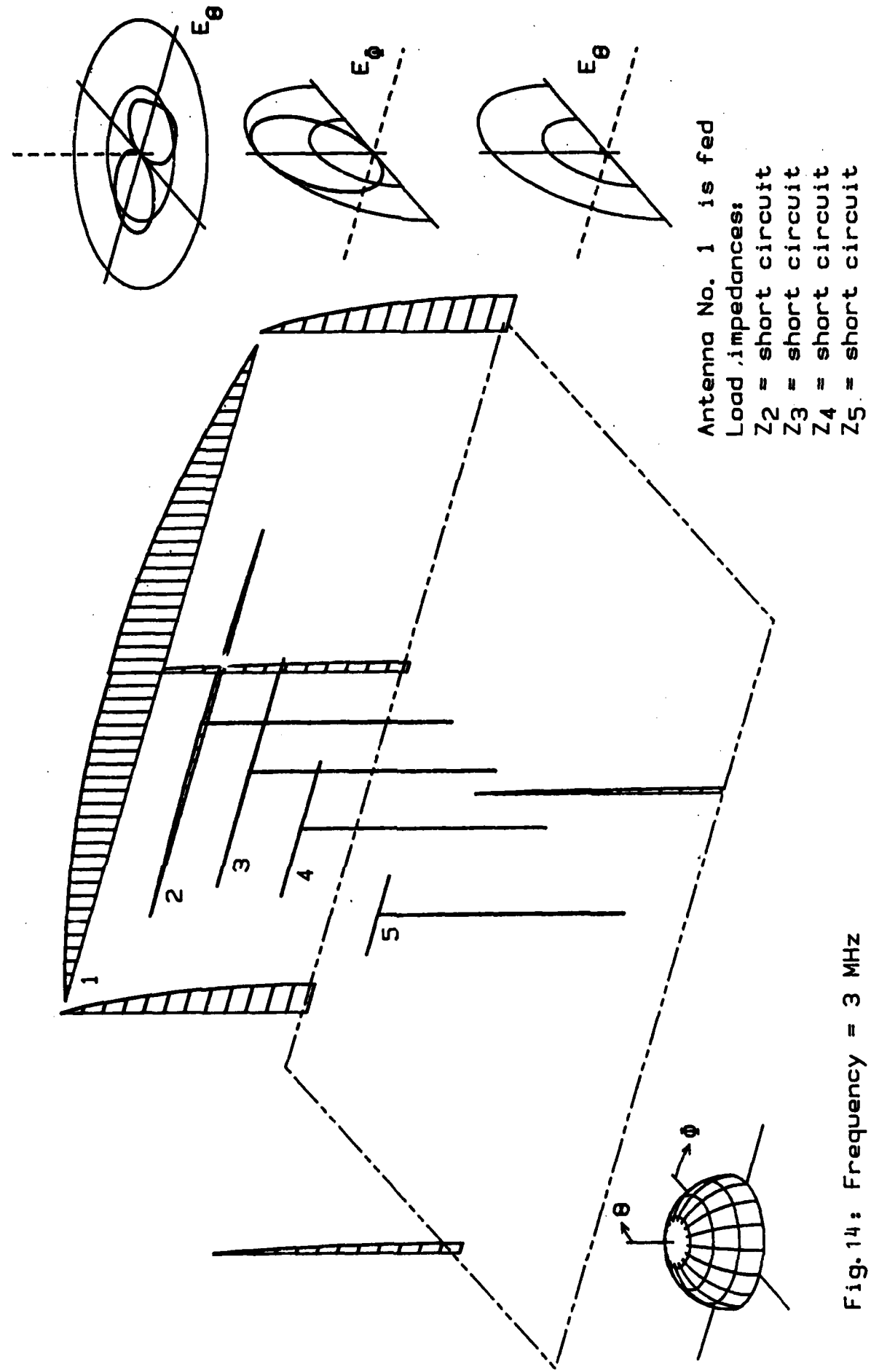
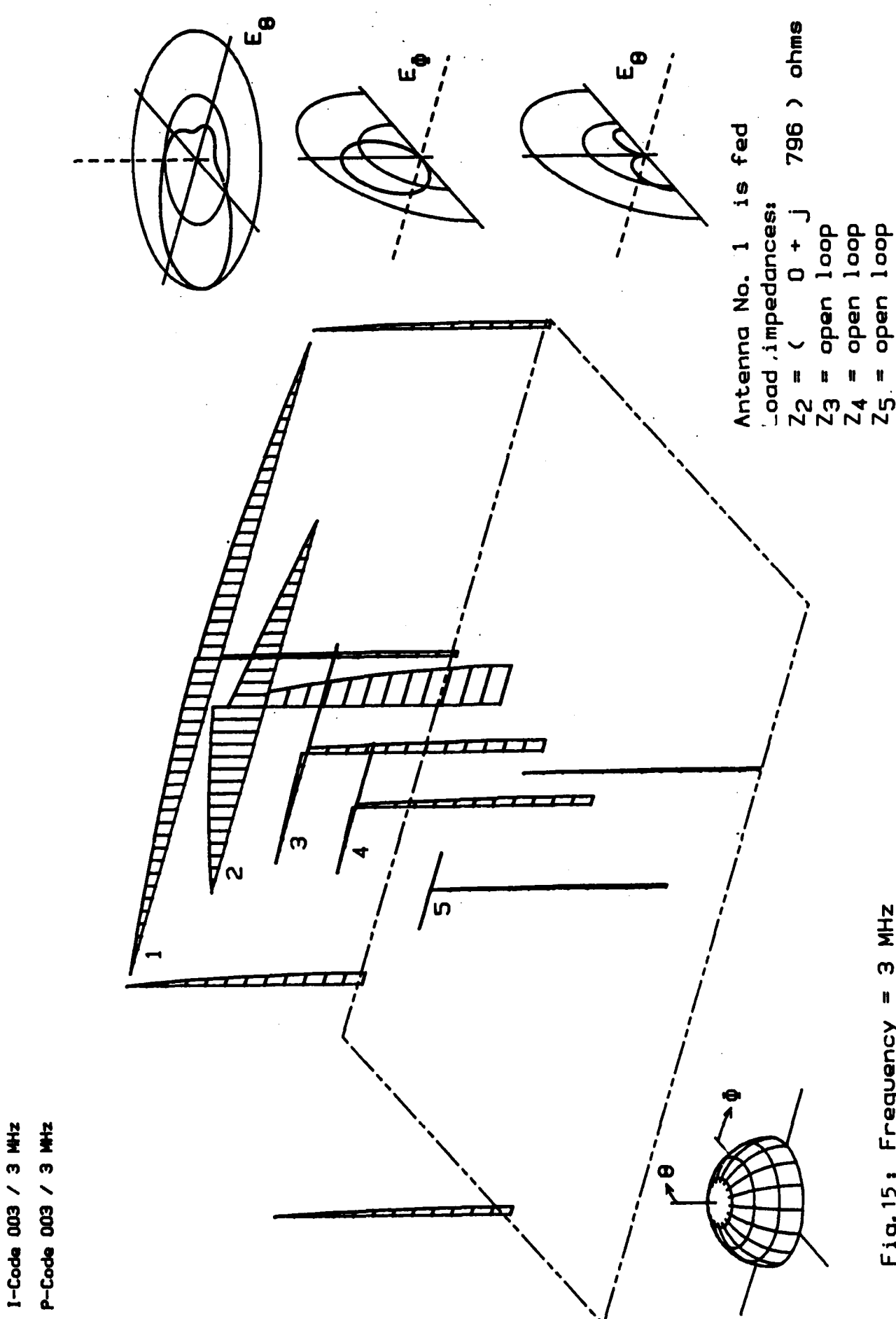


Fig. 14: Frequency = 3 MHz
Feeder type: Cobra head

inversion. U_1 is the feeding voltage of antenna 1.

As can be seen from the matrix equation the load impedances Z_2 through Z_5 influence the current distribution in conjunction with the internal impedance of the respective antenna. These internal impedances are grouped along the main diagonal of the Z-matrix in Table 1. For better recognition the internal impedances (Z_{11} , Z_{22} , Z_{33} , Z_{44} , and Z_{55}) are underlined. The internal impedances of the unfed antennas are in the order of magnitude of 1000 ohms and more. In this case the current in the unfed antennas is not very different between the cases where Z_2 through Z_5 are zero or infinite, respectively. The internal impedance alone is high enough to prevent sizeable currents within the parasitically coupled antenna.

This situation, however, changes dramatically if one or more load impedances are chosen to counteract the imaginary part of the internal impedance of the respective antennas. If, for instance, the load impedance of antenna 2 is chosen so that $Z_2 = (0+j796)$ ohms, then in the above matrix equation the respective element $Z_{22} + Z_2$ decreases to the value of the pure real part of the internal impedance Z_{22} which is as low as 41.38 ohms. (This condition is close to "complex conjugate" impedance termination. The only difference is that in our example the real part of the load impedance is set to zero.) In this case the induced current in antenna 2 increases dramatically. Fig. 15 shows the current distribution and the radiation pattern of this load condition. Antennas 3 through 5 are assumed to be open-loop terminated in this case. It can be seen that now the parasitically induced current in antenna 2 is higher than the feeder current of the fed antenna 1. The load impedance of antenna 2 generated a "resonance condition" at the feeder gap of antenna 2. Thus, antenna 2 acts as a weakly coupled resonator with the well-known current increase. This load termination will be referred to as "resonance termination" from here on.



To show the dependence of the current in antenna 2 close to the resonance condition two more cases have been analyzed with slightly varied load impedances. The following impedances have been chosen:

Fig. 16: $Z_{22} = (0 + j837)$ ohms, hence $Z_{22} + Z_2 = (41 + j41)$ ohms

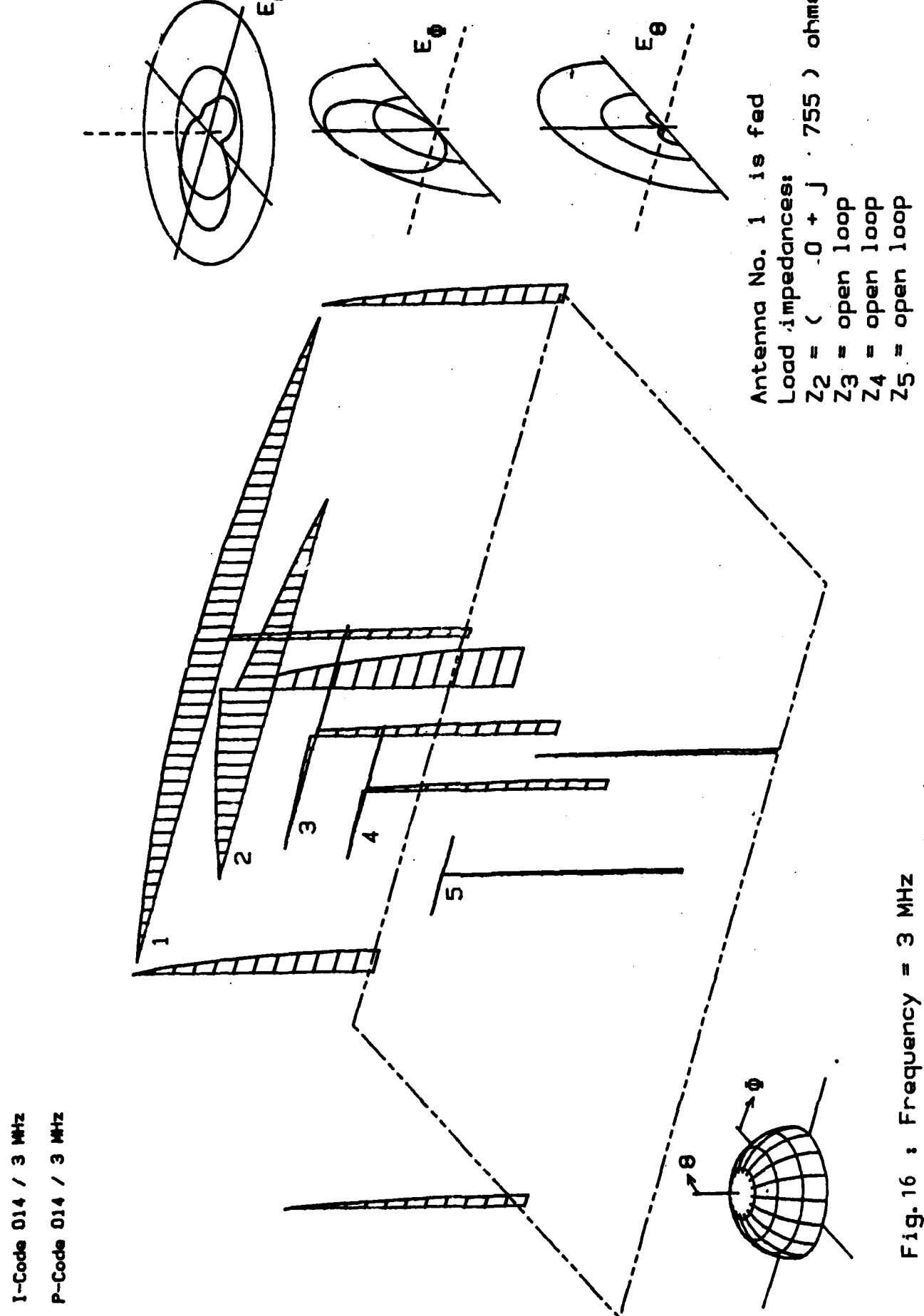
Fig. 17: $Z_{22} = (0 + j755)$ ohms, hence $Z_{22} + Z_2 = (41 - j41)$ ohms

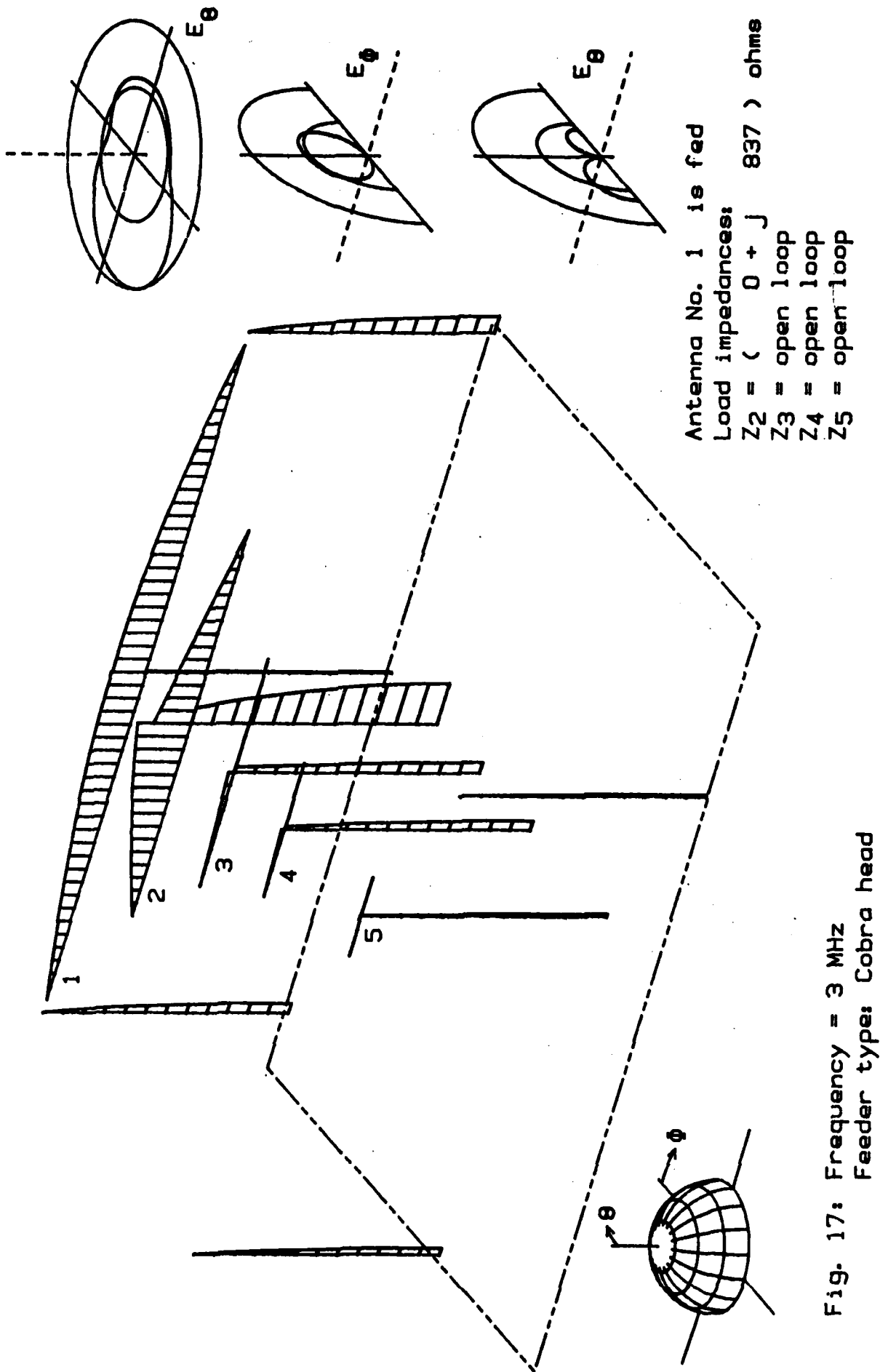
These are values comparable to the bandwidth condition of a resonance circuit. As can be seen from Figs. 16, 17, and 18 the current ratio between antenna 2 and antenna 1 really decreases about a factor of 0.707 from the resonance case.

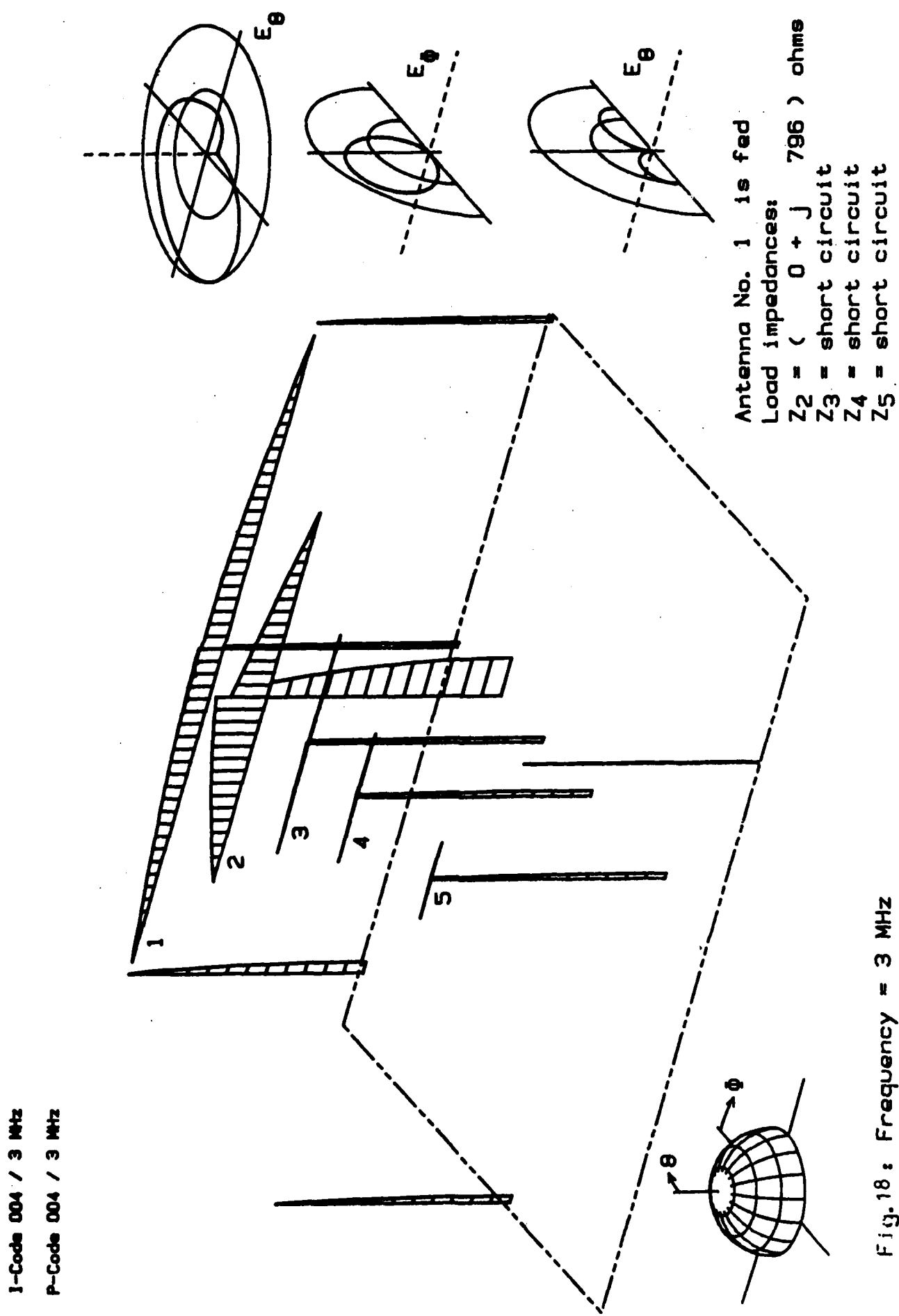
Note: The current distributions in the figures are normalized to the maximum current anywhere on the structure in order to avoid overlapping. In Figs. 15 through 17 the maximum current is observed in antenna 2. Therefore, a decrease of the current in antenna 2 can only be seen by noting the increase of the feeder current of antenna 1, as the maximum current (in antenna 2) is kept constant for drawing purposes.

Of course, an addition to the real part within the load impedance of antenna 2 could decrease the parasitic current in antenna 2. On the other hand, the radio transmitter or receiver which is connected to antenna 2 is supposedly for use in the 5 MHz region and has to be protected against power from the adjacent antennas. The respective filtering measures force a high reactive loading of antenna 2 in the frequency range of antenna 1, etc.

For completeness, Fig. 18 is a case where antenna 2 again is resonance terminated. The remaining antennas, however, are short circuited. As mentioned before, there are no major differences between the various cases of resonance termination of antenna 2 to the open-loop termination of the remaining antennas, since the internal impedances of these antennas are rather high. A







small, but physically interesting effect is the detuning of the "by-pass" resonances of the left-side halves of antennas 3 and 4 by short circuiting them to the respective right antenna halves.

The range of load impedances which produce disturbing currents can be estimated approximately. If, for instance, antenna m is fed and the critical load impedances of antenna n have to be determined one assumes all other antennas to be open-loop terminated. In this case the (feeder gap) currents I_n of the parasitically coupled antenna n and the feeder current I_m of the antenna m which is fed have a ratio

$$I_n/I_m = Z_{mn} / (Z_{nn} + Z_n) \quad (3)$$

In this expression Z_{mn} is the respective coupling impedance of the Z -matrix, Z_{nn} is the internal impedance of the parasitically coupled antenna, and Z_n is the load impedance of the parasitically coupled antenna.

If, for instance, the current of the parasitically coupled antenna is always less than 1/10 of the feeder current of the fed antenna, the equation

$$|Z_{nn} + Z_n| > 10 * |Z_{mn}| \quad (4)$$

has to be valid. If this equation is evaluated, it only shows possible solutions for the parasitically coupled antenna 2 if antenna 1 is fed. For all other antennas the parasitically coupled (feeder) current never reaches 1/10 of the feeder current of antenna 1. In Fig. 19 the result of equation 4 is evaluated concerning the earlier mentioned fact that the load terminations can only be highly reactive impedances. These load impedances are located along the imaginary axis in the Smith chart of Fig. 19. From Fig. 19 the probability can be estimated for which the load impedance of antenna 2 will be situated within the dangerous range. As this impedance will be generated

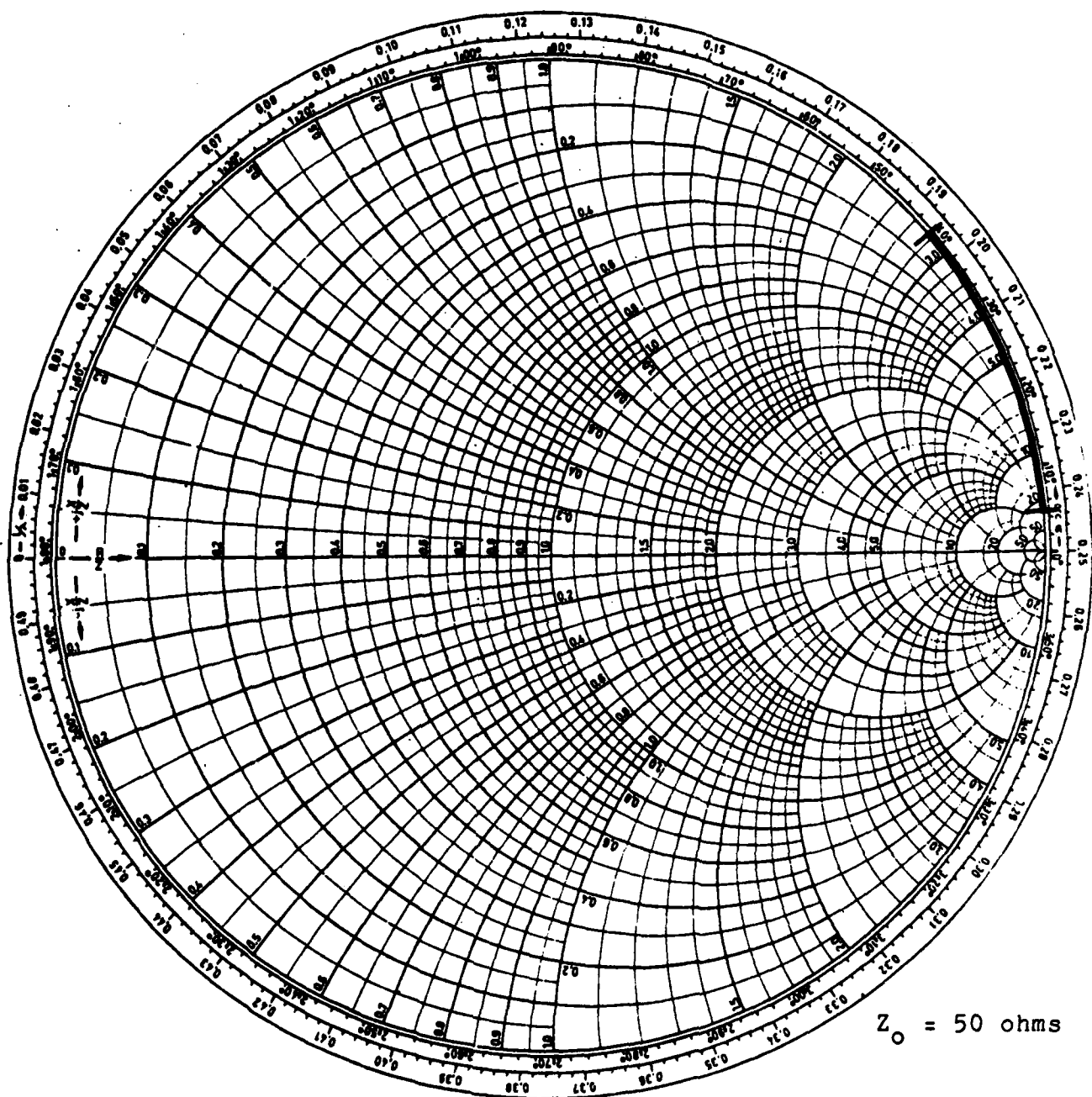


Fig. 19: Range of load impedances Z_2 of antenna 2 which can cause parasitic currents at the feeder gap of antenna 2 with a magnitude greater than $1/10$ of the feeder current of antenna 1.
(Antenna 1 is fed, $f = 3\text{MHz}$, Feeder type: cobra head)

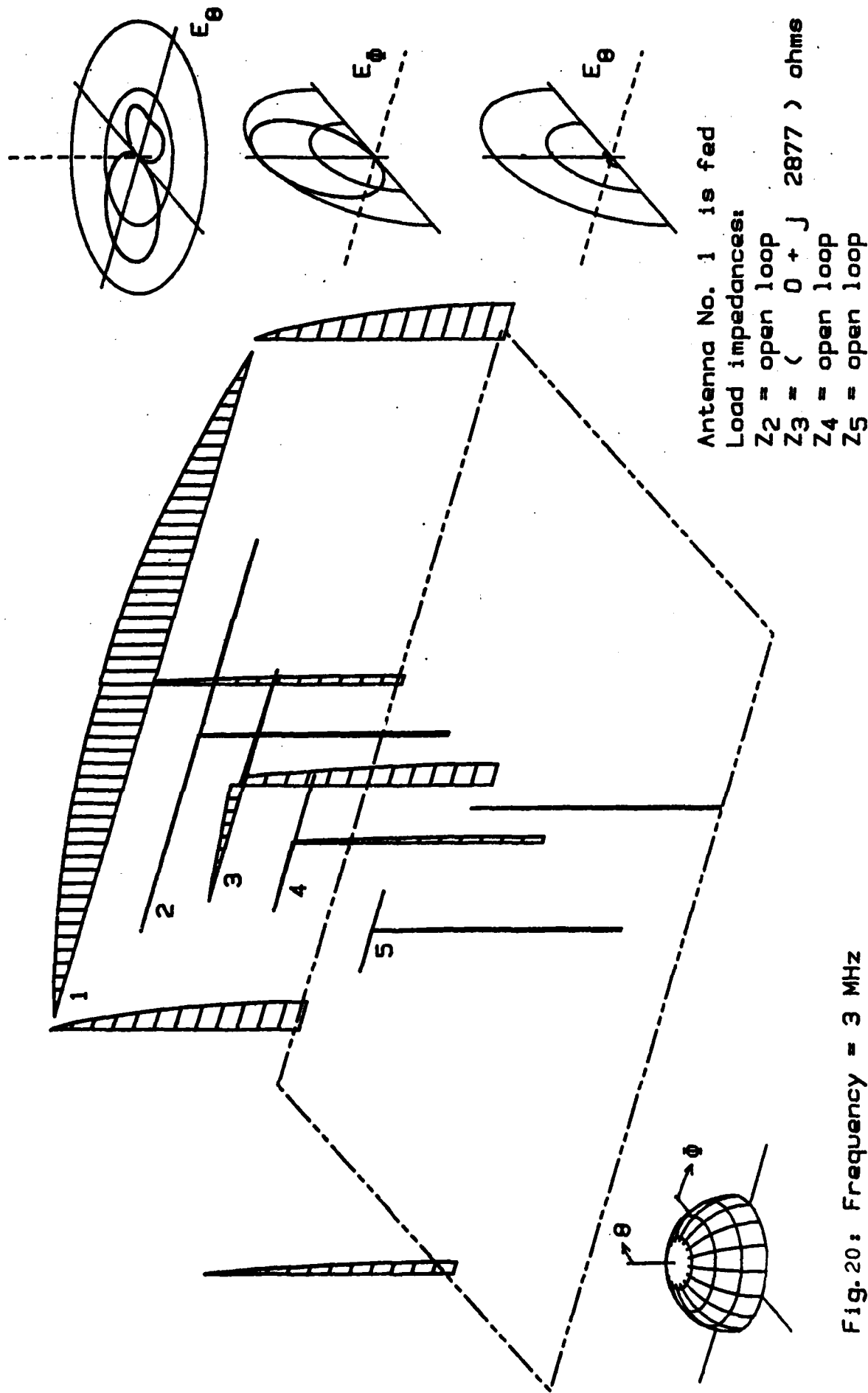
as a random reflection factor of the connected feeder line, the range has a probability which is directly proportional to the range of the angle of the reflection factor which it covers. It can be seen from Fig. 19 that this range is about 5° through 44° , leading to a probability of $39/360 = .11$ or 11%. In other words: In about 11% of all possible cases antenna 2 will have a parasitic current induced of more than 1/10 of the feeder current of antenna 1.

Note: Equation 3 only considers the currents in the feeder gaps of the parasitically coupled antennas. As seen in later examples, the "by-pass" currents due to structure resonances can reach very high values without being included in the Z-matrix! An example is shown in Fig. 23. In spite of the fact that equation 3 had no solution for the parasitically coupled antenna 3 this antenna structure has a current induced which is certainly higher than 1/10 of the feeder current of the fed antenna 1. A closer look shows that the high current is a "by-pass" current along the left-side half of the dipole and the feeder line. It cannot be included within the values of the Z-matrix. This is an example of the complexity of the problem. Definitely, each interesting assembly has to be recalculated. On the other hand, as mentioned before, a careful study of the five generic cases and the Z-matrix gives several hints on possible occurrences of negative influence.

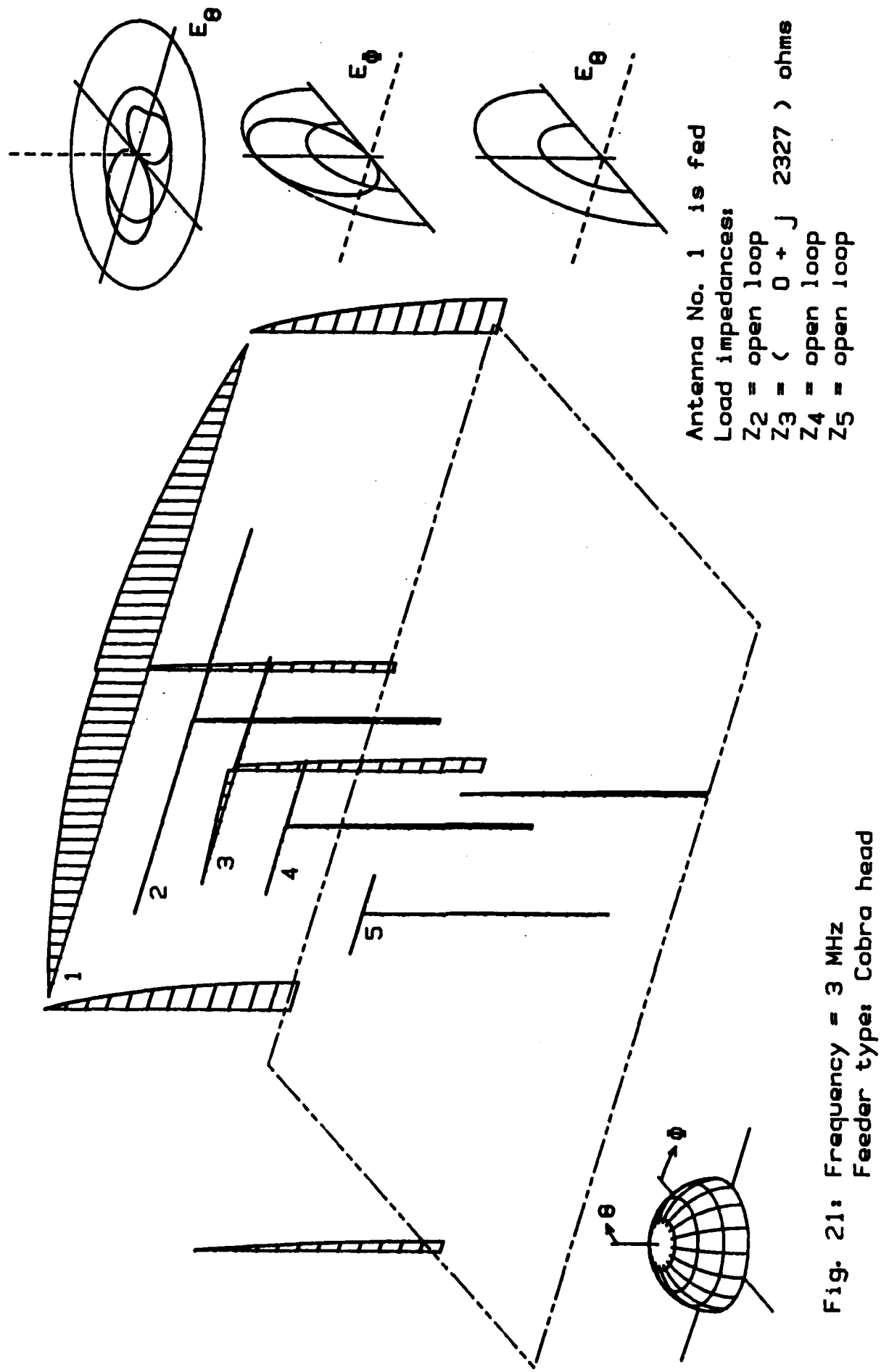
Fig. 20 shows a case where antenna 3 is resonance terminated. As expected from the low value of $|Z_{13}| = 40.3$ ohms compared to the high real part $\text{Re}(Z_{33}) = 550$ ohms of the element Z_{33} in the Z-matrix, the parasitic current in antenna 3 is rather low. However, in this case the "by-pass" current is also much higher than the current through the feeder gap of antenna 3.

Figs. 21 and 22 show cases where the resonance termination is "detuned" as far as getting an imaginary part equal to the real part in the determining expression $(Z_{33} + Z_3)$. Both figures

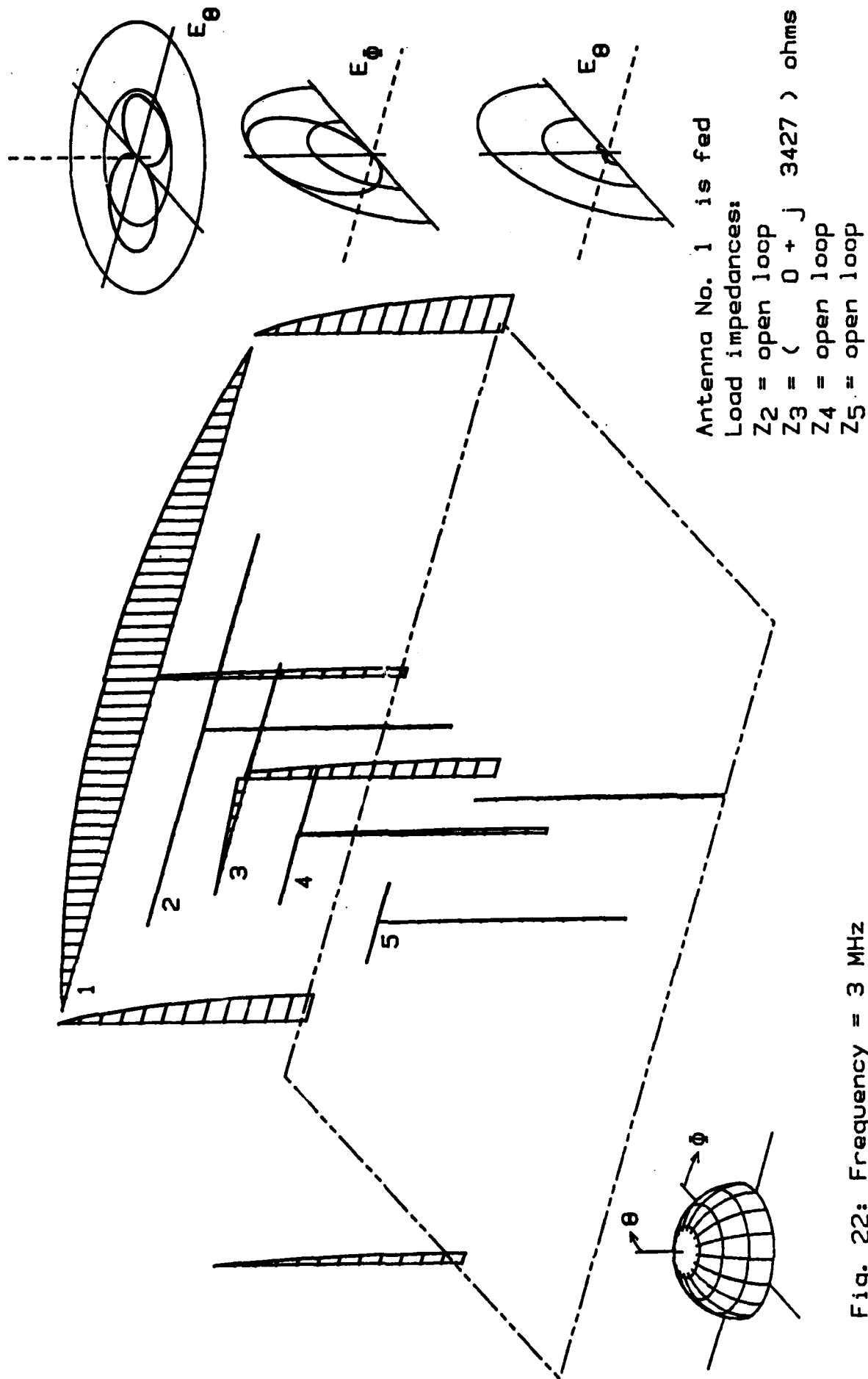
I-Code 008 / 3 MHz
P-Code 008 / 3 MHz



I-Code 016 / 3 MHz
P-Code 016 / 3 MHz



I-Code 017 / 3 MHz
P-Code 017 / 3 MHz



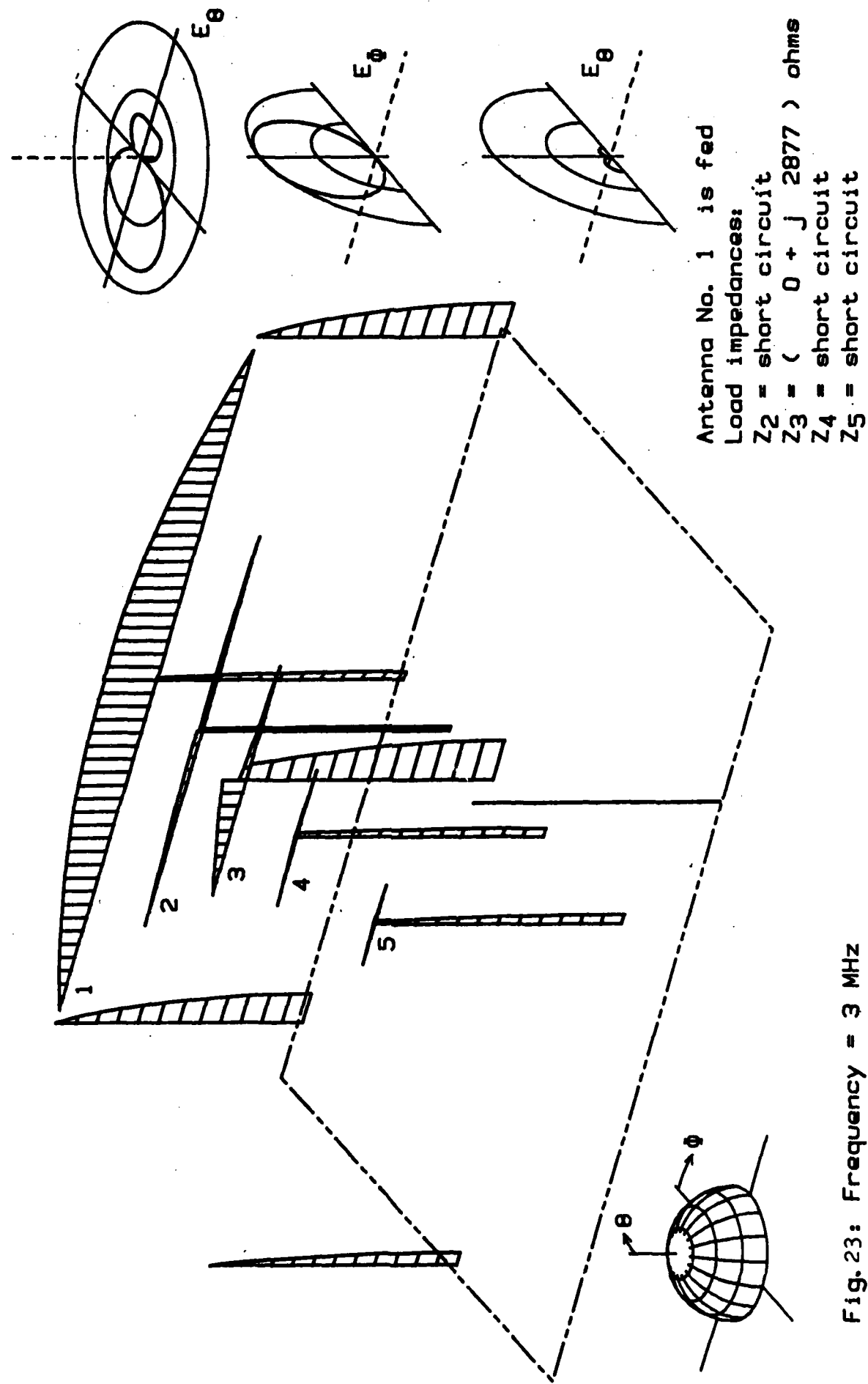
again show the decrease of the current by the approximate factor 0.707.

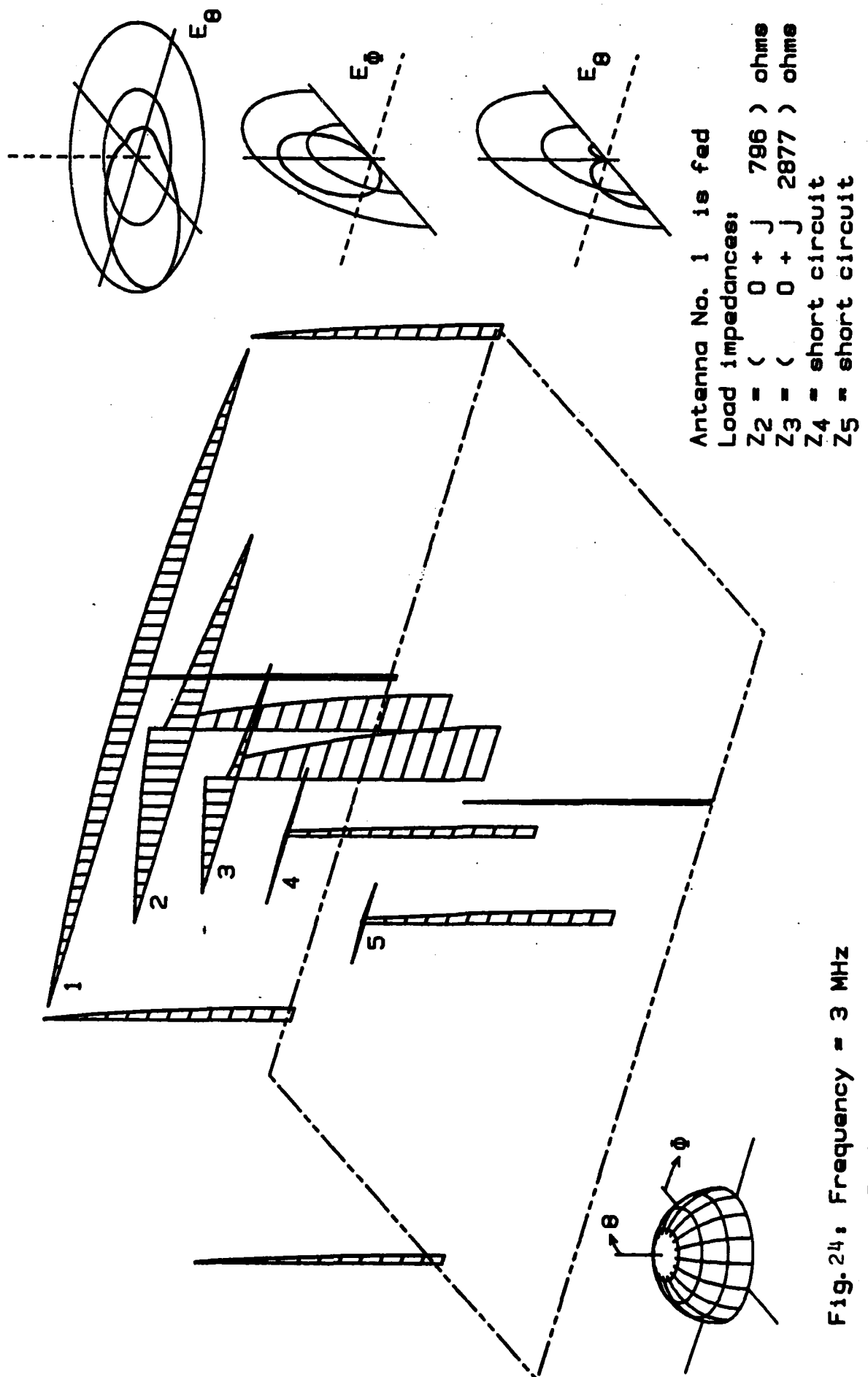
Fig. 23 again shows a resonance termination of antenna 3. In this case, however, antennas 2, 4, and 5 are short circuited. Due to multiple couplings the antenna current of antenna 3 is obviously increased over Fig. 20. The high current is a "by-pass" current due to the resonance of the left-side structure and the feeder line of antenna 3. As mentioned before, the "antenna current" which is flowing through the feeder gap towards the right-side dipole half is still less than 1/10 of the current through antenna 1.

Some more critical cases have been selected for Figs. 24 through 27. In Fig. 24 both antennas 2 and 3 have been resonance terminated. The result is rather negative concerning current distribution and radiation pattern. If the probability is estimated under which antenna 3 will be in a certain range of resonance termination, however, the combined probability of the occurrence of Fig. 24 is less than 1%. Figs. 25 and 26 show cases where antenna 4 and 5, respectively, are resonance terminated. Due to the values of Z_{14} , Z_{15} , Z_{44} , and Z_{55} the induced currents within antennas 4 and 5 in these cases are very low.

Fig. 27 finally shows resonance terminations of all unfed antennas. The result concerning the current distribution is rather dramatic. All antennas (including the feeder lines) show higher currents than the fed antenna. The only exception is antenna 3 with complex multiple mutual excitations that obviously cancel the exciting field for antenna 3. The probability of having this case in practice, however, is less than 0.01% if the load impedances of antennas 2 through 4 are randomly distributed.

I-Code 005 / 3 MHz
P-Code 005 / 3 MHz





I-Code 012 / 3 MHz
P-Code 012 / 3 MHz

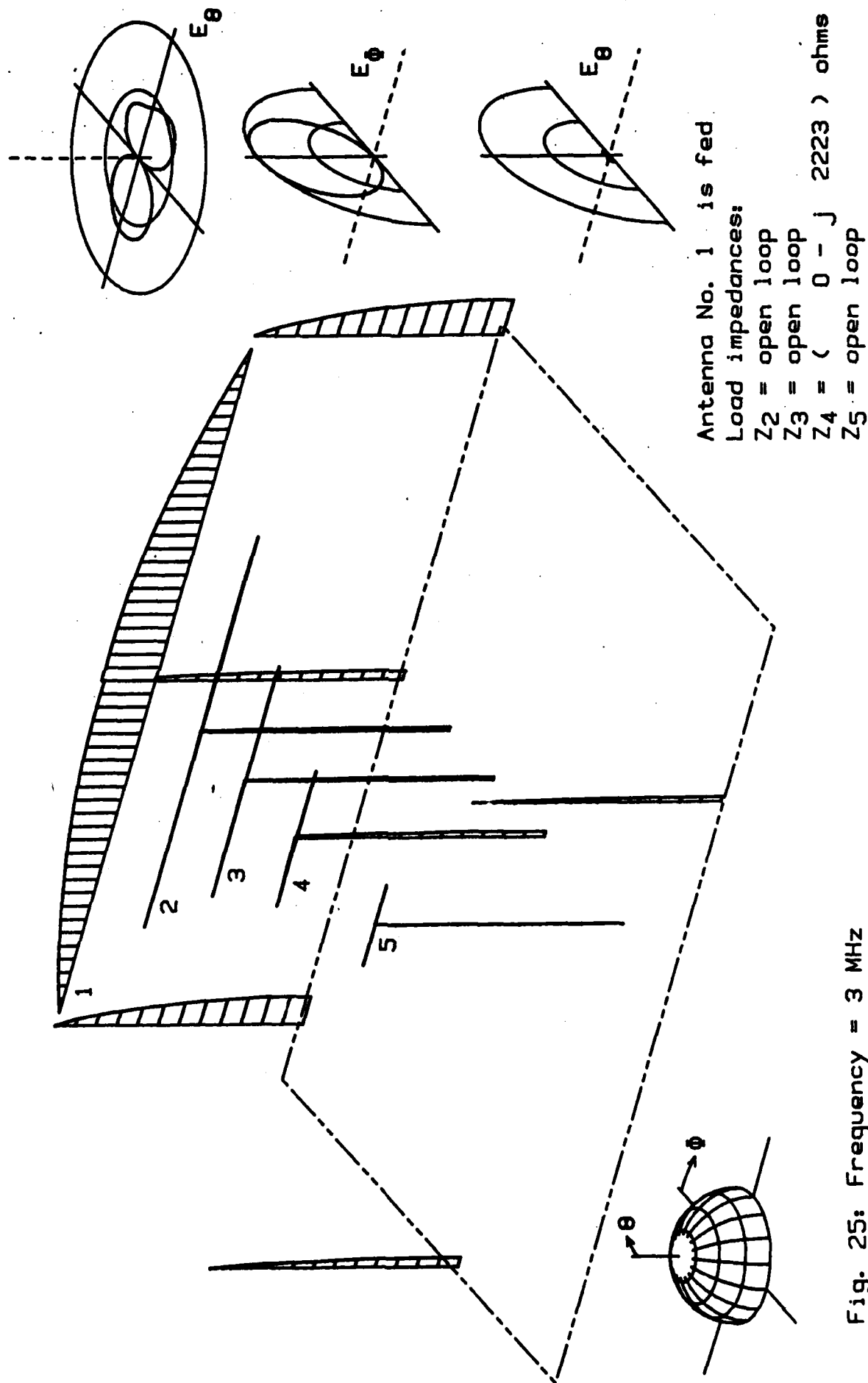


Fig. 25: Frequency = 3 MHz
CFFNER TYPE: COBRA HEAD

I-Code 013 / 3 MHz
P-Code 013 / 3 MHz

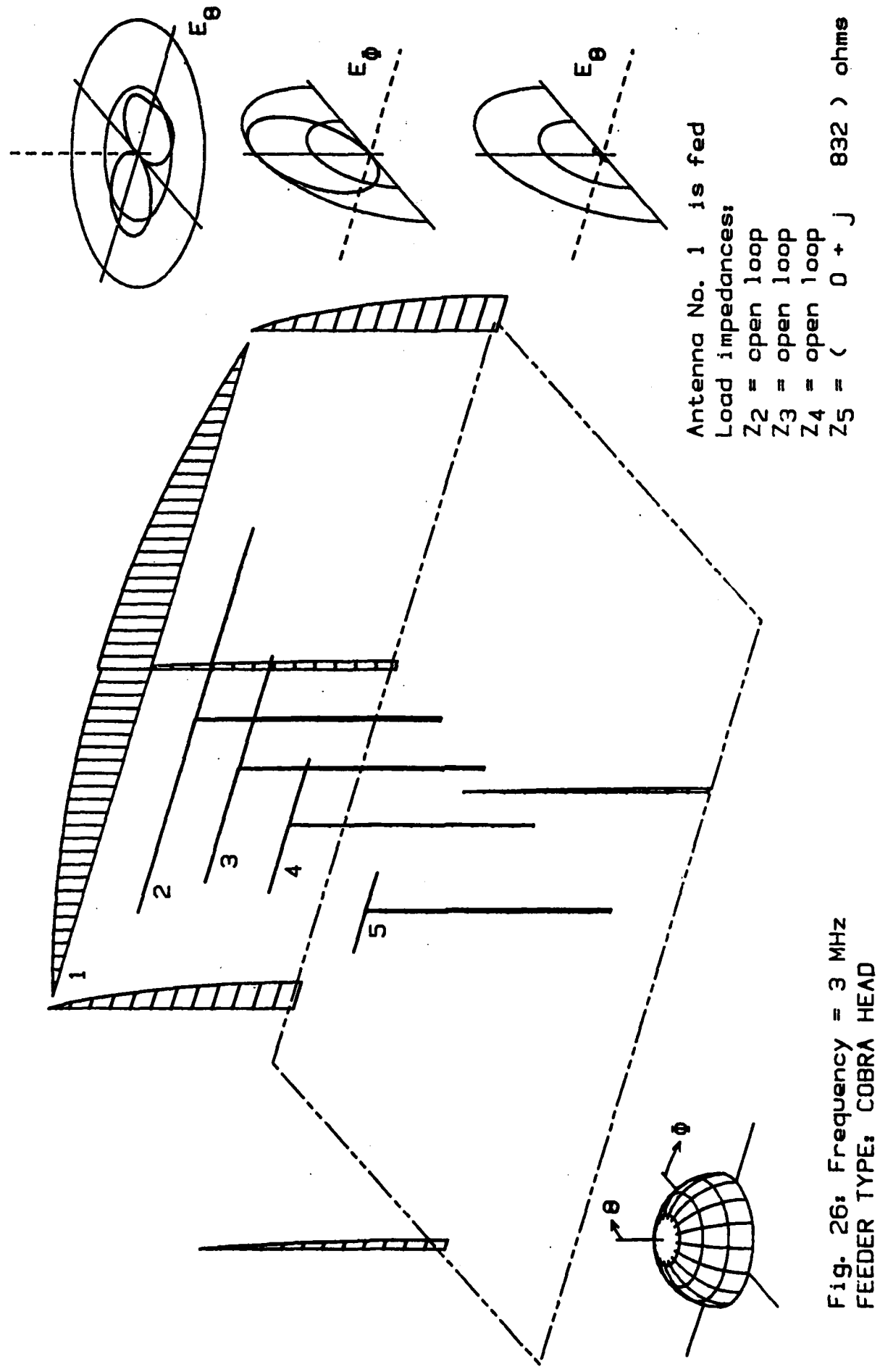
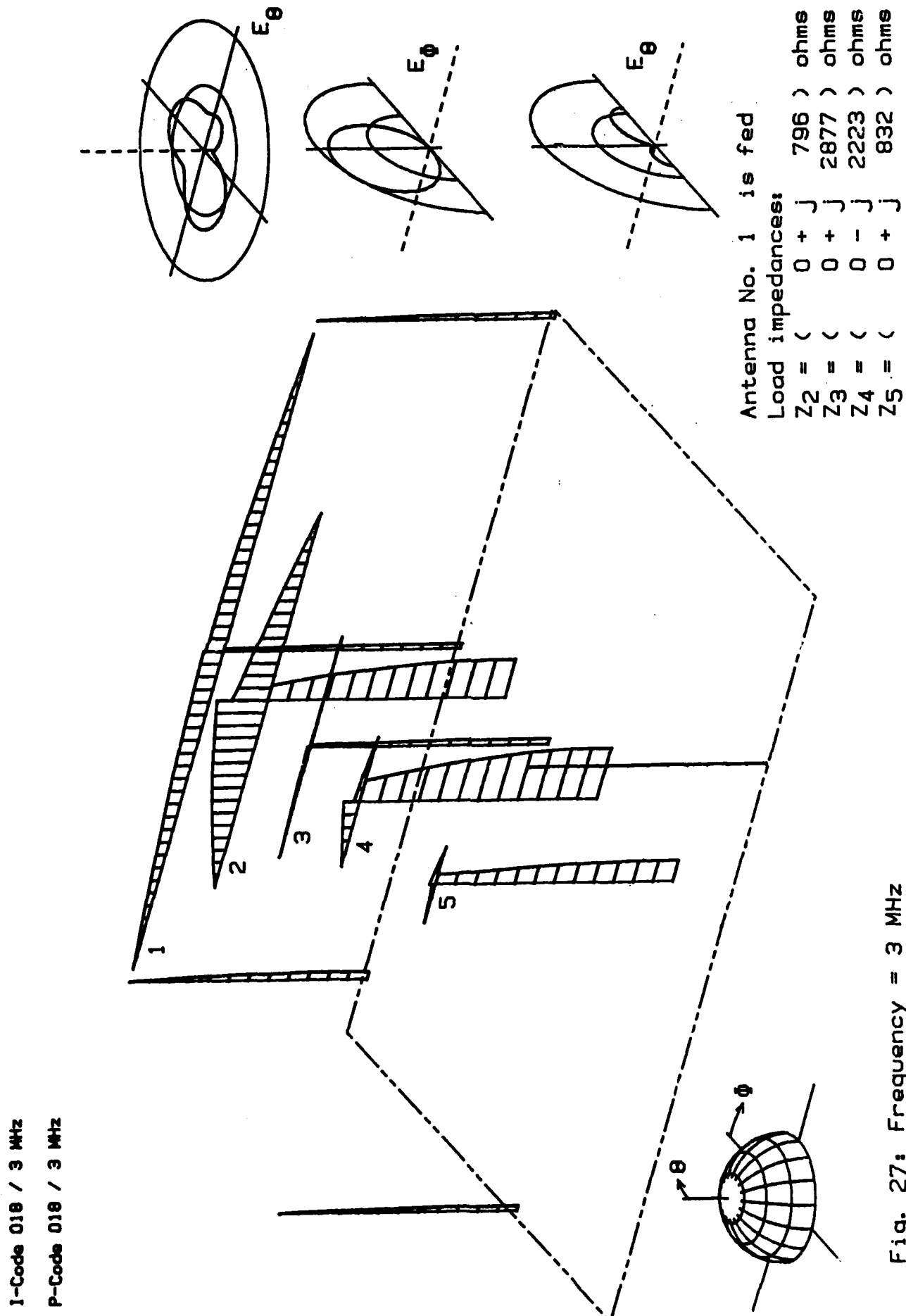


Fig. 26: Frequency = 3 MHz
FEEDER TYPE: COBRA HEAD



7. Analysis at 5.1MHz. Feeder type: Cobra head.

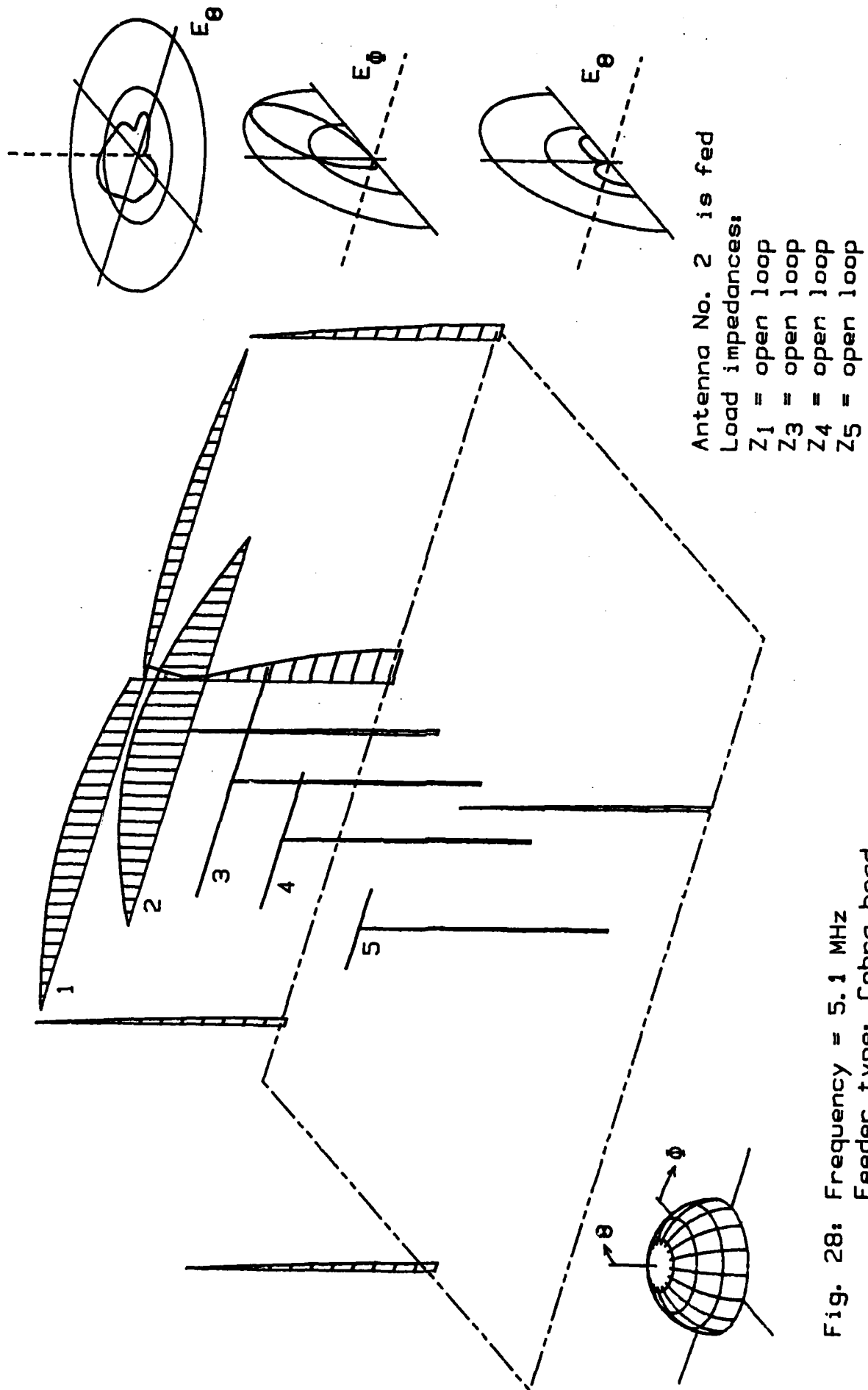
In Table 2 the Z-matrix for 5.1MHz and cobra-head feeding is presented. Figs. 28 through 32 show the generic cases. As the center frequency of antenna 2 is 5.1MHz only this antenna is intended for actual use at this frequency. Thus, Fig. 28 which deals with antenna 2 being fed is of special interest.

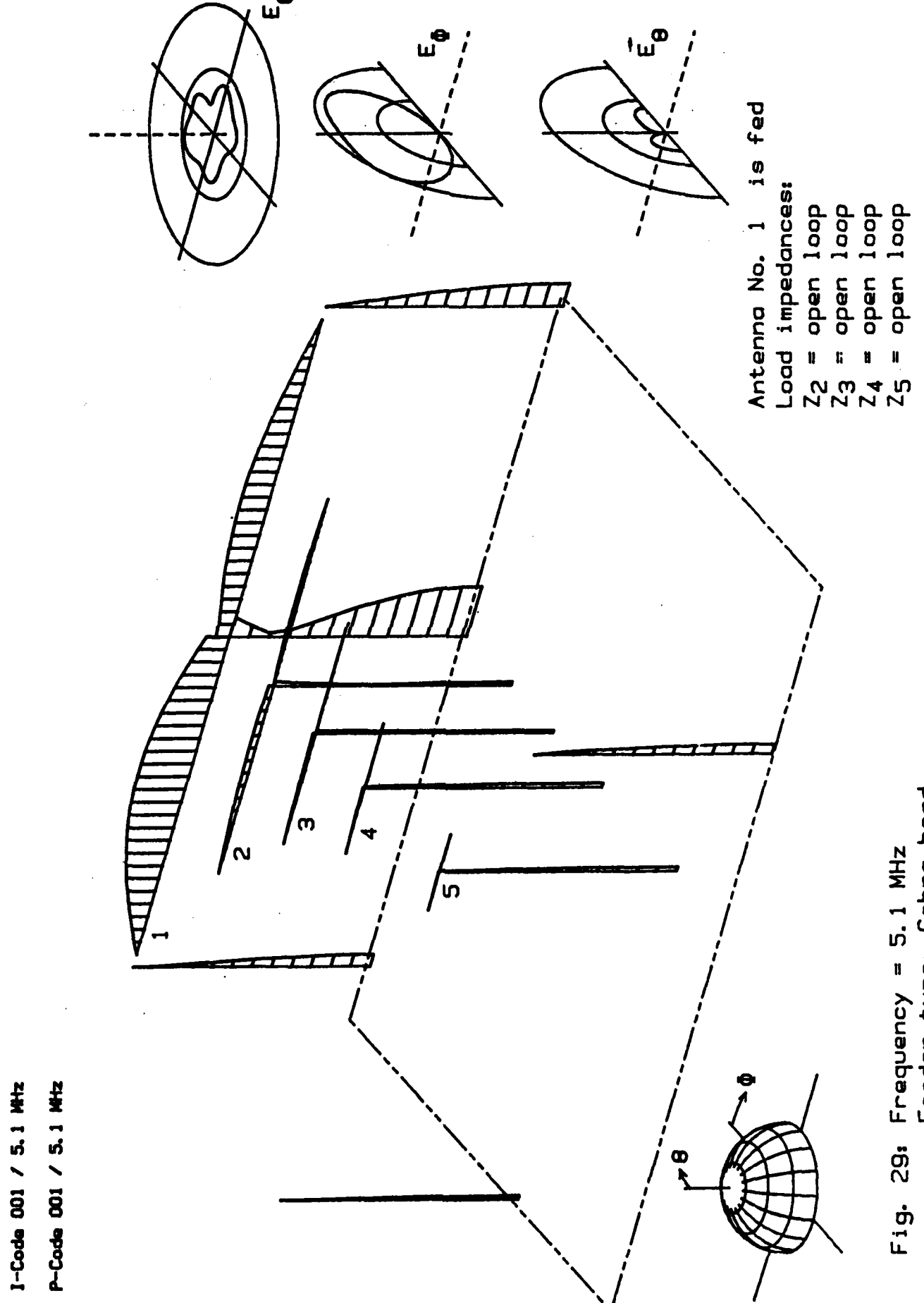
In Fig. 28 the remaining antennas are open loop terminated. As can be seen from the current distribution, the length of antenna 2 must be close to one half of the free-space wavelength. A very interesting effect is the high magnitude of the currents in the left-side dipole half and along the feeder line of antenna 1, due to a resonance in the structure of antenna 1. As can be seen from Figs. 2 and 3 the combined length of the left-side half of dipole 1 plus the feeder line is 43.3 m. This is .74 times the free-space wavelength of 58.8 m at 5.1MHz; therefore, the left antenna side of antenna 1 shows a three-quarter wavelength resonance at this operating frequency. This is another example of "by-pass" currents, this time to be expected at antenna 1.

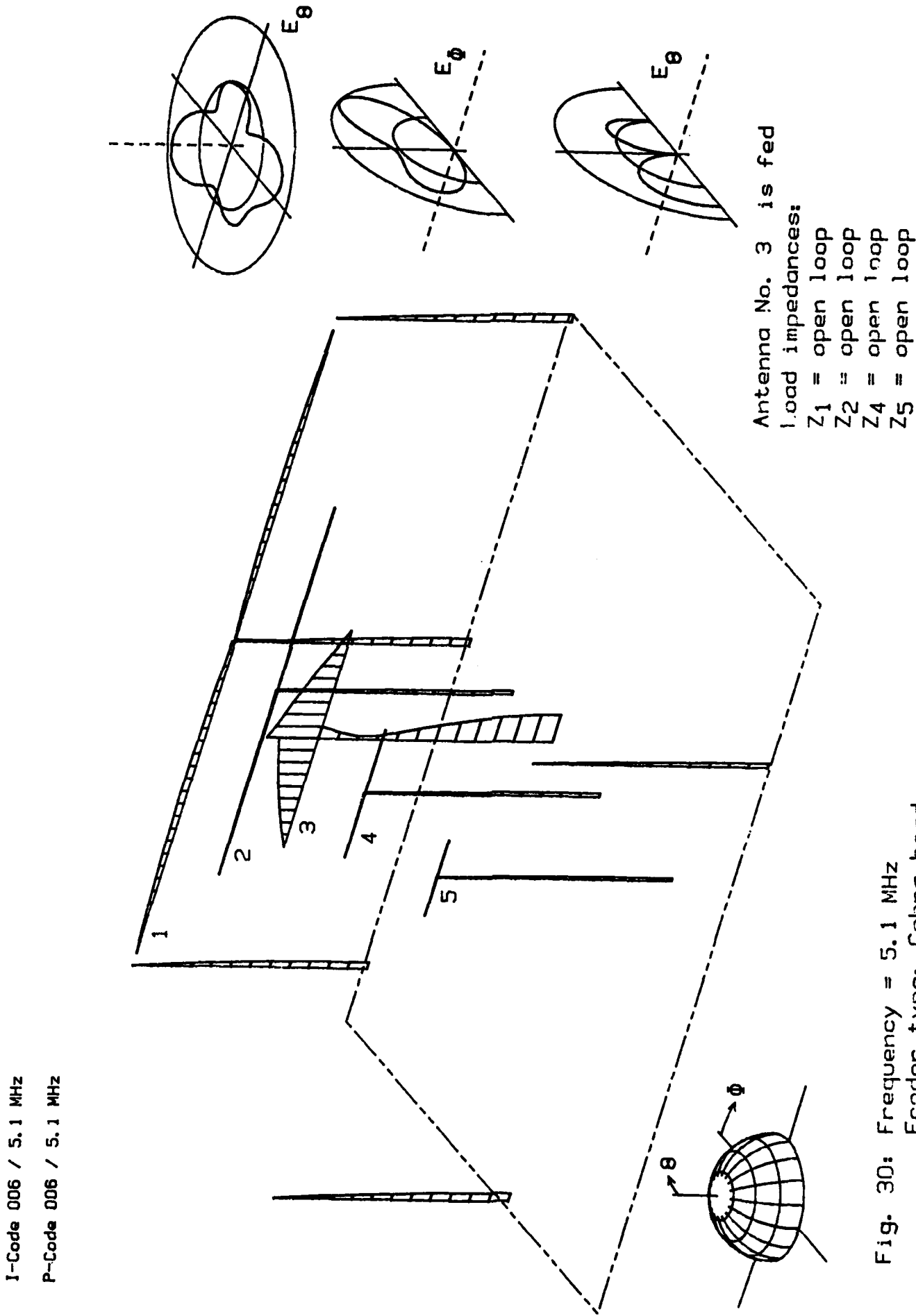
As the antenna height is now greater than 1/4 wavelength, the maximum radiation is no longer straight up. Instead, the radiation is maximum at some angle of elevation. The horizontally polarized radiation is, however, not symmetrical in the direction $\Theta = 0^\circ$ as can be seen from the patterns in Fig. 28 because of the high magnitude of the currents in antenna 1. Antenna 1 also produces a sizeable vertically polarized radiation due to the high magnitude of the parasitic current along the feeder line of antenna 1 and the currents induced from antenna 1 in poles 1 and 2. In contrast to the radiation of the poles at 3 MHz, the feeder line of antenna 2 now has a serious influence. This leads to the absolutely unsymmetrical radiation of E- Θ in the top radiation pattern of Fig. 28.

Table 2: I-Matrix for $f = 5.1$ MHz. Feeder type: Cobra head.

$I_{11} = (2758.82 + j 267)$ ohms	$I_{12} = (242.85 - j 383)$ ohms	$I_{13} = (38.60 - j 114)$ ohms	$I_{14} = (39.79 - j 13)$ ohms	$I_{15} = (56.71 - j 8)$ ohms
$I_{21} = (242.86 - j 383)$ ohms	$I_{22} = \underline{(50.01 + j 6)}$ ohms	$I_{23} = (24.32 - j 3)$ ohms	$I_{24} = (14.94 - j 7)$ ohms	$I_{25} = (4.04 - j 10)$ ohms
$I_{31} = (39.07 - j 113)$ ohms	$I_{32} = (24.35 - j 3)$ ohms	$I_{33} = \underline{(23.06 - j 553)}$ ohms	$I_{34} = (21.95 - j 6)$ ohms	$I_{35} = (12.00 - j 12)$ ohms
$I_{41} = (40.49 - j 13)$ ohms	$I_{42} = (14.97 - j 7)$ ohms	$I_{43} = (21.92 - j 6)$ ohms	$I_{44} = \underline{(30.46 - j 1043)}$ ohms	$I_{45} = (27.33 - j 4)$ ohms
$I_{51} = (57.24 - j 8)$ ohms	$I_{52} = (4.04 - j 11)$ ohms	$I_{53} = (11.95 - j 12)$ ohms	$I_{54} = (27.28 - j 4)$ ohms	$I_{55} = (39.75 - j 1619)$ ohms







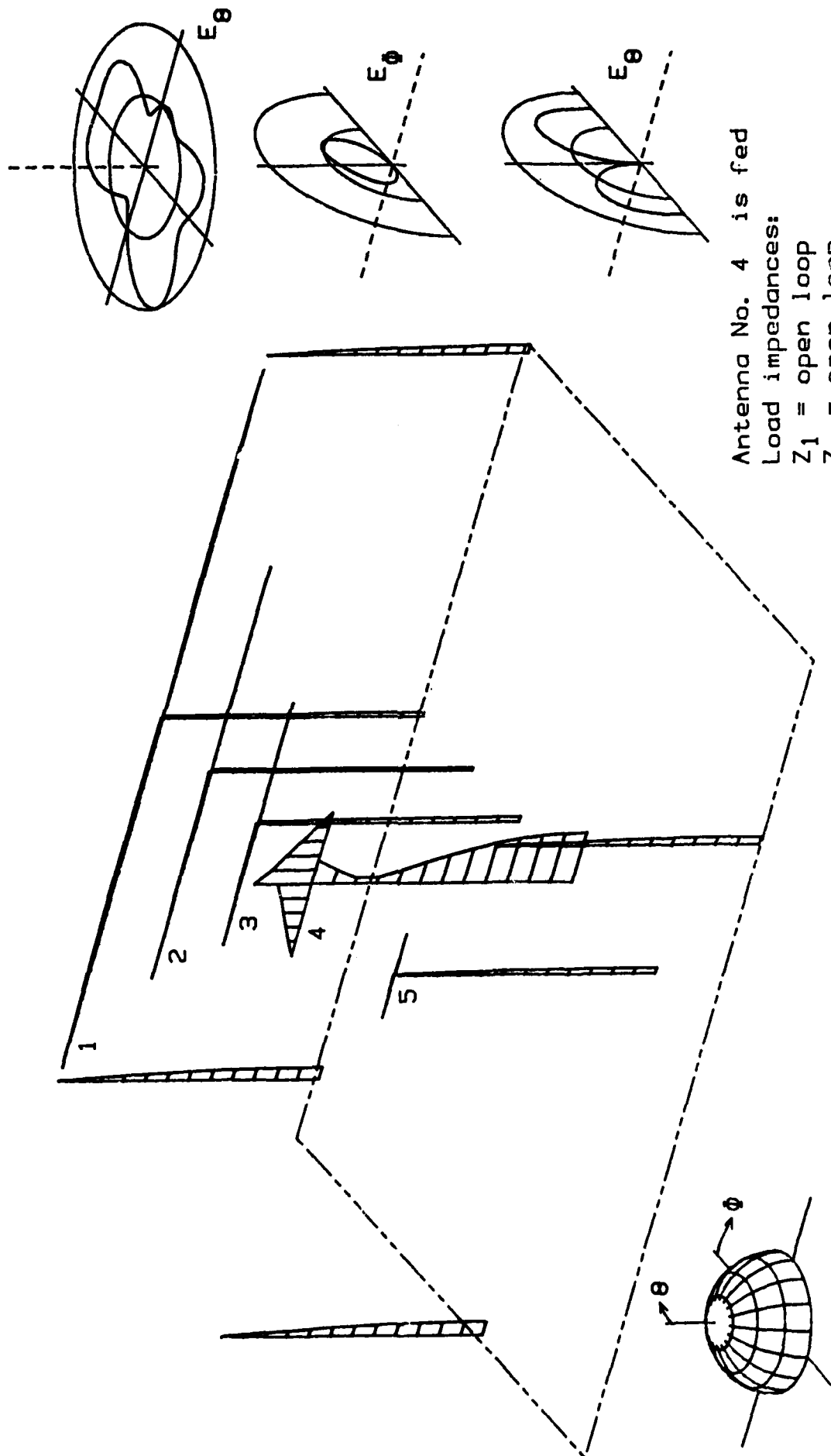


Fig. 31: Frequency = 5.1 MHz
Fodder type: Cobra head

I-Code 007 / 5.1 MHz

P-Code 007 / 5.1 MHz

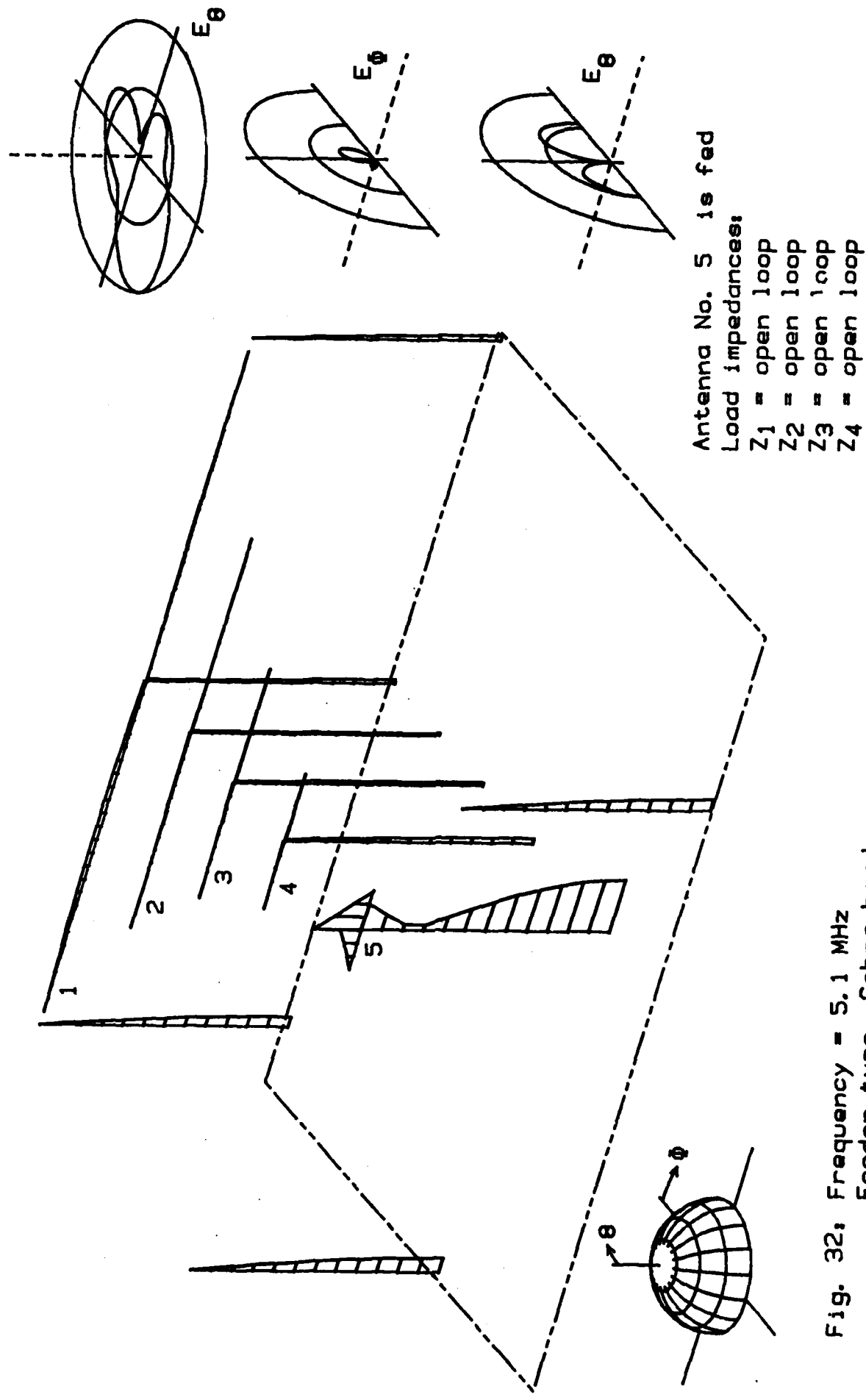


Fig. 33 is a case where antenna 2 is fed again but the remaining antennas are short circuited. Now the parasitic current in antenna 1 is very much less due to the fact that the resonance of the left-side dipole half and the feeder line has been disturbed by connecting the right-side dipole half to this structure. This is another effect which cannot be seen from the Z-matrix alone.

Figs. 34 and 35 are cases where antenna 3 is resonance terminated while antenna 1 is short circuited or open-loop terminated, respectively. In Figs. 36 and 37 the resonance termination of antenna 3 is detuned by varying the real and imaginary part of $(Z_{33} + Z_3)$ to be equal. Both figures should be compared to Fig. 34 and show the 0.707 decrease in the current ratio of I_3/I_2 . This is a relative increase of the same 0.707 of the currents in antenna 2 in these cases.

Some other cases of critical load terminations are shown in Figs. 38 through 42, partly a comparison between antenna 1 being open-loop terminated and short circuited. The joint occurrences of more than one critical parameters only appear with the combined probability. The conditions of Fig. 42, for instance, appear with the combined probability of less than 0.01%.

I-Code 004 / 5.1 MHz
P-Code 004 / 5.1 MHz

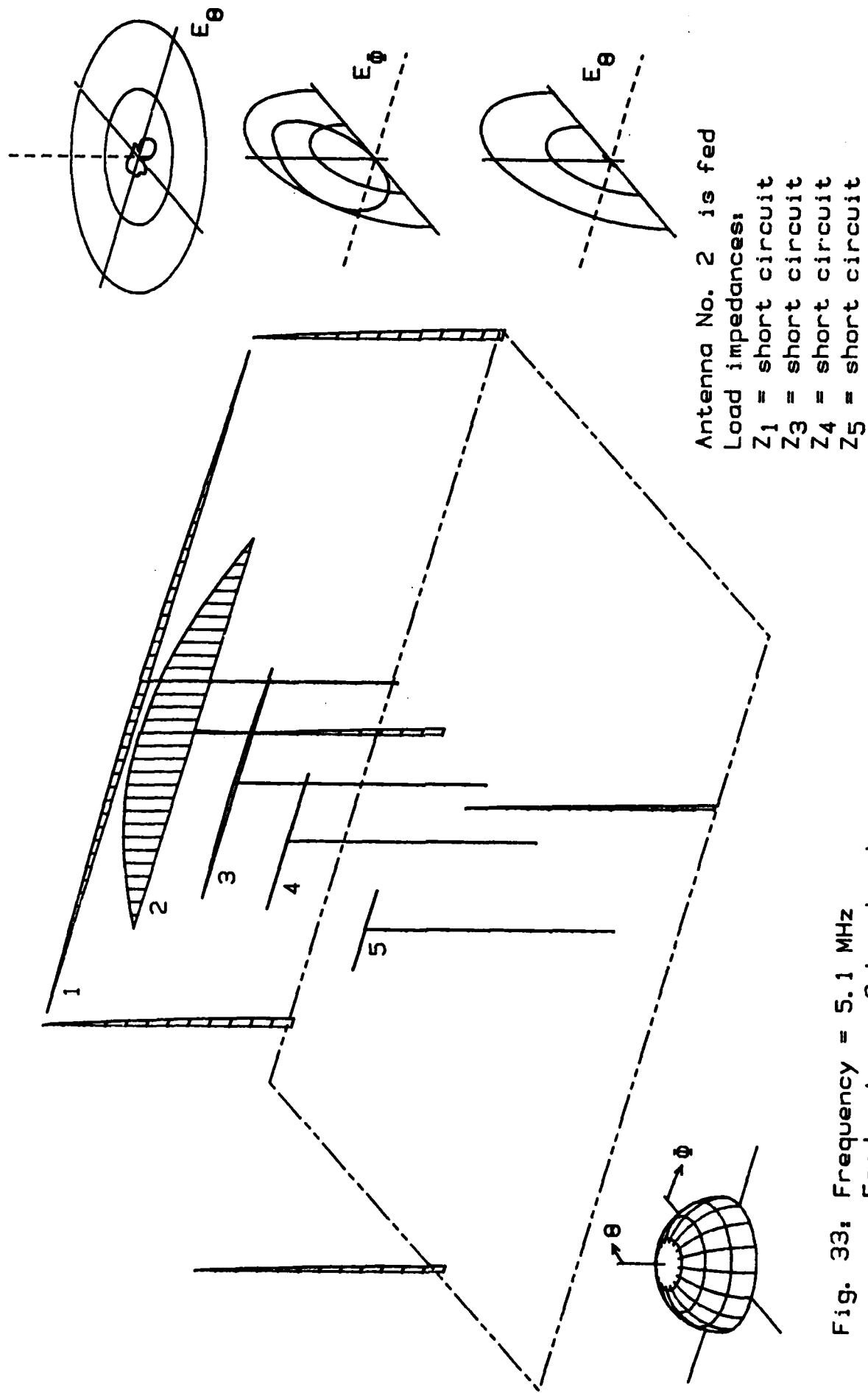
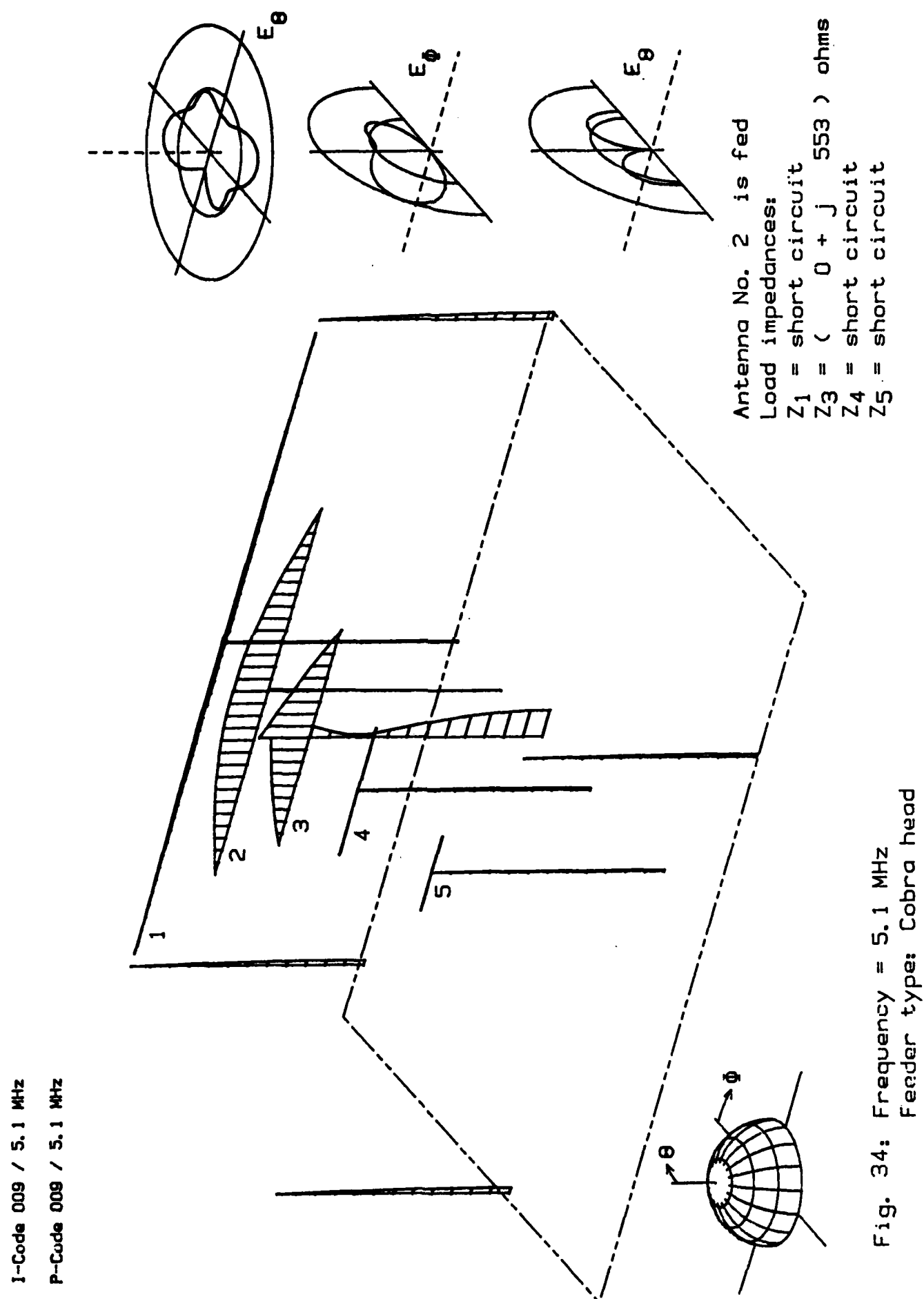
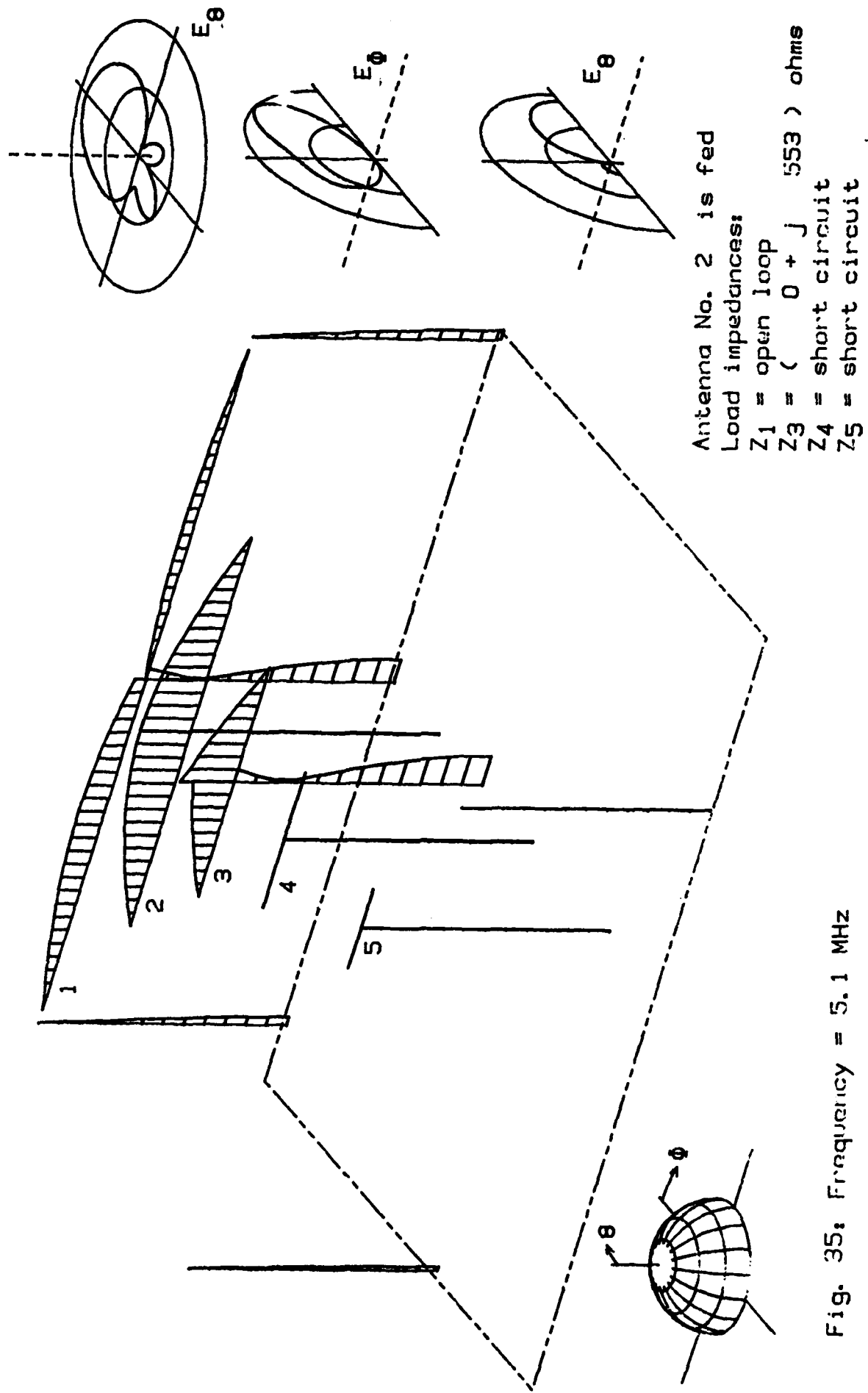


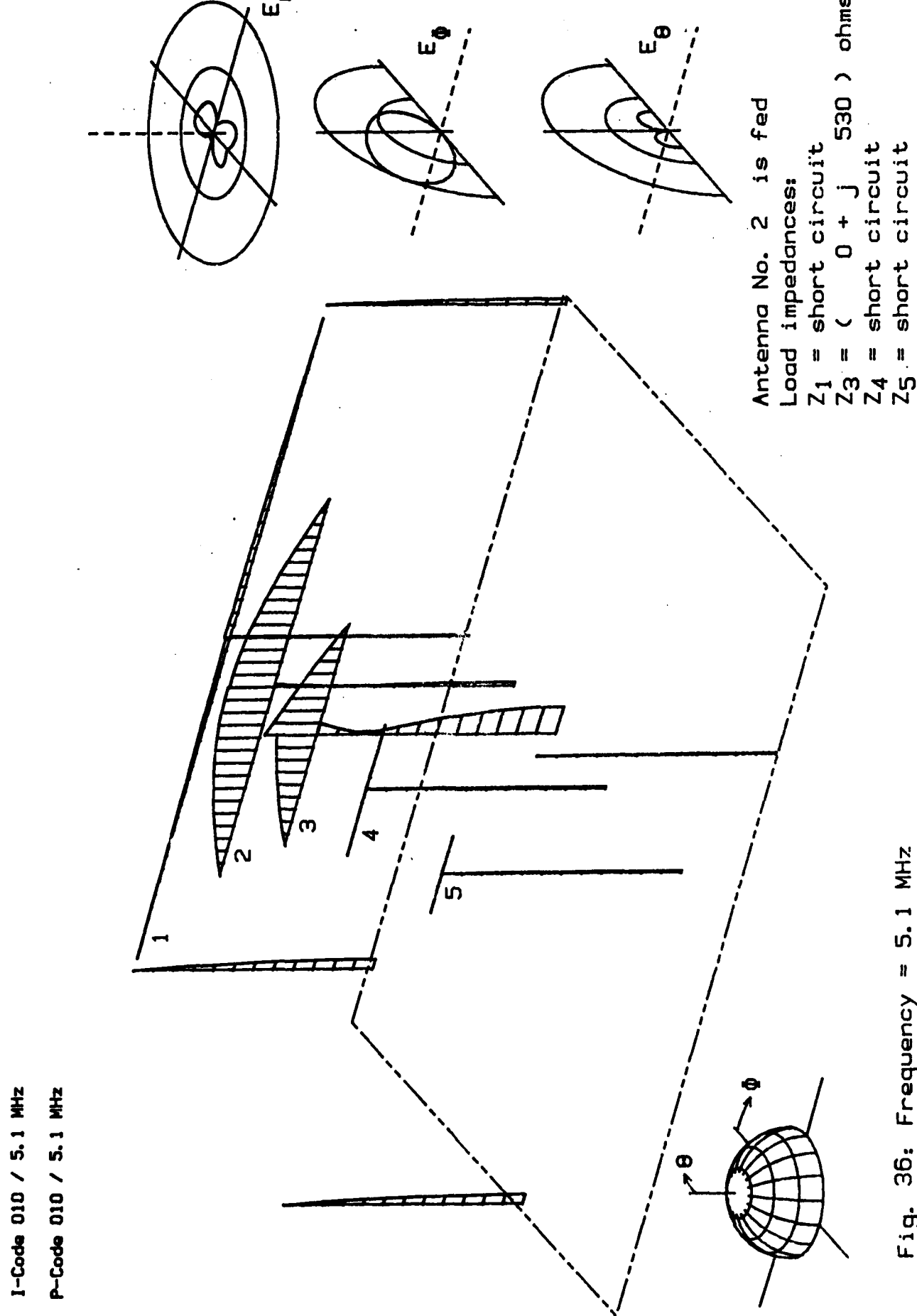
Fig. 33: Frequency = 5.1 MHz
Feeder type: Cobra head



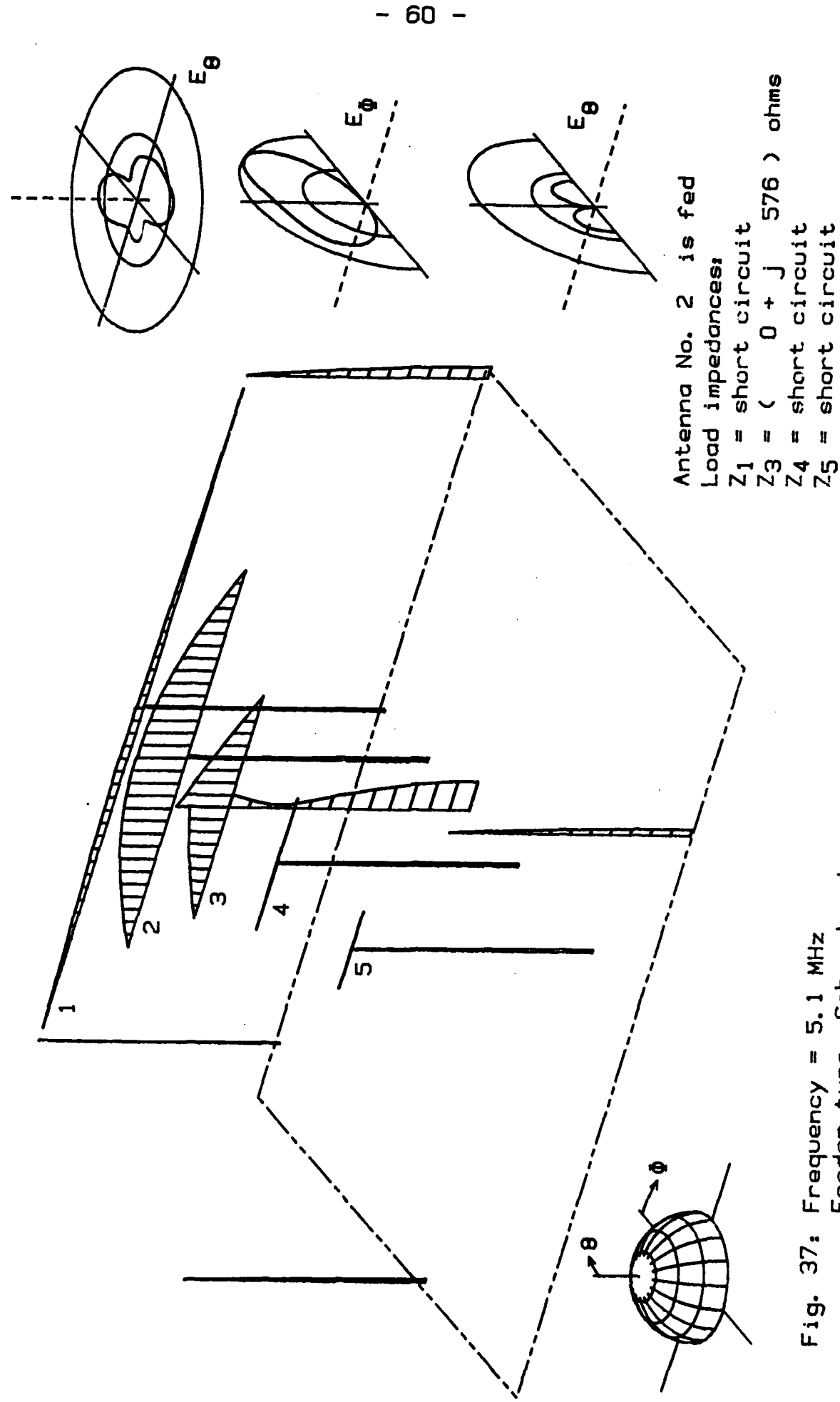
I-Code 012 / 5.1 MHz
P-Code 012 / 5.1 MHz

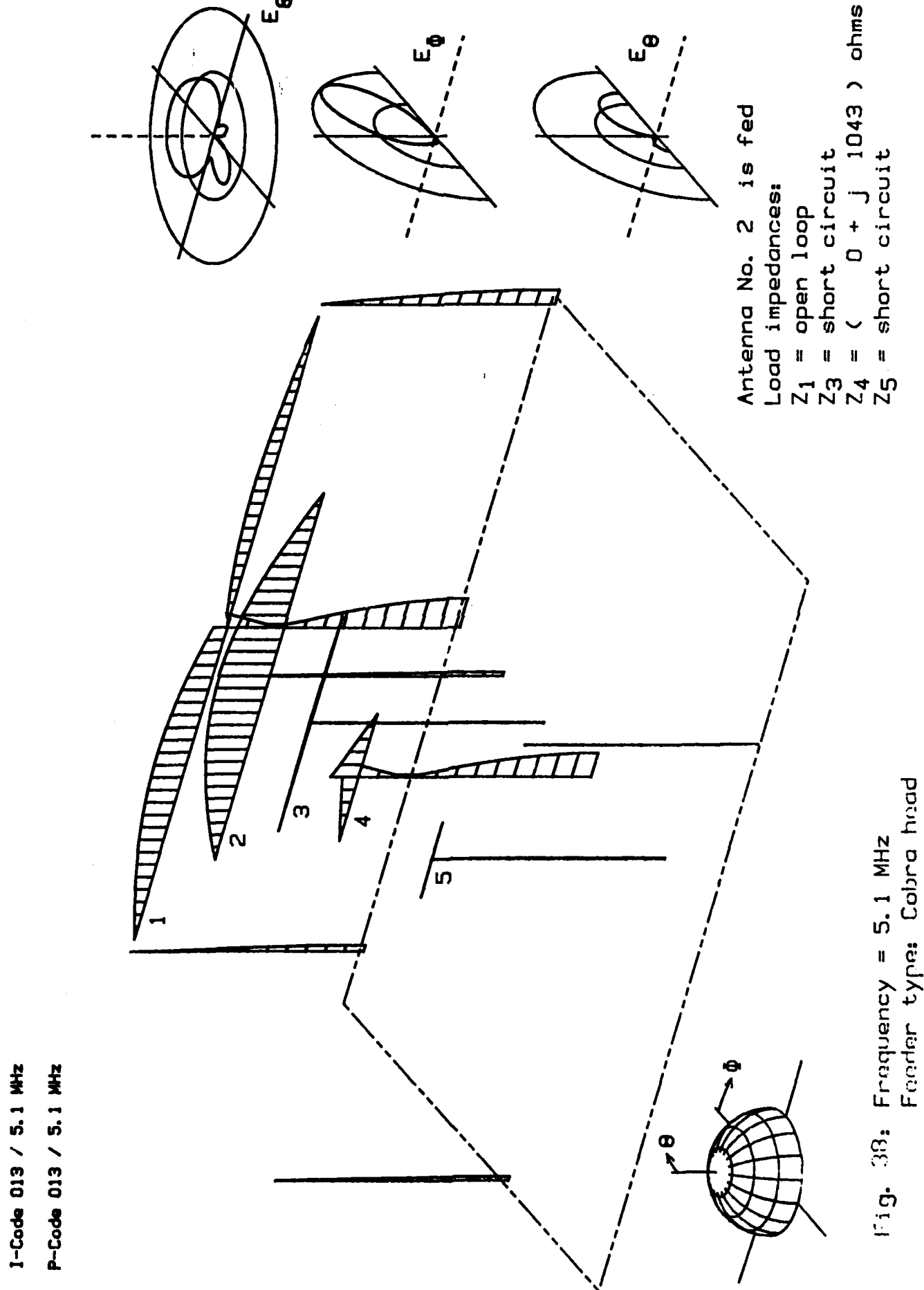
- 58 -

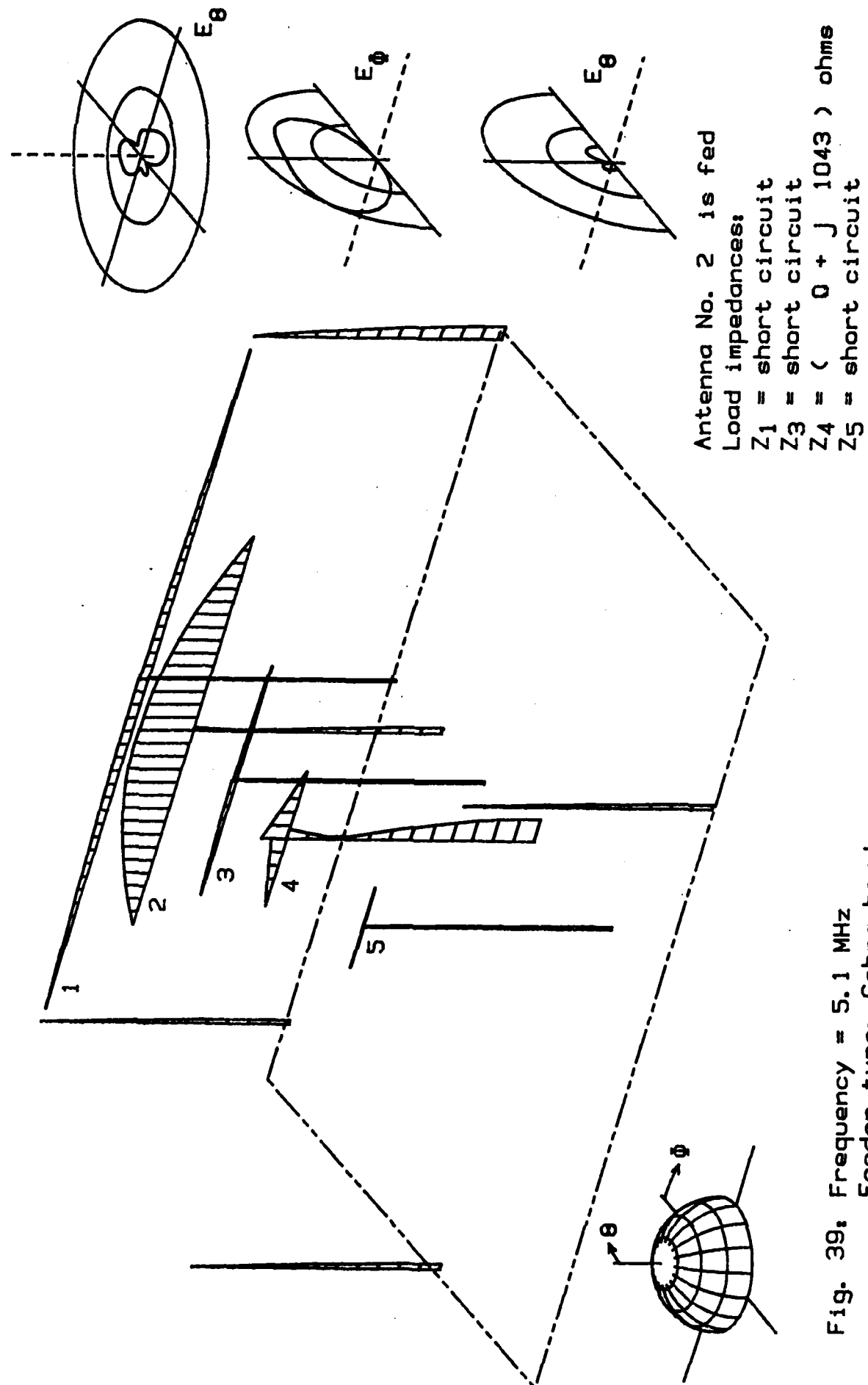




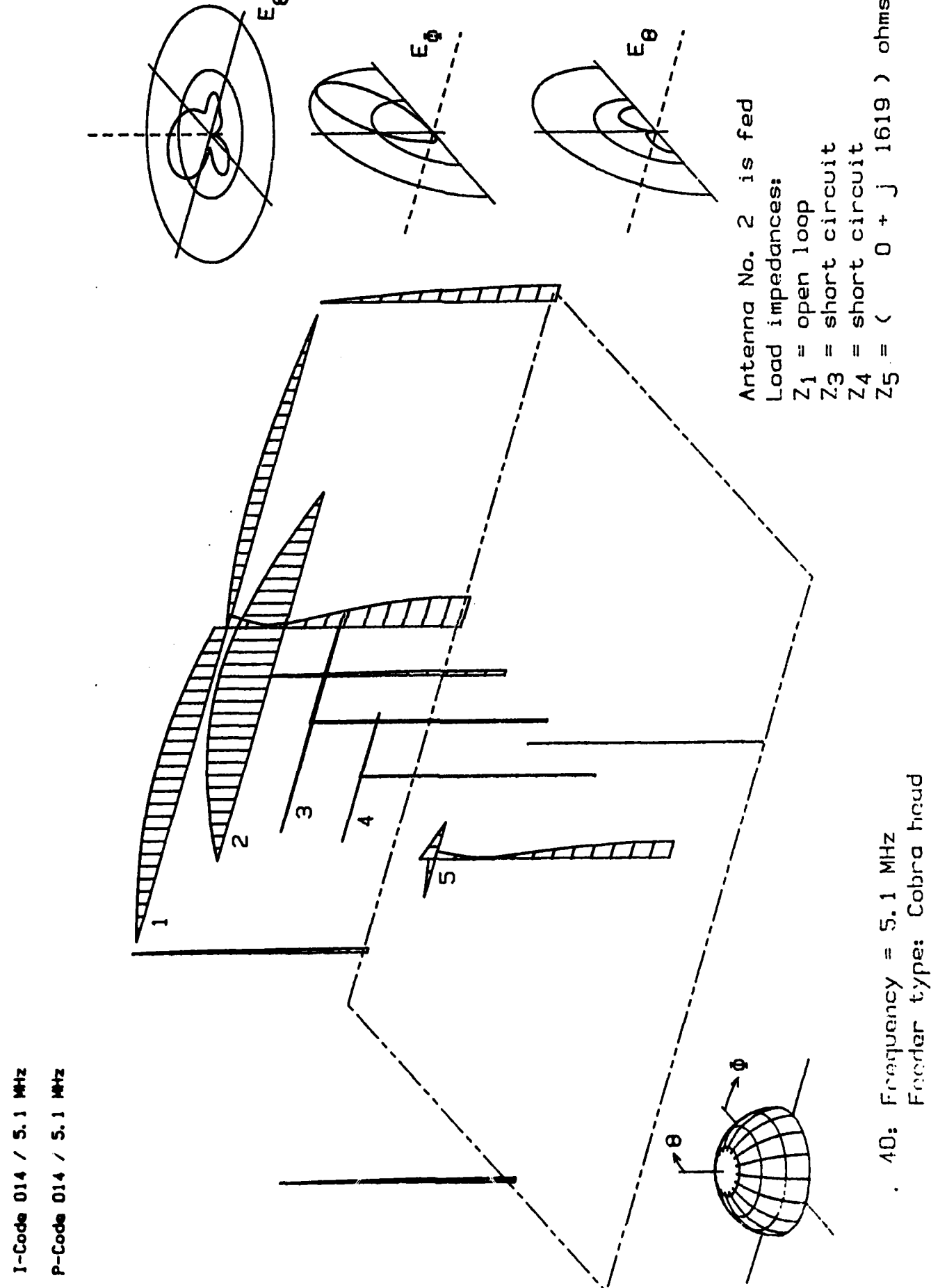
I-Code 011 / 5.1 MHz
P-Code 011 / 5.1 MHz





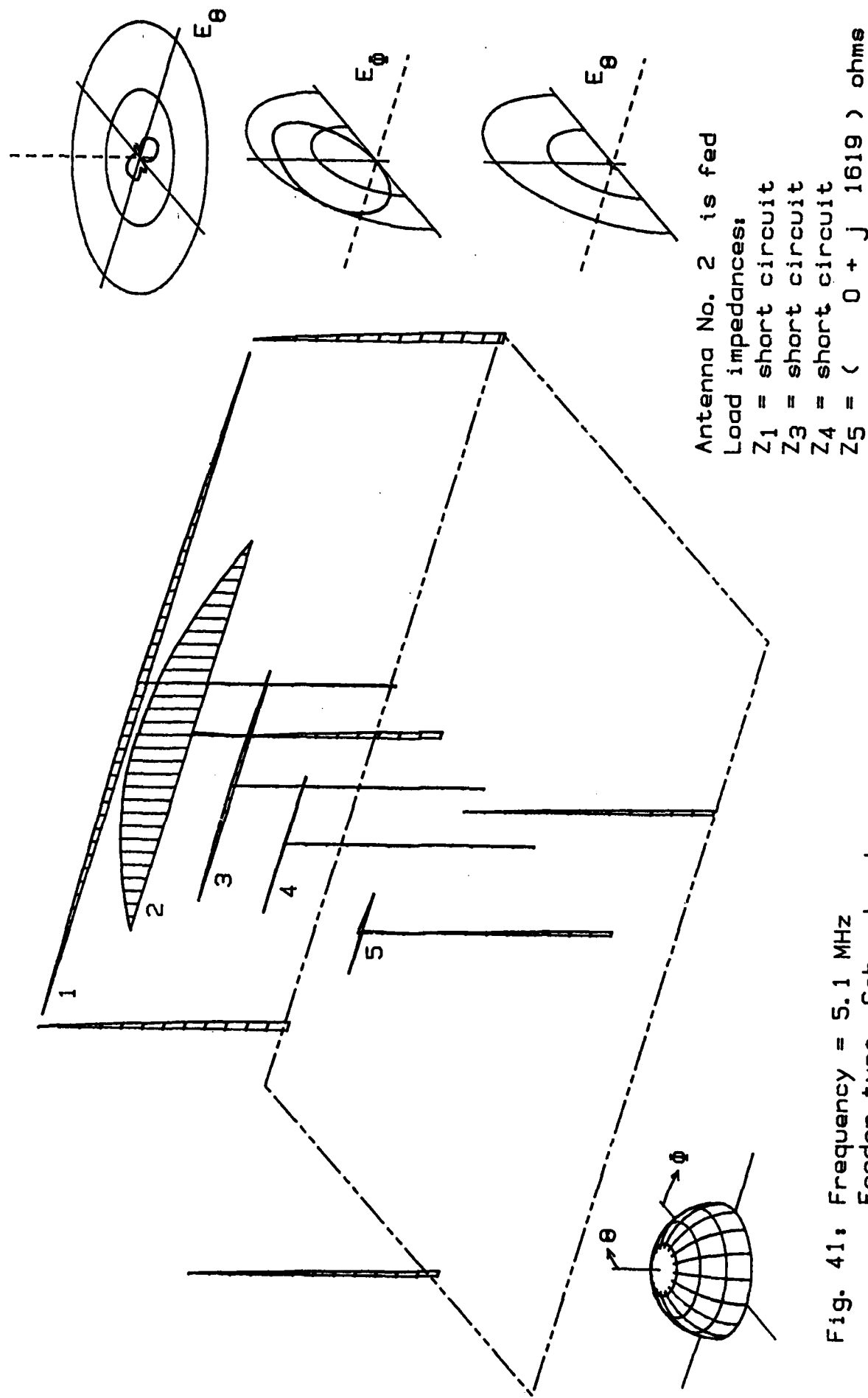


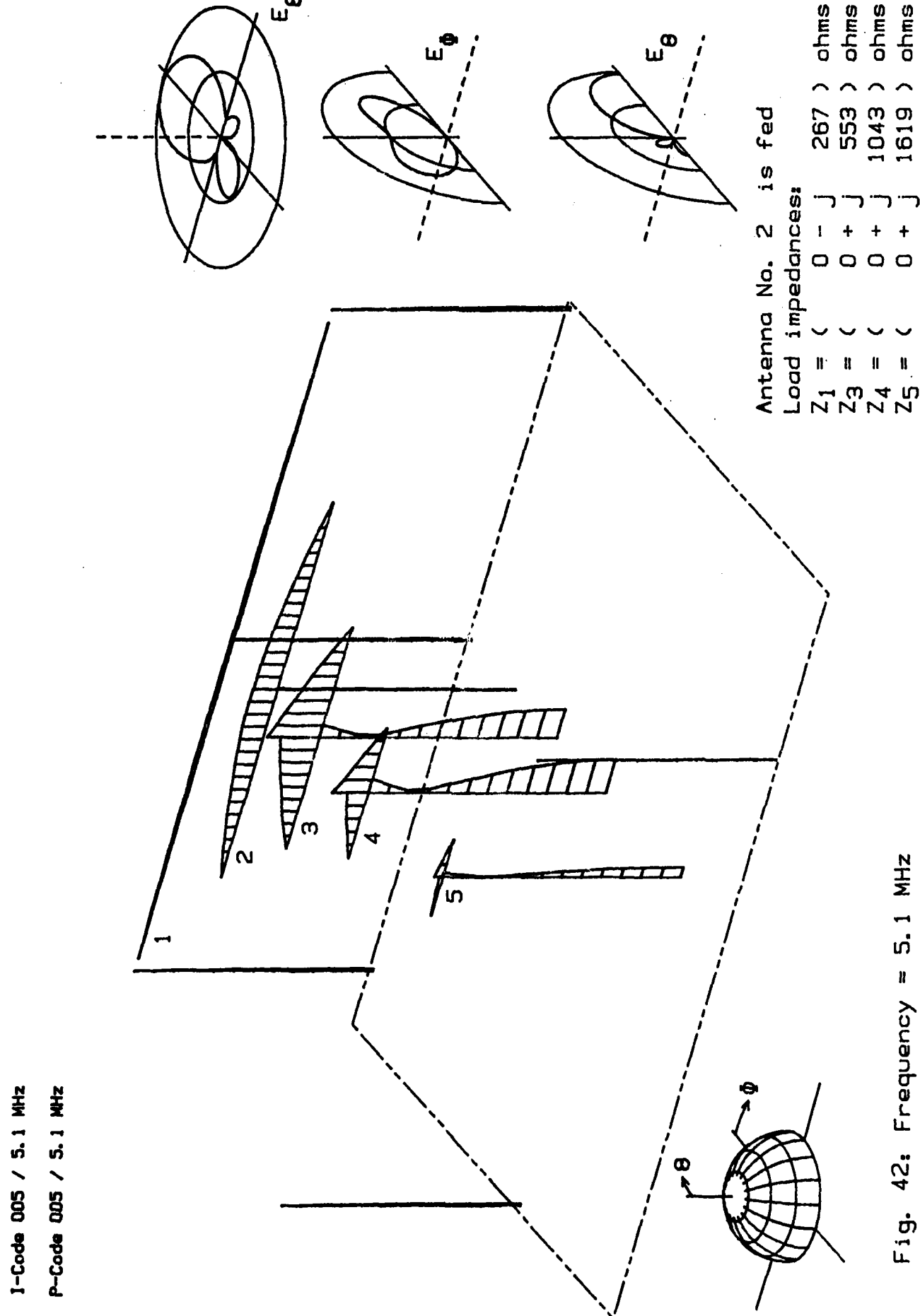
I-Code 015 / 5.1 MHz
P-Code 015 / 5.1 MHz



I-Code 016 / 5.1 MHz
P-Code 016 / 5.1 MHz

- 64 -





8. Analysis at 8.66MHz. Feeder type: Cobra head.

In Table 3 the Z-matrix for 8.66MHz and cobra-head feeding is presented. Figs. 43 through 47 show the generic cases. As the center frequency of antenna 3 is 8.66MHz only this antenna is intended for actual use at this frequency. Thus, Fig. 43 which deals with antenna 2 being fed is of major interest.

In Fig. 43 the remaining antennas are open loop terminated. From the current distribution along the feeder of antenna 3 it can be seen that the antenna height must be close to half a wavelength. At 8.66MHz the free space wavelength is 34.64 m. The height of the antennas of 18.3 m, therefore, corresponds to .53 lambda. This length transforms a short circuit from the ground plane to the feeder gaps. As a result a major part of the feeder current at antenna 3 flows as sheath current along the feeder line and not to the left-side of the dipole 3.

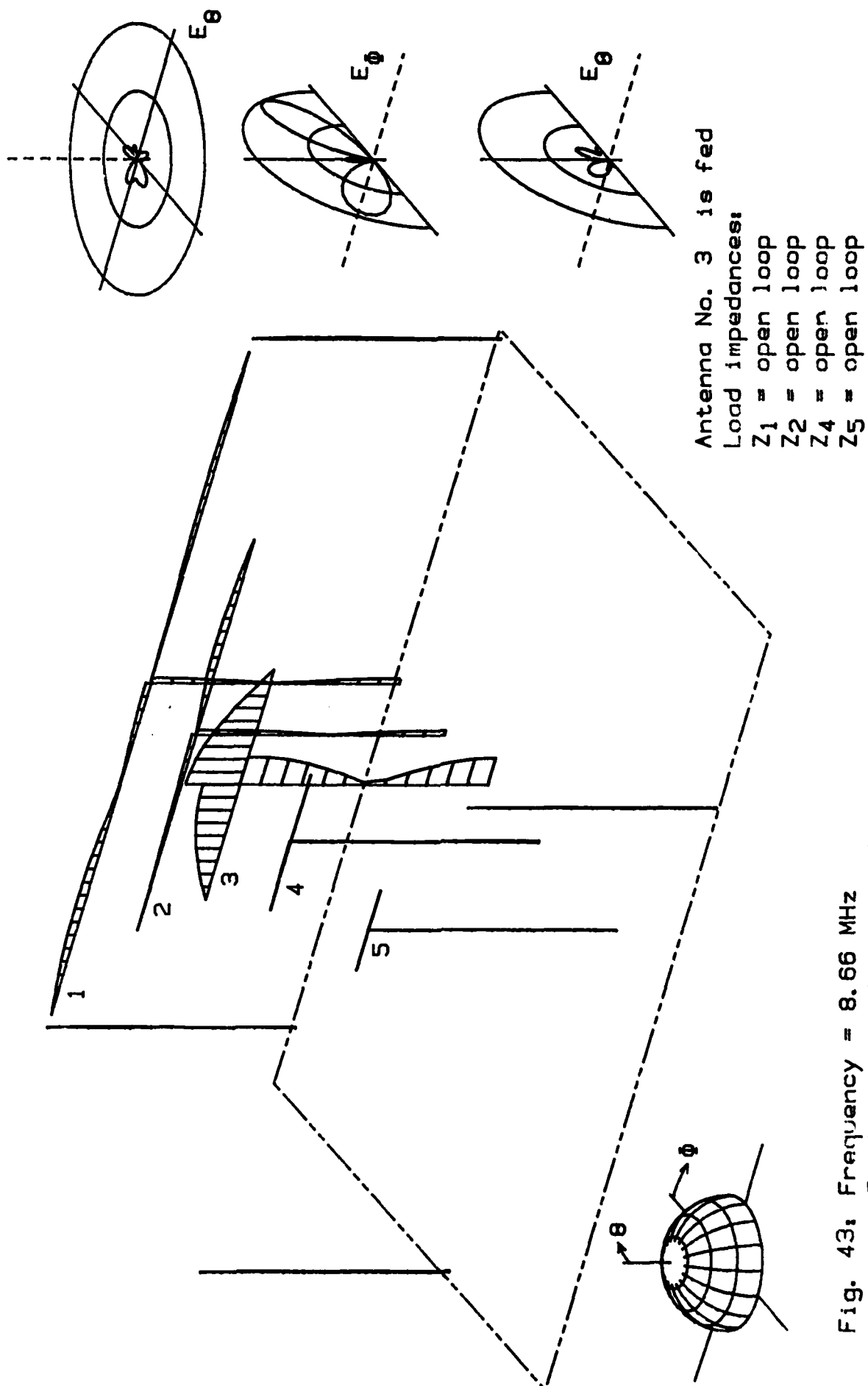
Another resonance can be detected in Fig. 43. The combined length of the left-side dipole half of antenna 1 plus the length of the feeder line is 43.3 m. This is exactly 5/4 wavelengths. It is only due to the weak coupling of both antennas that the "by-pass" current in antenna 1 is so small in this example.

The sheath current along the feeder line of antenna 3 in Fig. 43 is divided into two quarter-wavelength portions with 180° phase shift against another. This results in a cancellation effect in the coupling to the other feeder lines. Parasitic coupling via the feeder lines is therefore small at this frequency.

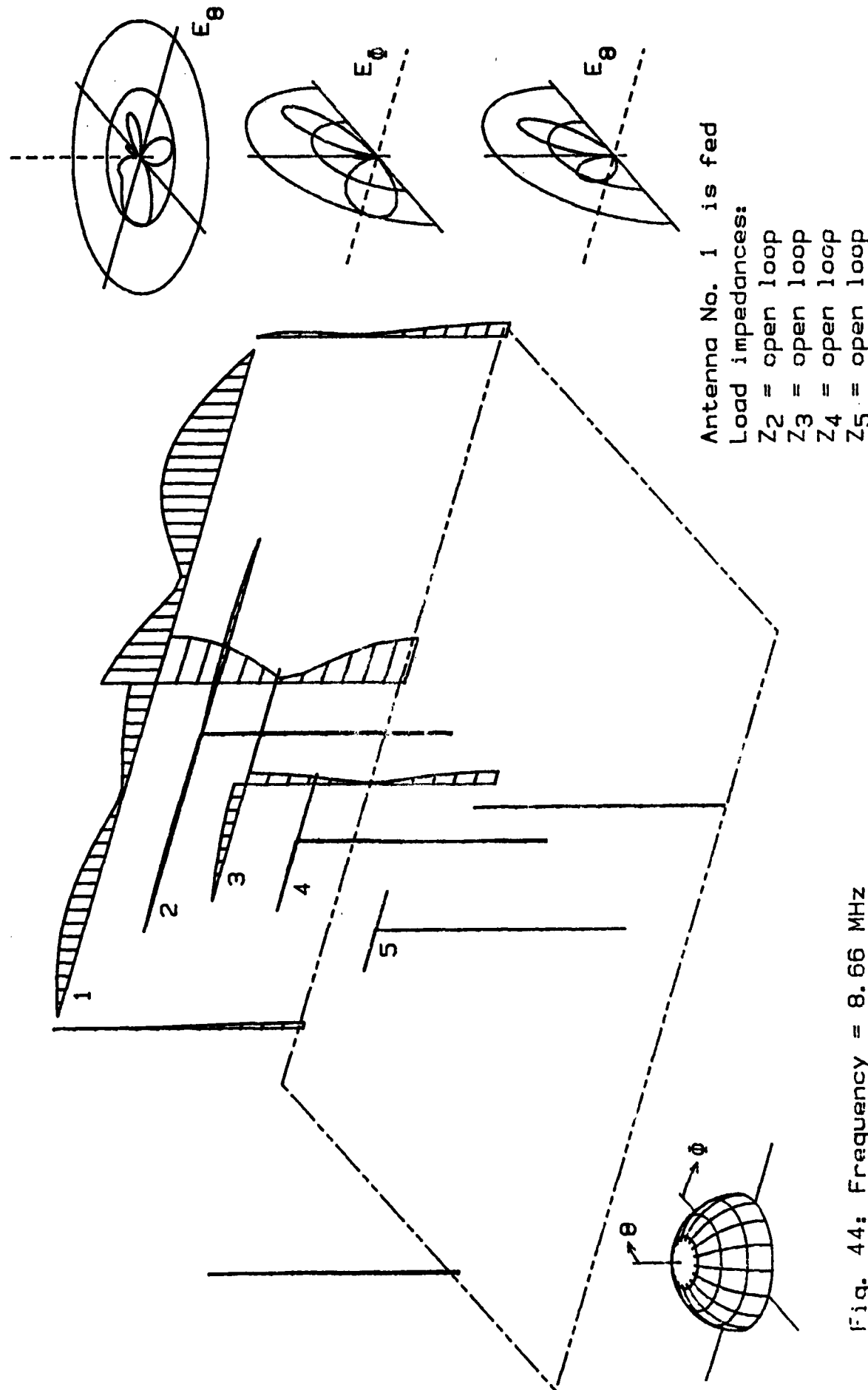
As the antenna height is about half a wavelength at 8.66MHz, the mirror images of the dipoles are one wavelength apart at this frequency resulting in a cancellation of the radiation in the upward direction as can be seen in the radiation patterns of Fig. 43. Radiation of the vertically polarized field is small

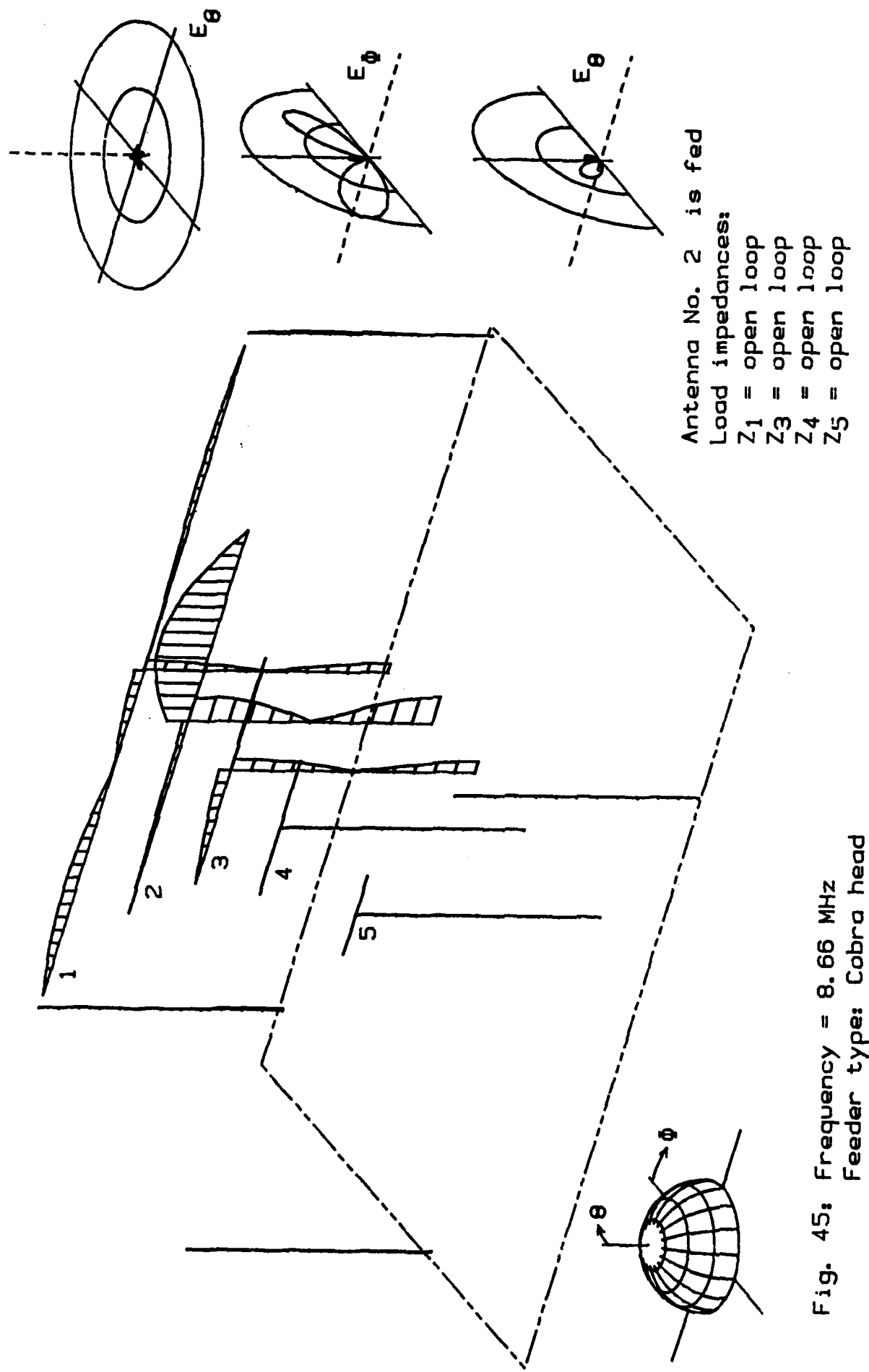
$l_{11} = (-83.80-j \ 68)$ ohms	$l_{12} = (-15.60+j \ 4)$ ohms	$l_{13} = (8.30-j \ 4)$ ohms	$l_{14} = (1.29-j \ 12)$ ohms	$l_{15} = (-4.57-j \ 2)$ ohms
$l_{21} = (-15.80+j \ 3)$ ohms	$l_{22} = (375.35+j \ 992)$ ohms	$l_{23} = (73.35-j \ 56)$ ohms	$l_{24} = (-17.15-j \ 41)$ ohms	$l_{25} = (-24.20+j \ 4)$ ohms
$l_{31} = (8.21-j \ 4)$ ohms	$l_{32} = (73.47-j \ 56)$ ohms	$l_{33} = (41.93+j \ 24)$ ohms	$l_{34} = (8.40-j \ 14)$ ohms	$l_{35} = (-5.07-j \ 6)$ ohms
$l_{41} = (1.23-j \ 12)$ ohms	$l_{42} = (-17.09-j \ 41)$ ohms	$l_{43} = (8.42-j \ 14)$ ohms	$l_{44} = (25.51-j \ 256)$ ohms	$l_{45} = (12.86-j \ 13)$ ohms
$l_{51} = (-4.59-j \ 2)$ ohms	$l_{52} = (-24.09+j \ 4)$ ohms	$l_{53} = (-5.06-j \ 6)$ ohms	$l_{54} = (12.83-j \ 13)$ ohms	$l_{55} = (18.46-j \ 602)$ ohms

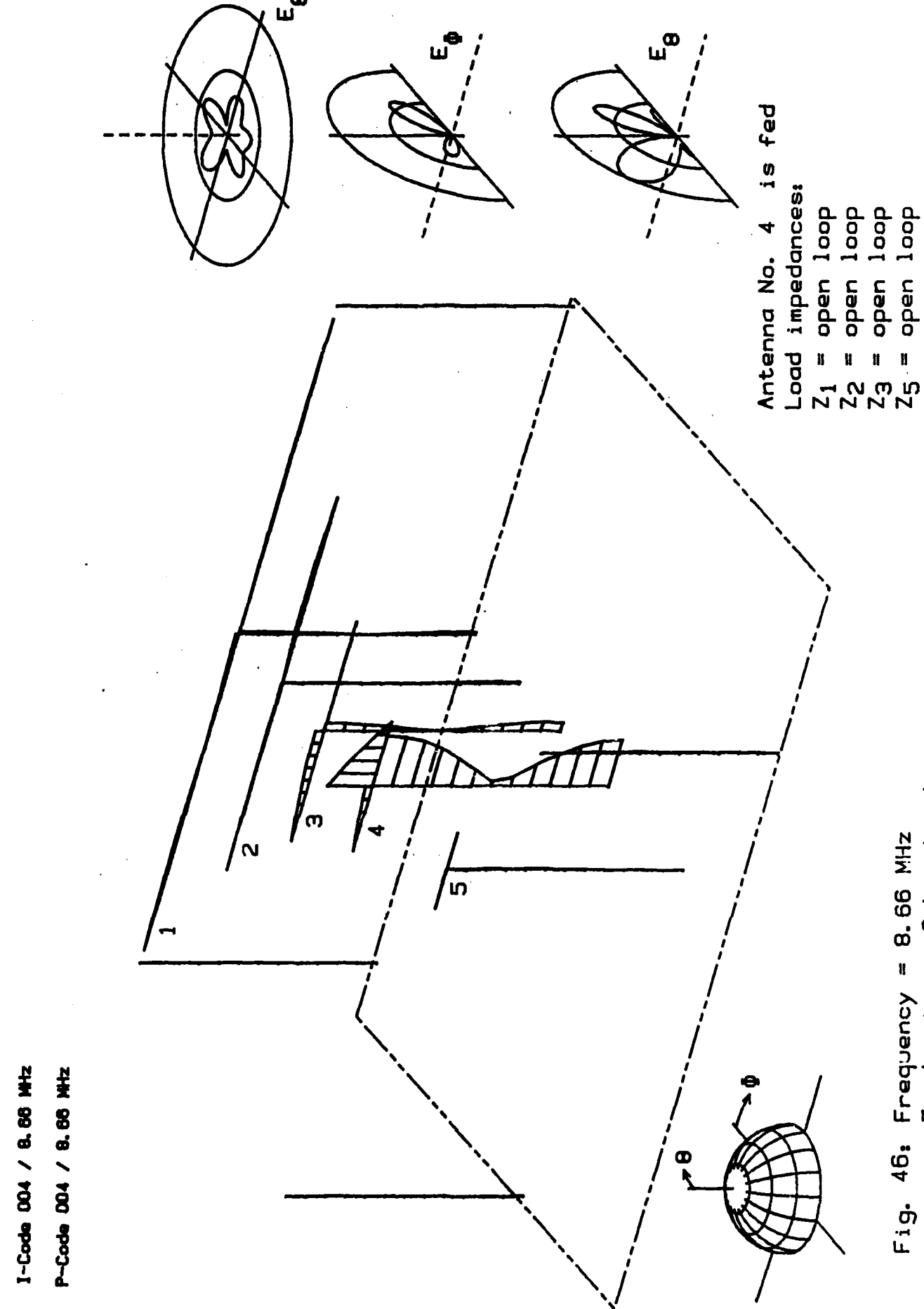
Table 3: Z-Matrix for $f = 8.66$ MHz. feeder type: cobra head.

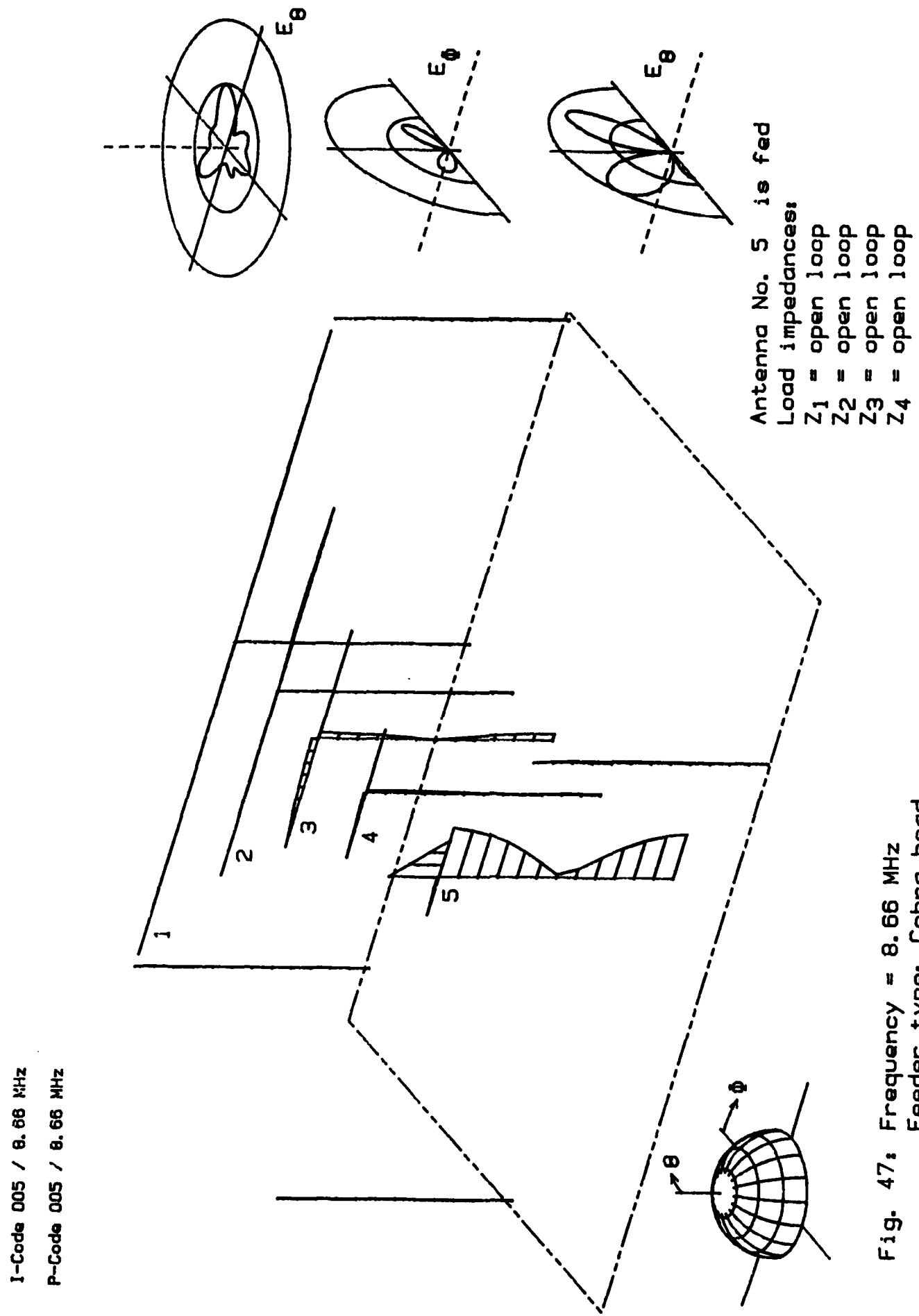


I-Code 002 / 8.66 MHz
P-Code 002 / 8.66 MHz









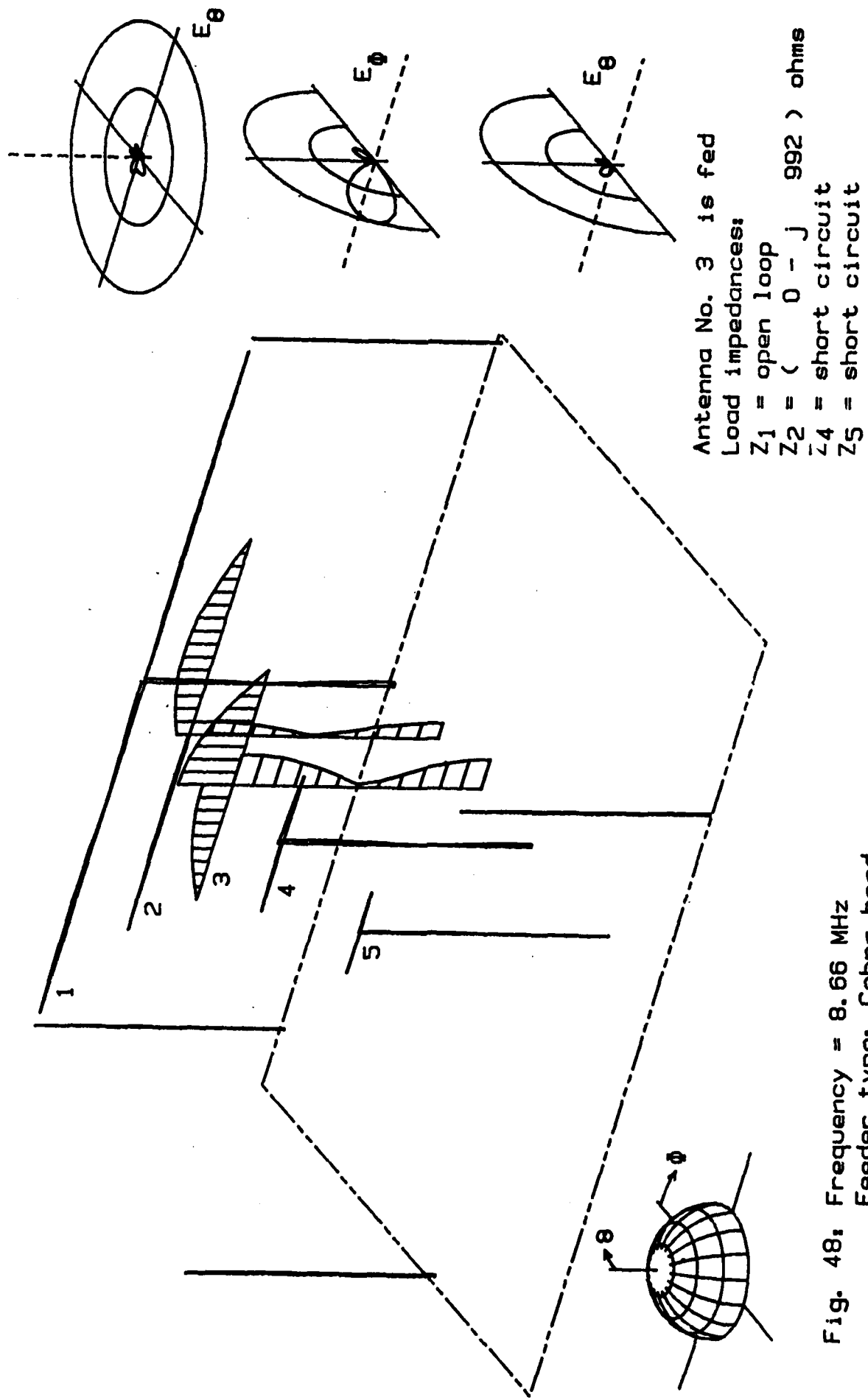
due to the half-wavelength height of all poles and antenna feeders.

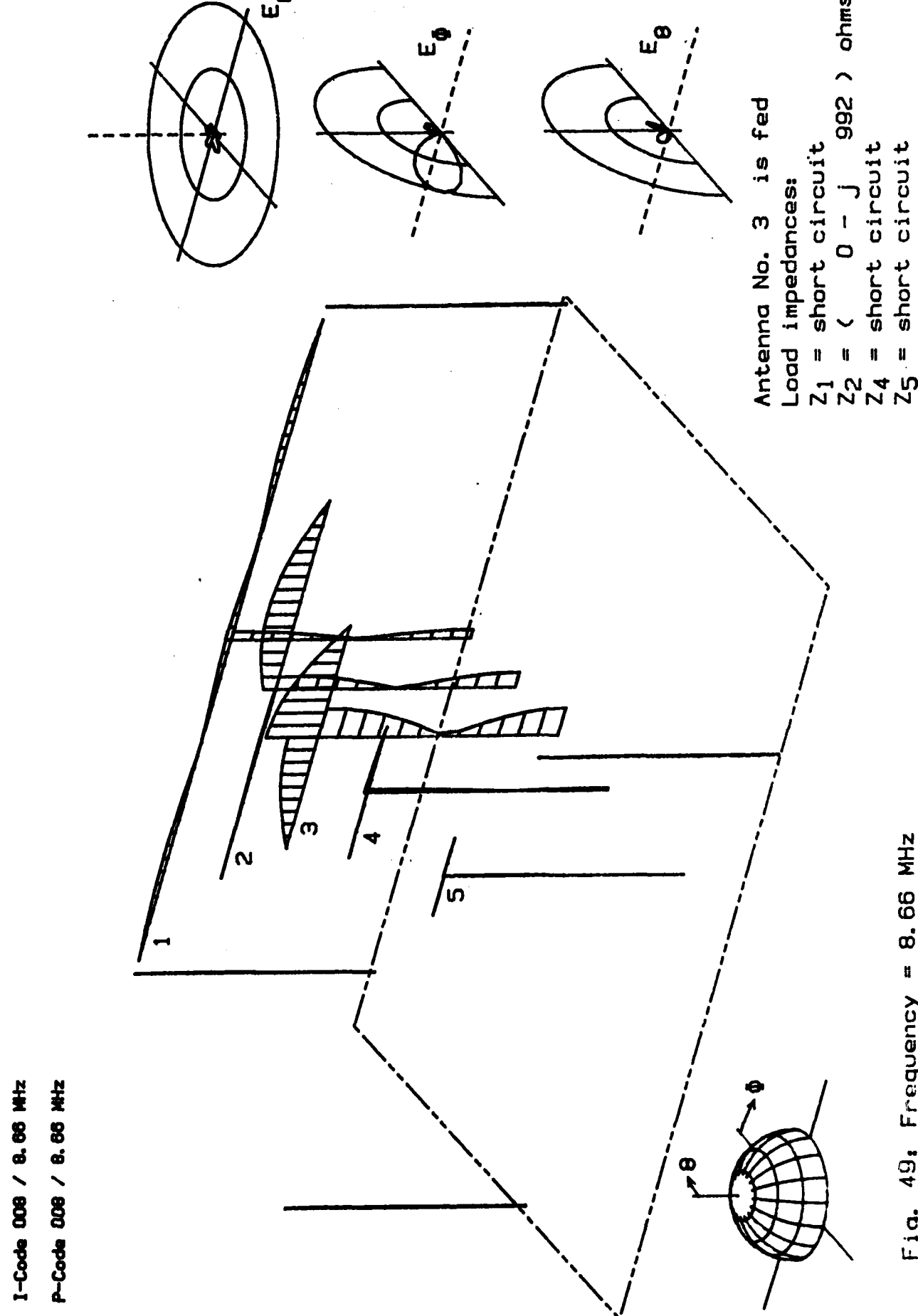
Figs. 44 through 47 show even more clearly the effect of the short circuit transformation of the half-wavelength feeder lines: In all these cases the excitation mainly takes place between the right-side half of the dipoles and the feeder line.

Some of the other interesting cases with resonance terminations are shown in Figs. 48 through 52. These cases have been selected for reasons similar to those of the previous frequencies.

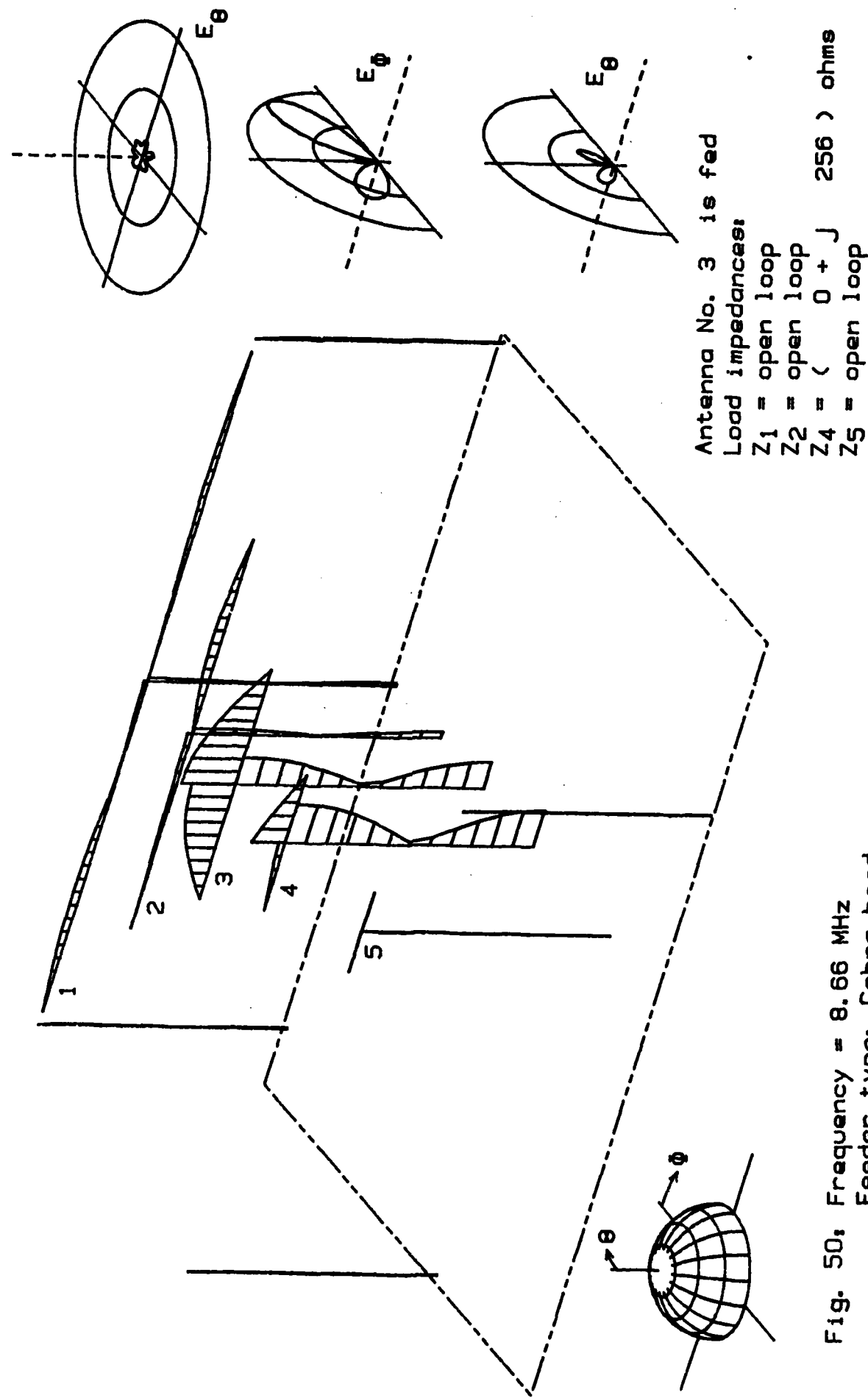
I-Code 007 / 8.66 MHz
P-Code 007 / 8.66 MHz

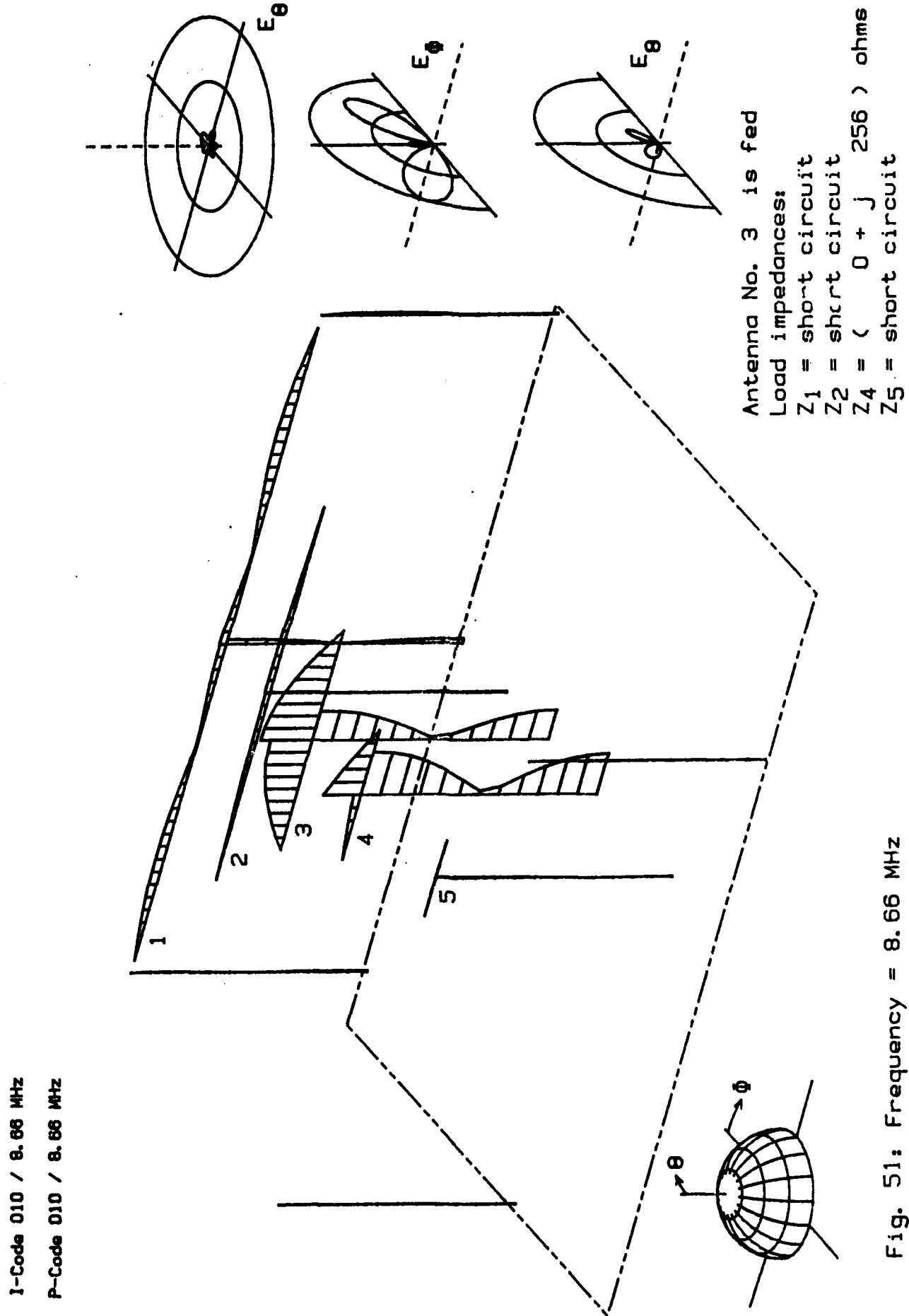
- 74 -

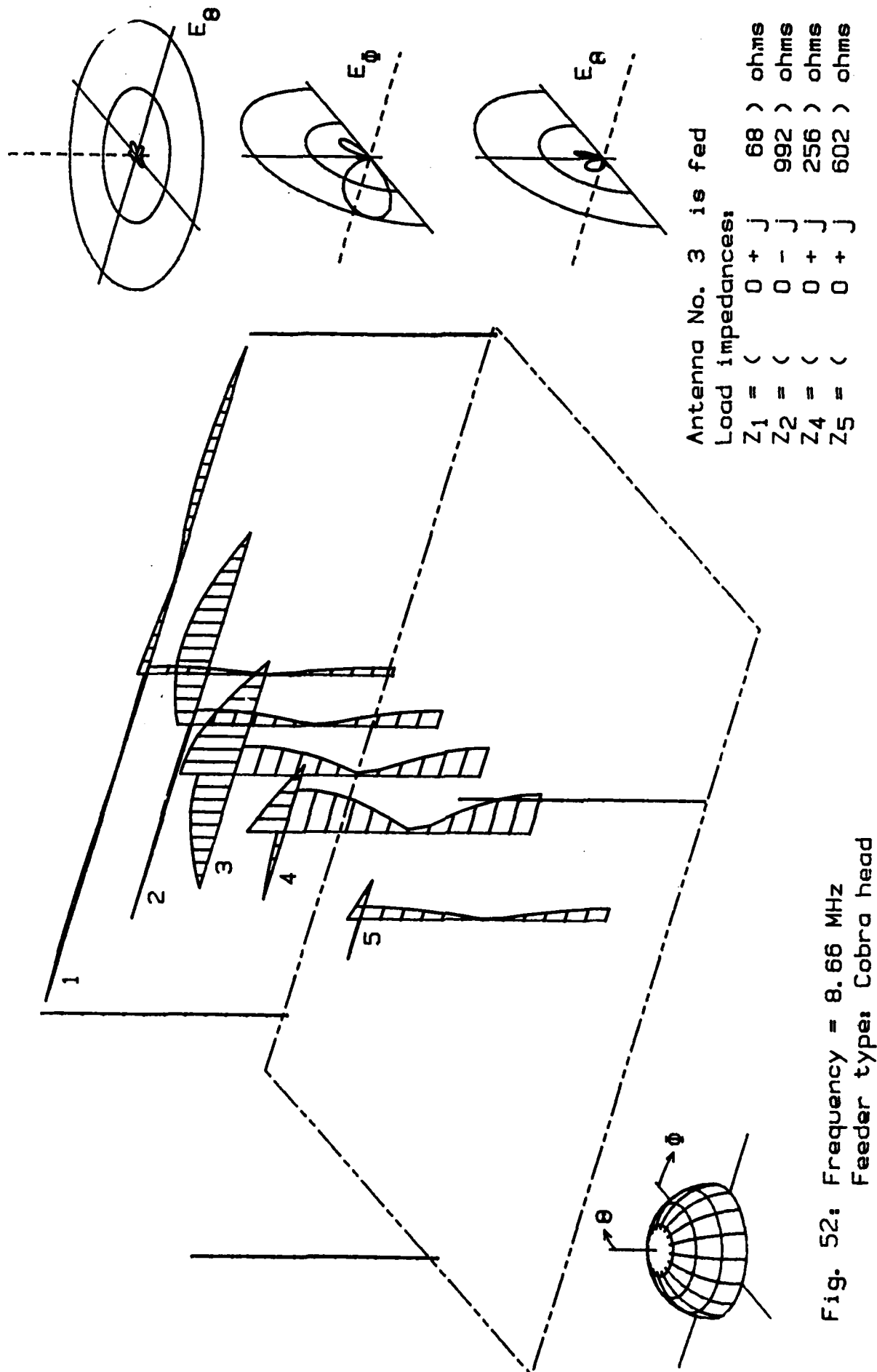




I-Code 009 / 8.66 MHz
P-Code 009 / 8.66 MHz







9. Analysis at 14.71MHz. Feeder type: Cobra head.

Table 4 shows the Z-matrix for 14.71MHz and cobra-head feeding. Figs. 53 through 57 show the generic cases. As the center frequency of antenna 4 is 14.71MHz, only this antenna is intended for actual use at this frequency. Thus, Fig. 53 with antenna 4 being fed is of major interest.

In the case of Fig. 53 the remaining antennas are open loop terminated. Now the combination of the left-side dipole half of antenna 3 and the feeder line shows a resonance behaviour. Its combined length is 26.95 m; the free-space wave length at 14.71 MHz is 20.4 m, resulting in a ratio of 1.32 which is close to a 5/4 wavelength resonance. Coupling to the other antennas is rather weak.

Due to the antenna height the pattern is rather spiked. Radiation in the vertical polarization, however, is small.

Figs. 58 through 63 show some more selected cases.

$Z_{11} = (-100.99-j134) \text{ ohms}$	$Z_{12} = (20.84-j6) \text{ ohms}$	$Z_{13} = (13.38-j3) \text{ ohms}$	$Z_{14} = (8.00-j1) \text{ ohms}$	$Z_{15} = (1.56+j4) \text{ ohms}$
$Z_{21} = (20.99-j6) \text{ ohms}$	$Z_{22} = (85.77-j127) \text{ ohms}$	$Z_{23} = (37.68-j3) \text{ ohms}$	$Z_{24} = (-25-j0) \text{ ohms}$	$Z_{25} = (1.03+j5) \text{ ohms}$
$Z_{31} = (13.27-j3) \text{ ohms}$	$Z_{32} = (37.84-j3) \text{ ohms}$	$Z_{33} = (519.71-j473) \text{ ohms}$	$Z_{34} = (-66.38+j24) \text{ ohms}$	$Z_{35} = (-6.14-j7) \text{ ohms}$
$Z_{41} = (-7.96-j1) \text{ ohms}$	$Z_{42} = (-.27-j0) \text{ ohms}$	$Z_{43} = (-66.40+j24) \text{ ohms}$	$Z_{44} = (100.39+j13) \text{ ohms}$	$Z_{45} = (-6.17-j10) \text{ ohms}$
$Z_{51} = (1.55+j4) \text{ ohms}$	$Z_{52} = (1.10+j3) \text{ ohms}$	$Z_{53} = (6.00-j7) \text{ ohms}$	$Z_{54} = (-6.19-j10) \text{ ohms}$	$Z_{55} = (21.92-j436) \text{ ohms}$

Table 4: Z-Matrix for $f = 14.71 \text{ MHz}$. Feeder type: Cobra head.

I-Code 001 / 14.71 MHz
P-Code 001 / 14.71 MHz

- 81 -

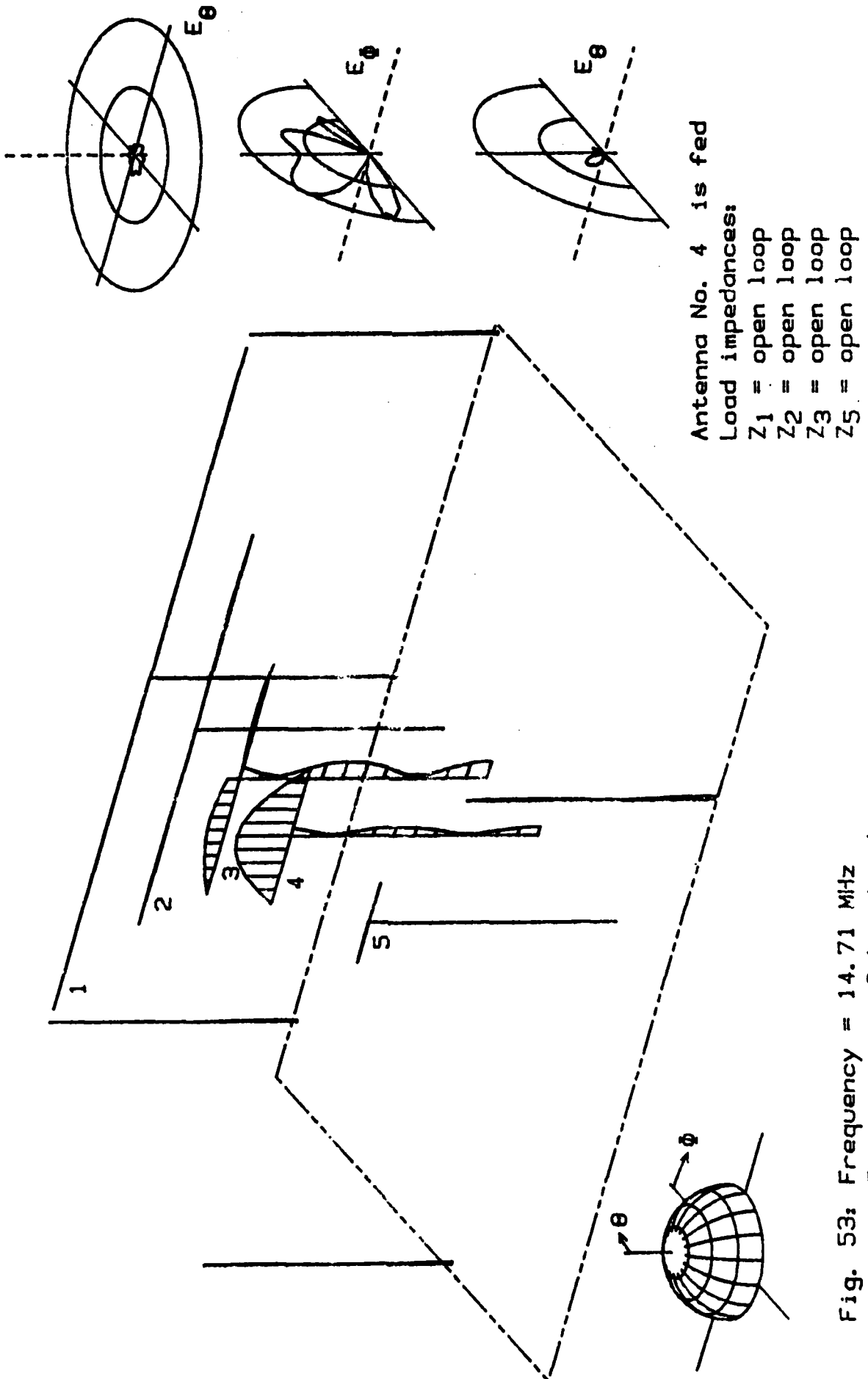
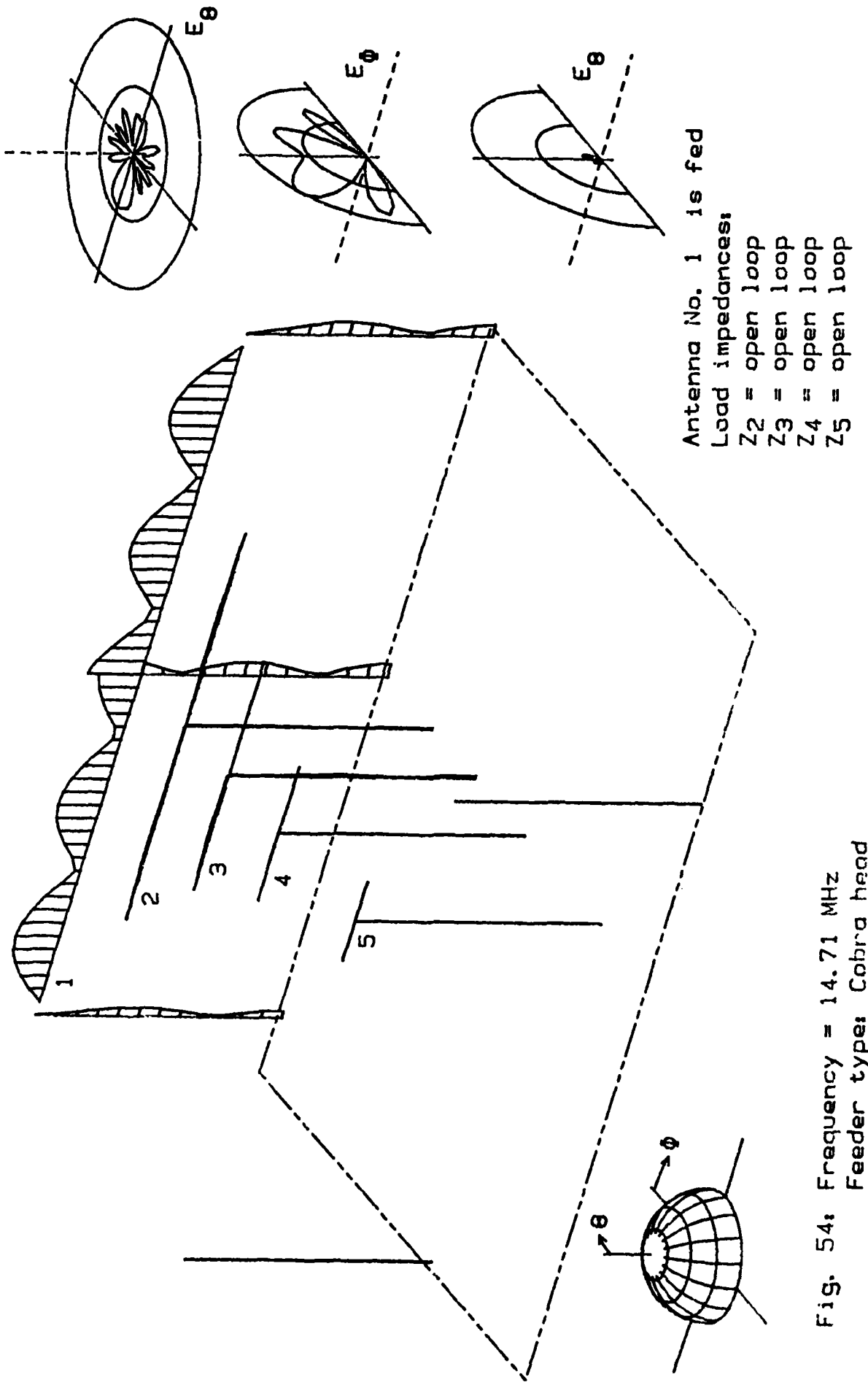
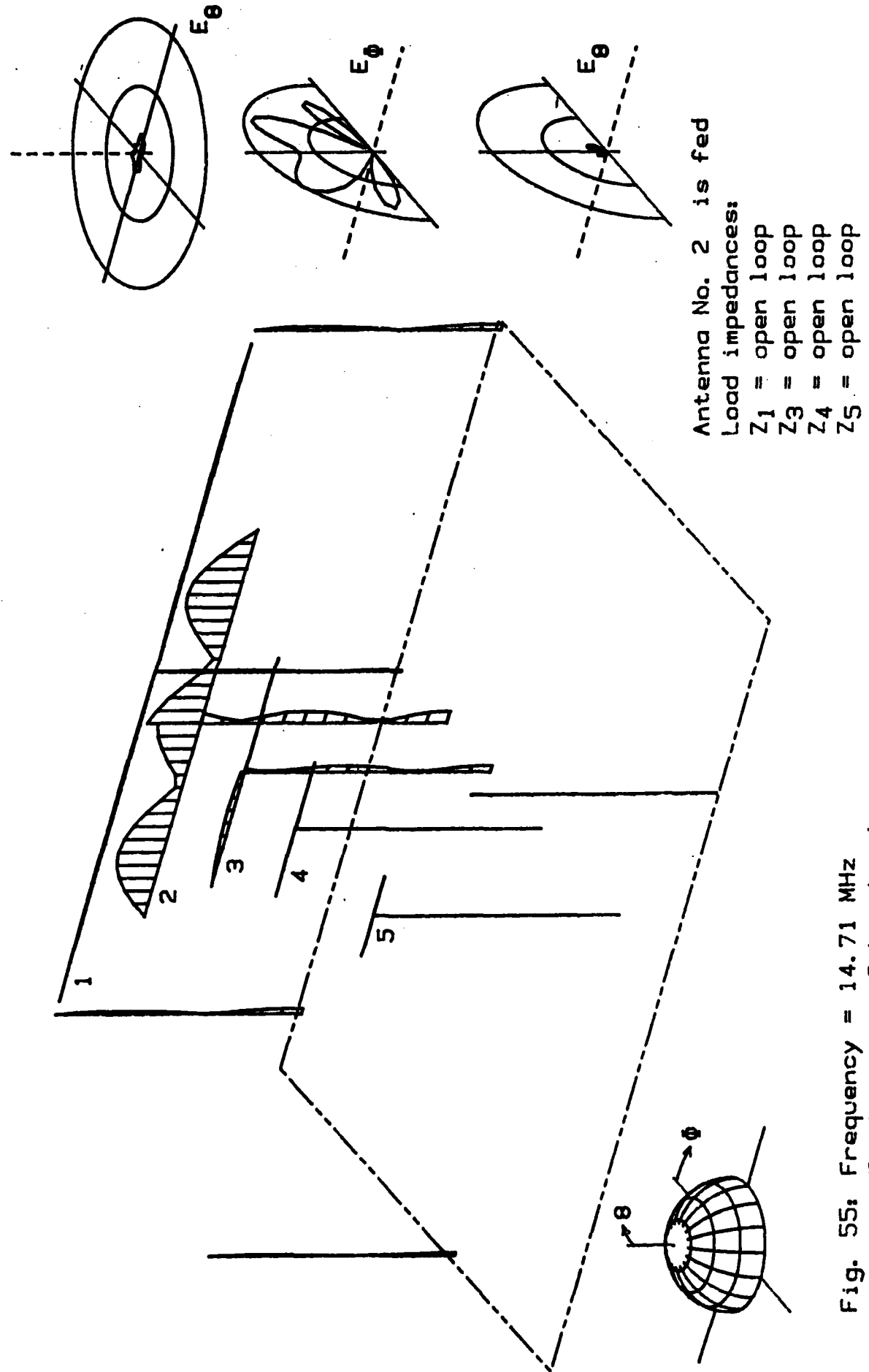


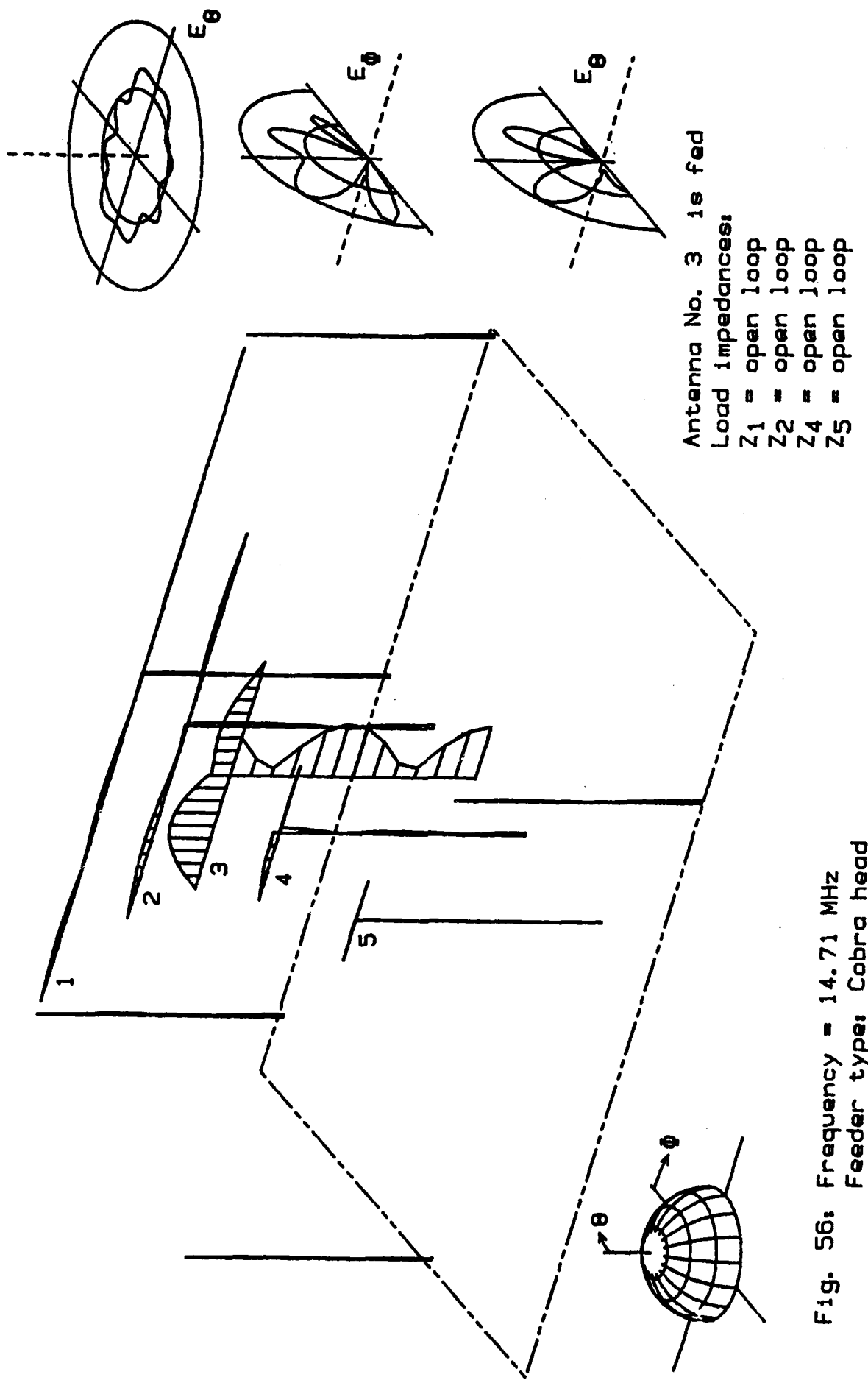
Fig. 53: Frequency = 14.71 MHz
Feeder type: Coax head

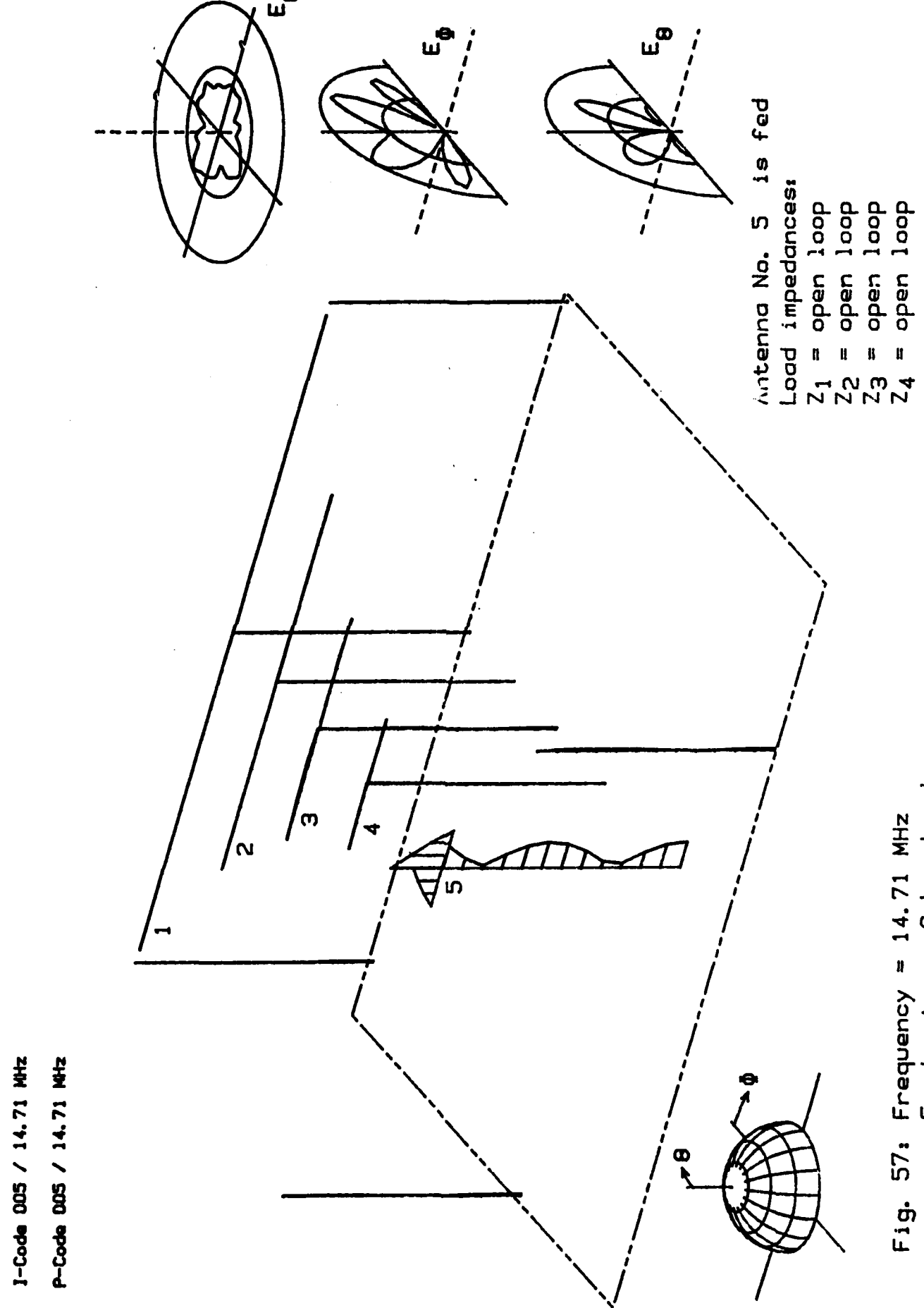


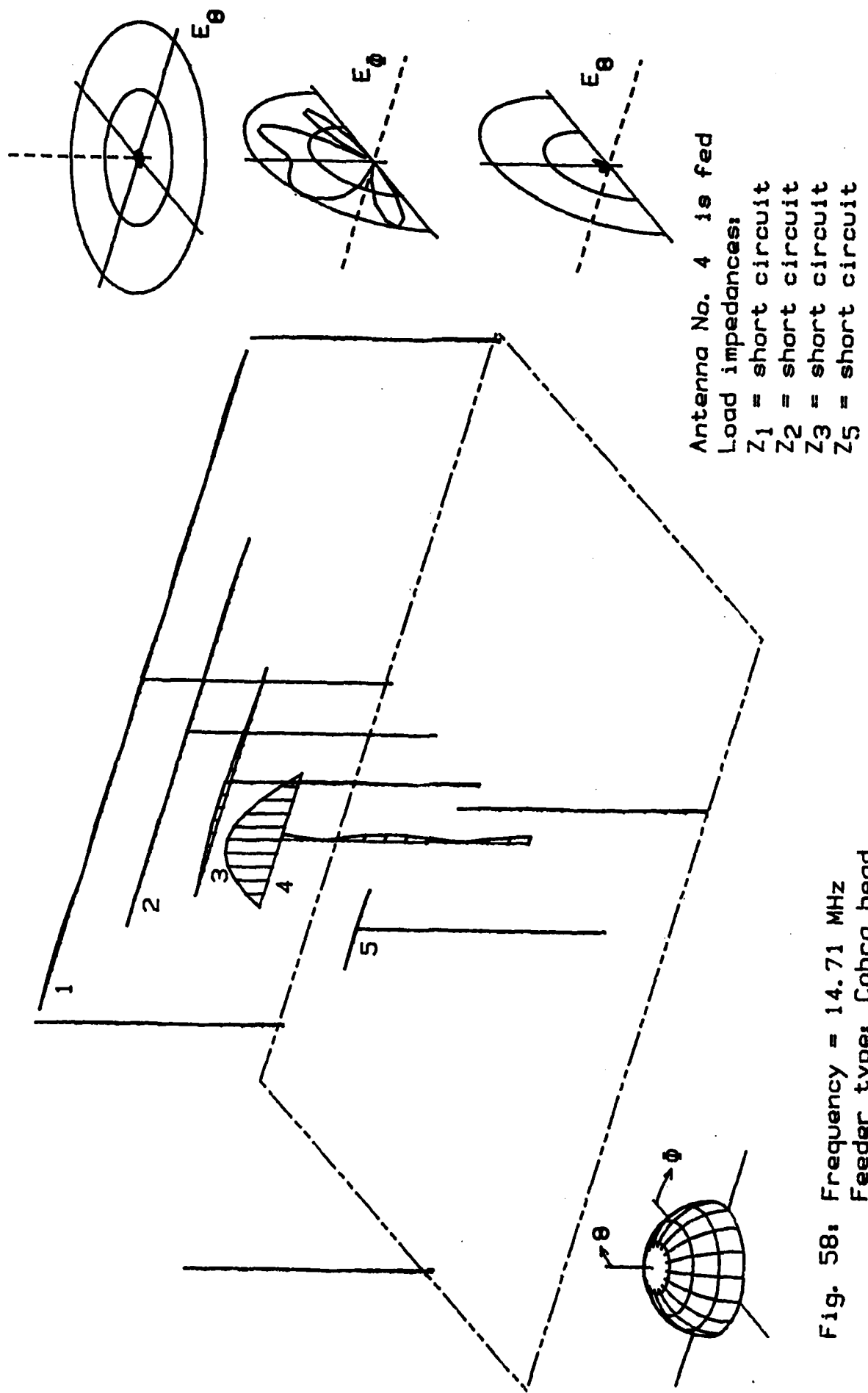
I-Code 003 / 14.71 MHz
P-Code 003 / 14.71 MHz

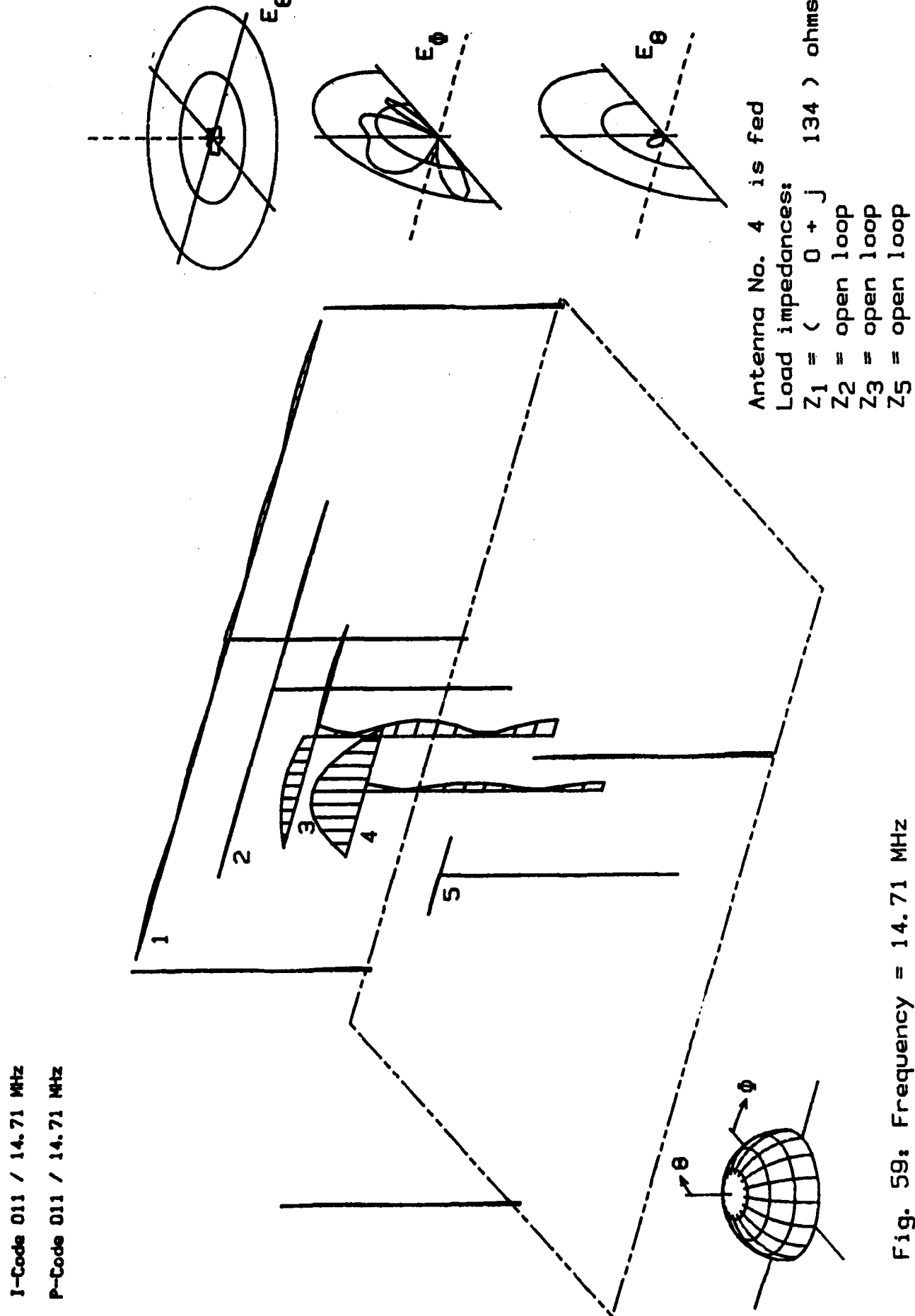


I-Code 004 / 14.71 MHz
P-Code 004 / 14.71 MHz

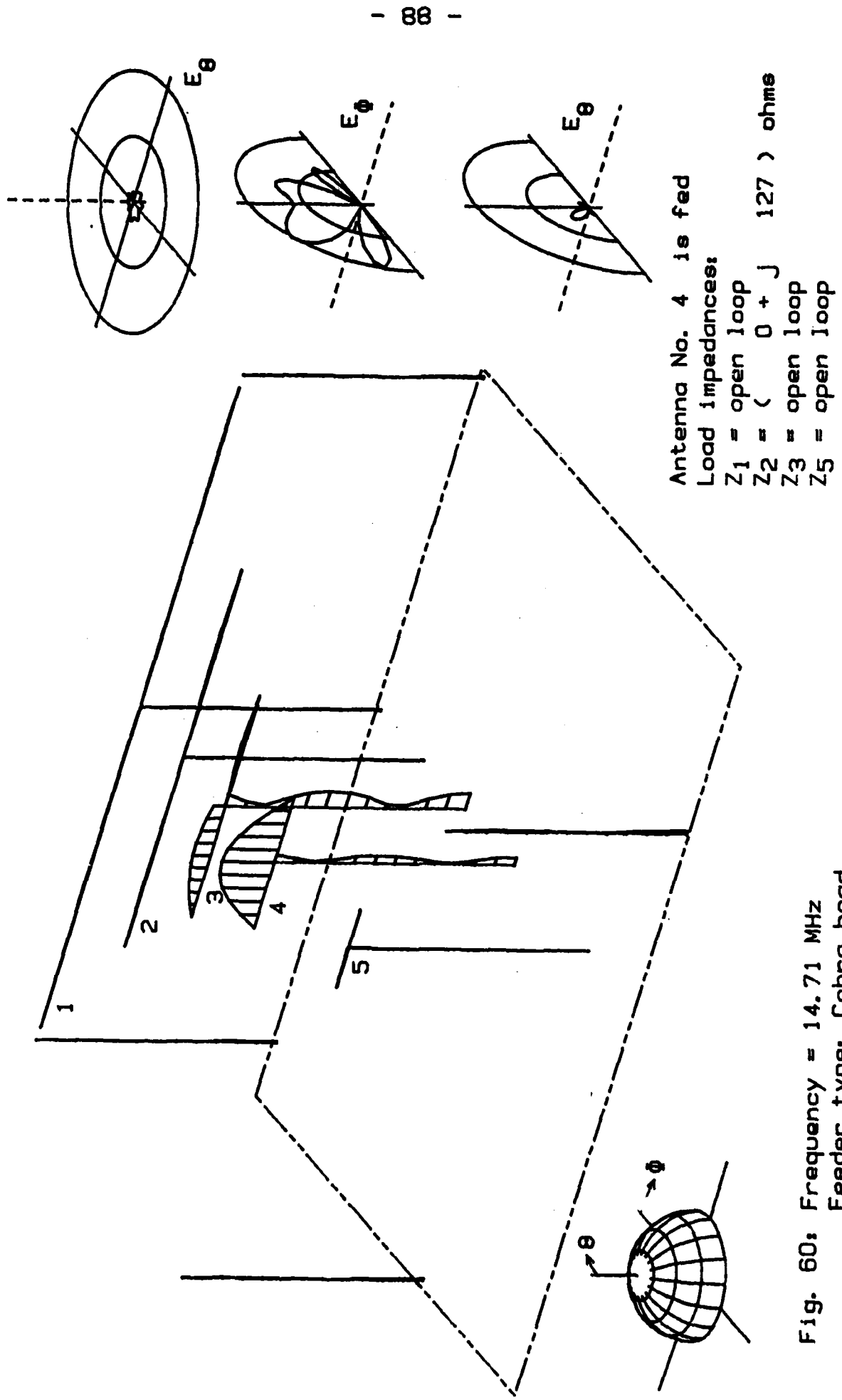


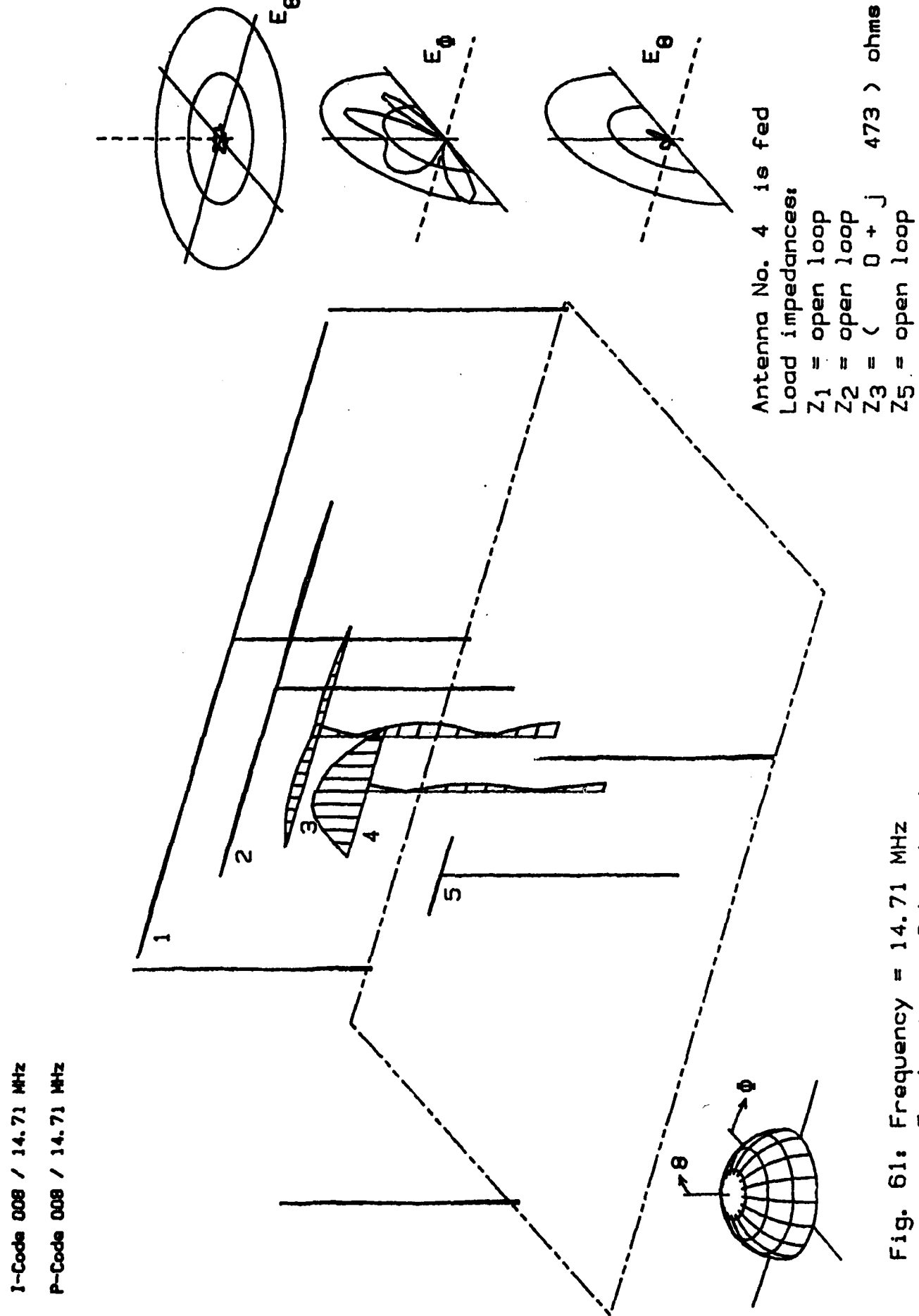






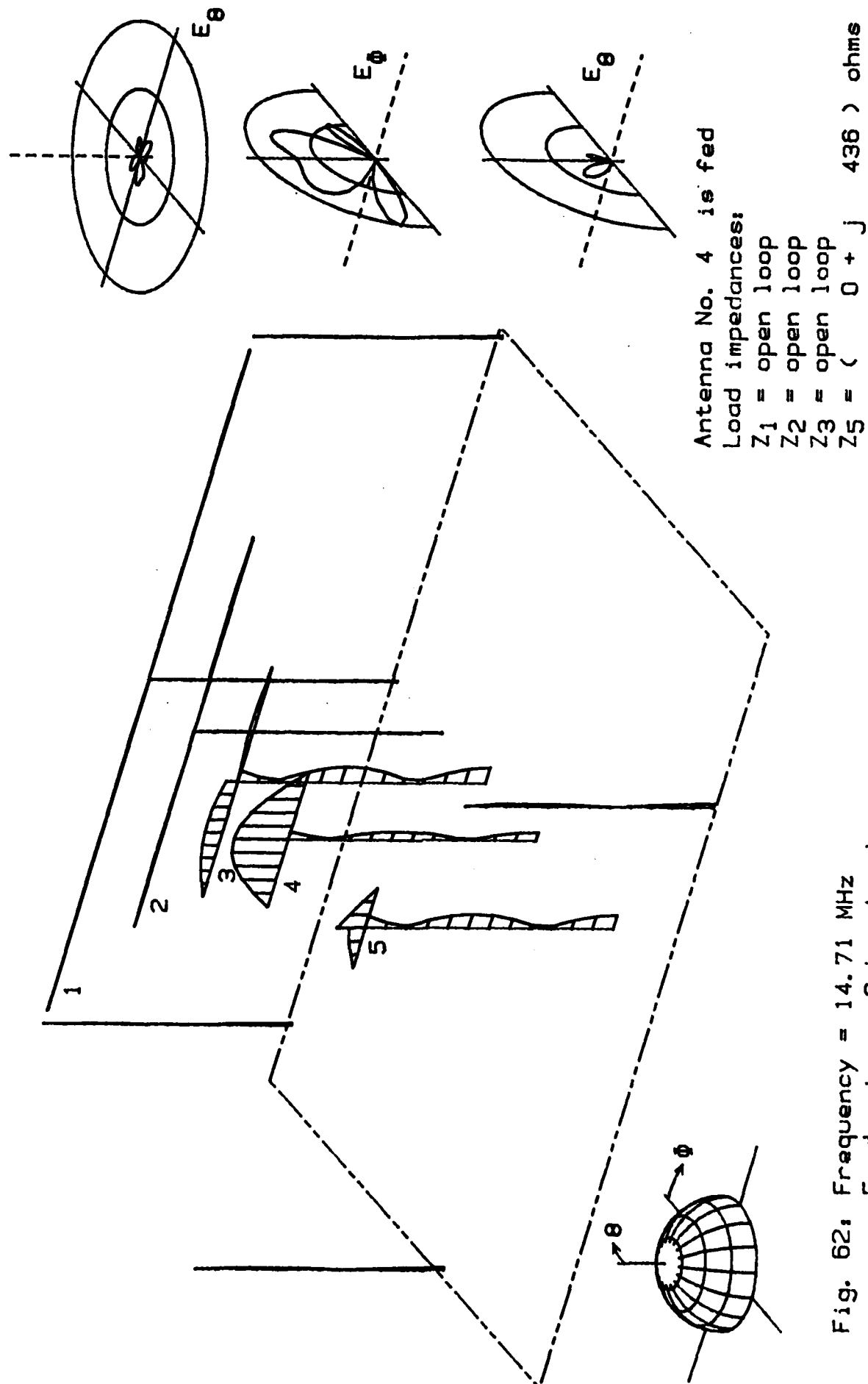
I-Code 010 / 14.71 MHz
P-Code 010 / 14.71 MHz

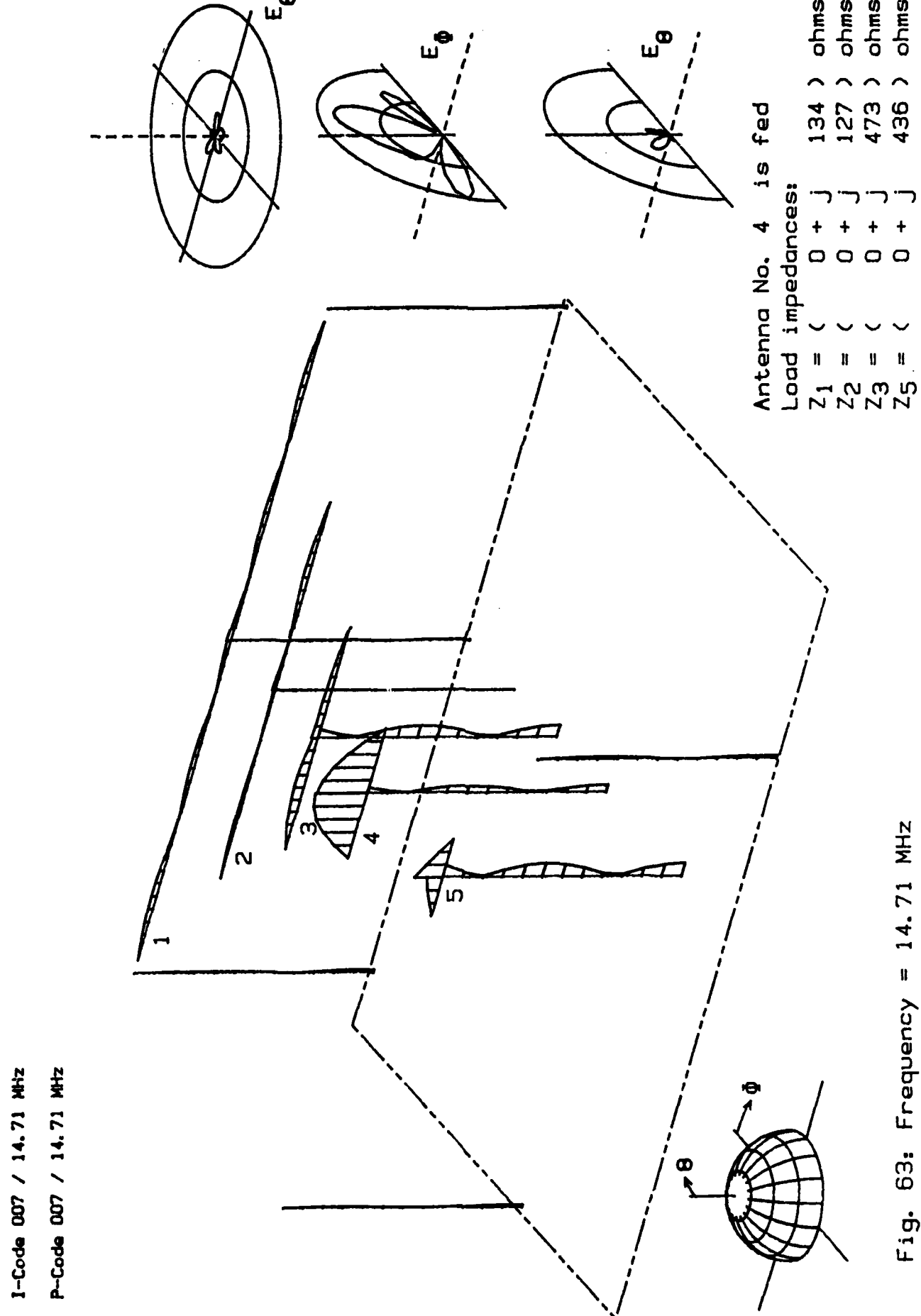




I-Code 009 / 14.71 MHz
P-Code 009 / 14.71 MHz

- 90 -





10. Analysis at 25 MHz. Feeder type: Cobra head.

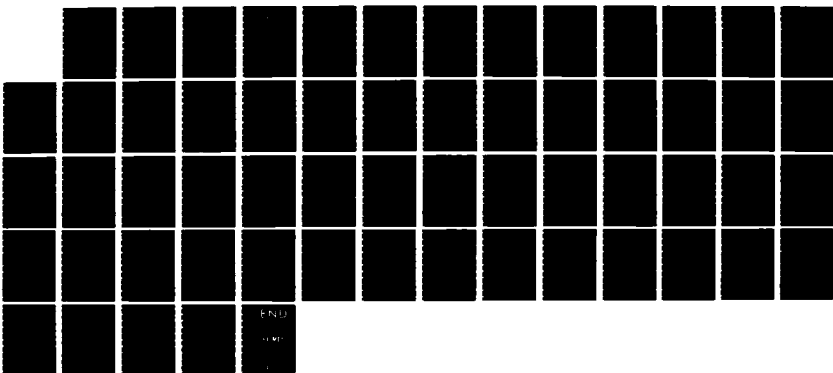
Table 5 shows the Z-matrix for 25 MHz and cobra-head feeding. Figs. 64 through 68 show the generic cases. As the center frequency of antenna 5 is 25 MHz, only this antenna is intended for actual use at this frequency. Thus, Fig. 64 with antenna 5 being fed is of major interest.

In Fig. 64 the remaining antennas are open loop terminated. At this frequency the feeder lines and poles have a length which is 1.5 times the free-space wavelength; therefore, the sheath current along the feeder line shows high values in this and all subsequent cases. Due to the height of the antenna the radiation pattern of the horizontally polarized field has many sidelobes.

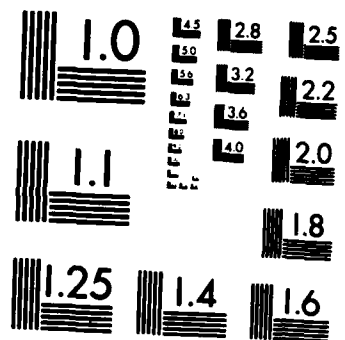
Figs. 69 through 74 show several interesting cases.

AD-A162 736 AN INVESTIGATION INTO PRINCIPLES FOR DESIGN OF A
MULTIPLE DIPOLE HF (HIGH) (U) HOCHSCHULE DER BUNDESWEHR
MUNICH (GERMANY F R) INST FOR HIGH- G FLACHENECKER
UNCLASSIFIED 15 JUN 84 R/D-4419-EE-09 DAJA45-83-M-0274 F/G 9/5 NL

272



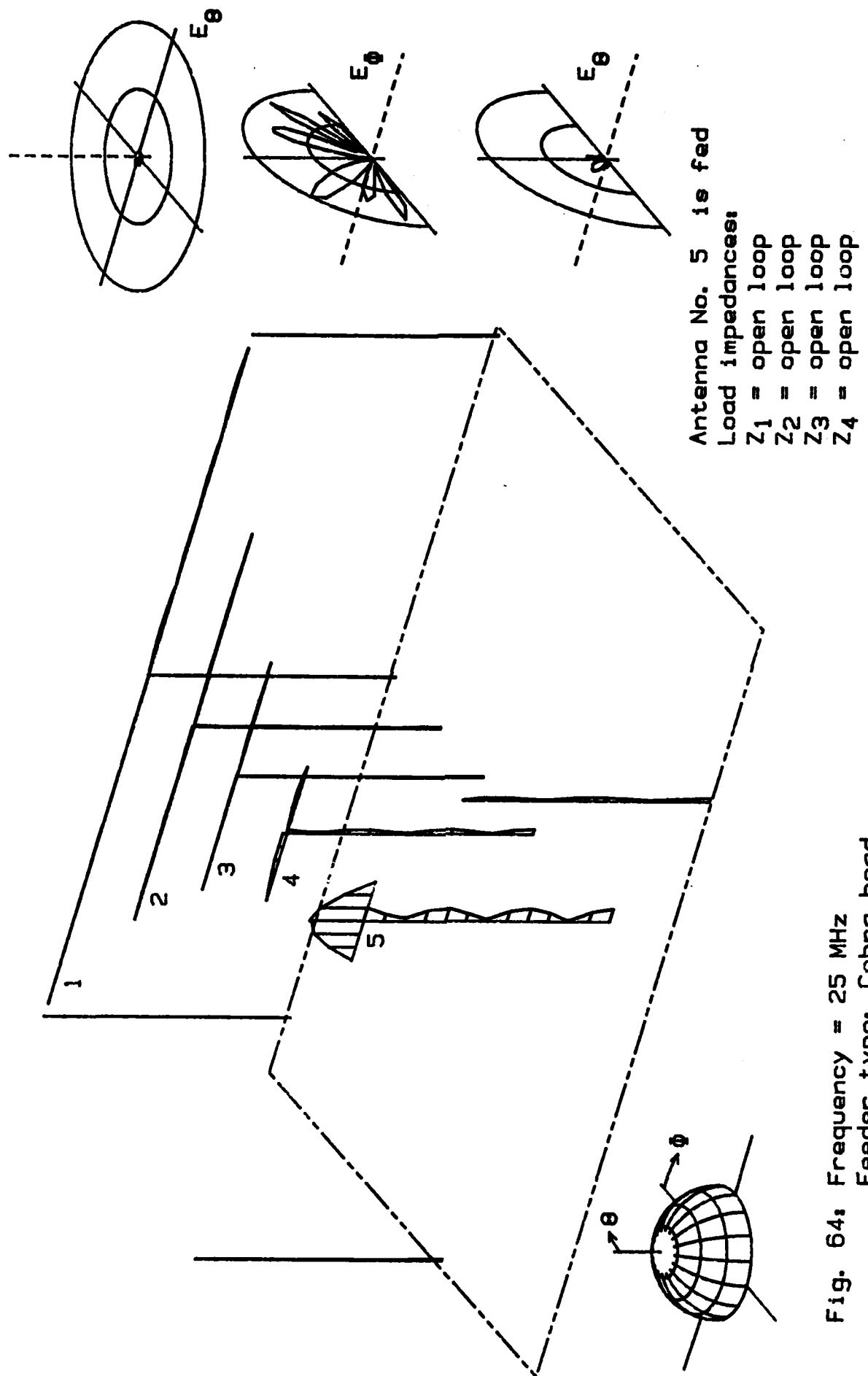
END

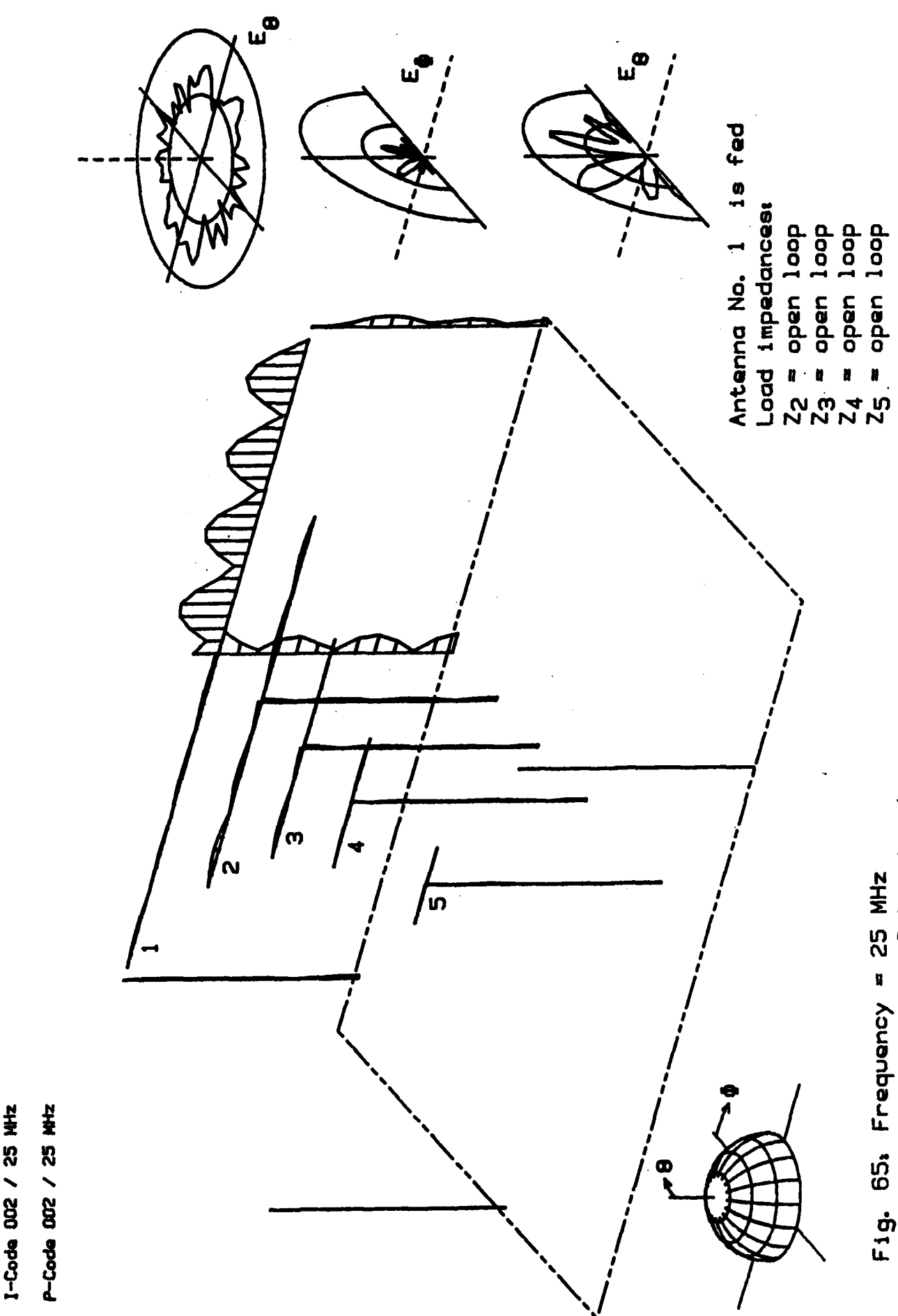


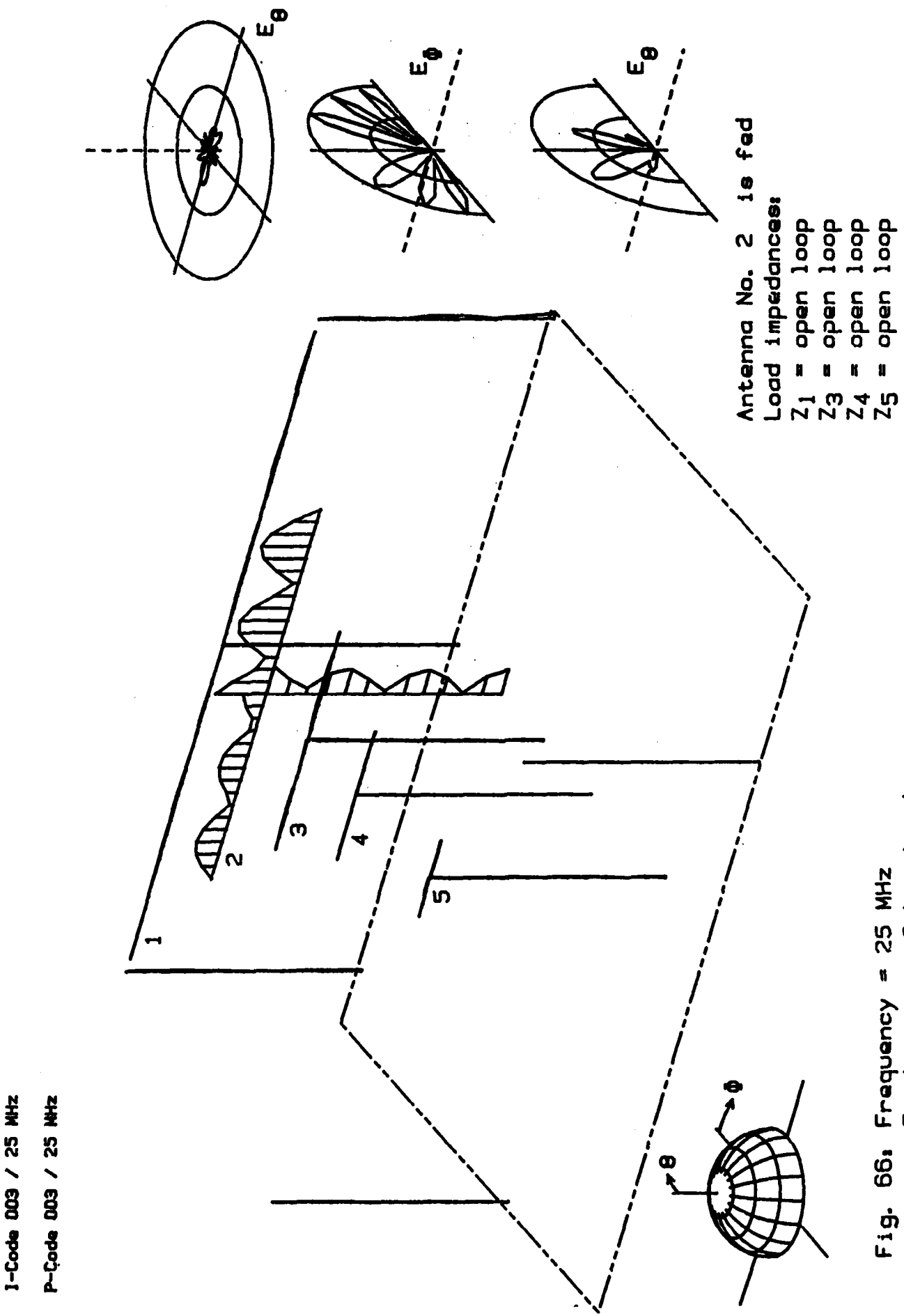
MICROCOPY RESOLUTION TEST CHART
NATIONAL BUREAU OF STANDARDS-1963-A

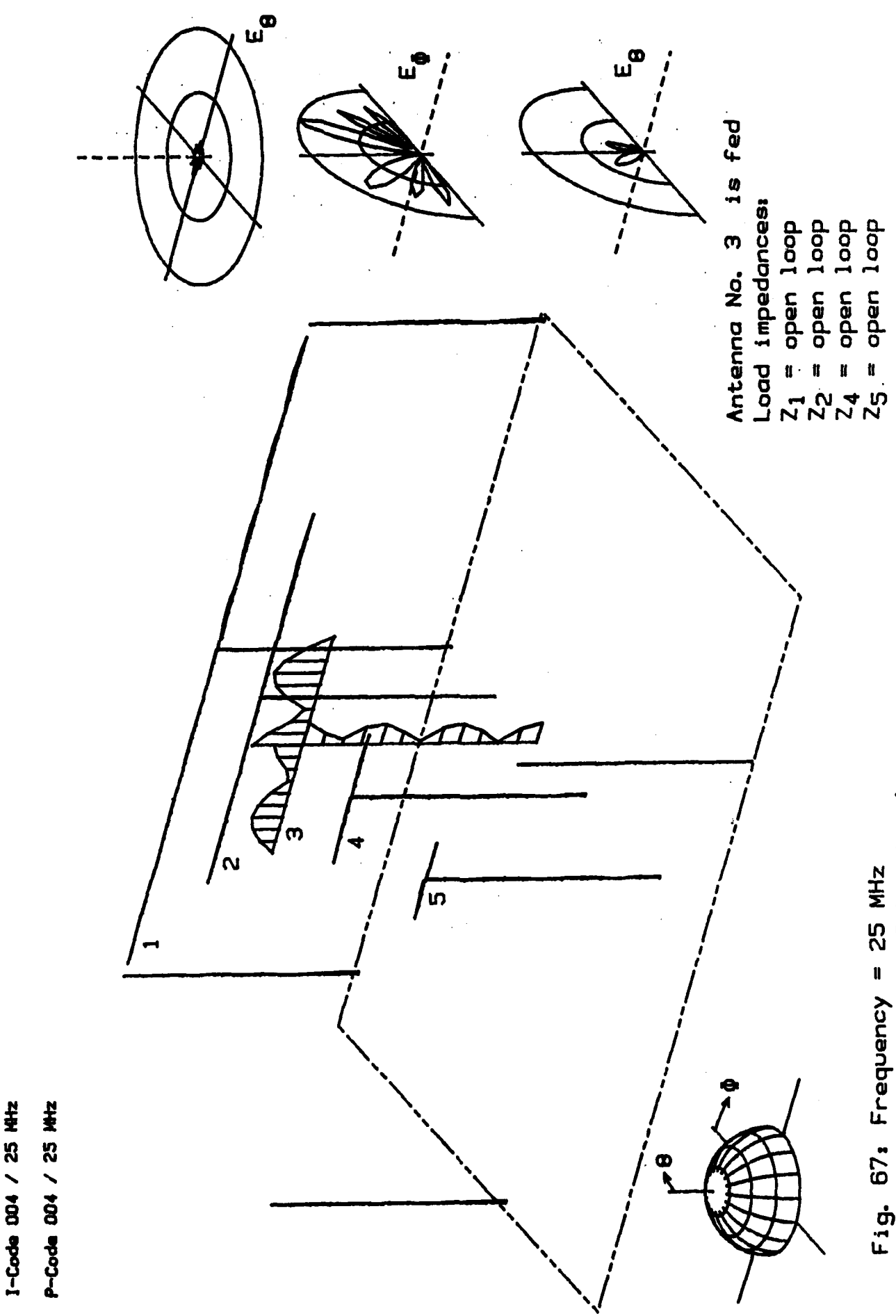
$L_{11} =$	$(480.27-j740)$ ohms	$L_{12} =$	$(7.21-j~11)$ ohms	$L_{13} =$	$(18.61-j~5)$ ohms	$L_{14} =$	$(20.65-j~5)$ ohms	$L_{15} =$	$(8.08+j~11)$ ohms
$L_{21} =$	$(6.90-j~11)$ ohms	$L_{22} =$	$\underline{(85.19-j~153)}$ ohms	$L_{23} =$	$(16.20-j~16)$ ohms	$L_{24} =$	$(-8.26-j~5)$ ohms	$L_{25} =$	$(2.30-j~8)$ ohms
$L_{31} =$	$(18.54-j~5)$ ohms	$L_{32} =$	$(16.26-j~16)$ ohms	$L_{33} =$	$\underline{(65.96-j~141)}$ ohms	$L_{34} =$	$(20.29-j~11)$ ohms	$L_{35} =$	$(6.22-j~3)$ ohms
$L_{41} =$	$(20.93-j~4)$ ohms	$L_{42} =$	$(-8.42-j~6)$ ohms	$L_{43} =$	$\underline{(20.22-j~11)}$ ohms	$L_{44} =$	$(175.48+j~421)$ ohms	$L_{45} =$	$(1.21+j~17)$ ohms
$L_{51} =$	$(8.11+j~11)$ ohms	$L_{52} =$	$(2.29-j~8)$ ohms	$L_{53} =$	$(6.22-j~3)$ ohms	$L_{54} =$	$(1.22+j~17)$ ohms	$L_{55} =$	$\underline{(66.64-j~8)}$ ohms

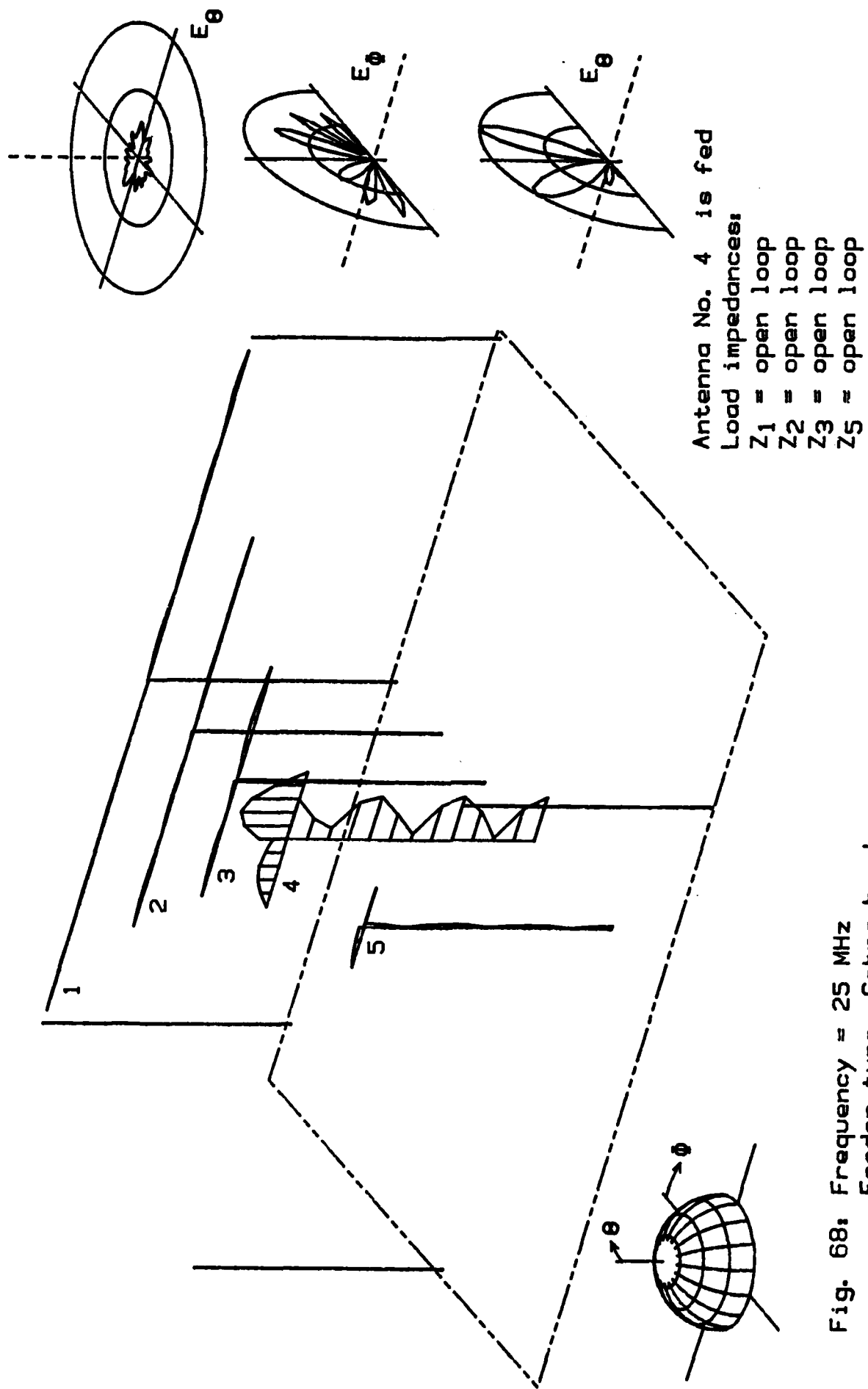
Table 5: Z-Matrix for f = 25 MHz. Feeder type: Cobra head.

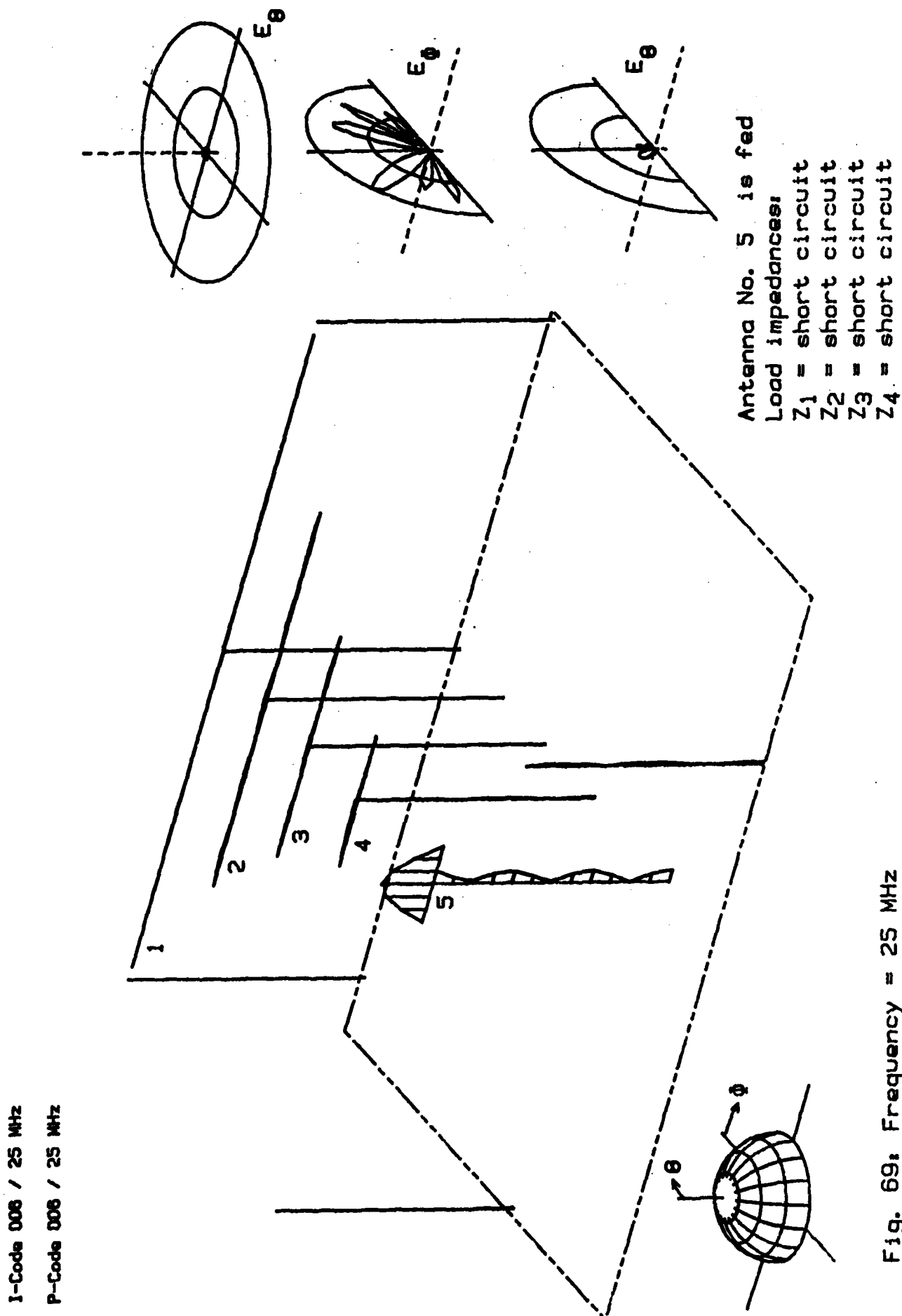


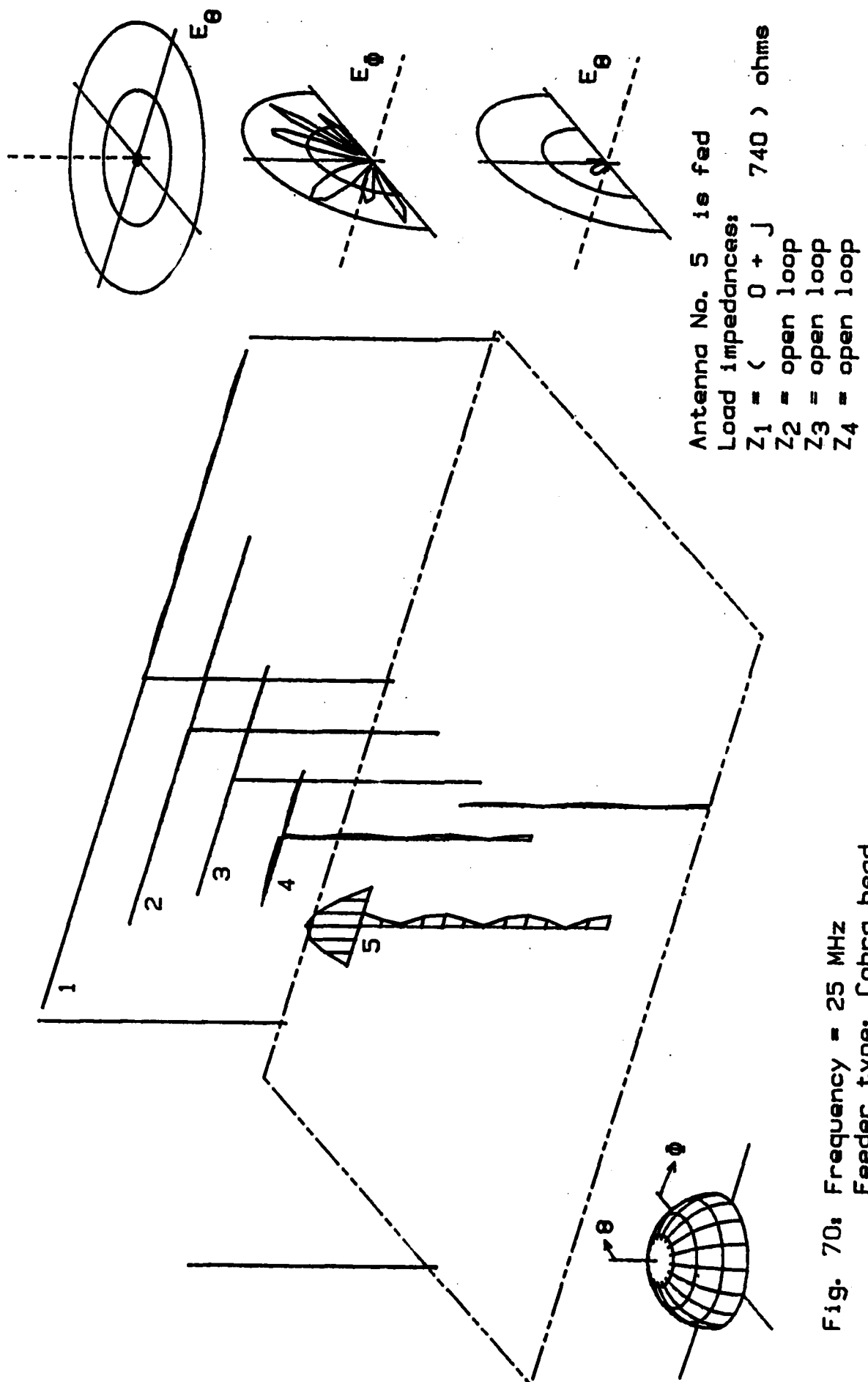


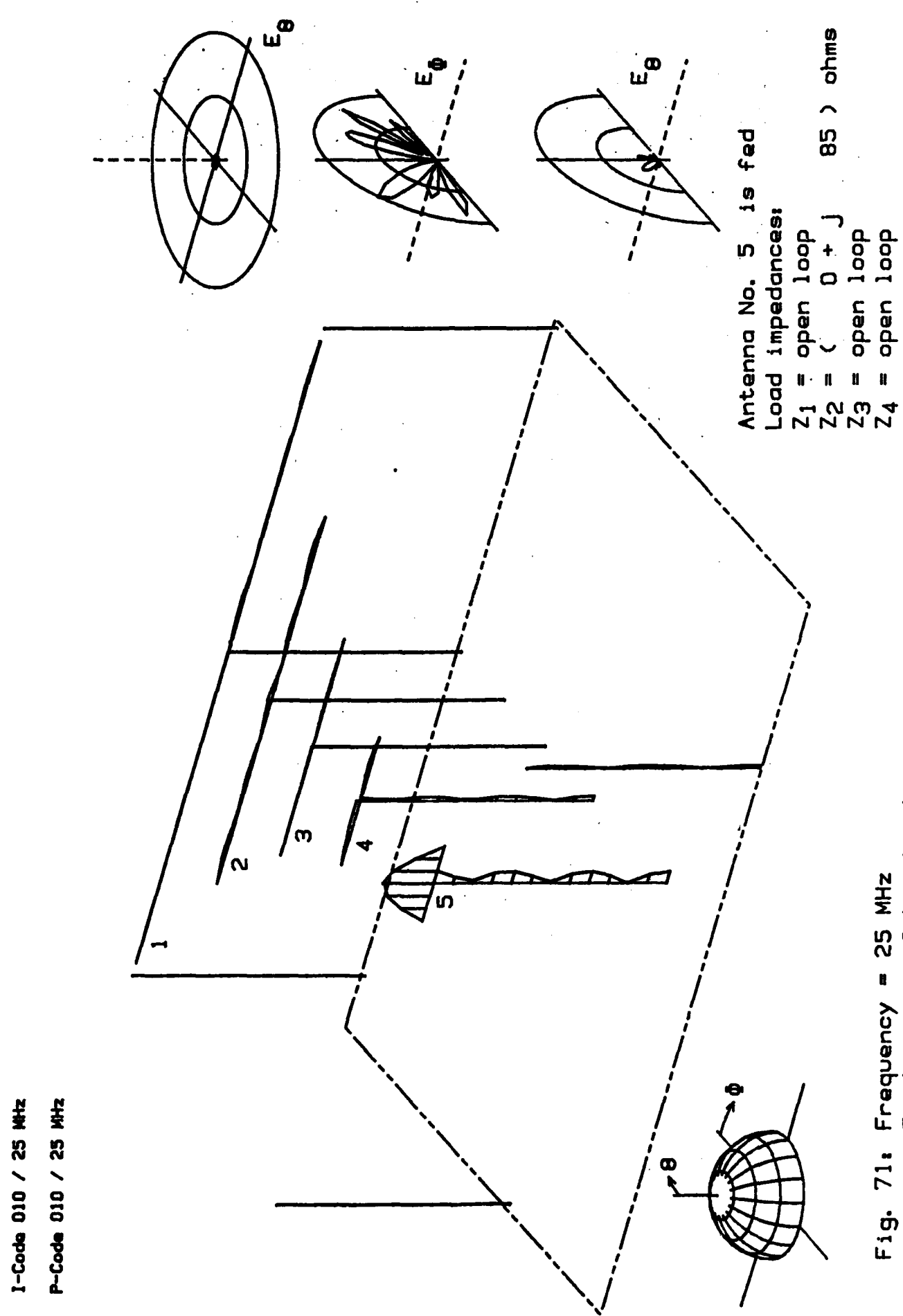


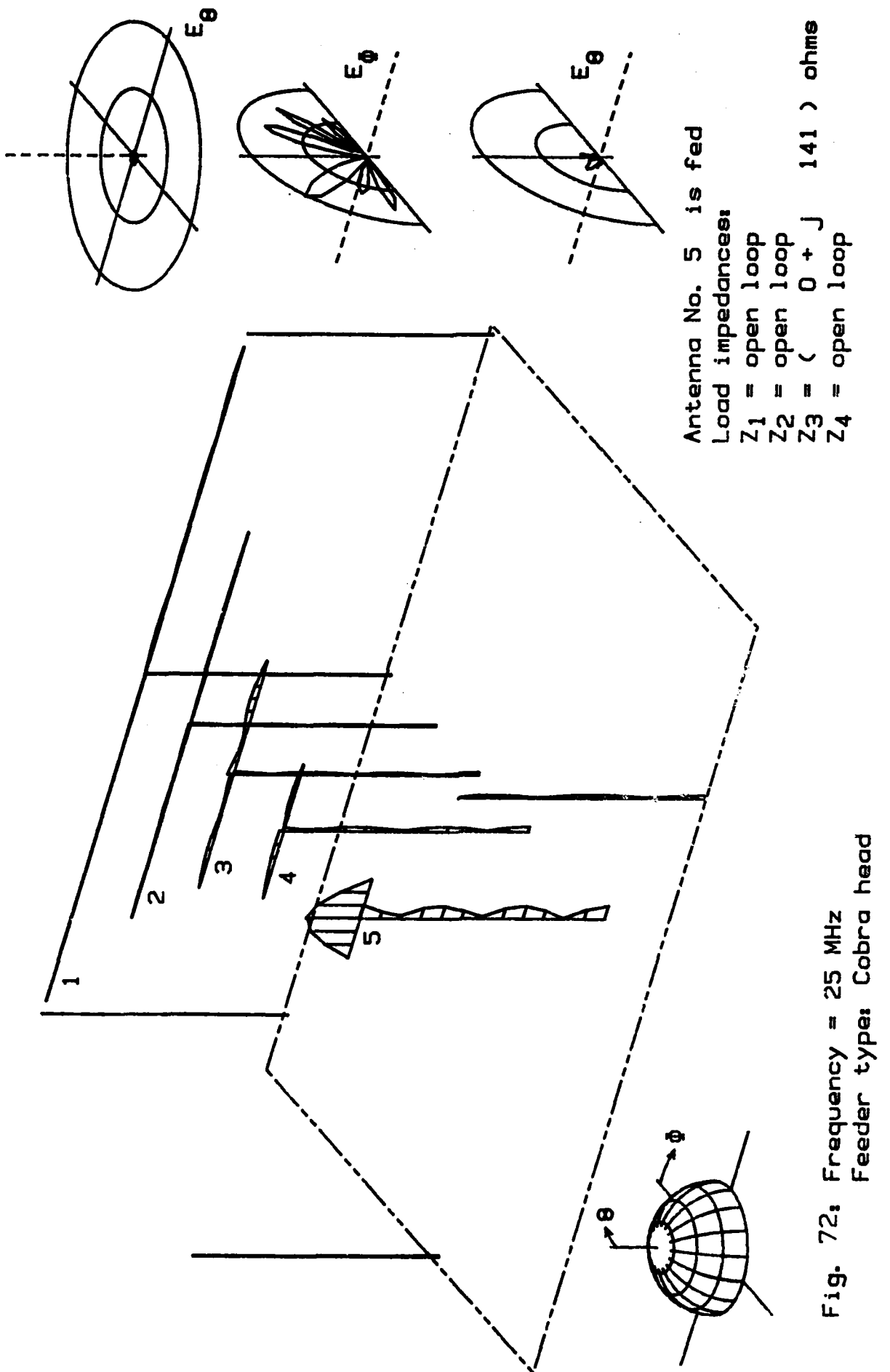


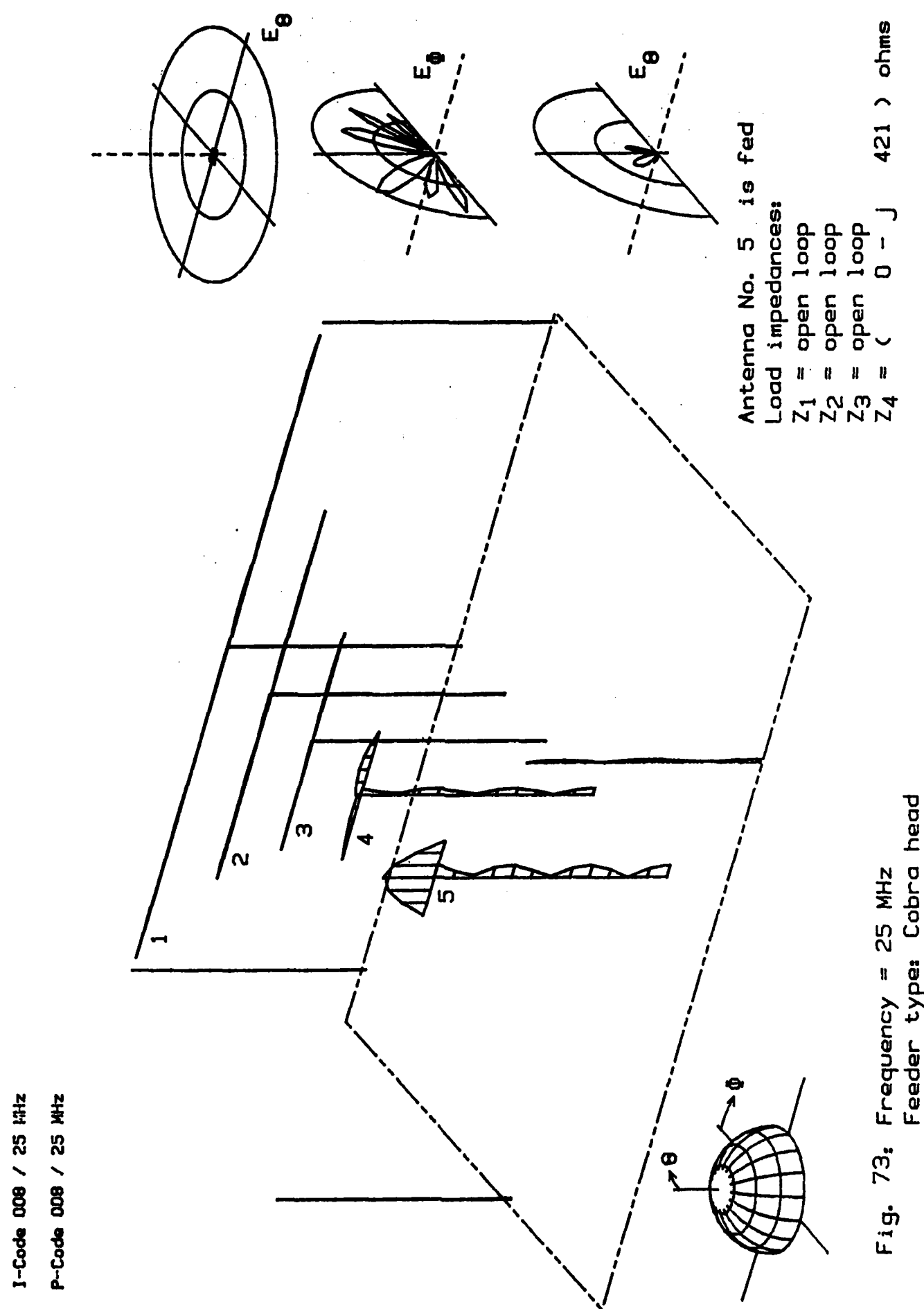


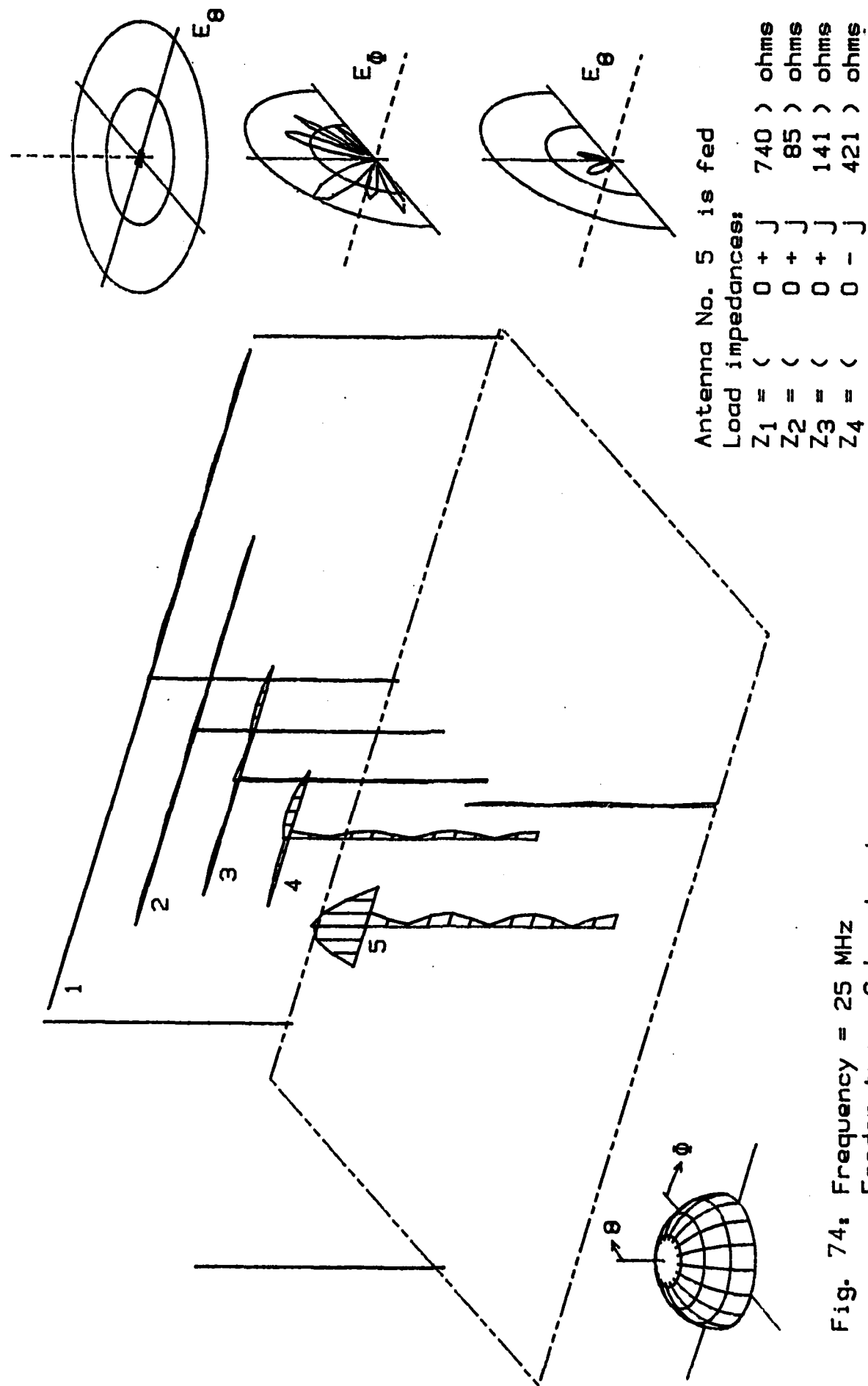












I-Code 007 / 25 MHz
P-Code 007 / 25 MHz

11. Analysis for the Feeder Type: Baluns at the Dipole Centers.

In the following, the same antenna configuration as in the preceding cases is analyzed. The only difference is the use of baluns at the antenna centers for symmetrical feeding of the antennas. In this case the balun as shown in Fig. 6a is used. A first glance at the results shows that all resonance problems concerning the feeder lines have disappeared. Feeder-line currents are no longer a problem.

In summary the results are presented in the following Tables and Figures:

3 MHz: Z-matrix in Table 6, page 108.

Selected cases of current distribution and radiation patterns in Figs. 75 through 81, pages 109 to 115.

5.1 MHz: Z-matrix in Table 7, page 116.

Selected cases of current distribution and radiation patterns in Figs. 82 through 88, pages 117 to 123.

8.66 MHz: Z-matrix in Table 8, page 124.

Selected cases of current distribution and radiation patterns in Figs. 89 through 95, pages 125 to 131.

14.71 MHz: Z-matrix in Table 9, page 132.

Selected cases of current distribution and radiation patterns in Figs. 96 through 102, pages 133 to 139.

25 MHz: Z-matrix in Table 10, page 140.

Selected cases of current distribution and radiation patterns in Figs. 103 through 109, pages 141 to 147.

The cases are selected under the same conditions as the previous investigations with the cobra head feeder. In one area, however,

a slight variation was necessary. In the case of the cobra head feeder, resonance terminations were chosen to cancel the imaginary part of the internal impedance of the respective antenna. In all these cases the real part of the load termination was assumed to be zero. This was allowed since the real part of the parasitically coupled antennas was rather high due to the radiation resistance produced by the sheath current along the feeder line. If, for instance, the internal impedance Z_{55} of antenna 5 at 3 MHz is noted in Table 1, a value of $Z_{55} = (370.1-j832)$ ohms can be read. In the case of the balun feeder, however, there are no feeder-sheath currents and, thus, the radiation resistance of the electrically short antenna is very low, as known from ideal short antenna theory. With the balun feeder at 3 MHz, the same antenna 5 shows an internal impedance $Z_{55} = (0.66-j3810)$ ohms. If in this case a load termination of $Z_5 = (0+j3810)$ ohms was assumed, the resulting resonance would result in a Q-factor of more than 5000. This would be quite unrealistic and would cause strange results in the current distribution and the radiation patterns.

Therefore, for the balun feeders, resonance terminations have been chosen which restrict the Q-factor of the respective resonance to the value 100. In Fig. 78, for instance, the real part of Z_3 is chosen to be 14 ohms which is 1/100 of the imaginary part of 1393 ohms. This selection of the load terminations is responsible due to the attenuation of the feeder lines.

The results in Figs. 75 through 109 show a rather ideal behaviour of the antenna arrangement. The major drawbacks of this system are:

- (a) A strong coupling between antenna 1 and poles 1 and 2 within the 3 MHZ frequency band.
- (b) A strong coupling between adjacent antennas if these

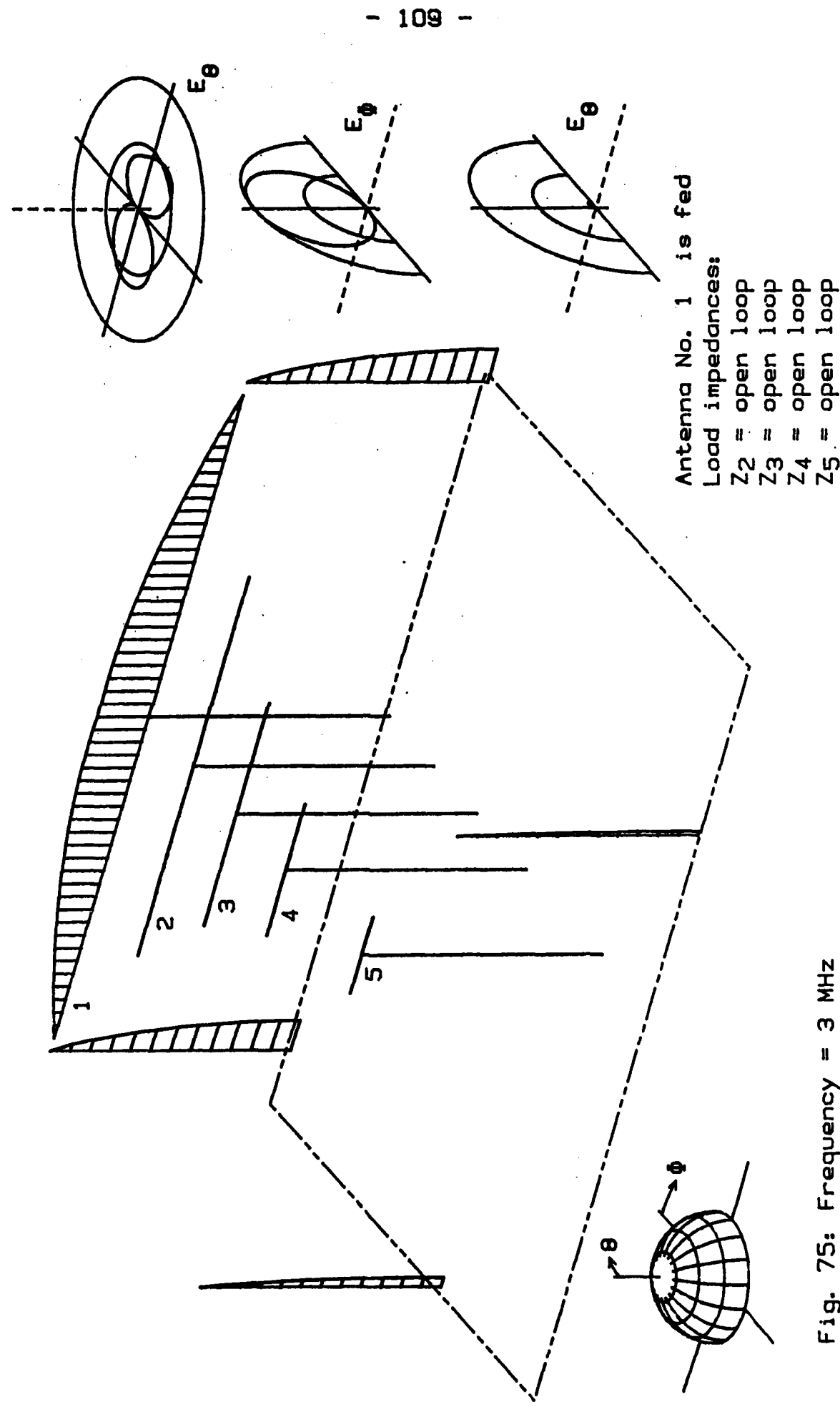
antennas are resonance terminated.

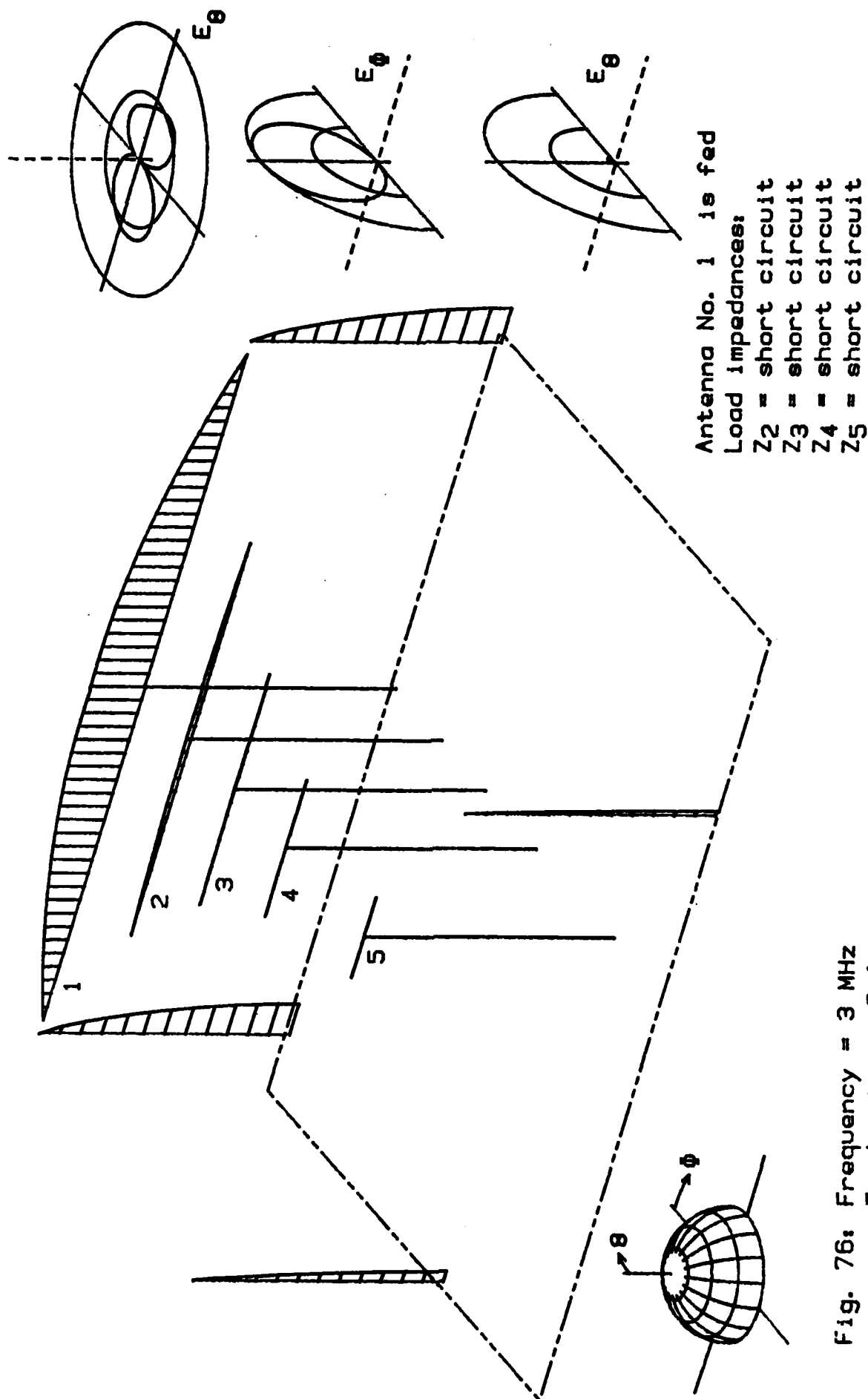
- (c) Many sidelobes at higher frequencies radiated from antennas 4 and 5 due to the fact that these antennas are mounted on the same level above ground as the lower frequency antennas. The mirror image of these antennas, which is separated by double the mounting height produces these side-lobe patterns at the higher frequencies.

$Z_{11} = (-112.71+j134) \text{ ohms}$	$Z_{12} = (49.58+j35) \text{ ohms}$	$Z_{13} = (24.30+j12) \text{ ohms}$	$Z_{14} = (11.76+j2) \text{ ohms}$	$Z_{15} = (4.97-j1) \text{ ohms}$
$Z_{21} = (49.63+j35) \text{ ohms}$	$Z_{22} = (22.89-j660) \text{ ohms}$	$Z_{23} = (11.68-j17) \text{ ohms}$	$Z_{24} = (5.94-j1) \text{ ohms}$	$Z_{25} = (2.74-j0) \text{ ohms}$
$Z_{31} = (24.33+j12) \text{ ohms}$	$Z_{32} = (11.68-j17) \text{ ohms}$	$Z_{33} = (6.19-j1393) \text{ ohms}$	$Z_{34} = (3.31-j15) \text{ ohms}$	$Z_{35} = (1.66-j0) \text{ ohms}$
$Z_{41} = (11.76+j3) \text{ ohms}$	$Z_{42} = (5.94-j1) \text{ ohms}$	$Z_{43} = (3.31-j15) \text{ ohms}$	$Z_{44} = (1.87-j2370) \text{ ohms}$	$Z_{45} = (1.03-j2) \text{ ohms}$
$Z_{51} = (4.95-j1) \text{ ohms}$	$Z_{52} = (2.73-j0) \text{ ohms}$	$Z_{53} = (1.65-j0) \text{ ohms}$	$Z_{54} = (1.03-j2) \text{ ohms}$	$Z_{55} = (.66-j3810) \text{ ohms}$

Table 6: Z-Matrix for f = 3 MHz. Feeder type: Baluns at the dipole centers.

I-Code 001 / 3 MHz
P-Code 001 / 3 MHz





I-Code 002 / 3 MHz

P-Code 002 / 3 MHz

I-Code 004 / 3 MHz
P-Code 004 / 3 MHz

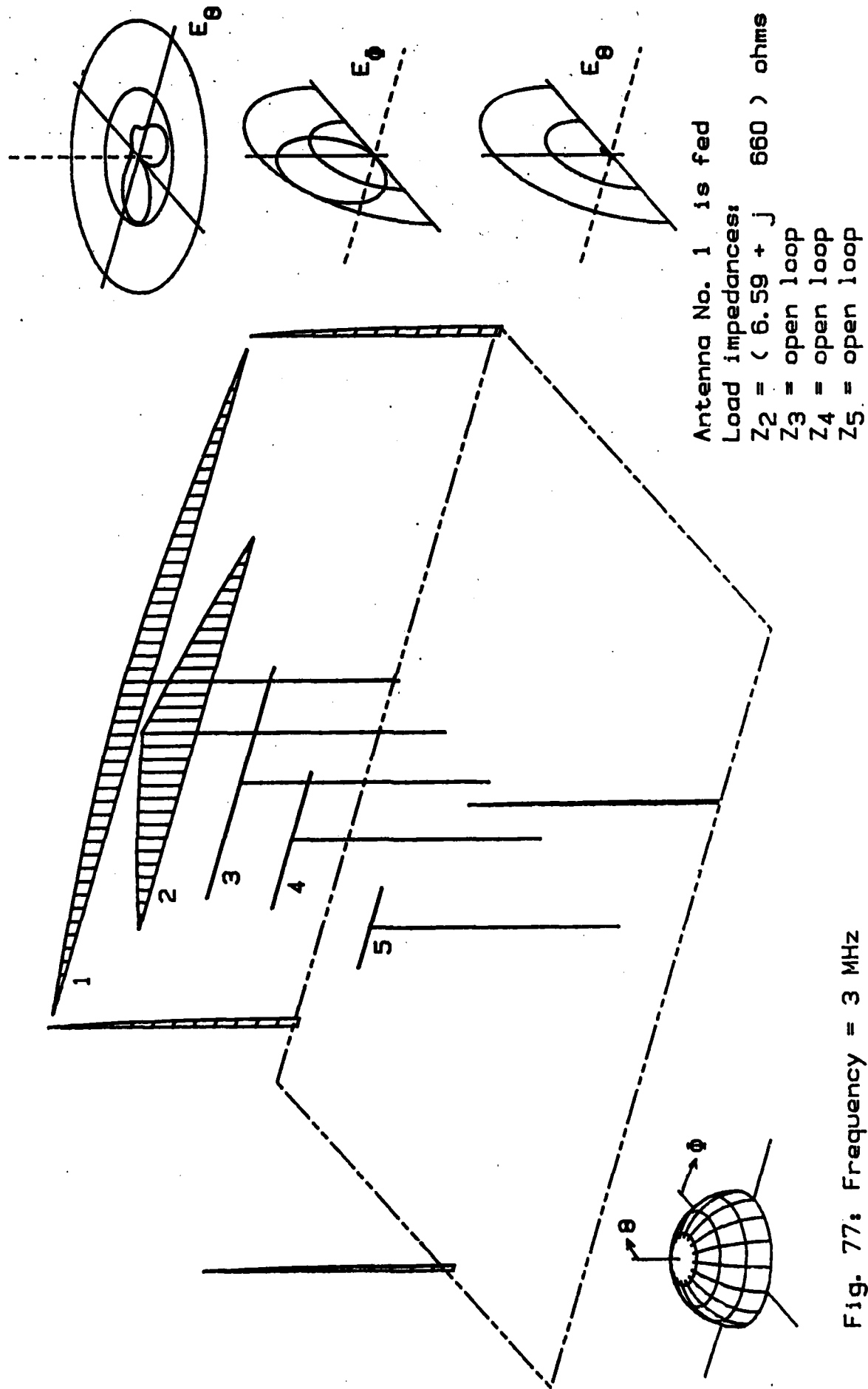
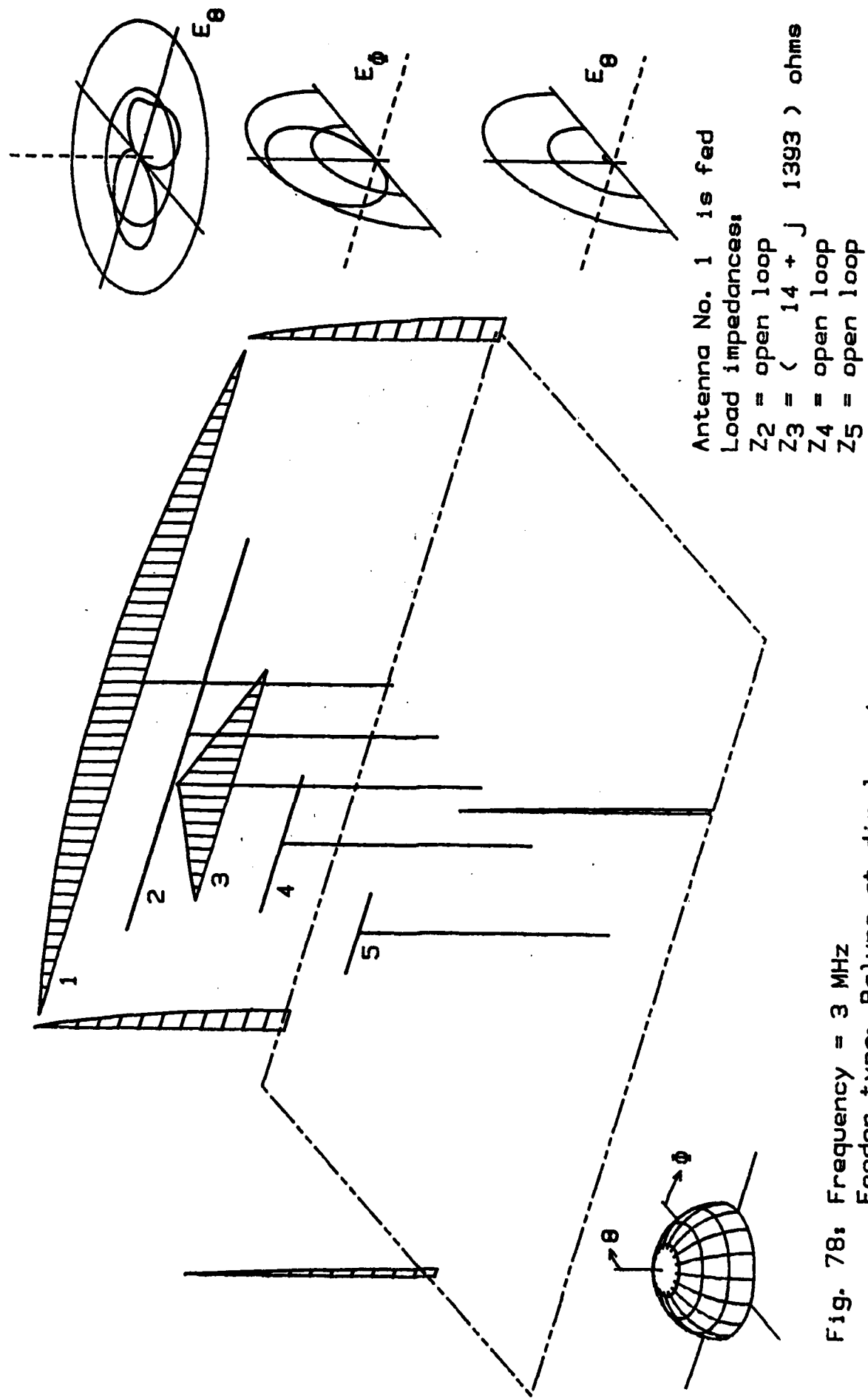


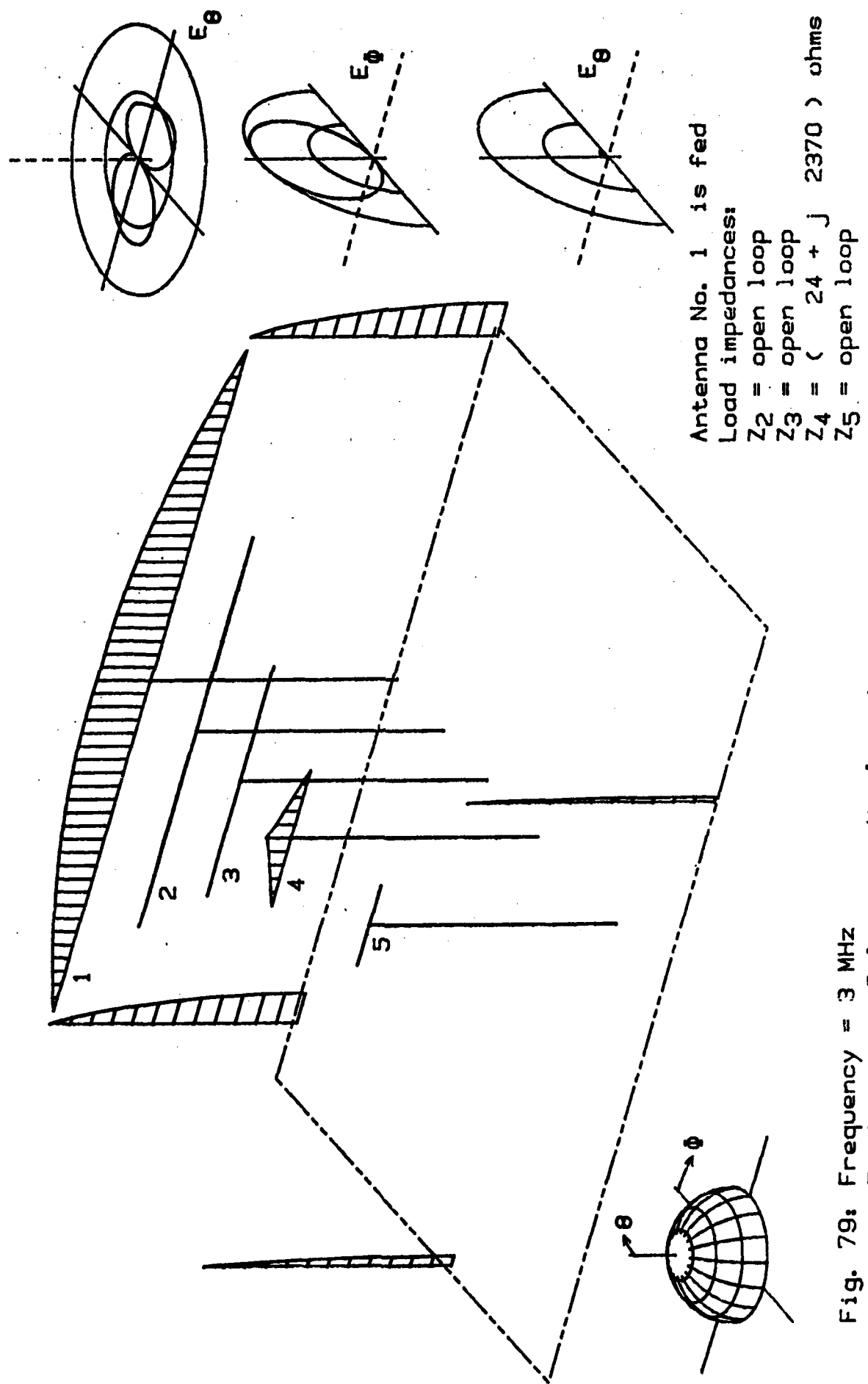
Fig. 77: Frequency = 3 MHz
Feeder type: Baluns at dipol centers

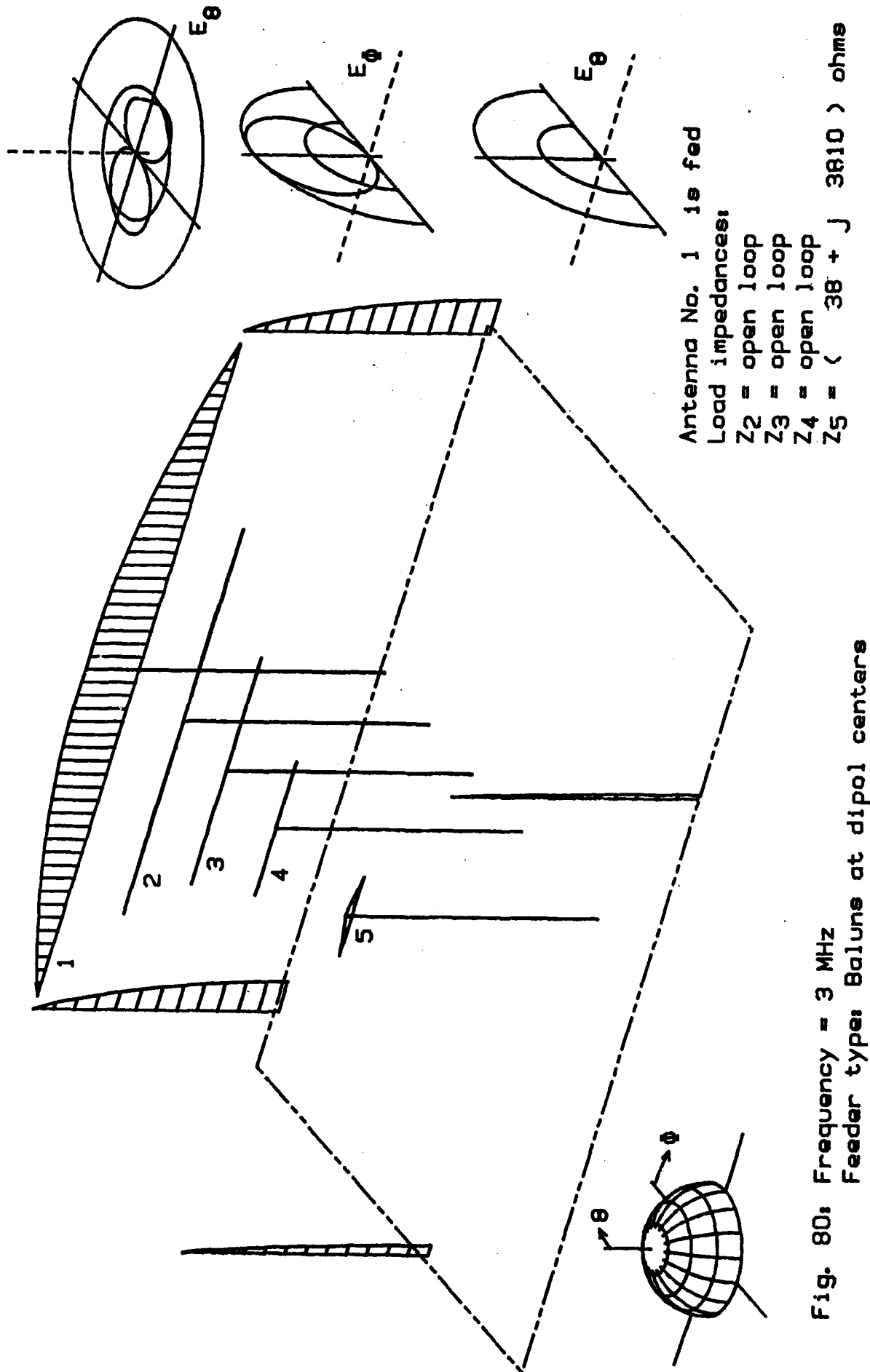
I-Code 005 / 3 MHz
P-Code 005 / 3 MHz

- 112 -

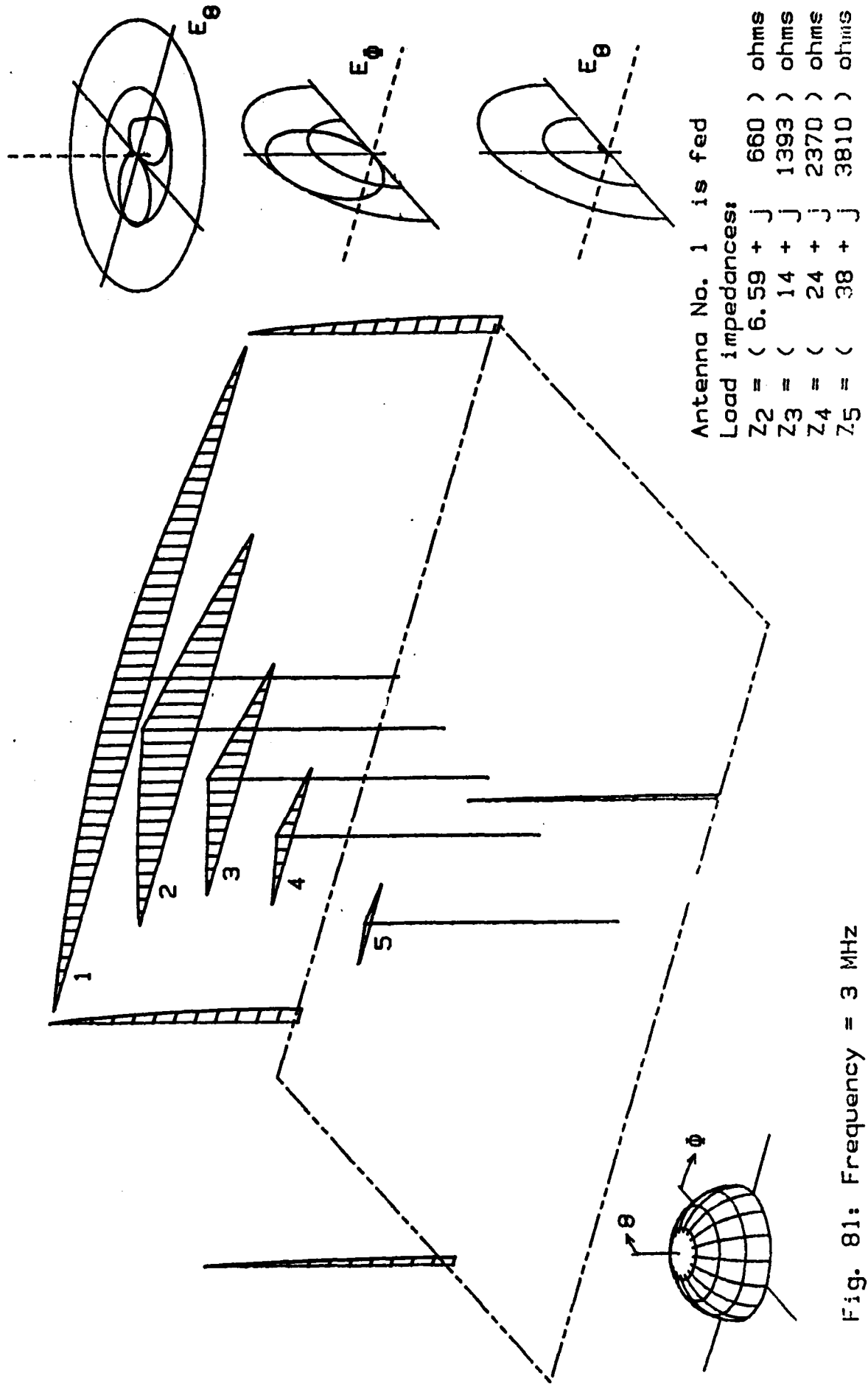


I-Code 006 / 3 MHz
P-Code 006 / 3 MHz





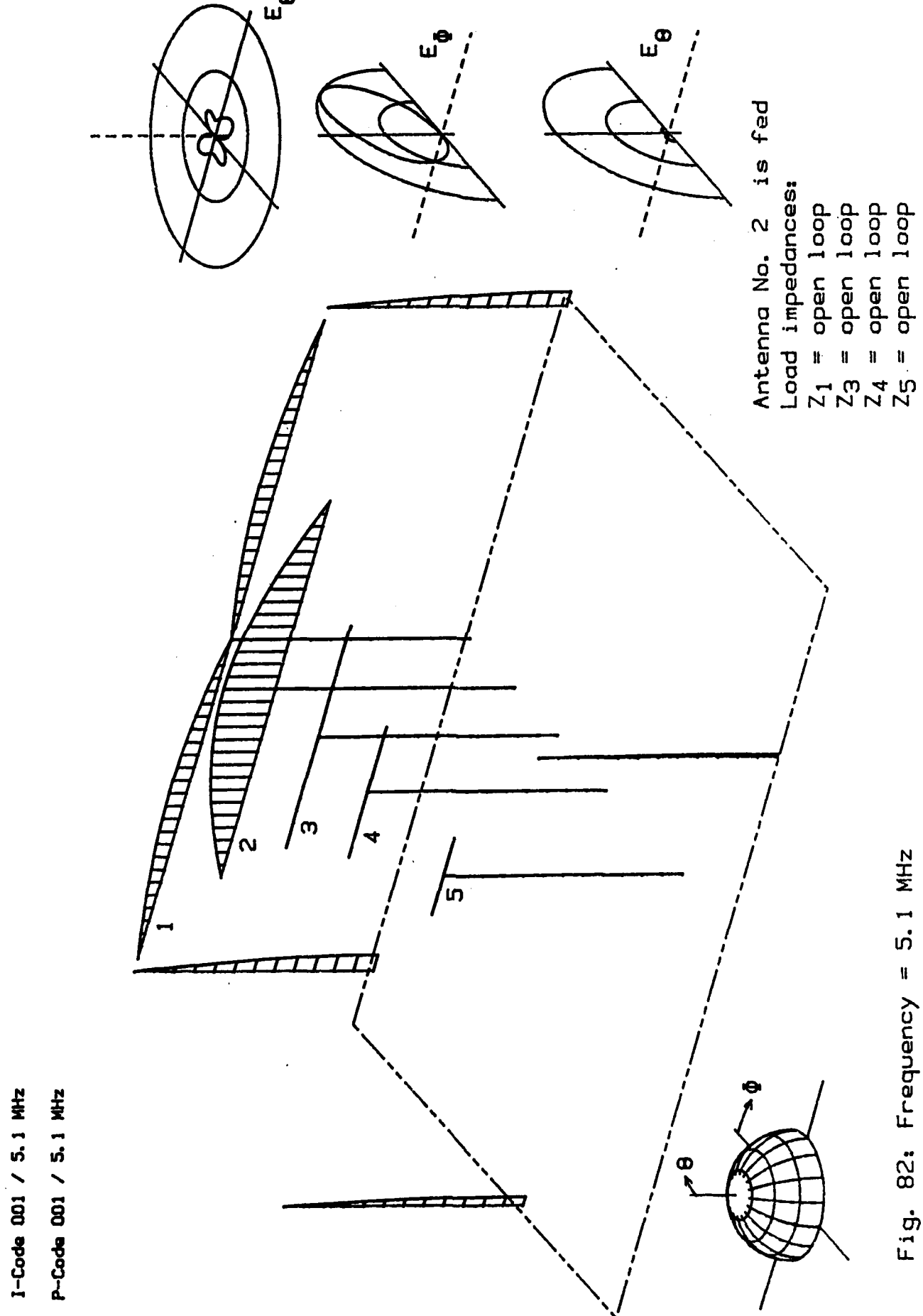
I-Code 003 / 3 MHz
P-Code 003 / 3 MHz

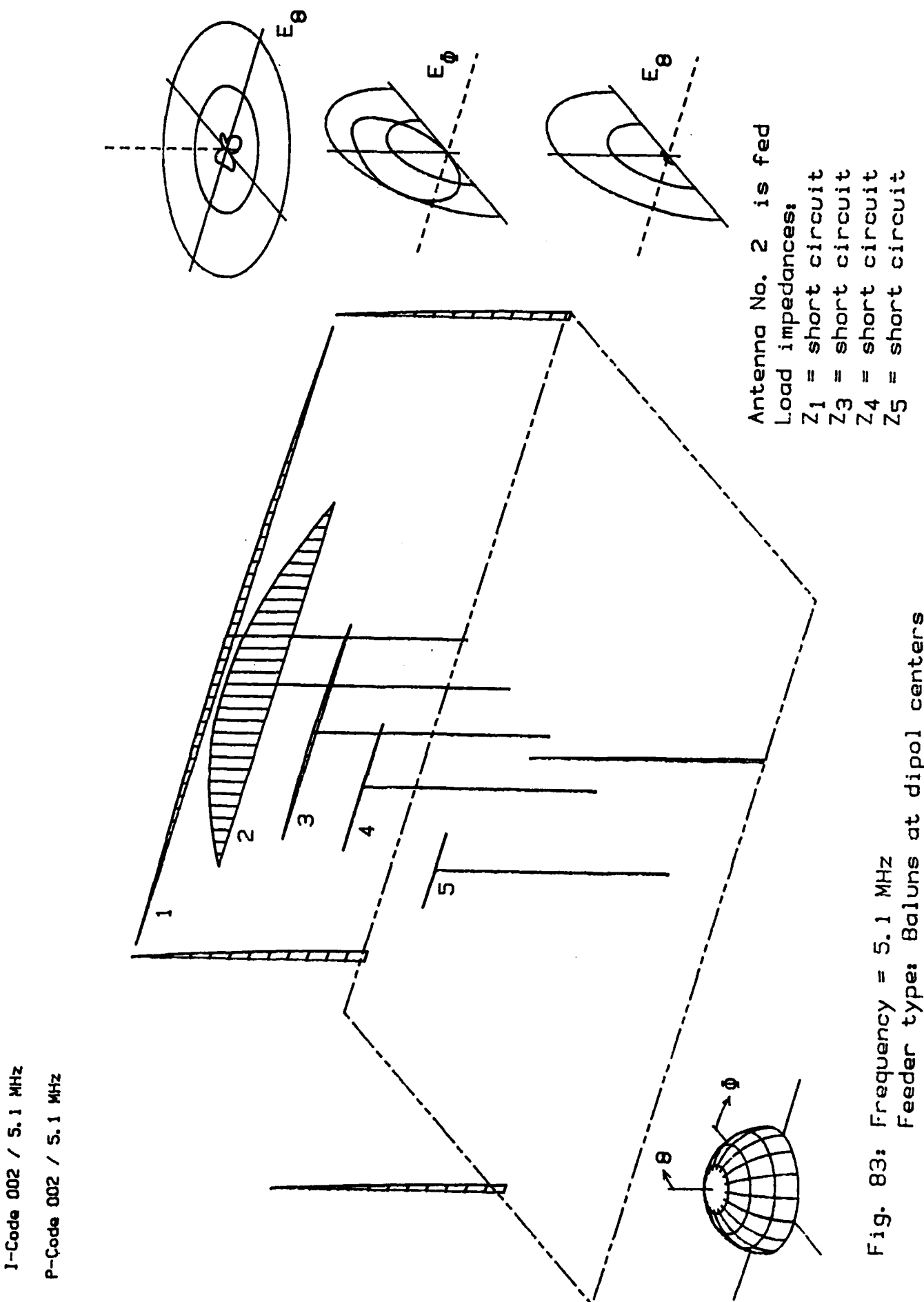


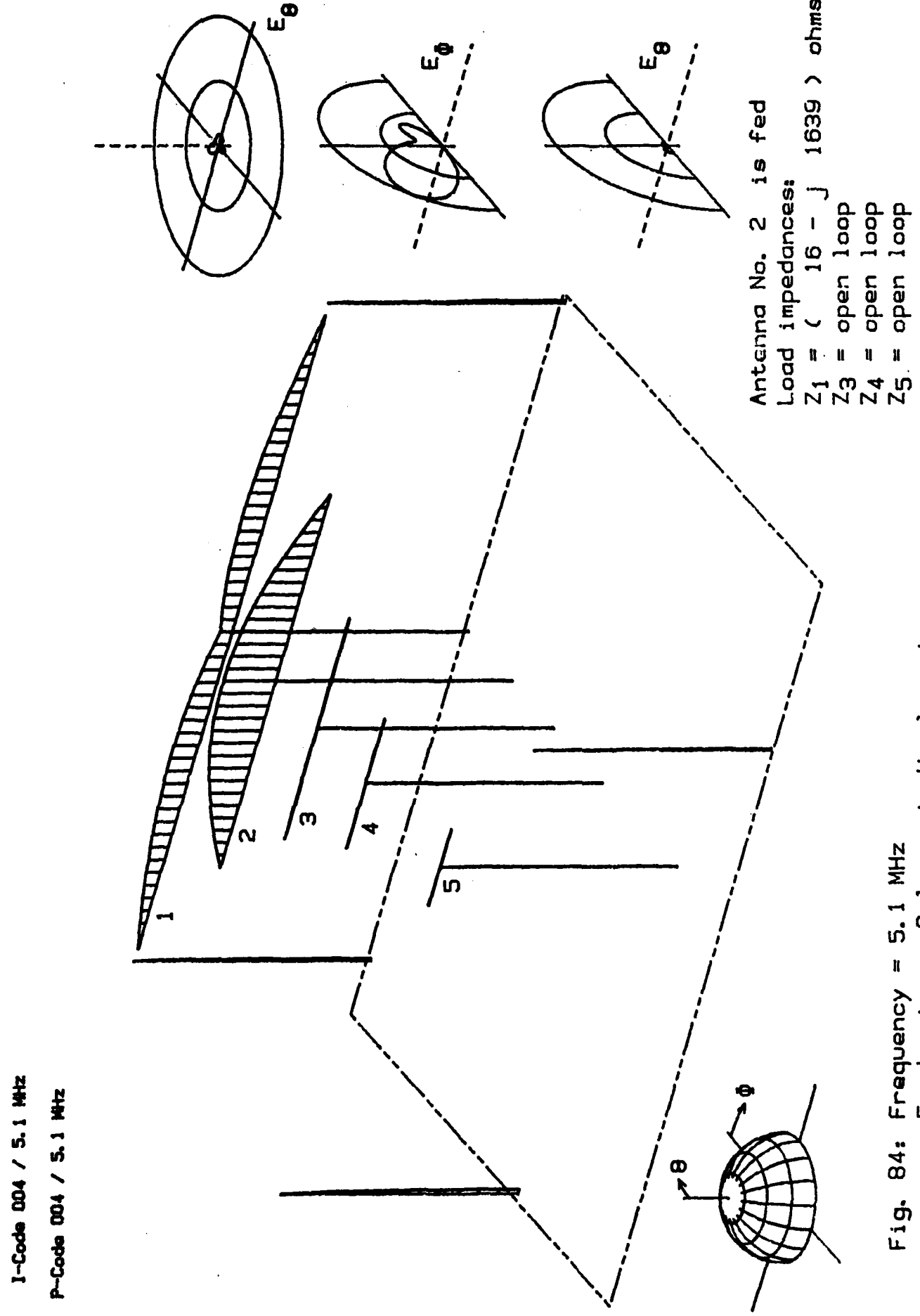
$z_{11} = (-1777.68 + j1639)$ ohms	$z_{12} = (-376.01 - j 117)$ ohms	$z_{13} = (98.29 - j 109)$ ohms	$z_{14} = (5.20 - j 62)$ ohms	$z_{15} = (-21.06 - j 17)$ ohms
$z_{21} = (375.88 - j 117)$ ohms	$z_{22} = (98.93 + j 9)$ ohms	$z_{23} = (36.29 - j 11)$ ohms	$z_{24} = (11.11 - j 9)$ ohms	$z_{25} = (-15 - j 5)$ ohms
$z_{31} = (98.22 - j 109)$ ohms	$z_{32} = (36.28 - j 11)$ ohms	$z_{33} = (18.36 - j 627)$ ohms	$z_{34} = (9.04 - j 6)$ ohms	$z_{35} = (2.98 - j 2)$ ohms
$z_{41} = (5.14 - j 62)$ ohms	$z_{42} = (11.10 - j 9)$ ohms	$z_{43} = (9.04 - j 6)$ ohms	$z_{44} = (6.29 - j 1294)$ ohms	$z_{45} = (3.30 - j 1)$ ohms
$z_{51} = (-21.14 - j 17)$ ohms	$z_{52} = (-19 - j 5)$ ohms	$z_{53} = (2.96 - j 2)$ ohms	$z_{54} = (3.29 - j 1)$ ohms	$z_{55} = (2.55 - j 2190)$ ohms

116 -

Table 7: Z-Matrix for $f = 5.1$ MHz. Feeder type: Baluns at the dipole centers.

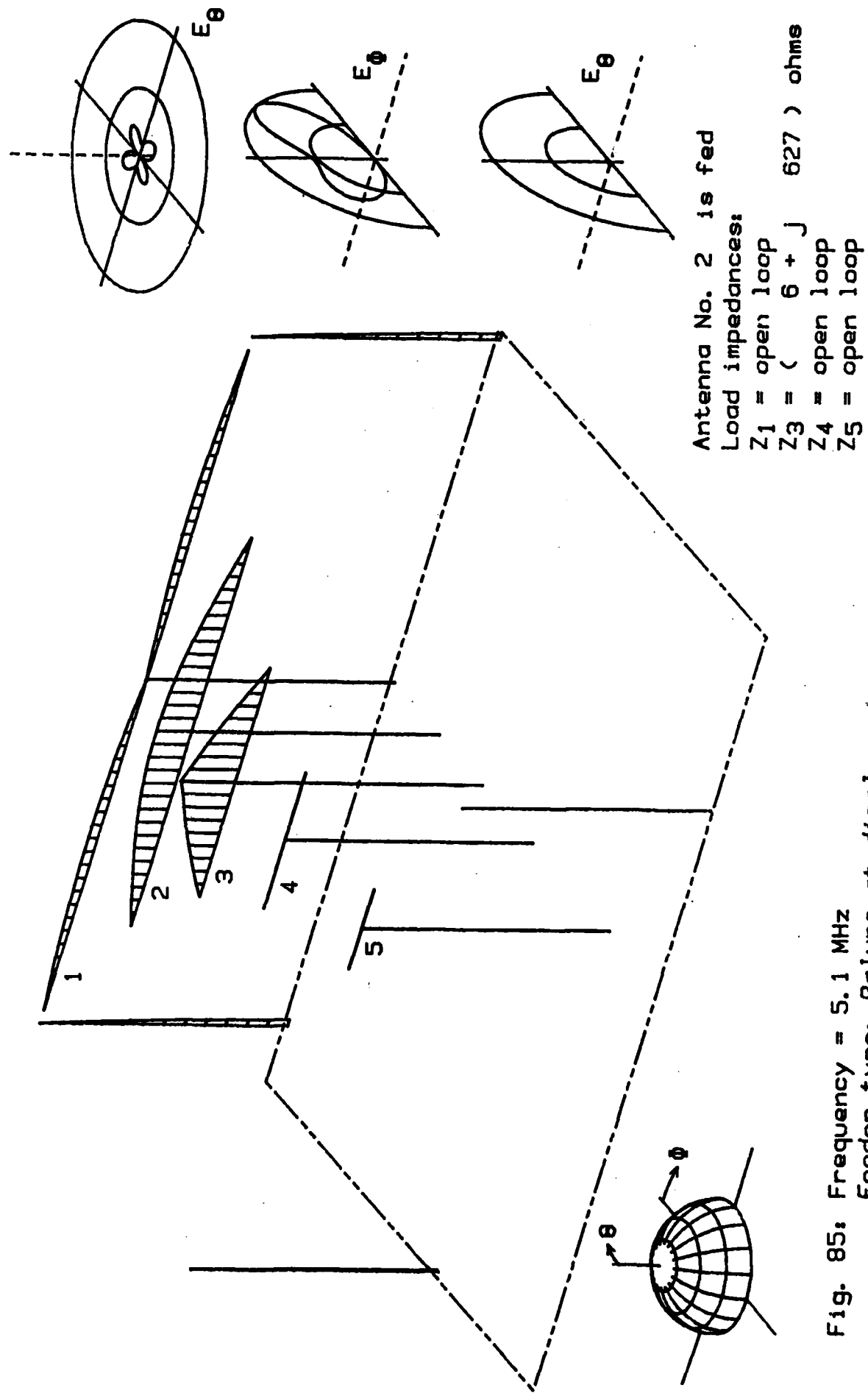


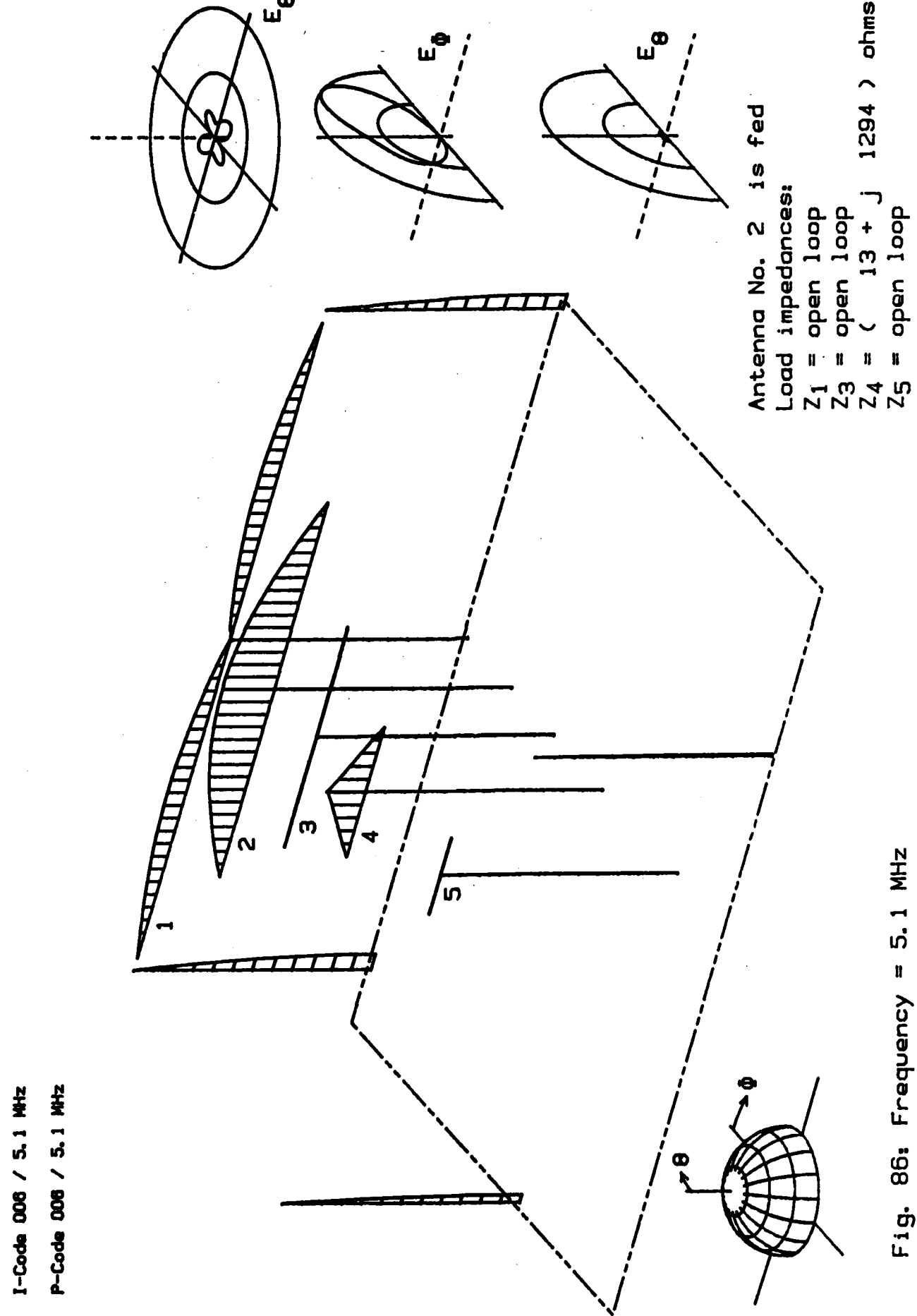




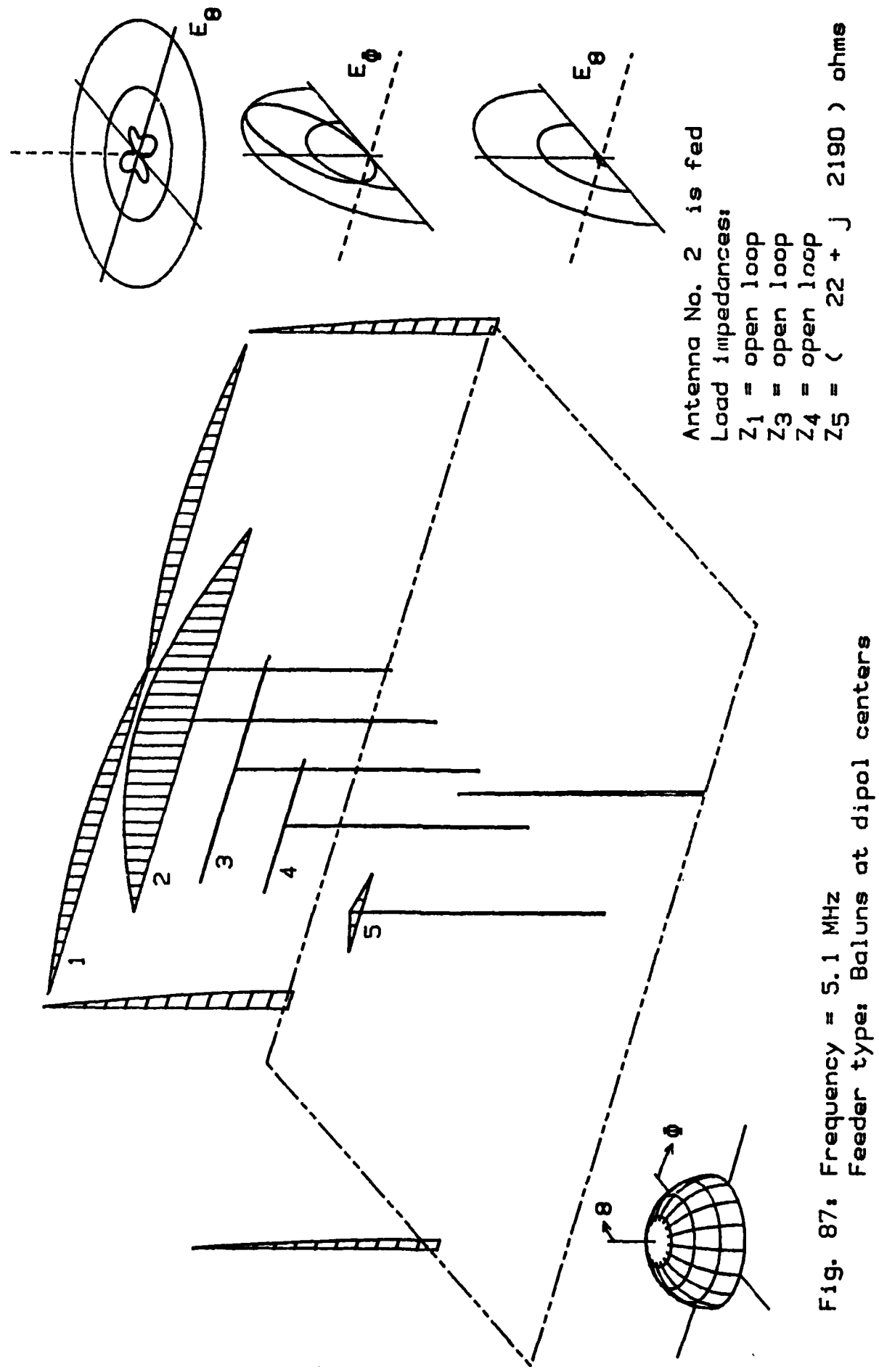
I-Code 005 / 5.1 MHz
P-Code 005 / 5.1 MHz

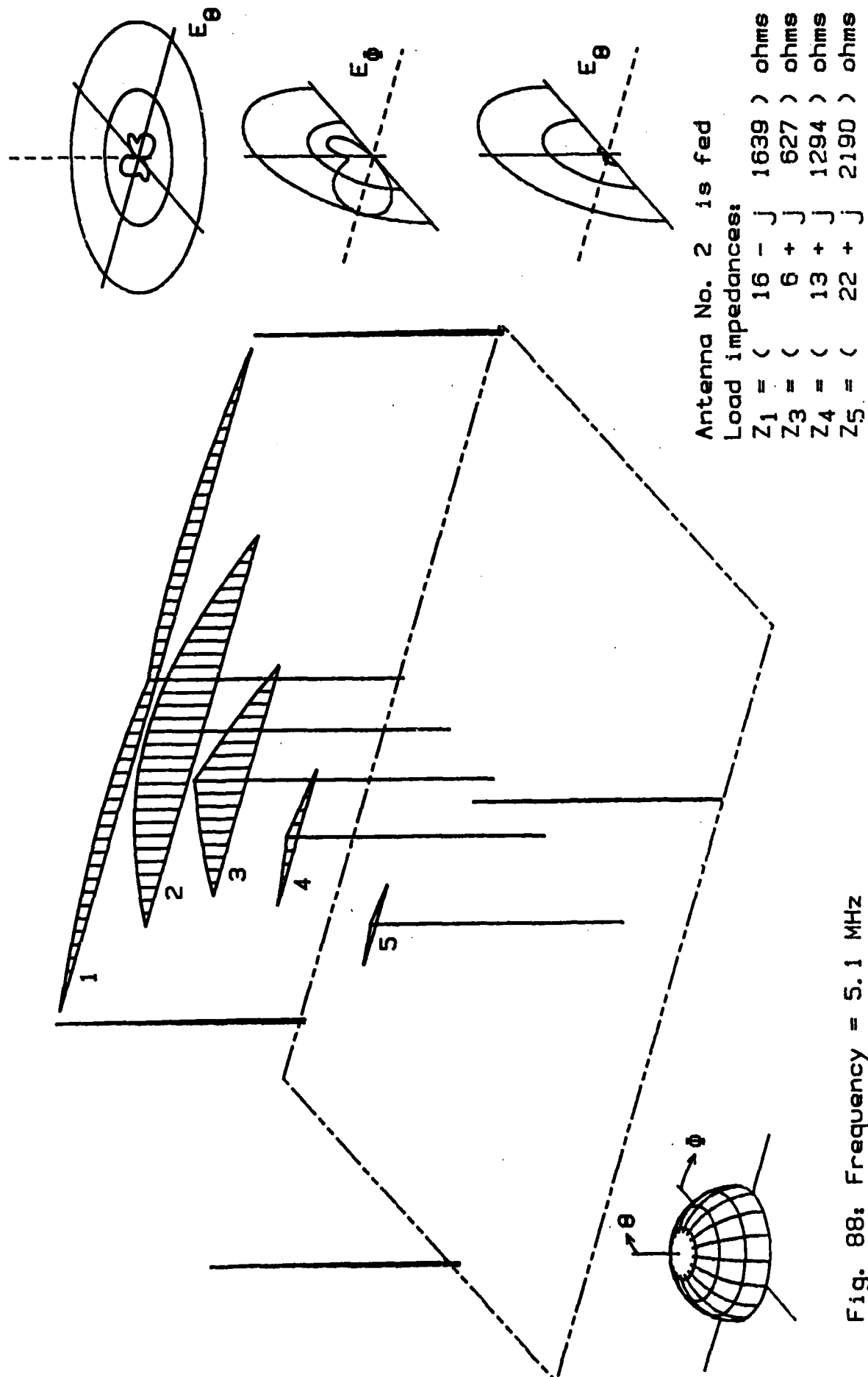
- 120 -





I-Code 007 / 5.1 MHz
P-Code 007 / 5.1 MHz



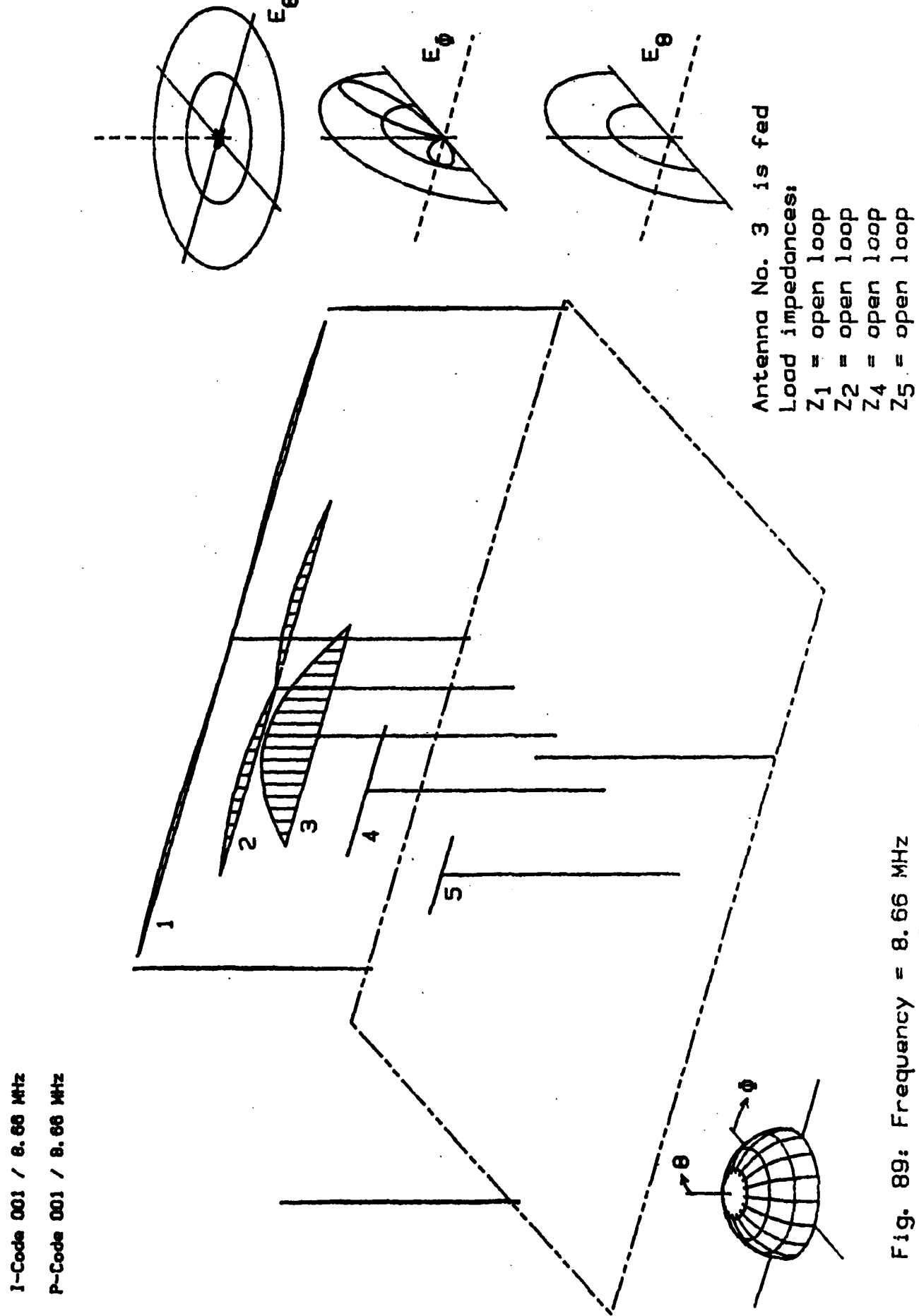


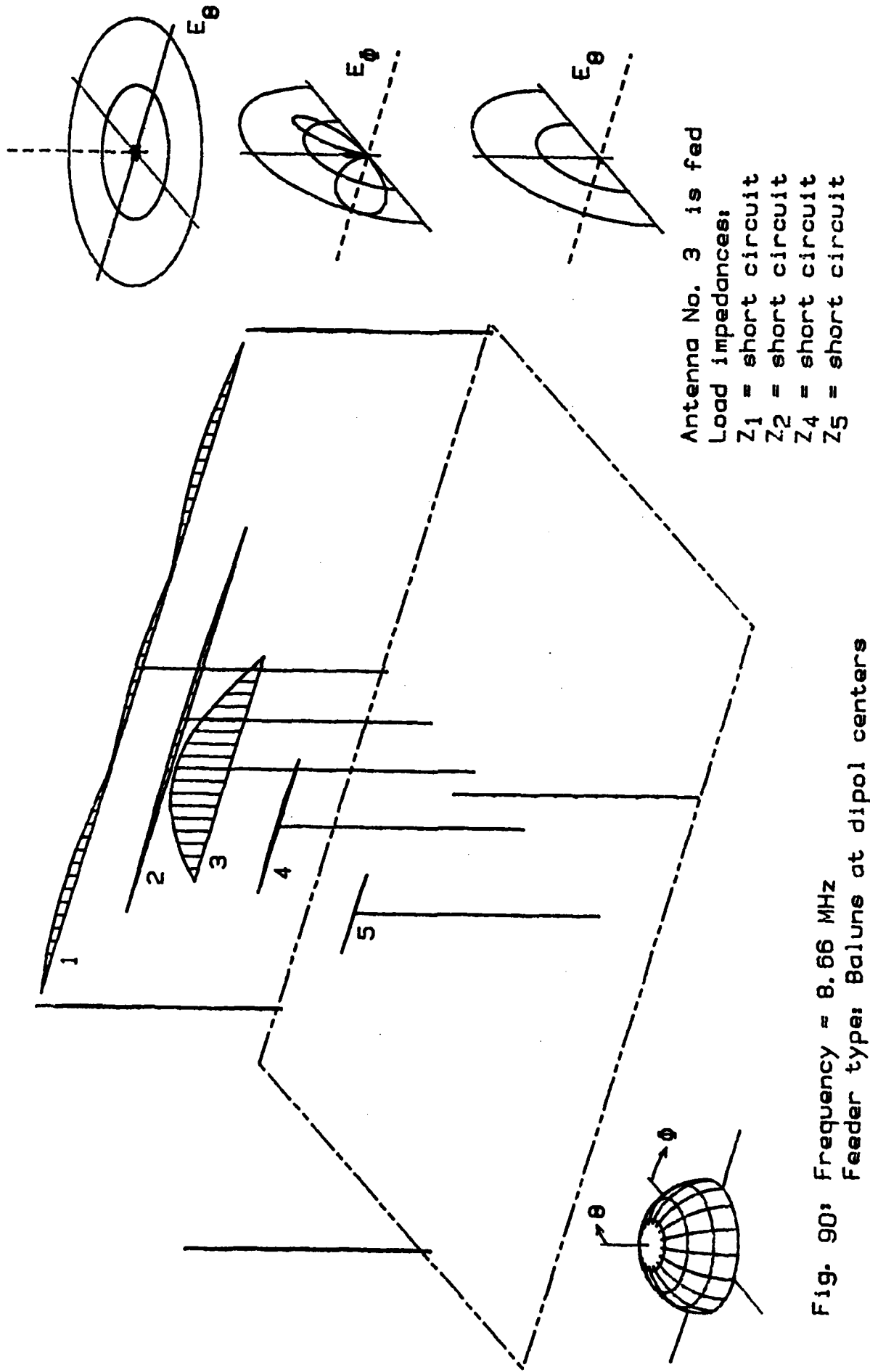
I-Code 003 / 5.1 MHz

P-Code 003 / 5.1 MHz

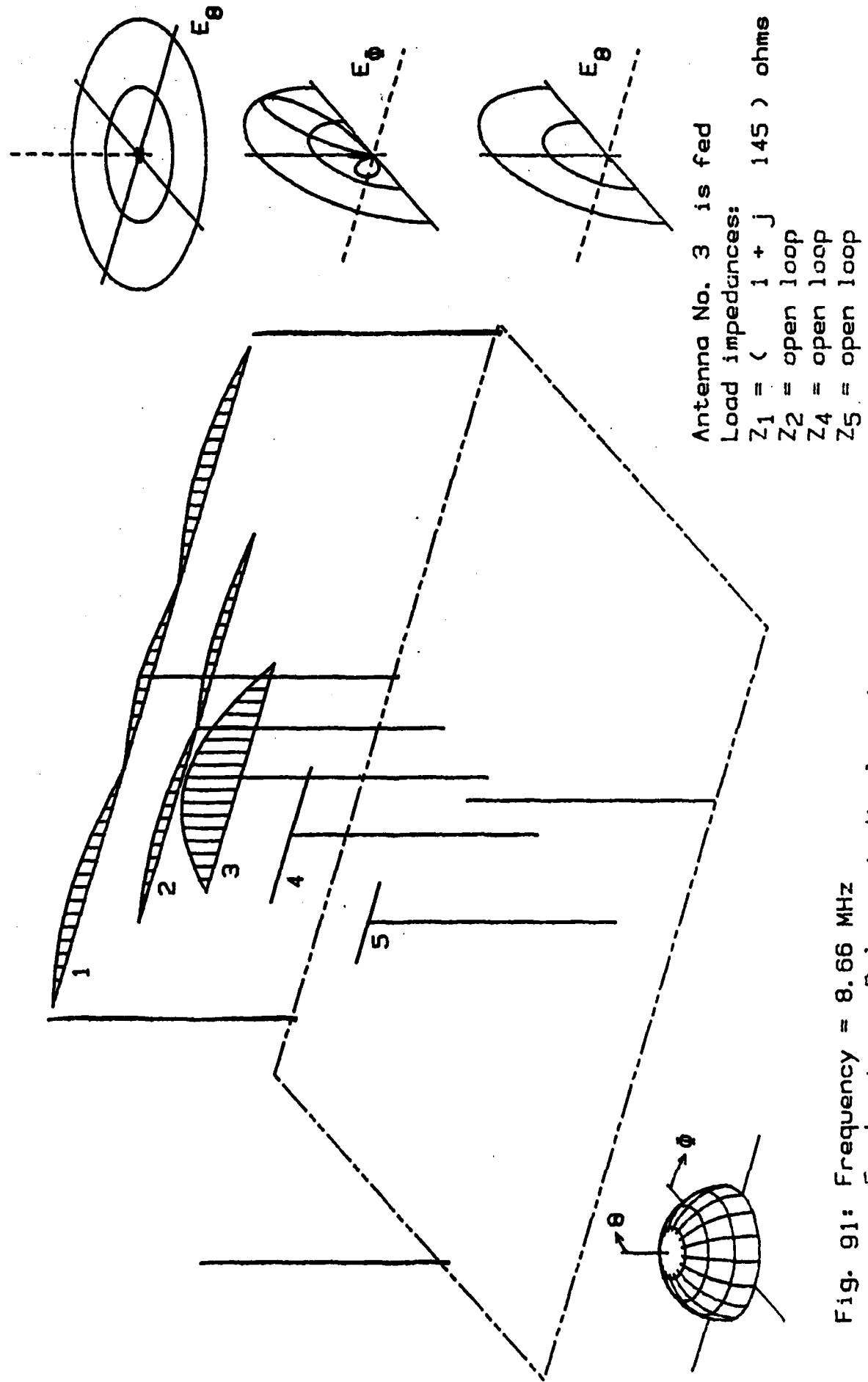
$Z_{11} = (-92.65-j145) \text{ ohms}$	$Z_{12} = (-57.25-j21) \text{ ohms}$	$Z_{13} = (-17.54-j11) \text{ ohms}$	$Z_{14} = (5.61-j9) \text{ ohms}$	$Z_{15} = (-3.73-j4) \text{ ohms}$
$Z_{21} = (-37.32-j21) \text{ ohms}$	$Z_{22} = (1280.04+j1814) \text{ ohms}$	$Z_{23} = (122.72-j192) \text{ ohms}$	$Z_{24} = (-78.31-j83) \text{ ohms}$	$Z_{25} = (-37.25+j41) \text{ ohms}$
$Z_{31} = (17.54-j11) \text{ ohms}$	$Z_{32} = (122.70-j192) \text{ ohms}$	$Z_{33} = (45.87+j19) \text{ ohms}$	$Z_{34} = (13.49-j11) \text{ ohms}$	$Z_{35} = (-5.30-j5) \text{ ohms}$
$Z_{41} = (5.60-j9) \text{ ohms}$	$Z_{42} = (-78.32-j83) \text{ ohms}$	$Z_{43} = (13.48-j11) \text{ ohms}$	$Z_{44} = (19.41-j586) \text{ ohms}$	$Z_{45} = (3.05-j9) \text{ ohms}$
$Z_{51} = (-3.74-j4) \text{ ohms}$	$Z_{52} = (-37.25+j41) \text{ ohms}$	$Z_{53} = (-5.30-j5) \text{ ohms}$	$Z_{54} = (3.05-j9) \text{ ohms}$	$Z_{55} = (4.11-j1203) \text{ ohms}$

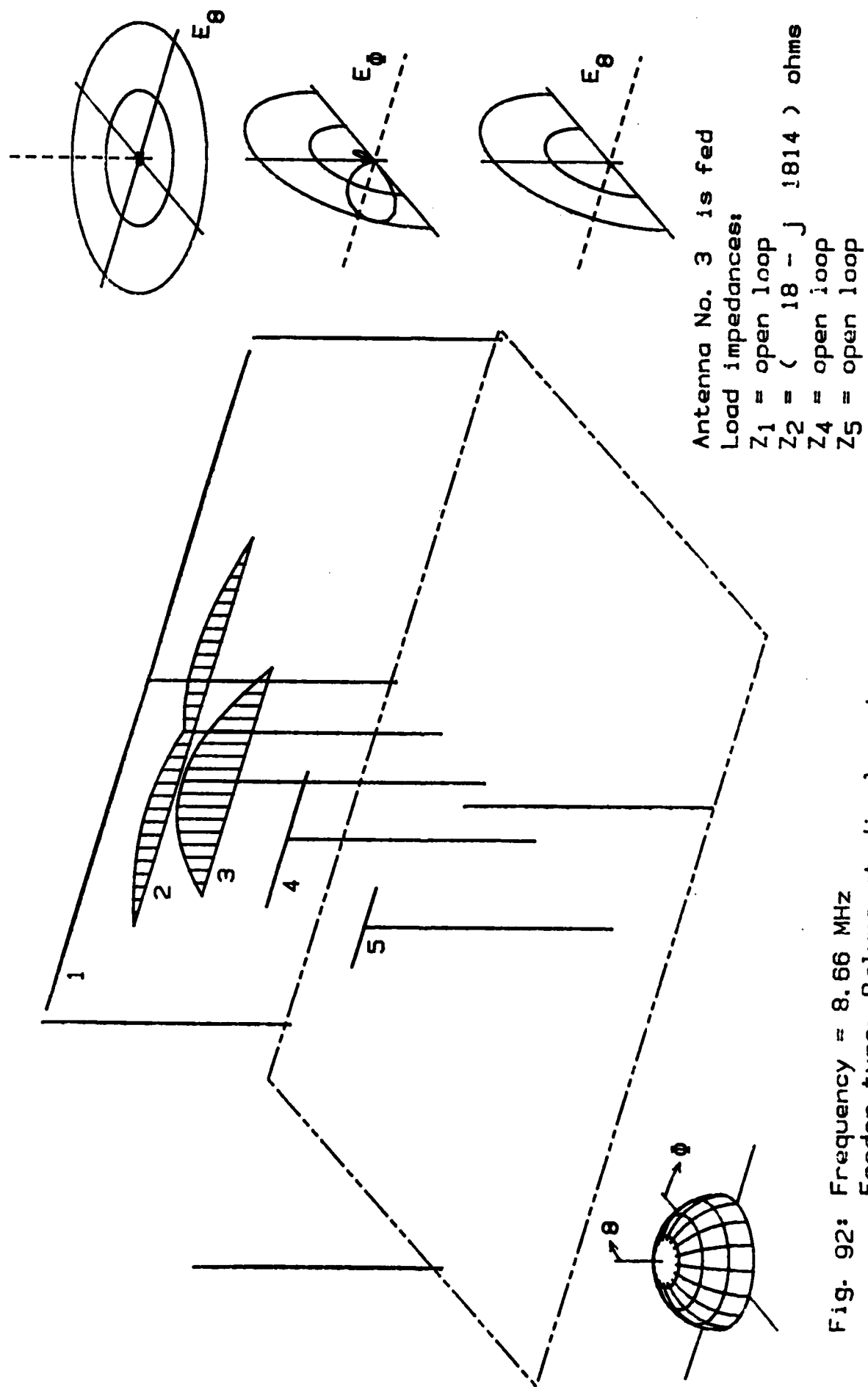
Table 8: Z-Matrix for $f = 8.66 \text{ MHz}$. Feeder type: Baluns at the dipole centers.



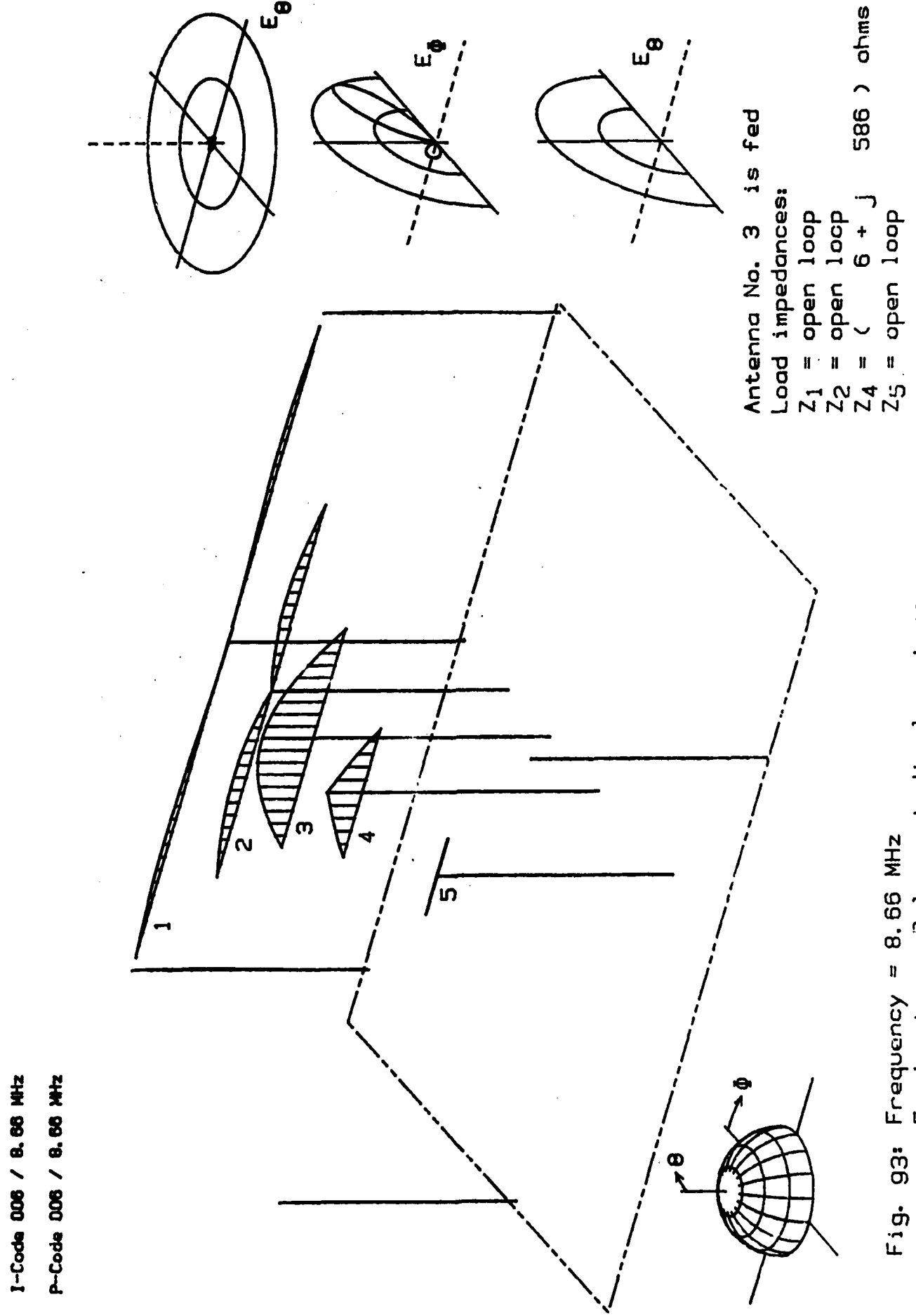


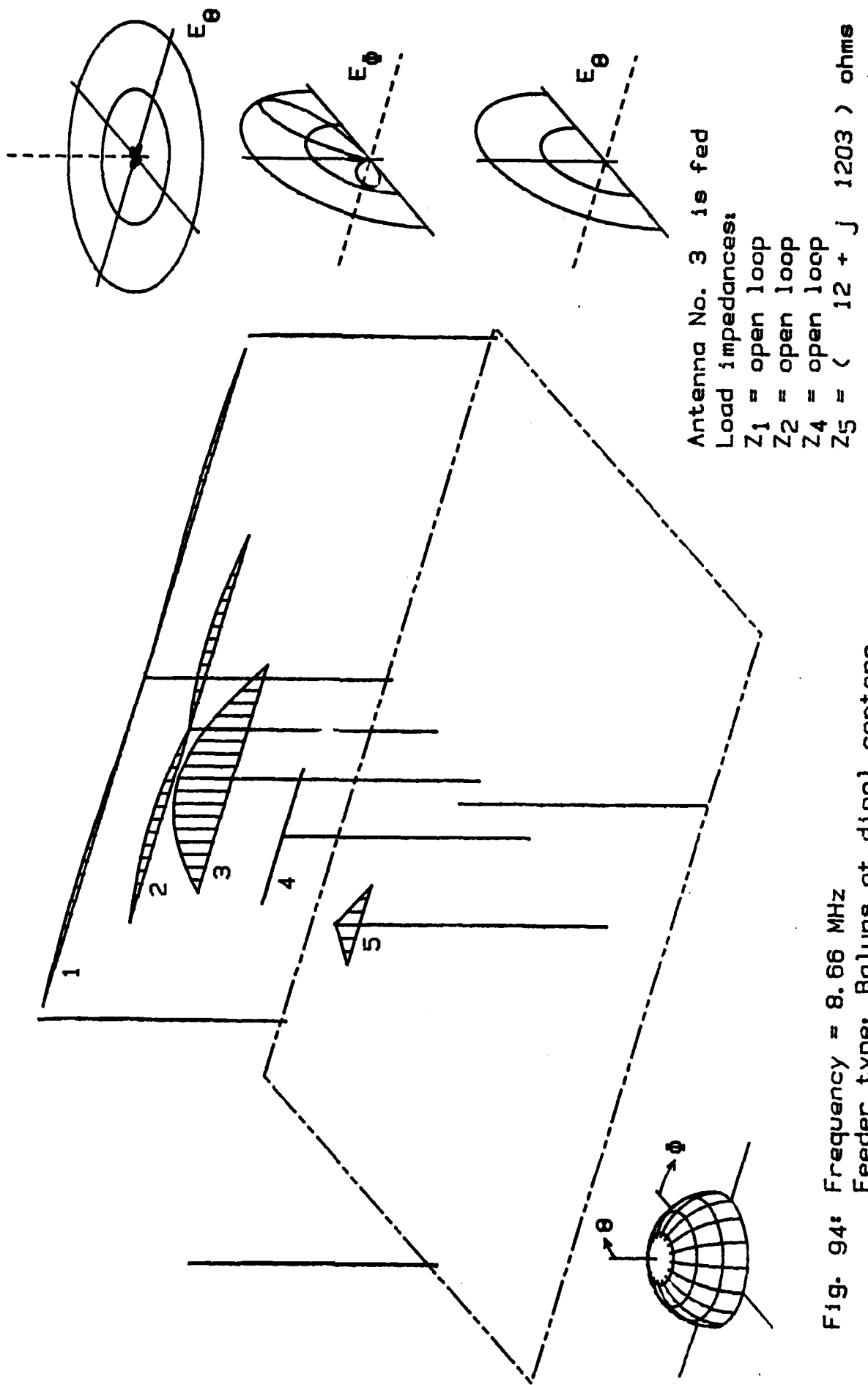
I-Code 004 / 8.66 MHz
P-Code 004 / 8.66 MHz



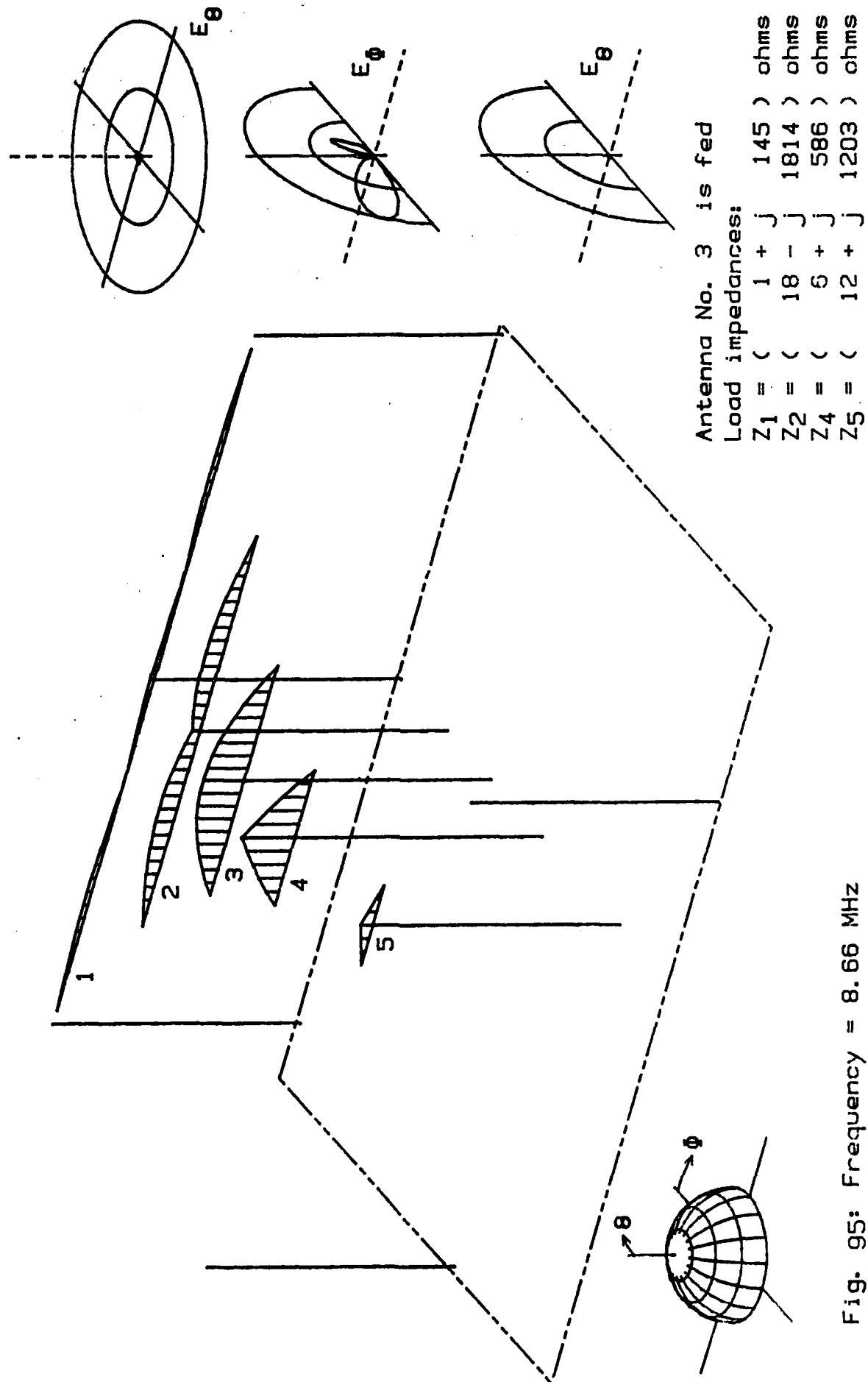


I-Code 005 / 8.66 MHz
P-Code 005 / 8.66 MHz





I-Codes 003 / 8.66 MHz
P-Codes 003 / 8.66 MHz



$Z_{11} = (-117.85-j143)$ ohms	$Z_{12} = (22.65-j 7)$ ohms	$Z_{13} = (-11.24+j 23)$ ohms	$Z_{14} = (-4.82-j 3)$ ohms	$Z_{15} = (1.95+j 6)$ ohms
$Z_{21} = (22.78-j 7)$ ohms	$Z_{22} = (96.00-j 136)$ ohms	$Z_{23} = (13.96+j 68)$ ohms	$Z_{24} = (6.33-j 6)$ ohms	$Z_{25} = (1.55+j 5)$ ohms
$Z_{31} = (-11.12+j 23)$ ohms	$Z_{32} = (13.99+j 67)$ ohms	$Z_{33} = (1569.54+j1213)$ ohms	$Z_{34} = (-61.94-j 202)$ ohms	$Z_{35} = (6.13+j 22)$ ohms
$Z_{41} = (-4.80-j 3)$ ohms	$Z_{42} = (6.32-j 6)$ ohms	$Z_{43} = (-61.95-j 202)$ ohms	$Z_{44} = (85.09+j 40)$ ohms	$Z_{45} = (-8.06-j 16)$ ohms
$Z_{51} = (1.95+j 6)$ ohms	$Z_{52} = (1.55+j 5)$ ohms	$Z_{53} = (6.12+j 22)$ ohms	$Z_{54} = (-8.06-j 16)$ ohms	$Z_{55} = (20.54-j 548)$ ohms

Table 9: Z-Matrix for $f = 14.71$ MHz. feeder type: Baluns at the dipole centers.

I-Code 001 / 14.71 MHz
P-Code 001 / 14.71 MHz

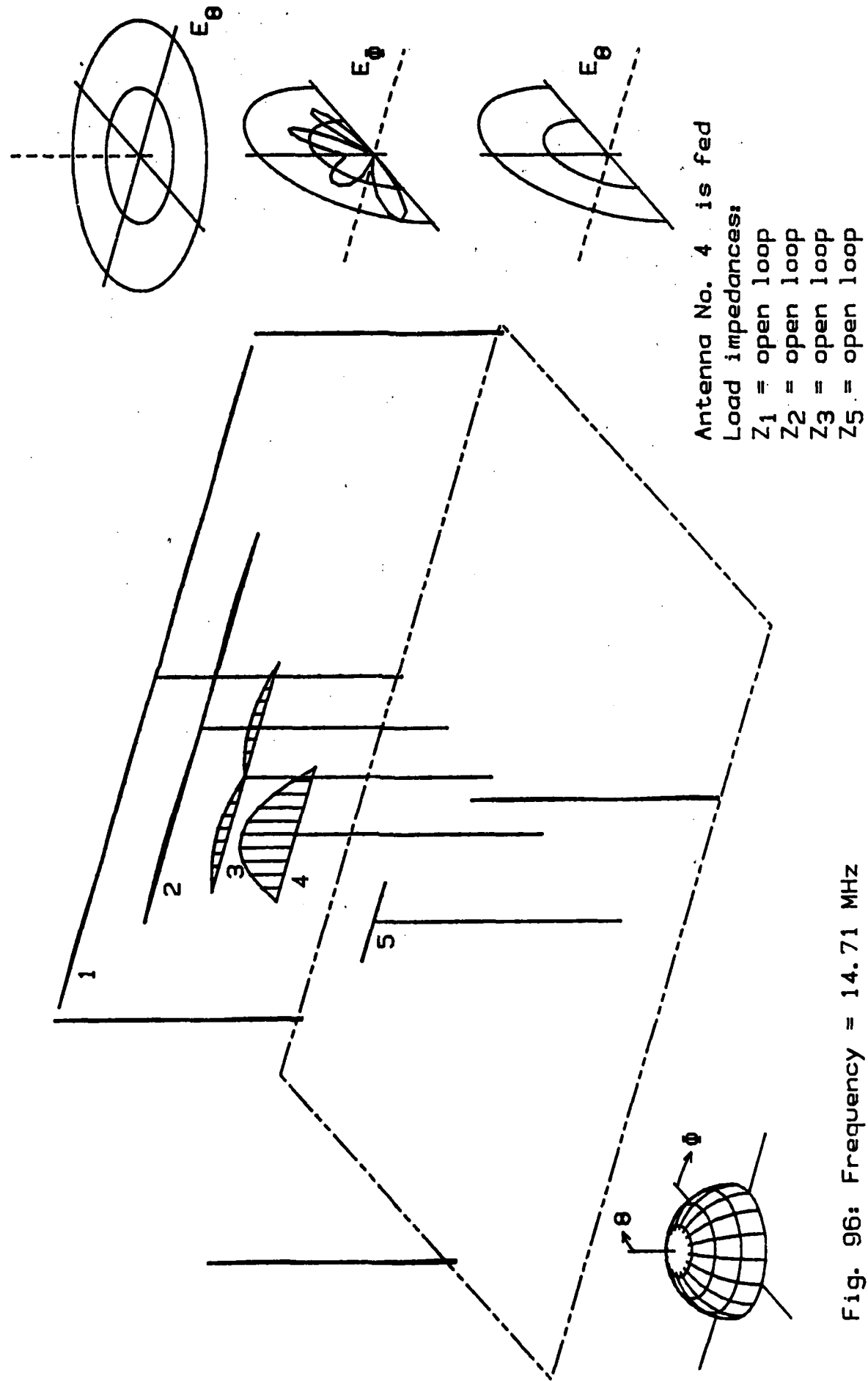
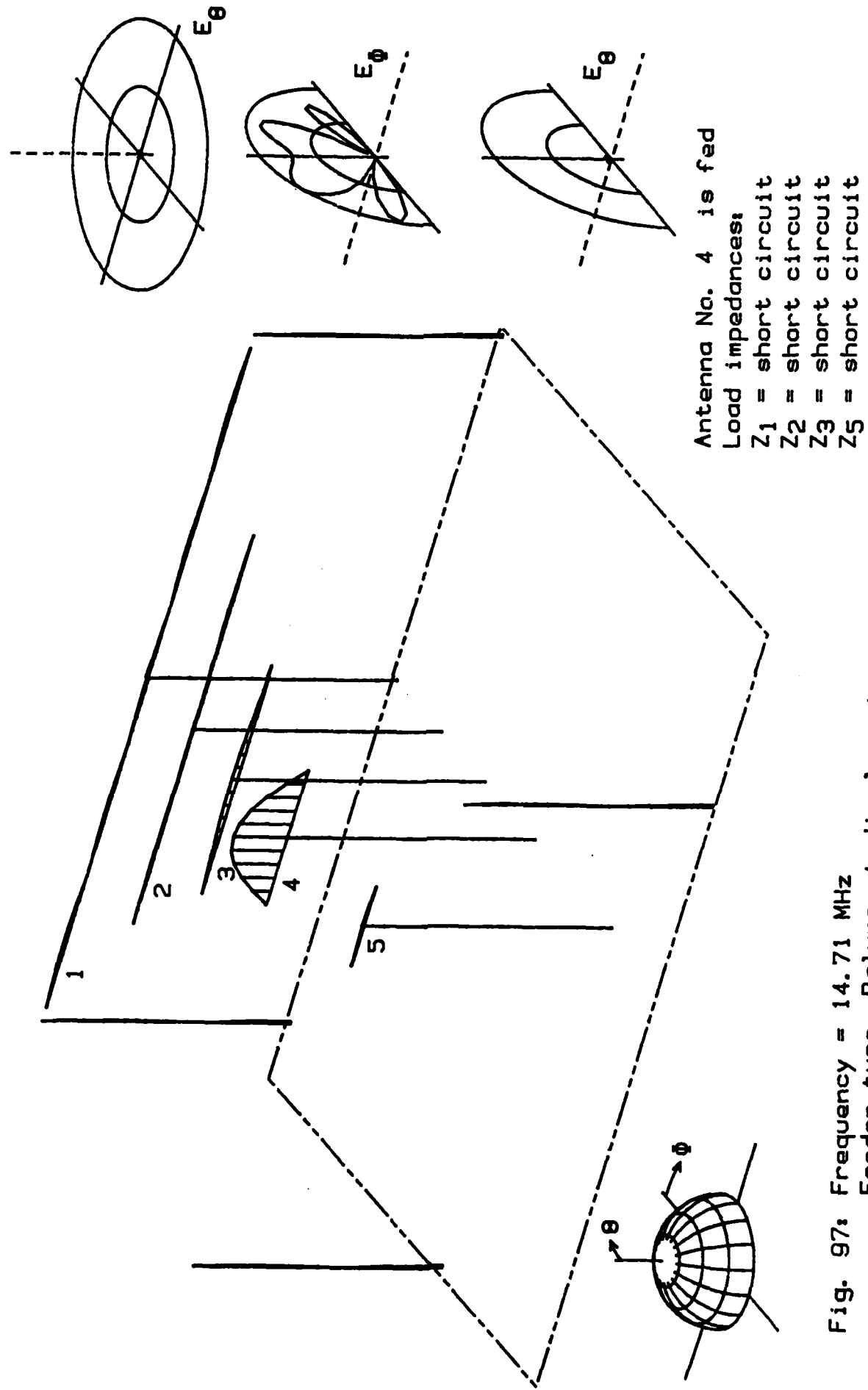
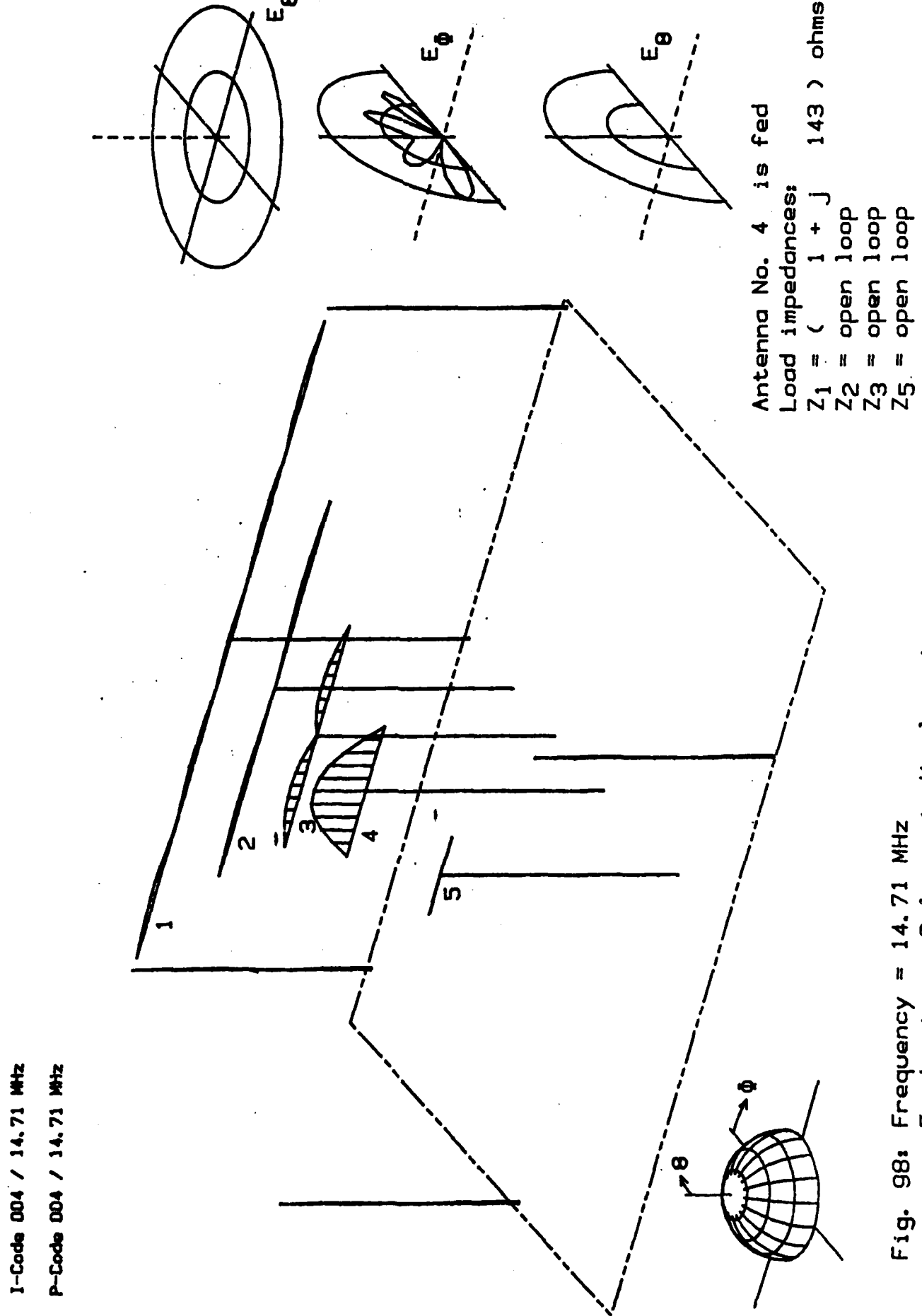
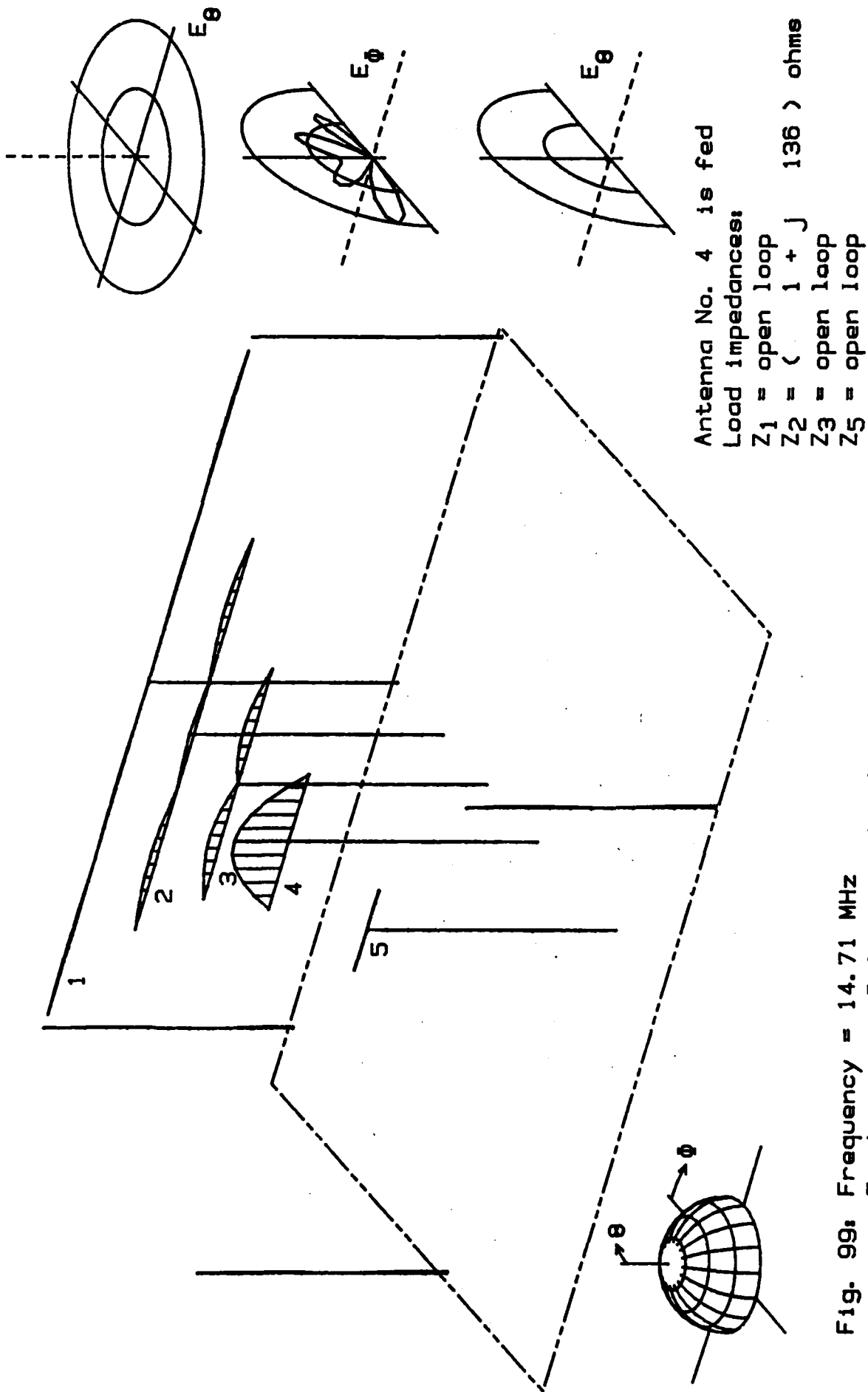


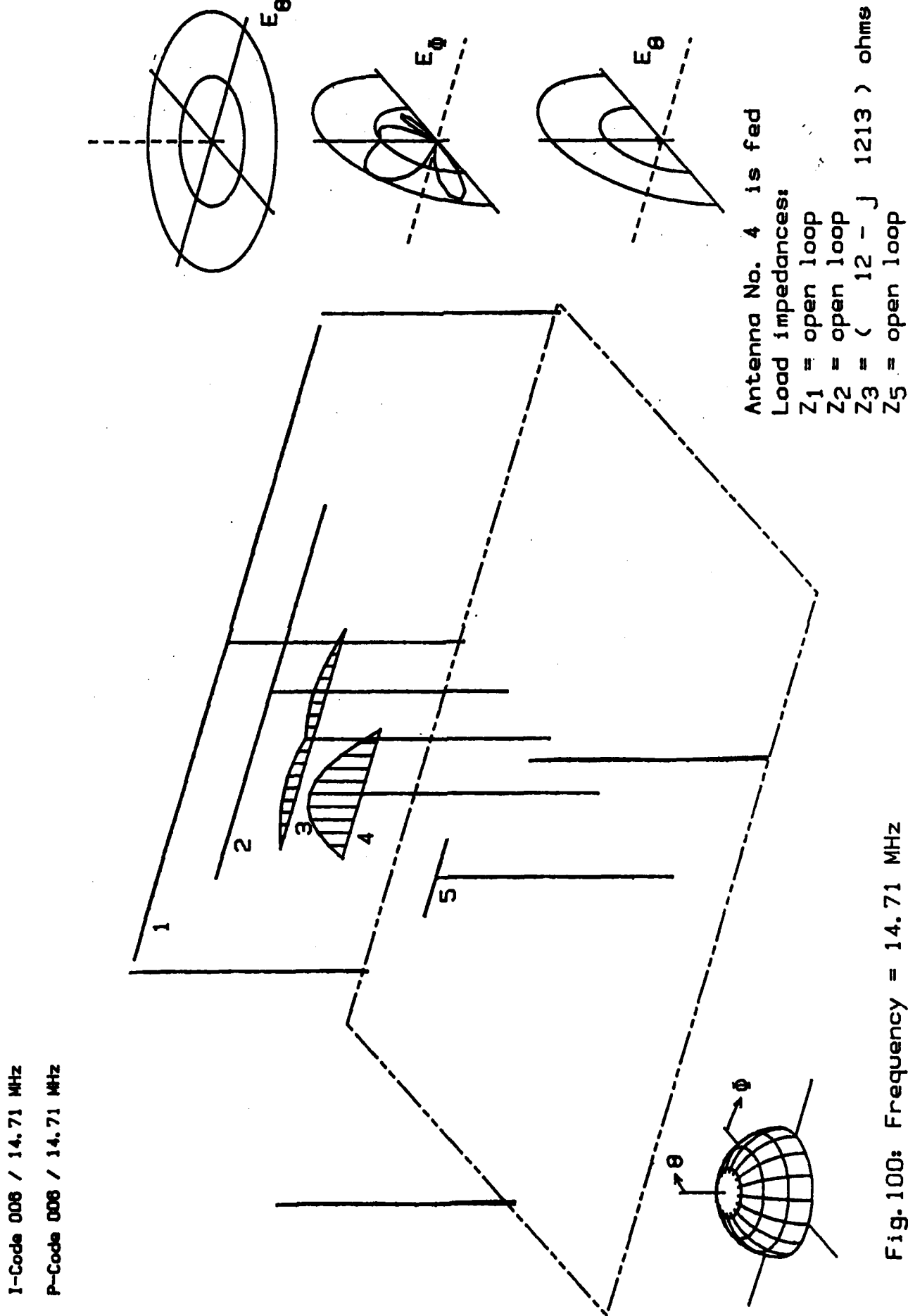
Fig. 96: Frequency = 14.71 MHz
Feeder type: Baluns at dipol centers

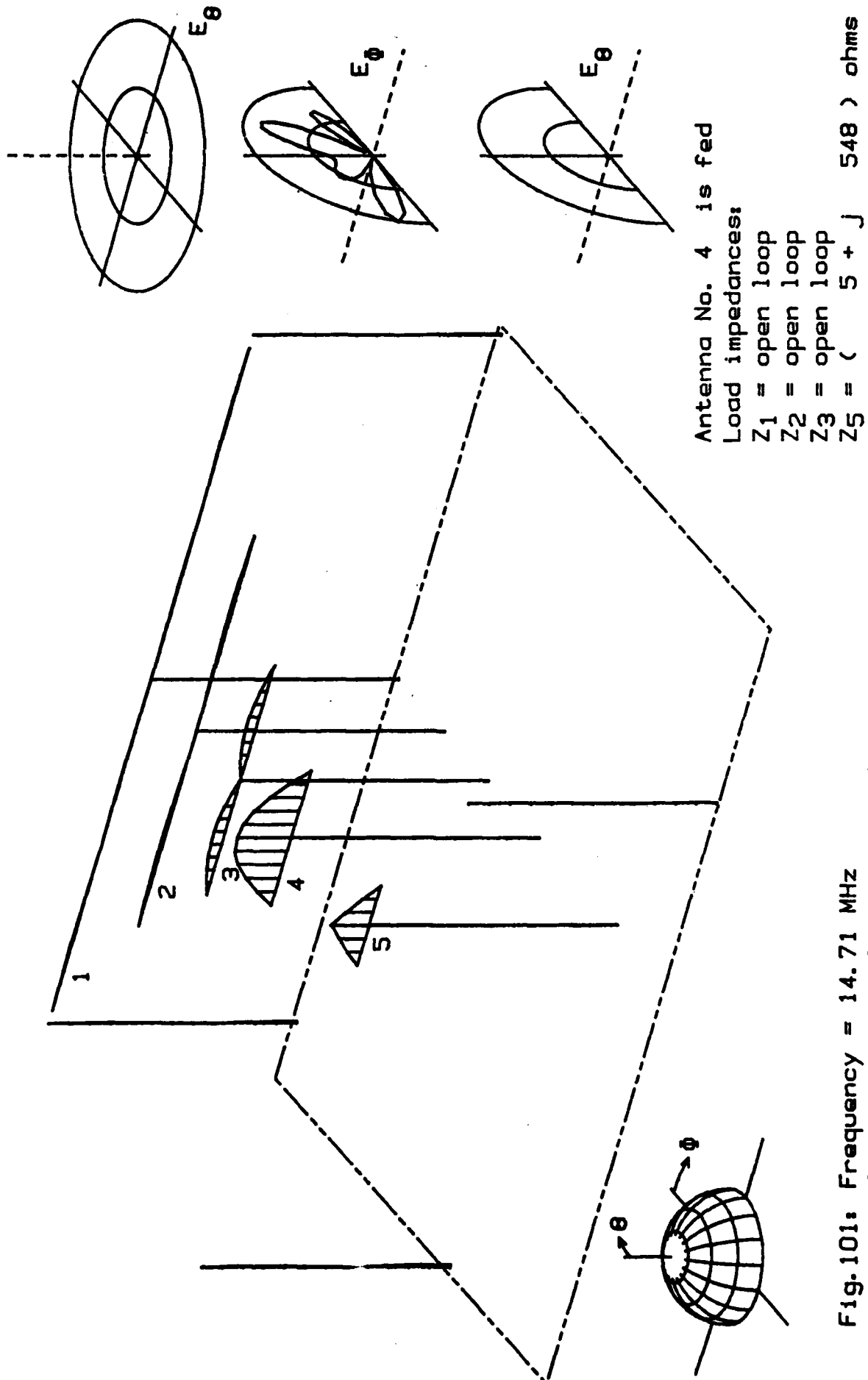
I-Code 002 / 14.71 MHz
P-Code 002 / 14.71 MHz





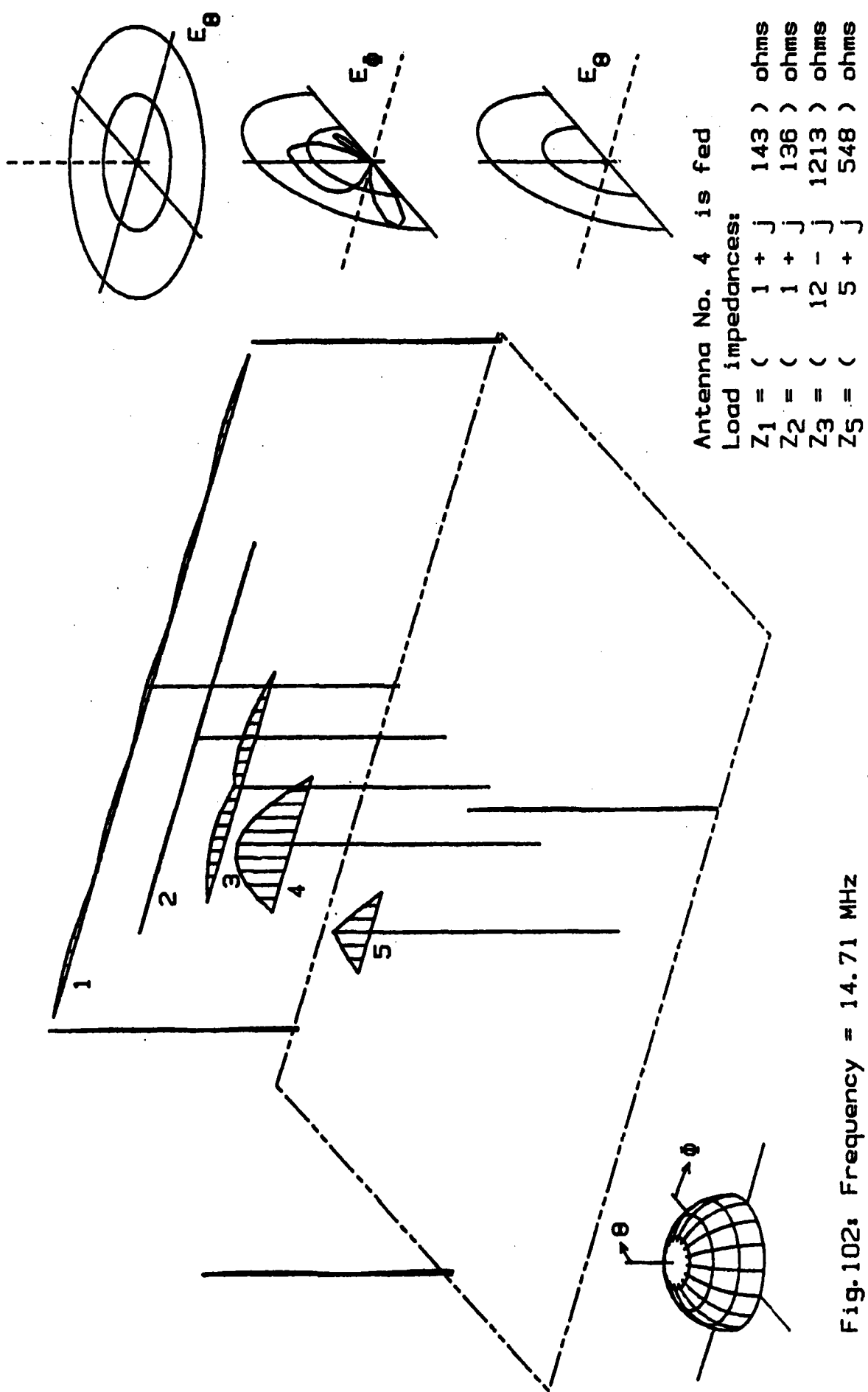






I-Code 007 / 14.71 MHz
P-Code 007 / 14.71 MHz

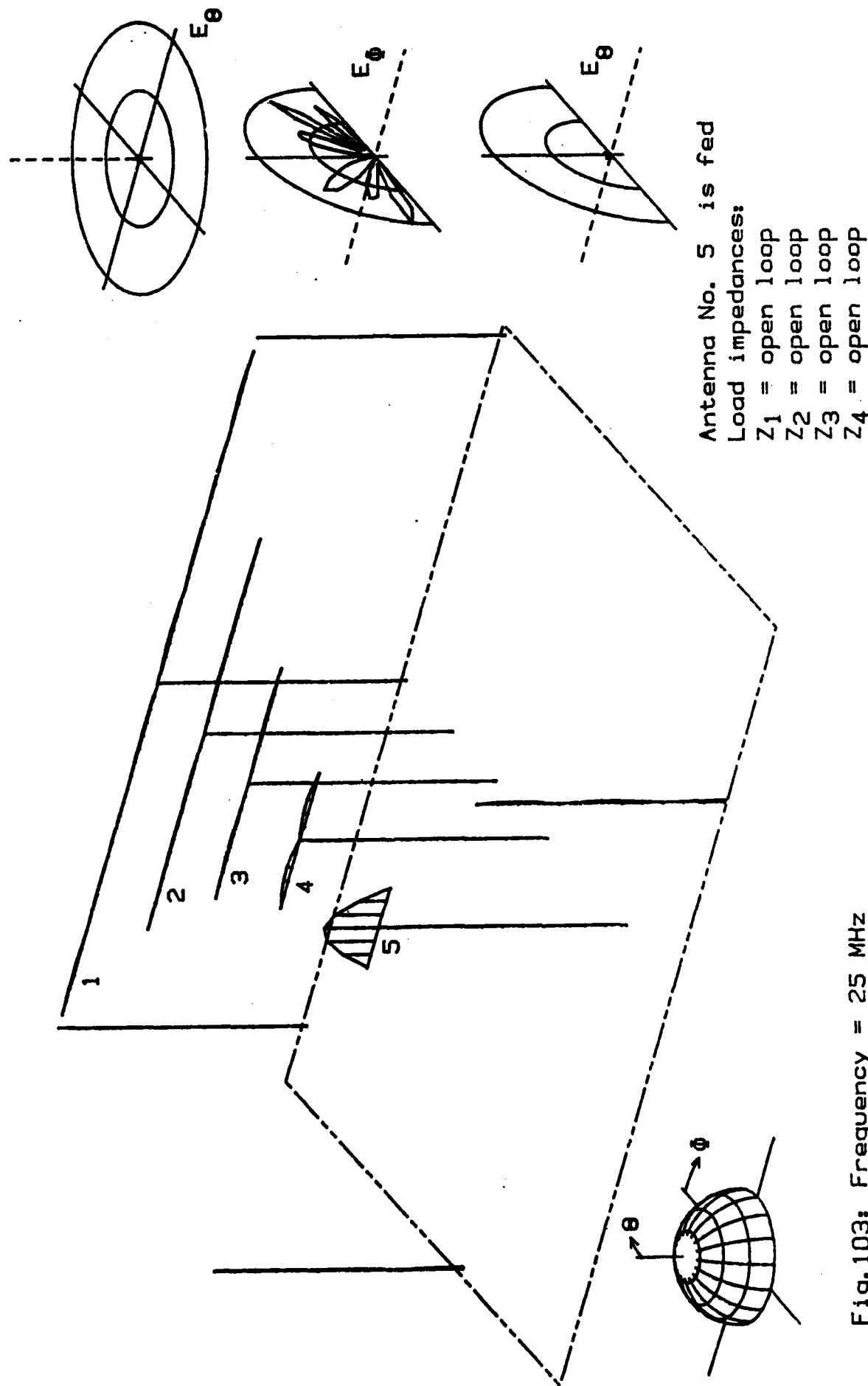
I-Code 003 / 14.71 MHz
P-Code 003 / 14.71 MHz



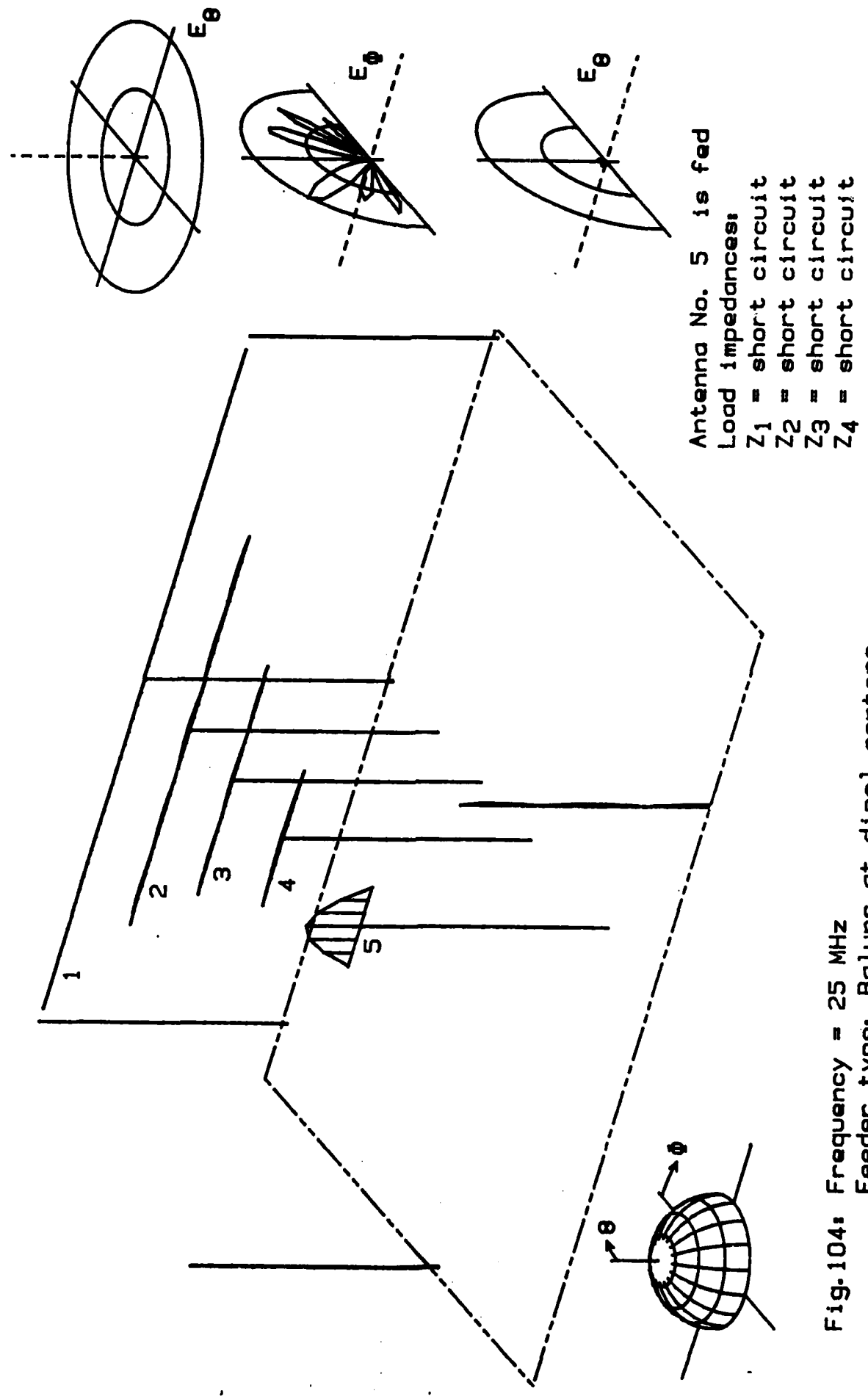
$l_{11} = (-782.26-j1231)$ ohms	$l_{12} = (-13.68-j 14)$ ohms	$l_{13} = (41.34+j 3)$ ohms	$l_{14} = (27.93-j 59)$ ohms	$l_{15} = (10.40+j 19)$ ohms
$l_{21} = (-13.91-j 13)$ ohms	$l_{22} = (116.51-j 208)$ ohms	$l_{23} = (16.92-j 22)$ ohms	$l_{24} = (-16.09+j 5)$ ohms	$l_{25} = (4.51-j 12)$ ohms
$l_{31} = (41.42+j 3)$ ohms	$l_{32} = (17.00-j 22)$ ohms	$l_{33} = (81.24-j 181)$ ohms	$l_{34} = (63.68-j 30)$ ohms	$l_{35} = (10.69-j 1)$ ohms
$l_{41} = (27.80-j 59)$ ohms	$l_{42} = (-16.04+j 5)$ ohms	$l_{43} = (63.64-j 30)$ ohms	$l_{44} = (1199.72+j1423)$ ohms	$l_{45} = (17.83+j 90)$ ohms
$l_{51} = (10.40+j 19)$ ohms	$l_{52} = (4.50-j 12)$ ohms	$l_{53} = (10.69-j 1)$ ohms	$l_{54} = (17.88+j 90)$ ohms	$l_{55} = (68.26+j 4)$ ohms

Table 10: Z-Matrix for f = 25 MHz. Feeder type: Baluns at the dipole centers.

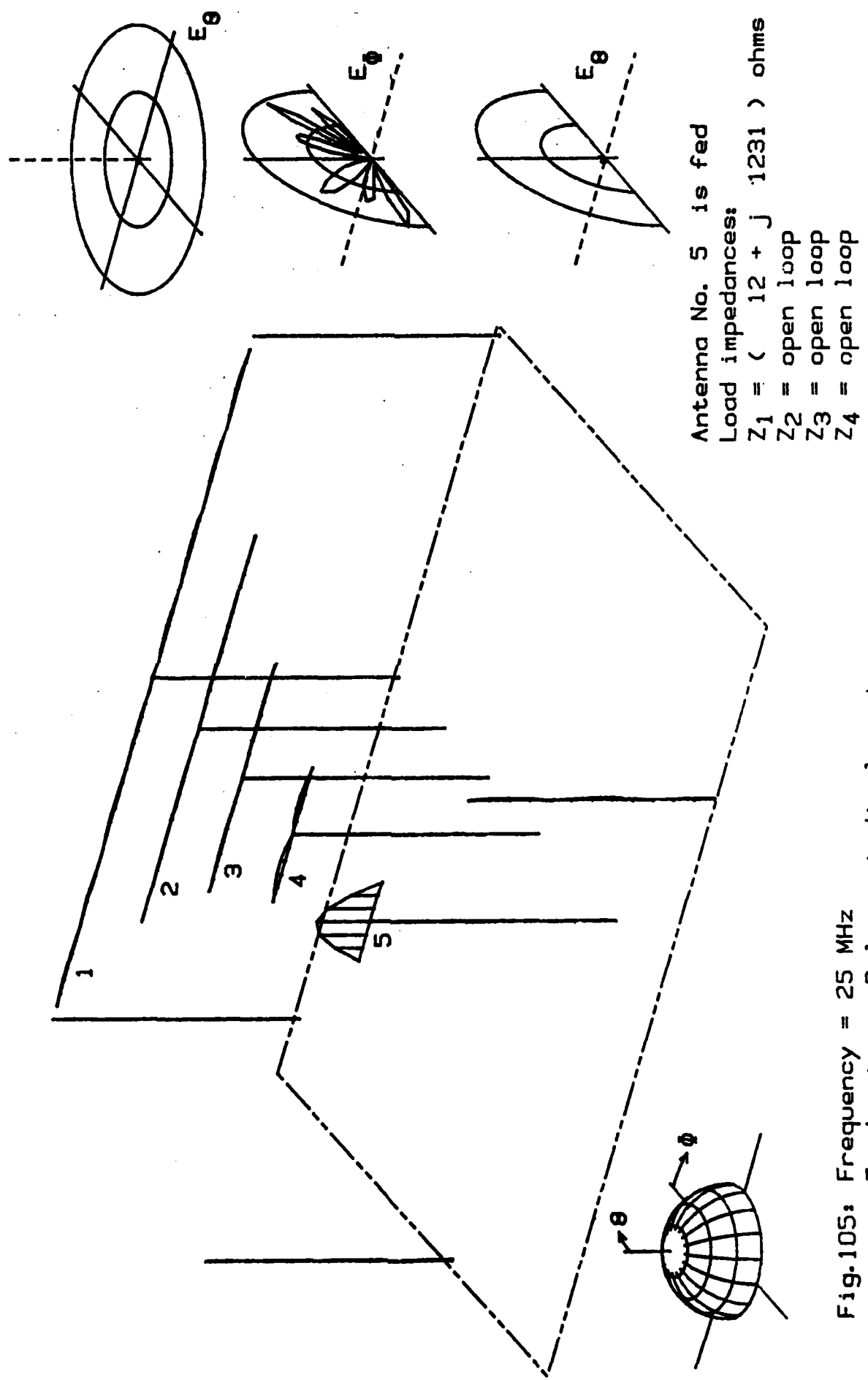
I-Code 001 / 25 MHz
P-Code 001 / 25 MHz



I-Code 002 / 25 MHz
P-Code 002 / 25 MHz

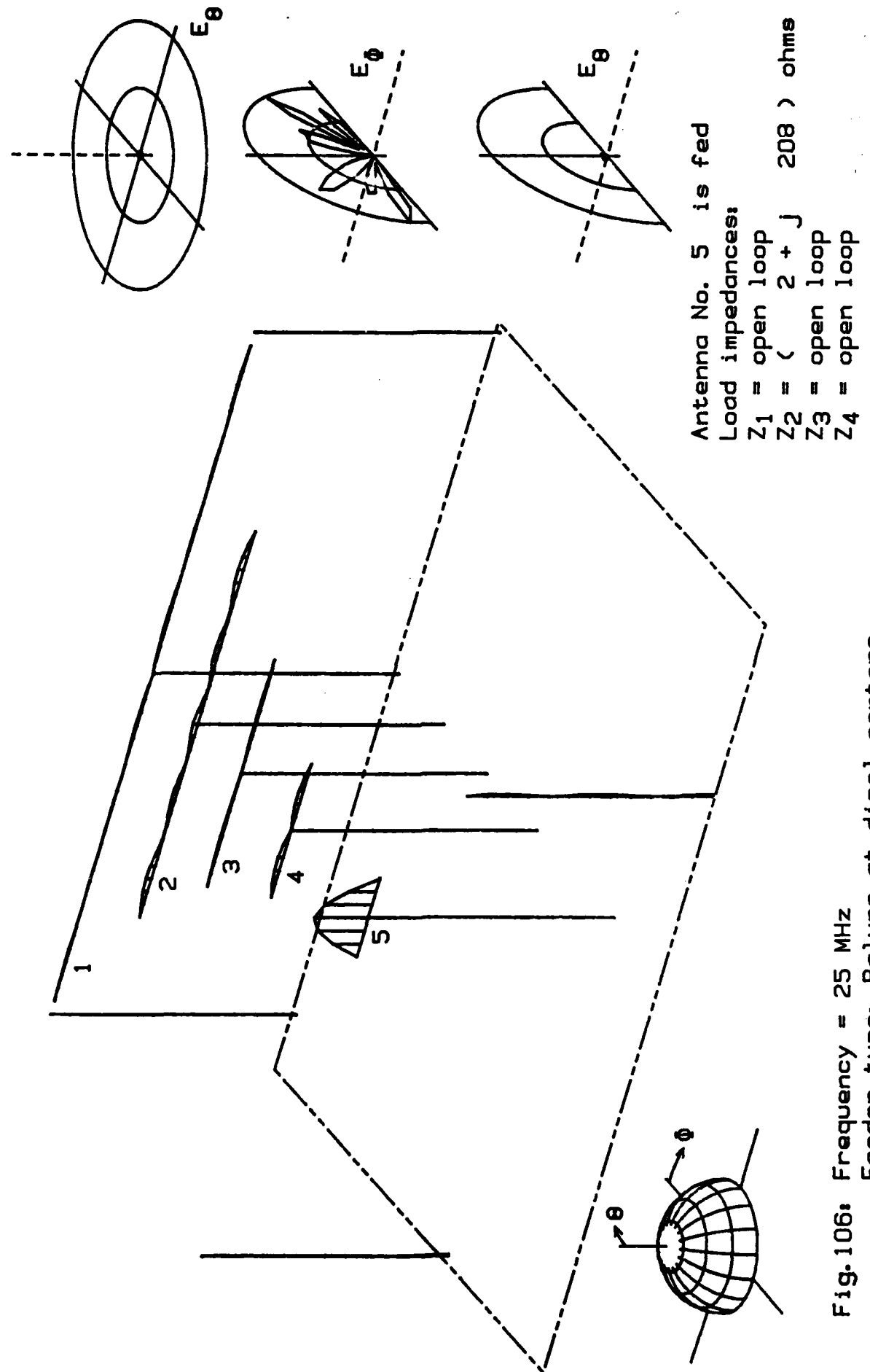


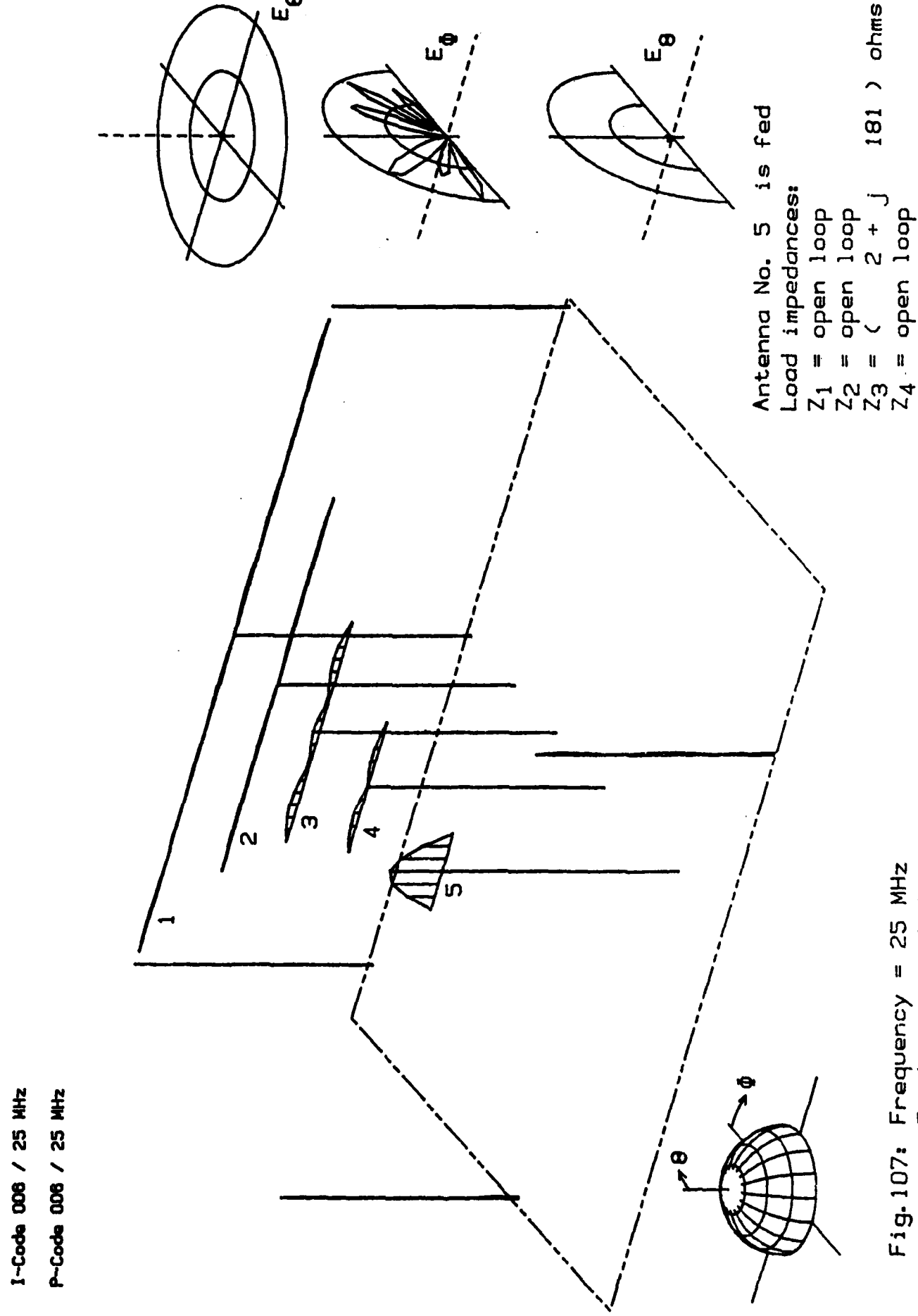
I-Code 004 / 25 MHz
P-Code 004 / 25 MHz



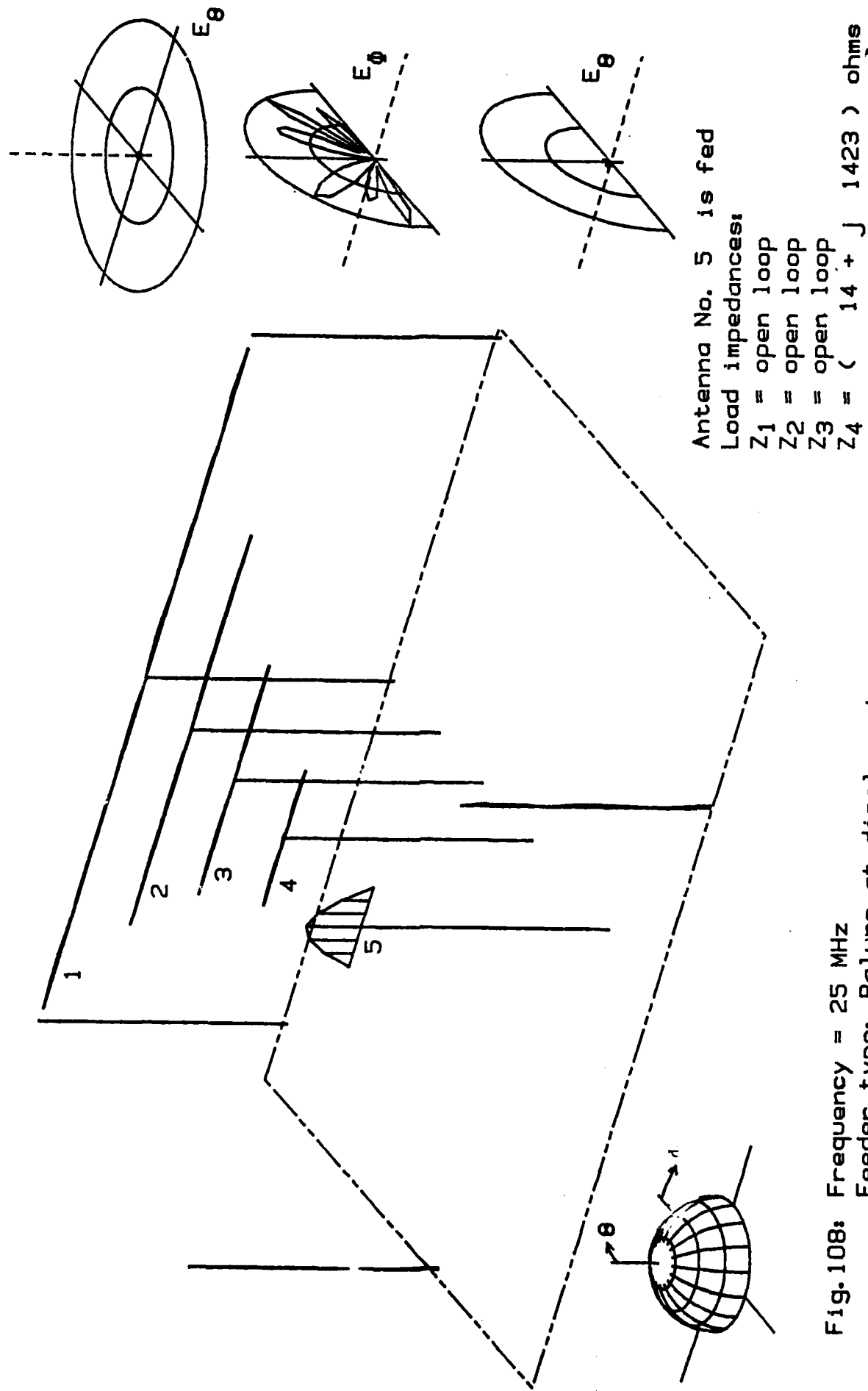
I-Code 005 / 25 MHz
P-Code 005 / 25 MHz

- 144 -

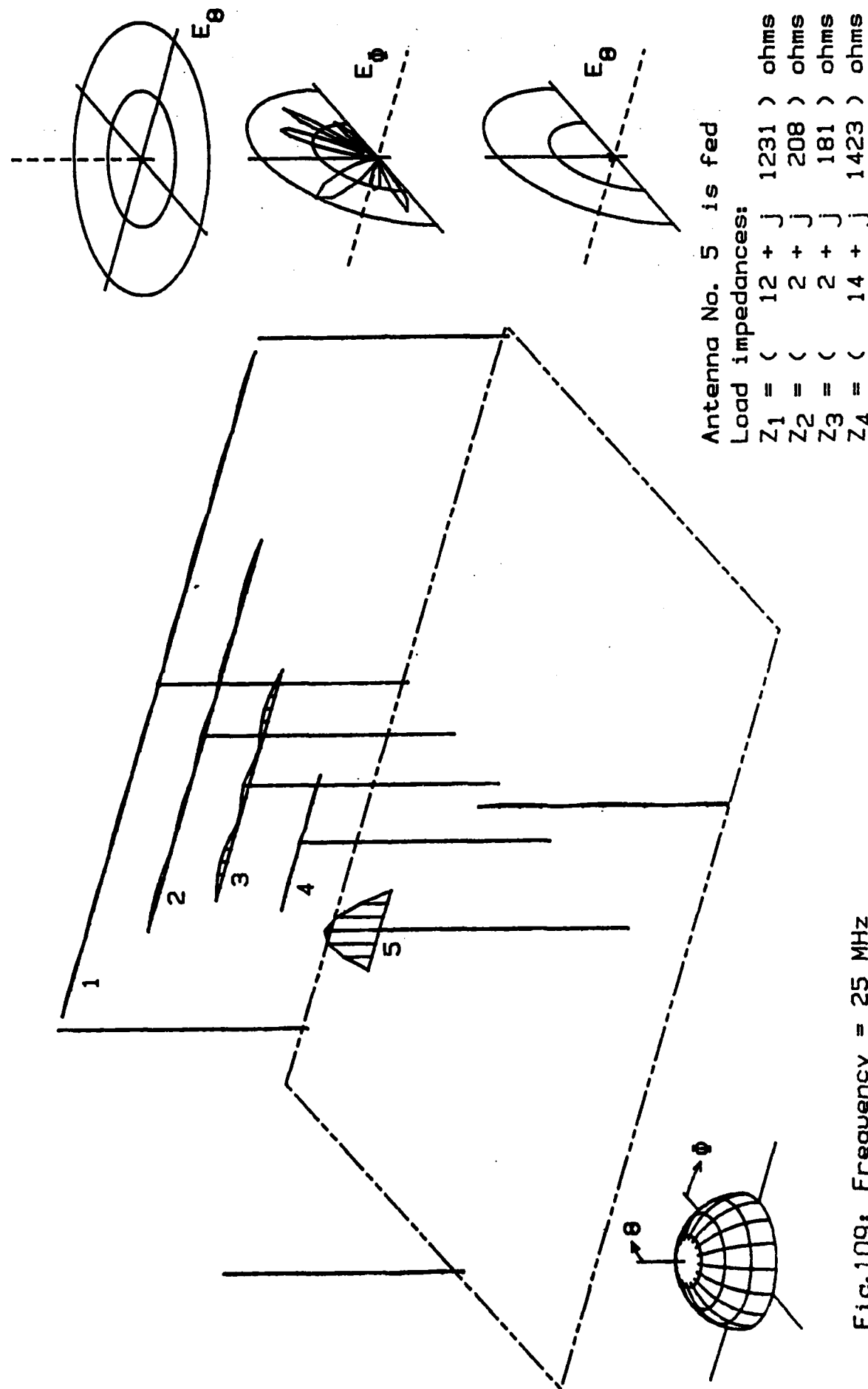




I-Code 007 / 25 MHz
P-Code 007 / 25 MHz



I-Code 003 / 25 MHz
P-Code 003 / 25 MHz



12. Conclusions - Recommendations

The main result of the preceding investigations is the disadvantage of the cobra head feeder. It can be stated as a general rule that the cobra head feeder should be avoided in any case because it forms an unsymmetry which seriously incorporates the feeder line into the radiating structure. As a result a major part of the radiated power is converted into the ground-wave radiation in an unpredictable manner. Additionally, the feeder line in connection with one half of the dipole antenna forms a structure which enables stray resonances at various frequencies. Over the wide frequency range which has to be covered by an HF-antenna site, multiple parasitic resonances can occur which are hard to predict without extended calculations. Even if those resonances are detected with the help of pre-calculations there are nearly no means to avoid them.

Coupling between the antennas and the supporting poles is stronger than might have been expected. In all previous calculations a distance of 1m has been assumed to exist between the tips of the dipole antenna 1 and poles 1 and 2. The capacity which is formed by this arrangement is large enough to produce parasitic currents in these poles which are of the same order of magnitude as the feeder currents of antenna 1 at about 3 MHz. These stray currents can be avoided by choosing a greater distance between the poles and the antenna tips (at least 5 m; more detailed calculations will be performed in the future), or by designing the poles to be non-conductive. In the latter case, a lightning protection would be provided by using randomly interrupted lightning conductors (realized with the help of spark gaps).

The supporting wires have been assumed to be non-conductive because of the limited computer memory. On the other hand, the

noted coupling between antenna 1 and the poles 1 and 2 seriously suggests the use of non-conductive supporting wires to avoid similar effects. In practice, "non-conductive" supporting wires can be achieved with a frequent interruption of conductive wires with insulators, if conductive wires must be used.

Long distance space-wave propagation in the HF-range can be performed best if the radiated power is launched under certain elevation angles which best fit to the reflection properties of the ionosphere (the same angle gives best performance for reception). These elevation angles are frequency dependent. However, the angle of maximum radiation depends on the mounting height of the antenna over ground compared to the wavelength. Thus, it is highly recommended that the different antennas not be mounted at the same height over ground level. Each antenna should be mounted at a height which is optimum for its frequency range and the reflection properties of the ionosphere at this frequency range.

The coupling between adjacent antennas depends on the load termination of the parasitically coupled antennas. In general, coupling effects seem to be more pronounced the closer the operating frequency range of adjacent antennas. This leads to the rule of mixing up long and short antennas instead of regularly spacing in ascending or descending lengths. Additional investigations on this subject are planned.

13. Acknowledgement.

The method for the calculation of the generic cases bases on a computer program developed by H. Lindenmeier and A. Schwab, who extensively contributed to this report. J. Harvey, R. Sauer, and R. Franklin supported this research work with several discussions and hints.

END

FILMED

2-86

DTIC